REXONEYE

QMR TECHNOLOGY

FOR THE EYE WELLNESS SOLUTION

CLINICAL STUDIES
UNIVERSITY RESEARCH
PUBLICATIONS

QUANTUM MOLECULAR RESONANCE
QMR
TECHNOLOGY
TELEA MEDICAL

www.resono.it

INDEX

CLINICAL OUTCOMES WITH THE REXON-EYE MEDICAL DEVICE

QMR TECHNOLOGY

QMR® TECHNOLOGY

The principle of operation of Rexon-Eye® is the Quantum Molecular Resonance (QMR®) Technology, which delivers a mild alternate electrical signal containing a specific mix of frequencies (from 4 MHz to 64 MHz) that has been shown **to stimulate the natural regeneration of cells** [3], in addition to having an important **anti-inflammatory action.** [1]

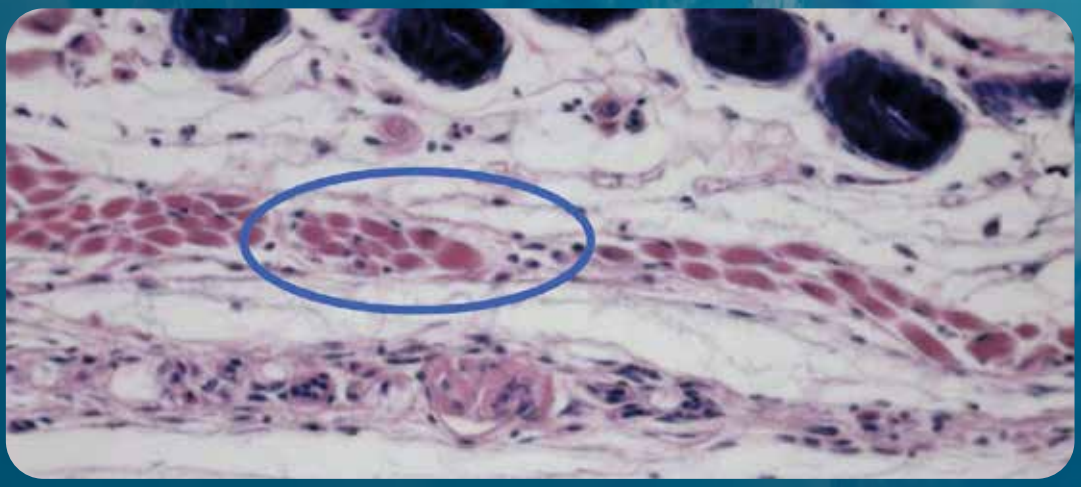

Effects of high frequency and low intencity currents: biostimulation and cell regeneration. Prof. C. Reggiani, Scientific Director of Research, University of Padova [4]

Studies showed that after a course of QMR® stimulation, the parvocellular infiltrate (black dots) appeared within the muscle fibers. This is a result of the regenerative process in progress.

THE UNIQUE ADVANTAGES OF REXON-EYE® THERAPY

What makes REXON-EYE® Therapy unique and innovative is its ability to stimulate biological tissue, enhancing the anti-inflammatory effect and promoting the natural regeneration of cells and tissues. The first application we selected is the treatment of dry eye, a condition affecting hundreds of millions of people worldwide.

THE ANTI-INFLAMMATORY EFFECT

Inflammation plays a key role in what is called the "**vicious circle of dry eye.**" Inflammation leads to tear film instability and ocular surface damage. As the eyes become drier, the level of inflammation increases. This heightened inflammation further exacerbates the dryness of the eyes.

REXON-EYE® Therapy interrupts this cycle through its anti-inflammatory effect. The technology acts to modulate macrophage polarization from the pro-inflammatory M1 phenotype towards the anti-inflammatory M2 phenotype. Macrophages M2 **reduce inflammation** by downregulating inflammatory cytokines and **releasing anti-inflammatory cytokines.** [1]

NATURAL REGENERATIVE EFFECT

QMR® technology emits packets of energy quanta capable of altering ion concentrations in the intracellular/extracellular matrix (biochemical effect), leading to significant changes in the transmembrane potential of the target cells. [2] These changes trigger metabolic pathways that **stimulate MSCs (Mesenchymal Stromal Cells).** Subsequently, MSCs differentiate into the required cell types.
Due to the properties of stem cells, **the regenerated biological tissue** possesses the same characteristics and functionality as the original tissue.

BIOLOGICAL SAFETY

QMR® Technology is proven to be biologically safe. Rigorous studies on chromosomes, apoptosis, and proteins have affirmed its biological safety, assuring **the absence of cellular damage in patients.** [2]

1. Paolucci et al., Antioxidants, 2023
2. Dal Maschio et al., BAM, 2009
3. Sella et al., PloS ONE, 2018
4. Prof. C. Reggiani, 2005

5 STEPS OF QMR REGENERATIVE PROCESS

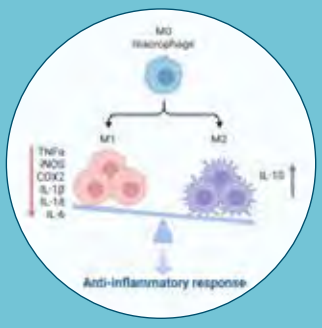

1

ANTI-INFLAMMATORY PROCESS

QMR reduces local inflammation by polarizing M1 macrophages towards M2 macrophages (the anti-inflammatory ones)

2

RESONANCE EFFECT

The energy package of QMR is capable of changing intra and extracellular ions, altering the transmembrane potential of stem cells and macrophages.

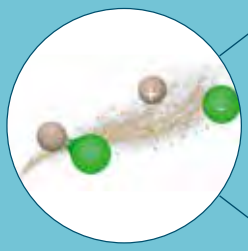

Phase 1
Breaks bonds without heat thanks to the resonance effects

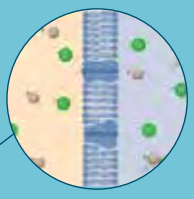

Phase 2
Modification of ions concentration in the intracellular/ extracellular matrix of the cells

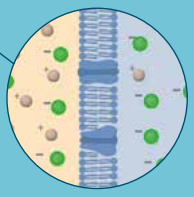

Phase 3
Generate significant changes in transmembrane potential of the target cells

3

STEM CELLS REPLICATION

The change in the transmembrane potential of the stem cells induces their replication. The stem cell regenerates asymmetrically, creating two stem cells named mother and daughter.

4

REGENERATIVE PROCESS

Through the immune system, the daughter goes to regenerate tissue of non-functional ocular structures.

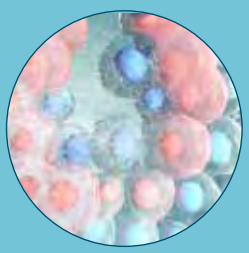

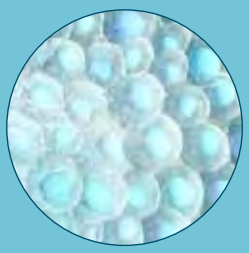

5

NATURAL REGENERATION COMPLETED

The regenerated tissue has the same functional characteristics as the tissue before the damage.

REXONEYE

QMR BIOLOGICAL SAFETY

Scientific Evidence In Vitro

Tested Cell Lines:

- Human fibroblasts MRC-5 (differentiated cells) [2]
- Mesenchymal stem cells (MSC) [1]
- Adipocytes, osteocytes, chondrocytes (differentiated cells) [2]
- Astrocytoma cells (tumor cells) [1]
- Glioblastoma cell lines [1]
- Endometrial adenocarcinoma cells [3]

Analyzed Parameters:

- Cell morphology
- Viability and mortality
- Cell proliferation rate
- Differentiation potential
- Cell cycle
- Apoptosis
- Karyotype
- Genomics and proteomics

Key Results:

- No karyotype variations. In vitro analyses confirmed the absence of associated genotoxic effects [2,4].
- No alterations in morphology, viability, cell cycle, or proliferation in treated cells [2,3,4].
- QMR treatment does not induce apoptosis or alter the differentiation of mesenchymal stem cells [2,4].
- In glioblastoma tumor cells cultured in vitro, QMR showed a cytostatic effect and enhancement of the effectiveness of chemotherapeutic treatment (e.g., temozolomide in glioblastomas), and reduced cell migration in more aggressive cell types [1].

[1] Selective cell cycle arrest in glioblastoma cell lines by quantum molecular resonance alone or in combination with temozolomide D. Catanzaro et al

[2] In-vitro analysis of Quantum Molecular Resonance effects on human mesenchymal stromal cells. S.Sella et al.

[3] In Vitro Gene Expression Profiling of Quantum Molecular Resonance Effects on Human Endometrium Models: A Preliminary Study A. Grassi et al.

[4] EFFECTS OF MOLECULAR QUANTUM RESONANCE IMAGING ON CULTURED HUMAN CELLS: SAFETY AND EFFICACY OF TREATMENT S. Sella

01

Efficacy of Quantum Molecular Resonance in Neuropathic Corneal Pain and Corneal Nerve Regeneration

Associate Professor Yu-Chi Liu, MD, MCI, PhD

Efficacy of Quantum Molecular Resonance in Neuropathic Corneal Pain and Corneal Nerve Regeneration

Associate Professor Yu-Chi Liu, MD, MCI, PhD

Department of Cornea and External Eye Disease, Singapore National Eye Centre, Singapore.
Singapore Eye Research Institute, Singapore.
Ophthalmology and Visual Sciences Academic Clinical Program, Duke-NUS Medical School, Singapore

[Preliminary Report and Unpublished Data]

Background

Neuropathic corneal pain (NCP) is an emerging condition resulting from dysfunctional corneal nerves and the diagnosis rate steadily increases yearly. Patients with NCP often experience burning, aching, shooting, or stabbing pain without corresponding clinical signs, and the symptoms are typically unresponsive to conventional dry eye treatments. The effects of NCP can range from mild discomfort impacting daily activities to severe symptoms that significantly impair physical and social well-being.
NCP is associated with various conditions, including dry eye disease, diabetic corneal neuropathy, herpes simplex keratitis, ocular trauma or surgeries. Psychological conditions like depression and anxiety, and chronic pain states such as fibromyalgia and trigeminal neuralgia also predispose to NCP. The pain management of NCP is challenging due to its multifaceted pathophysiology, often requiring a combination of treatment modalities. However, many patients have persistent pain despite multiple approaches, incurring huge indirect and direct economic costs.

Patients with NCP typically show impairment on sub-basal corneal nerves, which can be assessed using in vivo confocal microscopy (IVCM). Evidence has shown significant reduced corneal nerve fiber length, nerve fiber density, and nerve fiber fractal dimension, as well as increased corneal nerve fiber width in NCP patients compared with healthy individuals.

Furthermore, recent studies have indicated that electrotherapy can effectively reduce ocular pain intensity and promote nerve regeneration by delivering targeted electrical stimulation to affected nerves. We therefore hypothesize that QMR, as a form of electrotherapy, may potentially relieve pain symptoms and promote nerve regeneration in patients with NCP.

Aims

We aim to evaluate the efficacy of QMR in alleviating ocular pain symptoms of NCP, and to assess the potential impact of QMR on stimulating corneal nerve regeneration.

Methods

Our study has recruited 19 patients diagnosed with NCP. QMR treatment followed the protocol as recommended by Resono Ophthalmic. The Rexon-Eye device delivers stimulation to the epidermis of the closed eyelids, extending up to the lid border with an intensity setting of 4-5 on a scale of 0-10. All patients underwent 8 treatment sessions, with 1 session per week, each lasting 30 minutes. At each study

visit, we conducted standardized questionnaires including the Visual Analogue Scale (VAS) and the Ocular Pain Assessment Survey (OPAS) to evaluate eye pain intensity. At baseline, treatment visit 4 and 8, we conducted IVCM scanning to detect the changes of corneal nerves. At the end of treatment, we conducted acceptability and satisfaction questionnaire and end of treatment questionnaire.

Preliminary results

QMR treatment alleviates neuropathic corneal pain

The VAS scores showed a continuous decreasing trend throughout the QMR treatment process, with a statistically significant reduction observed after 4-week treatment (Figure 1 and Table 1).

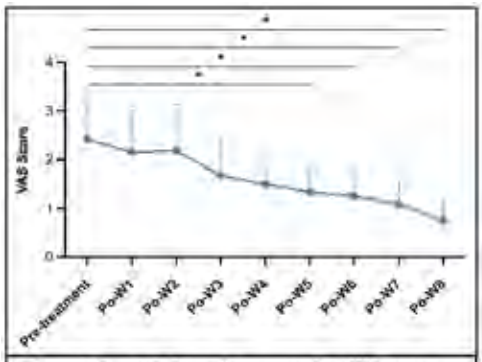

Figure 1. Eye pain intensity assessed by VAS scores.

Table 1. Change of the Visual Analogue Scale scores.

	VAS Score	*P* value
Pre-treatment	2.32 ± 3.20	-
Post-week 1	2.15 ± 3.08	0.339
Post-week 2	2.18 ± 3.19	0.586
Post-week 3	1.67 ± 2.57	0.056
Post-week 4	1.50 ± 2.69	0.128
Post-week 5	1.33 ± 1.97	**0.030**
Post-week 6	1.25 ± 1.86	**0.036**
Post-week 7	1.08 ± 1.73	**0.028**
Post-week 8	0.75 ± 1.42	**0.021**

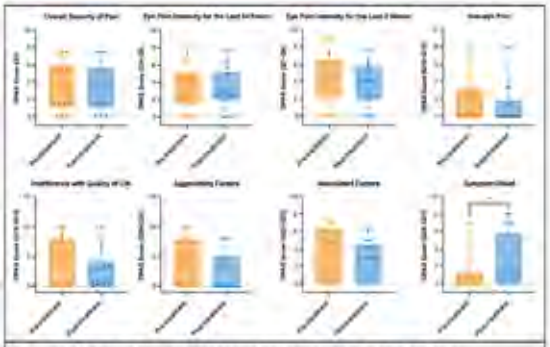

Figure 2. Eye pain characteristics assessed by OPAS scores.

Table 2. Comparison of OPAS scores pre- and post-QMR treatment.

OPAS Score (0–10)	Pre-treatment	Post-treatment	*P*
Overall severity of pain (Q1)	3.46 ± 2.94	3.32 ± 2.55	0.833
Eye pain intensity for the last 24 h (Q4-Q6)	3.55 ± 2.61	3.29 ± 2.25	0.443
Eye pain intensity for the last 2 weeks (Q7-Q9)	4.31 ± 2.68	3.74 ± 2.31	0.213
Non-eye pain (Q10-Q12)	1.40 ± 2.48	1.14 ± 2.32	0.753
Interference with quality of life (Q13-Q19)	4.47 ± 3.58	2.93 ± 3.00	0.126
Aggravating factors (Q20-Q21)	4.42 ± 3.73	2.54 ± 3.15	0.138
Associated factors (Q22-Q25)	3.57 ± 2.99	2.52 ± 2.11	0.247
Symptom relief (Q26-Q27)	1.50 ± 2.83	3.25 ± 3.45	**0.041**

Among various dimensions from the OPAS, a significant symptom relief was identified (Figure 2 and Table 2). Additionally, we observed a notable reduced interference on general activity, less pain exposed to volatile chemicals, and reduced eye pain accompanied by redness following QMR treatment (Figure 3).

QMR treatment potentially promotes corneal nerve regeneration

IVCM showed significant improvements in corneal nerve metrics including corneal nerve fiber density (CNFD), corneal nerve fiber length (CNFL), and corneal nerve total branch density (CTBD) following QMR treatment compared to baseline (Figure 4 and Table 3). Moreover, for the NCP patients who have undergone refractive surgeries, significant increases were observed in both CNFD (6.60±3.85/mm^2 vs. 3.27±2.34/mm^2) and CTBD (8.00±2.61/mm^2 vs. 4.15±1.27/mm^2; both P<0.05) following QMR treatment compared to baseline.

Table 3. Comparison of corneal nerve parameters pre- and post-QMR treatment.

Parameters	Pre-treatment	Post-treatment	*P* value
CNFD (/mm²)	7.54 ± 4.86	10.23 ± 5.48	**0.046**
CNBD (/mm²)	5.47 ± 6.19	9.15 ± 9.62	0.052
CNFL (mm/mm²)	5.63 ± 2.34	6.81 ± 3.14	**0.029**
CTBD (/mm²)	10.80 ± 8.38	15.49 ± 12.27	**0.037**
CNFA (mm²/mm²)	0.0028 ± 0.0009	0.0031 ± 0.0014	0.161
CNFW (mm/mm²)	0.0213 ± 0.0016	0.0214 ± 0.0010	0.880
CFractDim	1.33 ± 0.07	1.35 ± 0.06	0.058

CLEAR = corneal lenticule extraction for advanced refractive correction; SMILE = small incision lenticule extraction; CNFD = corneal nerve fiber density; CNBD = corneal nerve branch density; CNFL = corneal nerve fiber length; CTBD = corneal total branch density; CNFA = corneal nerve fiber area; CNFW = corneal nerve fiber width; CFracDim = corneal nerve fiber fractal dimension.

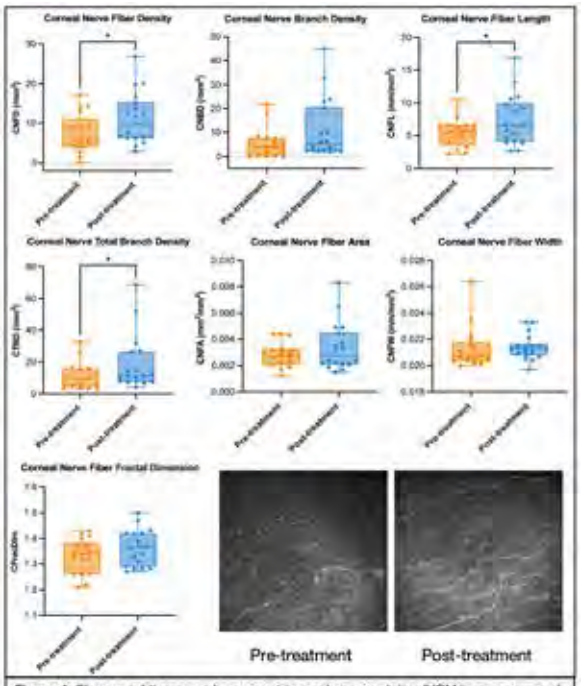

Figure 4. Changes of the corneal nerve metrics and representative IVCM images pre- and post-QMR treatment.

Patient feedback and satisfaction of QMR treatment

Over 60% of patients reported an overall improvement in their eye condition following QMR treatment compared with pre-treatment period. The majority of patients judged the treatment as pleasant (80%), effective (53.3%), durable (66.7%), comfortable (73.3%), convenient (60.0%), and satisfied (66.7%).

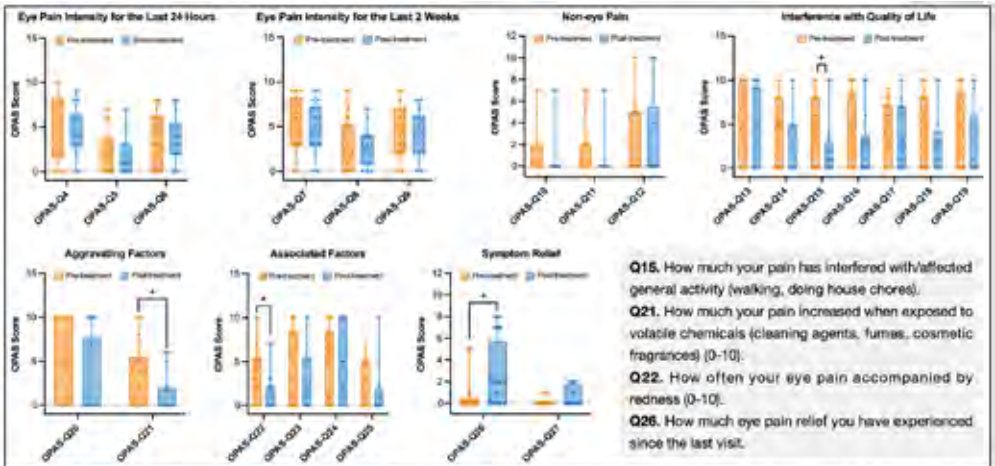

Figure 3. Individual item analysis of the OPAS showed significant improvement in Q15, Q21, Q22, and Q26 following QMR treatment compared to pre-treatment levels.

Table 4. Results of the End of Treatment questionnaire.

EoT Questions	Number	Percentage (%)
Q1. The situation compared to before treatment is now		
Better	**10**	**66.7**
Same	5	33.3
Worse	0	0.0
Q2. The situation compared to end of treatment is now		
Better	**9**	**60.0**
Same	6	40.0
Worse	0	0.0
Q3. The situation compared to 1 month after end of treatment is now		
Better	**9**	**60.0**
Same	6	40.0
Worse	0	0.0
Q4. During last week I experienced these eye symptoms		
Dryness	**15**	**100.0**
Pain	8	53.3
Burning	5	33.3
Sand	6	40.0
Photophobia	6	40.0
Q5. During last week I used tear substitutes during the day		
Yes	15	100.0
No	0	0.0
Q6. During last week I used tear substitutes during the evening/night		
Yes	15	100.0
No	0	0.0
Q7. In the last 2 months I had eye problems other than dry eye		
Yes	0	0.0
No	15	100.0
Q8. In the last 2 months I used tear substitutes		
Yes	**15**	**100.0**
No	0	0.0
Q9. In the last 2 months I tried to suspend using tear substitutes		
Yes, and it worked	0	0.0
Yes, but it did not work and I resumed using tear substitutes	3	20.0
No	12	80.0
Q10. Compared to before treatment my eyes now produce more tears		
Yes	3	20.0
No	5	33.3
Don't know	7	46.7
Q11. Compared to before treatment my eyes now are more wet (tears are more effective)		
Yes	4	26.7
No	4	26.7
Don't know	7	46.7
Q12. Compared to before treatment my eyes now feel better		
Yes	10	66.7
No	4	26.7
Don't know	1	6.7
Q13. Compared to before treatment I have reduced the use of tear substitutes		
Yes	2	13.3
No	**11**	**73.3**
Don't know	2	13.3
Q14. Overall, I judge the treatment as pleasant		
Yes	**12**	**80.0**
No	1	6.7
Neutral	2	13.3
Q15. Overall, I judge the treatment as effective		
Yes	**8**	**53.3**
No	4	26.7
Neutral	3	20.0
Q16. Overall, I judge the treatment as durable		
Yes	**10**	**66.7**
No	3	20.0
Neutral	2	13.3
Q17. Overall, I judge the treatment, with respect to other treatments I tried		
Better	**10**	**66.7**
Same	5	33.3
Worse	0	0.0

Table 5. Results of the acceptability and satisfaction questionnaire.

Acceptability and Satisfaction Questions	Mean score	Number	Percentage (%)
Q1. Do you feel your eyes are comfortable after the treatment? (0-3)	1.80±0.77	-	-
0: Very uncomfortable	-	1	6.7
1: Slightly uncomfortable	-	3	20.0
2: Slightly comfortable	-	**9**	**60.0**
3: Very comfortable	-	**2**	**13.3**
Q2. Is it convenient if you have to do this once a week for 4 times? (0-3)	1.67±0.82	-	-
0: Not convenient	-	1	6.7
1: Slightly inconvenient	-	5	33.3
2: Slightly convenient	-	**7**	**46.7**
3: Very convenient	-	**2**	**13.3**
Q3. Would you recommend this to someone else who has similar dry eyes? (0-3)	2.00±1.00	-	-
0: No	-	2	13.3
1: Perhaps	-	1	6.7
2: Yes, will recommend	-	**7**	**46.7**
3: Yes, strongly recommend	-	**5**	**33.3**
Q4. Overall, how satisfied are you with the treatment? (0-3)	1.73±0.96	-	-
0: Not satisfied at all	-	2	13.3
1: Neutral	-	3	20.0
2: Quite satisfied	-	**7**	**46.7**
3: Very satisfied	-	**3**	**20.0**

Conclusions

Based on our preliminary data, QMR treatment is effective in alleviating neuropathic eye pain, and reducing the interference on general activities in NCP patients. QMR treatment potentially promotes corneal nerve regeneration. The treatment is well-tolerated without adverse events reported during the study period. Larger-scale clinical trials with longer follow up are ongoing.

02

Randomized, double-masked, sham-controlled trial of efficacy and safety of quantum molecular resonance for treating meibomian gland dysfunction

L. Uthaithammarat, N. Kasetsuwan, U. Reinprayoon, Y. Chongpison, W. Quanchareonsap , P. Dissaneevate

The ROYAL COLLEGE of OPHTHALMOLOGISTS

www.nature.com/eye

ARTICLE OPEN

Check for updates

Randomized, double-masked, sham-controlled trial of efficacy and safety of quantum molecular resonance for treating meibomian gland dysfunction

Lita Uthaithammarat[1], Ngamjit Kasetsuwan[1,2]✉, Usanee Reinprayoon[1,2], Yuda Chongpison[3], Wiyada Quanchareonsap[1] and Paphaphat Dissaneevate[4]

© The Author(s) 2025

BACKGROUND: This randomized, double-blind, sham-controlled trial aimed to evaluate the novel quantum molecular resonance (QMR) device for meibomian gland dysfunction (MGD) treatment.
METHODS: Eighty participants diagnosed with MGD were randomized into QMR or sham-QMR groups. Each procedure was performed on days 0, 7, 14, and 21. Primary (meibum quality score) and other secondary outcomes were examined at baseline and weeks 7 and 11. Tear osmolarity and interleukin (IL)-6 and IL-1 receptor agonist levels were evaluated at baseline and week 7. Adverse events were recorded. A multilevel mixed-effect linear regression model was used for data analysis.
RESULTS: Meibum quality ($p = 0.008$), corneal/conjunctival fluorescein staining score ($p = 0.036$), telangiectatic vessel area ($p = 0.008$), and superior ($p = 0.011$) and inferior ($p = 0.020$) lid meiboscale were significantly improved in the QMR group than those in the sham-treated group at week 11. Superior lid meiboscale ($p = 0.027$) and meibomian gland plugging grade (MGPG) ($p = 0.017$) were significantly improved in the QMR group at week 7. In the QMR group, Ocular Surface Disease Index (OSDI) scores and lid margin thickening grades were significantly lesser at weeks 7 ($p = 0.002$ and <0.001, respectively) and 11 (both $p < 0.001$) than the baseline values. At week 7, IL-6 levels were significantly decreased only in the QMR group ($p = 0.016$). All other parameters did not significantly differ. No serious adverse event occurred.
CONCLUSIONS: The QMR device was effective for MGD treatment, with improvements in meibum quality, corneal/conjunctival staining, telangiectatic vessels, MGPG, superior and inferior lid meiboscale, and decreased OSDI score, lid margin thickening grade, and tear IL-6 level.

Eye; https://doi.org/10.1038/s41433-025-03890-3

INTRODUCTION

Meibum is an essential component of the tear film, protecting it from hyperevaporation. Meibomian gland dysfunction (MGD), a chronic abnormality of lipid secretion from meibomian glands in the upper and lower eyelids, is characterized by duct obstruction or qualitative/quantitative changes in meibum secretion. Abnormal meibum secretion may lead to evaporative dry eye disease, which is the most common type of dry eye [1]. Patients' symptoms vary from no symptoms to ocular discomfort, redness, itching, or photophobia. If these conditions are left untreated, inflammation can occur and damage the ocular surface.

Currently, a gold-standard MGD treatment has not been established; however, recommendations include warm compressions and lid massages to liquefy the meibum, reopen the obstructed gland, and remove the meibum. Moreover, anti-inflammatory agents are used to decrease inflammation and improve meibum quality [2]. In addition, various novel device-based treatments are available. A quantum molecular resonance (QMR)-based device was recently suggested as an effective treatment for MGD and dry eye disease [3–7]. QMR is a physical effect that occurs when tissues are stimulated with weak alternating electric current patterns at 4–64 MHz. This randomized sham-controlled trial aimed to ascertain the efficacy, safety, and mechanisms of MGD treatment using this QMR device.

METHODS

This study was approved by the Institutional Review Board of the Faculty of Medicine, Chulalongkorn University, Thailand, and adhered to the tenets of the Declaration of Helsinki. This trial was registered at ClinicalTrials.gov (NCT05165342). Written informed consent was obtained from all participants. Additionally, written informed consent for the publication of identifiable patient photographs (Supplementary Fig. 1B) was obtained from the patient prior to publication.

Participants diagnosed with MGD according to the "International Workshop on Meibomian Gland Dysfunction: Report of Subcommittee on Management and Treatment of Meibomian Gland Dysfunction" [2] at the outpatient clinic, Department of Ophthalmology, King Chulalongkorn Memorial Hospital, Thailand, were recruited between December 10, 2021,

[1]Department of Ophthalmology, Faculty of Medicine, Chulalongkorn University and King Chulalongkorn Memorial Hospital, Bangkok, Thailand. [2]Center of Excellence for Cornea and Stem Cell Transplantation, Department of Ophthalmology, Faculty of Medicine, Chulalongkorn University, Bangkok, Thailand. [3]Center of Excellence in Biostatistics, Research Affairs, Faculty of Medicine, Chulalongkorn University, Bangkok, Thailand. [4]Faculty of Medicine, Chulalongkorn University, Bangkok, Thailand. ✉email: ngamjitk@gmail.com

Received: 5 June 2024 Revised: 19 May 2025 Accepted: 12 June 2025
Published online: 27 June 2025

SPRINGER NATURE

and April 30, 2022. The inclusion criteria were (1) age 18–80 years, (2) ability and willingness to comply with the treatment/follow-up schedule, and (3) stage 1–4 MGD diagnosis in one or both eyes. Exclusion criteria are presented in Supplementary Data.

The sample size was calculated using the meibum quality score as the primary outcome with 80% power ($\beta = 0.2$). Eleven participants were required for each of the QMR and sham-QMR groups to detect a clinically significant difference in five scores between these groups. With a two-sided statistical significance level of 5% ($\alpha = 0.05$), the mean meibum quality score and pooled standard deviation (SD) were calculated as 13.8 and 4.10 [4, 8].

Experimental design

This was a prospective, randomized, double-blind, sham-controlled clinical trial. In the randomization step, a treatment sequence was randomly permuted in blocks of six and eight, with block sizes allocated unequally in a ratio of 1:4:6:4:1 (Pascal's triangle) for the first 34 participants. Subsequently, minimization [9] was used to assign participants to the sham-QMR or QMR group according to sex, age (≤60 or >60 years), and MGD stage (1/2 or 3/4). The unit of randomization/minimization was the individual participant. The sequences were placed in an opaque, sealed envelope and stored by a researcher (W.Q.). All investigators and participants were blinded to the treatment assignments for the duration of their involvement. Upon study completion, a research assistant unmasked the randomization sequence and forwarded the results to the study team for data analysis. A single evaluator (L.U.) examined patients throughout the study.

Treatment

This study used the QMR Rexon-Eye device (Resono Ophthalmic, Trieste, Italy). All participants underwent either QMR or sham-QMR treatment performed by a single research assistant on days 0, 7, 14, and 21. The QMR treatment protocol was recommended by the company that developed the Rexon-Eye device. The treatment was administered using goggles for 20 min per visit and applied to the closed upper and lower eyelids. The intensity was set at 5 (custom units), corresponding to an average power of 12 W, with 60 V voltage and 200 mA current between the goggle electrode and the neutral electrode attached to the participant's chair (Supplementary Fig. 1). The sham-QMR group received the same treatment except that the power was set to zero. During the procedure, sound was perceived the same in the QMR and sham-QMR groups. All participants were required to use only preservative-free artificial tears (0.18% sodium hyaluronate) at least four times daily, together with lid hygiene (lid scrub and warm compression) twice daily. Their compliance was checked by a research assistant.

Clinical assessment

For each participant, the eye with the higher MGD stage was evaluated. Primary (meibum quality score) and secondary (Ocular Surface Disease Index [OSDI] score, tear meniscus height [TMH, mm], noninvasive tear break-up time [NITBUT, s], bulbar conjunctival hyperemia [grade], tear film lipid layer thickness [TFLLT, nm], corneal and conjunctival fluorescein staining score, Schirmer's test [mm], area of lid telangiectasia [pixel], lid margin thickening and irregularity grade, meibomian gland plugging grade [MGPG], superior and inferior lid meiboscale, and meibum expressibility grade) outcomes were examined at baseline, 7-week (1 month after the last treatment), and 11-week (2 months after the last treatment) visits. Tear osmolarity (mOsm/L) and interleukin (IL)-1 receptor agonist (IL-1Ra) and IL-6 levels (pg/mL) were evaluated at baseline and 7-week visits. Best-corrected visual acuity (BCVA), uncorrected visual acuity (UCVA), and intraocular pressure (IOP, mmHg) were recorded on days 0, 7, 14, and 21, week 7, and week 11. The sequence and details of the clinical assessment are provided in Supplementary Data.

Statistical analysis

Demographics and baseline clinical characteristics are reported as mean with SD, median with first and third quartiles, or frequency with percentage. Linear mixed model regression with an adjusted baseline was used to analyze all parameters over time. The results are presented as estimated means and 95% confidence intervals (CIs). To determine whether each outcome measure in the two groups changed differently over time, a time–treatment group interaction term was included if $p_{\text{interaction}}$ was <0.2. To control for type 1 errors, Scheffé's method was used as a post hoc test for multiple comparisons. The baseline cytokine concentration was described as a geometric mean with a percent coefficient of variation (%CV). Normal distribution was assessed with a histogram and the Shapiro–Wilk test after logarithmic transformation. Linear mixed model regression with adjusted log-transformed baseline cytokine value was used to evaluate differences in logarithmic mean values of cytokine concentrations. Intention-to-treat analyses of efficacy outcomes were conducted. For all analyses, statistical significance was set at an alpha level of 0.05. Stata version 15.1 was used (StataCorp, College Station, TX).

RESULTS

Of 80 eligible participants, seven were lost to follow-up (Supplementary Fig. 2). The baseline characteristics and clinical and laboratory parameters of the QMR and sham-QMR groups are shown in Supplementary Table 1. All estimated outcomes calculated from linear mixed models are shown in Table 1, Figs. 1 and 2.

Primary outcome: meibum quality

The meibum quality score was significantly lower in the QMR group than that in the sham-QMR group at 11 weeks ($p = 0.008$). In the QMR group, the 7-week score was significantly lower than that at baseline ($p = 0.034$). All other pairwise comparisons showed no significant group differences.

Secondary outcomes

All secondary outcomes were presented in Table 1, Figs. 1 and 2. The area of lid telangiectasia and tear cytokine levels are presented in Supplementary Fig. 3 and Fig. 3, respectively.

Safety profile

BCVA, UCVA, and IOP. Pairwise comparisons of these parameters at each time point were not significantly different (Supplementary Table 2), and the ocular examinations of all participants were normal throughout.

Adverse events. After the first QMR treatment, three participants of the QMR group experienced mild upper eyelid redness, which resolved without treatment within 3 days. The reason was that the goggles were too tight, and no further complaints were reported.

Temperature of the upper eyelid skin. The mean temperatures at baseline and on days 7, 14, and 21 are presented in Supplementary Table 3. The estimated mean difference between the temperatures before and after treatment was significantly higher in the QMR than in the sham-QMR group on days 0, 7, 14, and 21 (all $p < 0.001$; Table 2).

DISCUSSION

This is the first prospective, randomized, double-blind, sham-controlled trial comparing QMR with sham-QMR treatment for MGD. We found that QMR treatment significantly improved MGD-related signs compared to the sham-QMR group, including meibum quality, corneal and conjunctival staining, lid margin telangiectasia, MGPG, and lid meiboscale. In the QMR group, OSDI scores, lid margin thickening grades, and tear IL-6 levels were significantly improved after treatment compared to the baseline values.

Electrical stimulation with low-intensity currents has demonstrated successful outcomes in tissue regeneration [10–13]. The meibomian glands' regenerative potential has been previously reported using topical diquafosol [14], intraductal meibomian gland probing [15], and lid hygiene [16]. This suggests that QMR can induce their regeneration. The QMR's specific current pattern

Table 1. All clinical estimated mean outcomes at baseline, 1 month after the last treatment (week 7), and 2 months after the last treatment (week 11).

Outcome (95% confidence interval)	Group	Baseline	1 month after the last treatment	1 month vs baseline	QMR vs Sham (1 month)	2 months after the last treatment	2 months vs baseline	QMR vs Sham (2 months)
OSDI score (0–100)	QMR	27.01; [24.00, 30.02]	19.34; [16.24, 22.45]	$P = 0.002$*	$P = 0.161$	17.84; [14.83, 20.86]	$P < 0.001$*	$P = 0.999$
	Sham-QMR	27.80; [24.79, 30.82]	20.13; [16.99, 23.27]	$P = 0.002$*		18.63; [15.61, 21.67]	$P < 0.001$*	
TMH (mm)	QMR	0.24; [−0.001, 0.47]	0.27; [0.03, 0.51]	$P = 1.000$	$P = 0.979$	0.43; [0.19, 0.66]	$P = 0.893$	$P = 0.979$
	Sham-QMR	0.12; [−0.11, 0.37]	0.16; [−0.09, 0.41]	$P = 1.000$		0.32; [0.08, 0.56]	$P = 0.893$	
NITBUT (s)	QMR	9.24; [8.11, 10.37]	9.01; [7.85, 10.17]	$P = 1.000$	$P = 1.000$	10.00; [8.87, 11.14]	$P = 0.944$	$P = 1.000$
	Sham-QMR	9.06; [7.93, 10.20]	8.83; [7.65, 10.02]	$P = 1.000$		9.83; [8.68, 10.97]	$P = 0.944$	
Bulbar conjunctival hyperemia (JENVIS scale, 0–4)	QMR	1.25; [1.06, 1.45]	1.43; [1.23, 1.64]	$P = 0.847$	$P = 0.940$	1.23; [1.03, 1.43]	$P = 1.000$	$P = 0.940$
	Sham-QMR	1.37; [1.17, 1.57]	1.55; [1.34, 1.76]	$P = 0.847$		1.35; [1.15, 1.55]	$P = 1.000$	
Tear film lipid layer thickness (nm)	QMR	54.86; [49.40, 60.32]	56.92; [51.33, 62.51]	$P = 0.996$	$P = 1.000$	53.01; [47.54, 58.48]	$P = 0.997$	$P = 1.000$
	Sham-QMR	55.31; [49.84, 60.77]	57.36; [51.67, 63.07]	$P = 0.996$		53.45; [47.95, 58.96]	$P = 0.997$	
Tear osmolarity (mOsm/L)	QMR	297.70; [294.40, 300.99]	302.15; [298.76, 305.54]	$P = 0.169$	$P = 0.998$	-	-	-
	Sham-QMR	298.09; [294.82, 301.35]	302.54; [299.05, 306.03]	$P = 0.169$		-	-	
Sodium fluorescein staining score (0–15)	QMR	2.12; [1.79, 2.44]	1.42; [1.09, 1.75]	$P = 0.114$	$P = 0.610$	1.24; [0.92, 1.57]	$P = 0.013$*	$P = 0.036$*
	Sham-QMR	1.85; [1.52, 2.18]	1.89; [1.54, 2.24]	$P = 1.000$		2.06; [1.73, 2.39]	$P = 0.975$	
Schirmer's test (mm)	QMR	14.55; [12.39, 16.71]	14.54; [12.33, 16.77]	$P = 1.000$	$P = 0.999$	15.25; [13.09, 17.41]	$P = 0.999$	$P = 0.545$
	Sham-QMR	16.47; [14.30, 18.63]	13.77; [11.46, 16.08]	$P = 0.686$		12.07; [9.88, 14.26]	$P = 0.121$	
Telangiectatic vessel (pixel)	QMR	30,732.69; [28,188.34, 33,277.04]	29,755.25; [27,177.81, 32,332.70]	$P = 0.997$	$P = 0.297$	26,259.85; [23,646.30, 28,873.40]	$P = 0.231$	$P = 0.008$*
	Sham-QMR	28,600.29; [26,082.36, 31,118.22]	34,406.38; [31,793.07, 37,019.69]	$P = 0.039$*		33,839.81; [31,155.88, 36,523.75]	$P = 0.102$	
Lid margin thickening grade (0–2)	QMR	1.23; [1.10, 1.35]	0.75; [0.63, 0.88]	$P < 0.001$*	$P = 0.070$	0.76; [0.64, 0.89]	$P < 0.001$*	$P = 0.885$
	Sham-QMR	1.23; [1.10, 1.35]	1.06; [0.92, 1.19]	$P = 0.602$		0.89; [0.76, 1.01]	$P = 0.009$*	
Lid margin irregularity grade (0–2)	QMR	1.04; [0.88, 1.20]	1.06; [0.90, 1.22]	$P = 1.000$	$P = 0.769$	0.98; [0.82, 1.14]	$P = 0.997$	$P = 0.769$
	Sham-QMR	1.18; [1.02, 1.34]	1.20; [1.03, 1.37]	$P = 1.000$		1.12; [0.96, 1.28]	$P = 0.997$	
MG plugging grade (0–3)	QMR	2.40; [2.14, 2.66]	1.72; [1.45, 1.98]	$P = 0.009$	$P = 0.017$*	1.71; [1.45, 1.97]	$P = 0.007$	$P = 0.054$
	Sham-QMR	2.36; [2.10, 2.62]	2.44; [2.16, 2.71]	$P = 0.999$		2.33; [2.07, 2.59]	$P = 1.000$	
Superior lid meiboscale (0–4)	QMR	1.78; [1.69, 1.88]	1.65; [1.55, 1.75]	$P = 0.454$	$P = 0.027$*	1.66; [1.56, 1.75]	$P = 0.475$	$P = 0.011$*
	Sham-QMR	1.80; [1.70, 1.90]	1.91; [1.81, 2.02]	$P = 0.653$		1.93; [1.83, 2.03]	$P = 0.460$	
Inferior lid meiboscale (0–4)	QMR	1.23; [1.17, 1.28]	1.20; [1.15, 1.25]	$P = 0.987$	$P = 0.658$	1.18; [1.12, 1.23]	$P = 0.772$	$P = 0.020$*
	Sham-QMR	1.24; [1.19, 1.29]	1.27; [1.22, 1.33]	$P = 0.957$		1.31; [1.26, 1.37]	$P = 0.323$	

Table 1. continued

Outcome (95% confidence interval)	Group	Baseline	1 month after the last treatment	1 month vs baseline	QMR vs Sham (1 month)	2 months after the last treatment	2 months vs baseline	QMR vs Sham (2 months)
Meibum quality score (0–24)	QMR	16.16; [15.15, 17.17]	13.79; [12.75, 14.82]	$P = 0.034$*	$P = 0.193$	14.16; [13.15, 15.17]	$P = 0.116$	$P = 0.008$*
	Sham-QMR	16.30; [15.28, 17.30]	15.86; [14.78, 16.94]	$P = 0.996$		17.06; [16.03, 18.08]	$P = 0.939$	
Meibum expressibility grade (0–3)	QMR	0.79; [0.51, 1.08]	0.62; [0.33, 0.91]	$P = 0.970$	$P = 0.761$	0.40; [0.11, 0.68]	P = 0.411	$P = 0.761$
	Sham-QMR	1.03; [0.75, 1.31]	0.85; [0.56, 1.15]	$P = 0.970$		0.63; [0.35, 0.92]	$P = 0.411$	
Tear Cytokine (log-pg/ml)								
IL-6 level	QMR	3.23; [2.95, 3.52]	2.73; [2.44, 3.02]	$P = 0.016$	$P = 0.146$	-	-	-
	Sham-QMR	3.10; [2.82, 3.38]	3.05; [2.74, 3.35]	$P = 0.806$		-	-	
IL-1Ra level	QMR	12.45; [12.20, 12.70]	12.33; [12.06, 12.59]	$P = 0.498$	$P = 0.106$	-	-	-
	Sham-QMR	12.39; [12.14, 12.64]	12.64; [12.06, 12.59]	$P = 0.194$		-	-	

IL interleukin, *NITBUT* noninvasive tear break-up time, OSDI Ocular Surface Disease Index, *TMH* tear meniscus height
* $P < 0.05$

differs from that of other transcutaneous electrical stimulation (TES) approaches [17, 18]. This study showed that meibomian gland function and structure significantly improved after QMR treatment. Improvement in corneal staining indicates a decrease in ocular surface inflammation, showing reversibility of corneal epithelium damage [19]. Improvements in meiboscale, meibum quality, and meibomian gland plugging, which is positively correlated with meibomian gland dropout [20], suggested the reversibility of meibomian gland damage. These findings are consistent with the theory that electrical stimulation facilitates tissue regeneration.

Additionally, QMR alleviates inflammation as demonstrated by decreased matrix metalloproteinase (MMP)-9 levels [3] and leukocyte infiltration in tissues [10] reported by other studies and reductions in IL-6 levels with a trend toward decreasing IL1-Ra levels according to our study.

The meibomian gland is not only regulated by hormones but is also influenced by nerve stimulation, with nerve density playing a crucial role in its function [21]. The alternating current patterns of QMR may stimulate nerves innervating meibomian glands, potentially leading to nerve and subsequent glandular regeneration.

A study examining QMR effects on human mesenchymal stromal cells revealed its impact on transcriptional regulation by modulating genes associated with developmental processes and cellular pathways, including metabolism, kinase activity, and cellular regulation. Real-time polymerase chain reaction showed significantly increased *MMP1*, *PLAT*, and *ARHGAP22* expression after QMR treatment, whereas *A2M* expression was significantly decreased [22]. These genes are involved in extracellular matrix remodeling, angiogenesis, embryogenesis, inflammation reduction, and wound healing promotion. The impact at transcriptional and cellular levels may decrease inflammatory cytokine levels, e.g., IL1-Ra and IL-6 levels, and improve ocular surface staining, as indicated by our results. A previous study showed a strong association between ocular surface staining and ocular surface inflammation [23]. The QMR effects on transcriptional regulation suggest that its effectiveness may persist for an extended period after treatment.

The meibum quality score was significantly lower in the QMR group at 11 weeks than that in the sham-QMR group and at 7 weeks than the baseline values. At week 7, MGPG was much lower in the QMR group than MGPG in the sham-QMR group. Moreover, MGPG in the QMR group was significantly improved at week 7 than the baseline values. This aligns with the findings of previous studies [3, 4]. Additionally, the superior and inferior lid meiboscales were significantly improved in the QMR group. Likewise, Kavroulaki et al. [6] reported such improvements 2 months after the last treatment; this effect persisted for at least 2 months after treatment in our study. In contrast, Trivli et al. found no change in meiboscale results [3].

Interestingly, meibum expressibility reflecting meibum secretion [24] did not improve in our study. Meibum lipids contribute to tear film stability and protect tears from hyperevaporation [24]. Accordingly, NITBUT, reflecting tear film stability, and TFLLT, reflecting the amount of lipids in the tear film, did not improve after treatment in our study. This aligns with the findings of Foo et al. [7]; however, other studies reported different findings [3, 4, 6, 17]. Although meibum quality was significantly improved, meibum expressibility was unchanged after treatment in our study. Meibum quality was reported to be a sensitive and specific test for MGD, whereas meibum expressibility has poor efficacy owing to variable secretory activity of individual glands depending on their location [25]. NITBUT and TFLLT may require longer follow-up periods to detect changes.

In both study groups, patient-reported dry eye symptoms reflected by OSDI scores significantly improved at 7- and 11-week follow-ups compared with the baseline values without significant

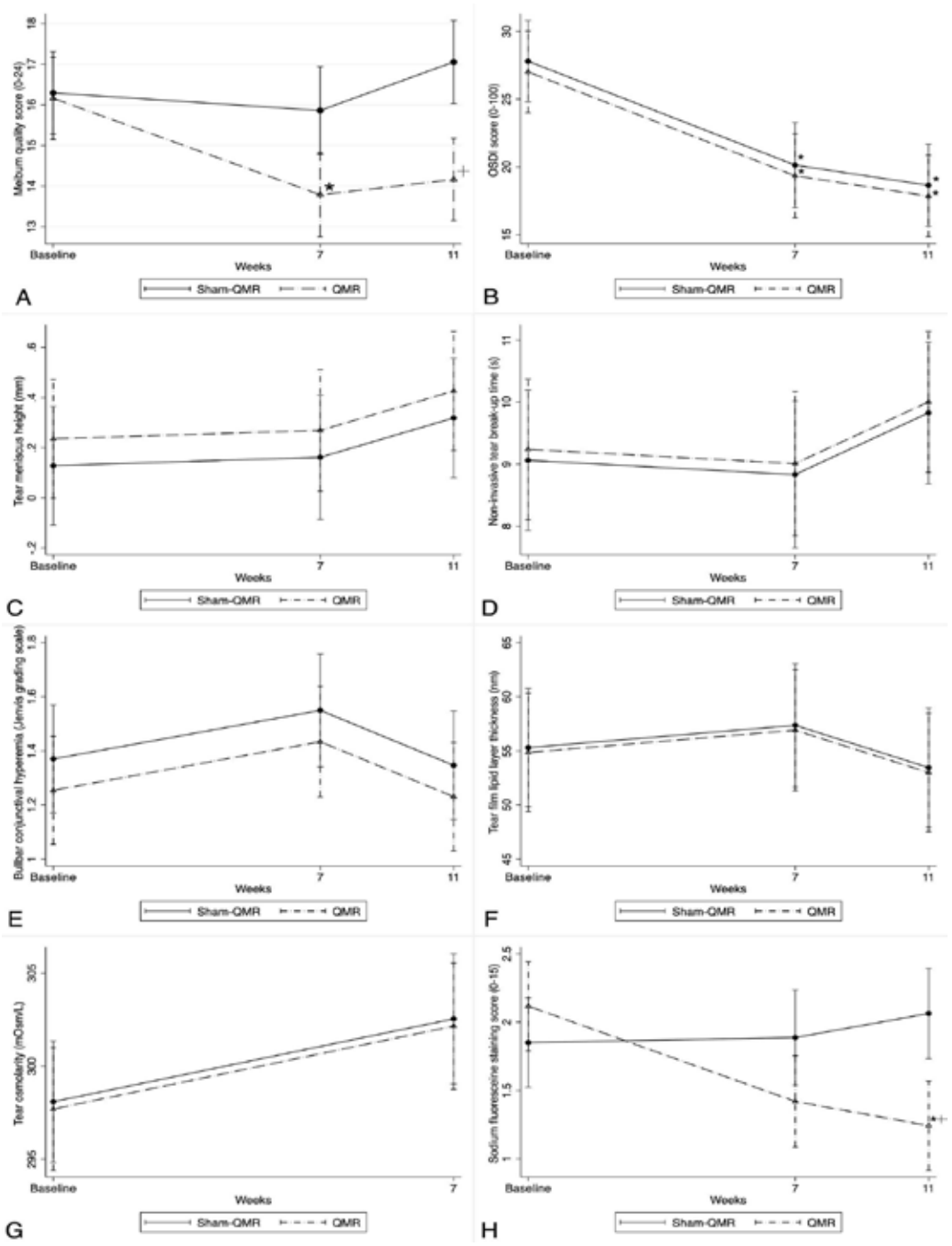

Fig. 1 Eight outcomes in the QRM and sham-QRM groups at baseline and 7- and 11-week follow-ups. A Meibum quality score, **B** Ocular Surface Disease Index score, **C** tear meniscus height, **D** noninvasive tear break-up time, **E** bulbar conjunctival hyperemia, **F** tear film lipid layer thickness, **G** tear osmolarity, and **H** sodium fluorescein staining score. + $p < 0.05$, comparison between the two study groups; * $p < 0.05$, comparison with baseline within each study group. QMR quantum molecular resonance.

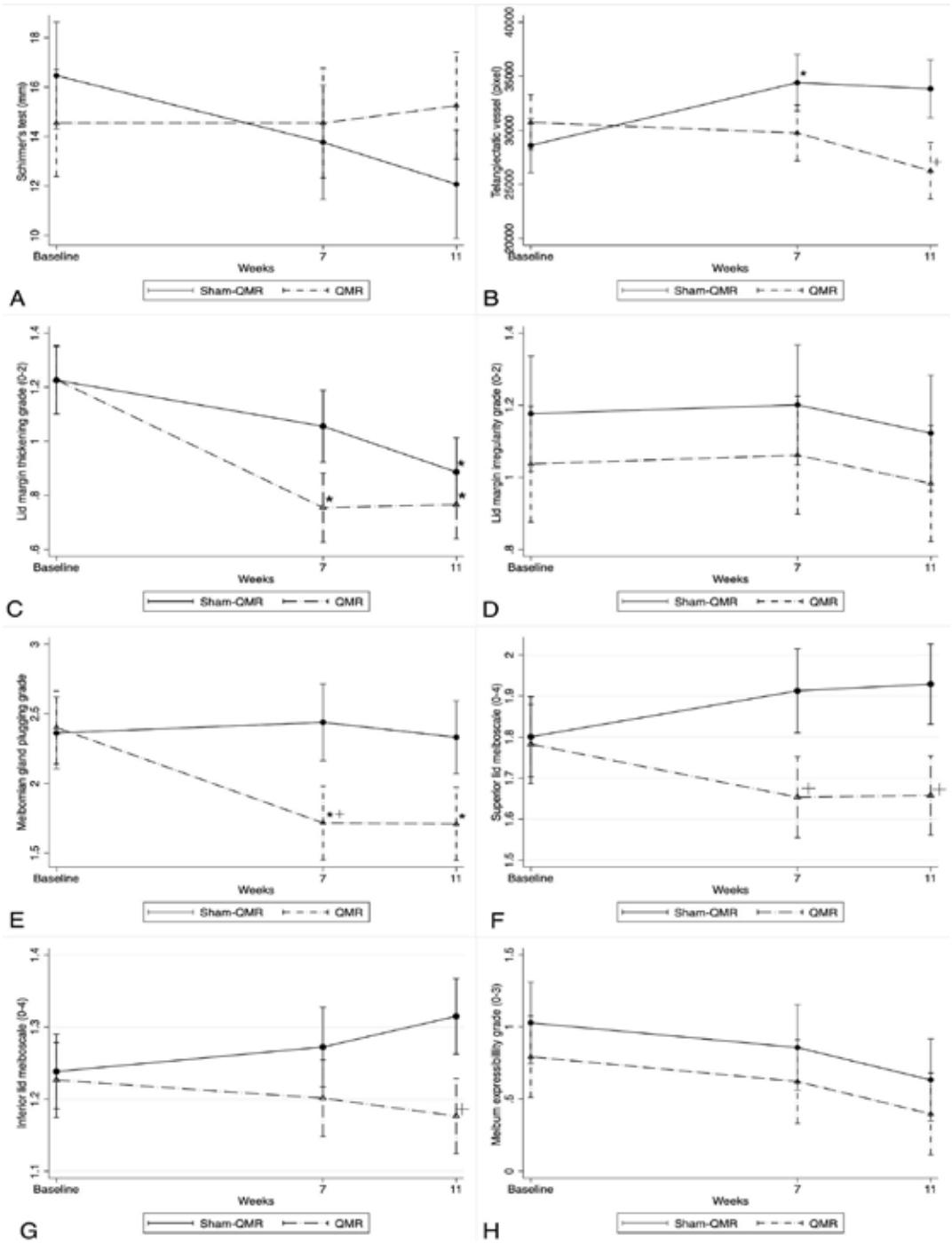

Fig. 2 Eight outcomes in the QRM and sham-QRM groups at baseline and 7- and 11-week follow-ups. A Schirmer's test, **B** area of telangiectasia vessels, **C** lid margin thickening grade, **D** lid margin irregularity grade, **E** meibomian gland plugging grade, **F** superior lid meiboscale, **G** inferior lid meiboscale, and **H** meibum expressibility grade. + $p < 0.05$, comparison between the two study groups; * $p < 0.05$, comparison with baseline within each study group. QMR quantum molecular resonance.

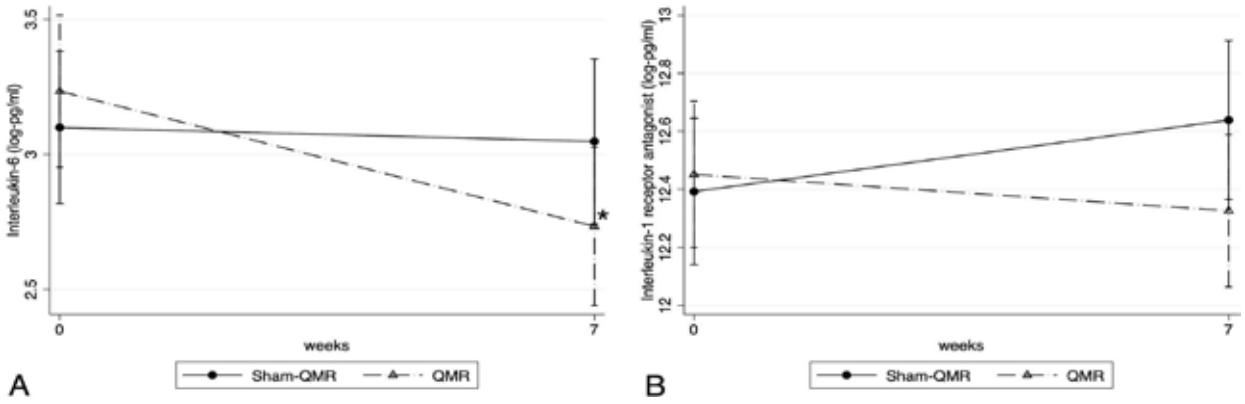

Fig. 3 Logarithmic mean values of tear cytokine levels in the QRM and sham-QRM groups at baseline and 7-week follow-up. Levels of (**A**) interleukin-6 and (**B**) interleukin-1 receptor antagonist in tear fluid. * $p < 0.05$, comparison with baseline within each study group. QMR quantum molecular resonance.

Table 2. Estimated mean difference with 95% confidence interval of the upper eyelid temperature between immediately after and just before the intervention.

Difference of Temperature (After-Before, Celsius)	QMR	Sham-QMR	*P*
Day 0	1.67; [1.39, 1.95]	0.27; [-0.04, 0.51]	<0.001
Day 7	1.46; [1.19, 1.74]	0.03; [-0.24, 0.31]	<0.001
Day 14	1.77; [1.50, 2.05]	0.34; [0.06, 0.61]	<0.001
Day 21	1.50; [1.22, 1.77]	0.06; [-0.21, 0.34]	<0.001

group differences. The application of artificial tears with lid hygiene (standard treatment) may have caused this. The OSDI and Standard Patient Evaluation of Eye Dryness Questionnaire scores were also significantly improved in previous QMR [3–7] and TES [17] studies. Moreover, the OSDI score primarily reflects the patients' subjective perceptions. Notably, the patients were treatment-naïve, and they compared their symptoms before and after receiving the standard treatment together with the intervention (either QMR or sham-QMR), resulting in improved scores. Several studies have reported an inconsistent association between clinical signs and subjective symptoms of dry eye disease [26–29], and in this study, the sham-QMR group similarly exhibited symptomatic improvement despite the absence of significant changes in clinical signs.

According to our findings, QMR alleviated inflammation in patients with MGD. IL-6 levels were significantly decreased at week 7, with a decreasing trend in IL1-Ra levels after treatment. Trivli et al. reported that QMR treatment significantly reduced tear MMP-9 levels [3]. Moreover, IL-6, IL1-Ra, and MMP-9 are associated with evaporative dry eye, including MGD [30–32]. Abnormalities in meibomian gland secretion contribute to tearing hyperosmolarity and further induce stress to the ocular surface, in which epithelial cells express IL-6. Furthermore, IL-6 amplifies the process by recruiting both innate and adaptive immune cells to the site of inflammation, promoting the vicious cycle of dry eye disease and ocular surface inflammation [33]. Additionally, ocular surface inflammation contributes to MGD [34]. In a previous study, IL-6 levels were significantly associated with MGD and non-Sjögren aqueous tear deficiency [30, 35]. As QMR can decrease IL-6 levels, it may eliminate one of the factors leading to the vicious cycle of dry eye and MGD. IL1-Ra is a natural antagonist of the pro-inflammatory cytokine IL1β by competitively binding to type 1 IL1 receptors. The spare receptor effect causes IL1-Ra levels to be higher than IL1β levels in normal tear fluid [36]. Moreover, IL1-Ra tear levels were higher in patients with MGD than in healthy participants [36], and they were nonsignificantly decreased after applying QMR, which led us to infer that QMR may mitigate IL1-Ra levels. Foo et al. found nonsignificant changes in the levels of 11 cytokines, including IL-6, in tears of patients with dry eye [7]. Desiccating dry eye stress increased the number of sloughing and stained corneal cells [37]. Although in our study IL-6 and IL1-Ra levels decreased in week 7, corneal and conjunctival fluorescein staining significantly improved in 11 weeks. Inflammation-associated clinical signs improve 1 month after cytokine reduction. Five previous TES/QMR studies showed significant improvements in corneal and conjunctival fluorescein levels in the treatment group [3–5, 7, 17]. However, bulbar conjunctival hyperemia was not significantly changed in our study. Lid telangiectasia is an MGD characteristic and reflects exposure to insults, including inflammation [38, 39]. Our findings showed the efficacy of QMR treatment in decreasing lid margin telangiectasia areas at 7 and 11 weeks, whereas in the sham-QMR group, this area was significantly increased at 7 weeks. The QMR-induced amelioration of inflammation supports the hypothesis that QMR can improve lid margin telangiectasia.

It was hypothesized that QMR promotes tear secretion [40]. Previous studies demonstrated QMR effectiveness in increasing Schirmer's test results [4, 5] and improving TMH [6]. However, others found that QMR did not affect TMH or Schirmer's test results [3, 7, 17]. According to Han et al., tear osmolarity significantly improved at 12 weeks [17]. Our study found no significant improvements in TMH, Schirmer's test results, or tear osmolarity in the QMR group, whereas Schirmer's test was worse in the sham-QMR group at 11 weeks. We postulate that longer follow-up or more QMR treatments are needed to detect significant improvements in Schirmer's test and other tear volume-associated outcomes because Schirmer's test results were improved after a 12-month follow-up [5].

Lid margin thickening is reportedly associated with MGD-related meibomian gland morphological features except for

meibomian gland dropout [20]. In our study, lid margin thickening was significantly improved at 7 and 11 weeks in the QMR group and at 11-week follow-up in the sham-QMR group. The improvement in the sham-QMR group might be due to lid hygiene, but our results suggest that QMR treatment with lid hygiene decreases lid thickening more effectively and faster than lid hygiene alone. Conflicting results have been reported regarding the association between MGD and lid margin irregularity [20, 41, 42]. In our study, lid margin irregularity did not change after QMR treatment.

By contrast, thermal pulsation proximal to a distal peristaltic motion device introduces heat of 42.5 °C to the eyelid. Thermal pulsation for MGD treatment involves liquefying and evacuating meibum. The positive effect persisted for 3 months in one study and for 12 months in another [43]. However, patients with a short fornix and small palpebral aperture size reported discomfort and soreness after treatment [43]. Another novel approach to effectively treating MGD is IPL therapy. Underlying mechanisms include reducing inflammation, thrombosing telangiectatic vessels, and stimulating mitochondria of meibomian glands, thereby promoting cell activity and consecutive improvement of the meibomian gland microstructure. Its effects last 45 days to 27 months, depending on severity. However, side effects after IPL treatment were reported, including cheek swelling, conjunctival cysts, skin blistering, and hair loss at the brow and forehead [43]. Compared with these two device-based therapies, QMR has fewer limitations of use and fewer side effects, and the impact at the transcriptional level may persist longer after QMR treatment. The longest study confirmed that transcutaneous electrical stimulation (TES), which shares similar principles with QMR, is effective in improving dry eye disease over a 12-month period [5].

The phase-transition temperature of MGD (35 °C) is higher than that of healthy meibomian glands (32–33 °C) [44]. Thus, heat-based MGD treatment requires at least 40–45 °C for eyelid compression to melt pathologically altered meibum [2]. In our study, the lid temperature significantly increased only by 1.50–1.77 °C after QMR treatment. Therefore, the QMR-induced increase in lid temperature may not be important for meibum quality improvement.

Regarding the QMR safety profile, BCVA, UCVA, and IOP did not change throughout the study. Despite an increased eyelid skin temperature after treatment, adverse events like upper eyelid redness were mild and resolved without treatment within 3 days. Moreover, ocular examinations did not reveal any abnormalities throughout the study.

Our study had some limitations. First, our evaluations may not have been frequent enough. This could have affected our findings regarding certain parameters, including TMH, NITBUT, TFLLT, tear osmolarity, Schirmer's test, lid margin irregularity, and meibum expressibility. Second, a longer follow-up time might be needed to show the changes of some parameters. Third, because the microbiome and *Demodex* mites were found to be associated with MGD [2], further studies on the effects of bacteria and *Demodex* load are needed. Finally, seven participants were lost to follow-up in this study (two and five participants of the QMR and sham-QMR groups, respectively); more participants might be needed to identify adverse QMR effects. However, the number of participants exceeded the calculated minimum sample size.

CONCLUSION

In conclusion, the use of a QMR-based device is a promising and less invasive alternative to MGD treatment. It improved meibum quality and alleviated inflammation of the ocular surface, as demonstrated by clinical improvements of the cornea and conjunctival staining and decreased IL-6 levels in tears.

SUMMARY

What was known before

- Quantum molecular resonance could be used as an alternative treatment for meibomian gland dysfunction; however, there is no previous randomized controlled trial of quantum molecular resonance and meibomian gland dysfunction.

What this study adds

- This study is the first randomized controlled trial study which showed that quantum molecular resonance (QMR) could help meibomian gland dysfunction (MGD). QMR showed a significant reduction in IL-6 cytokine in the tear and facilitated meibomian gland regeneration. This study found that meibomian gland plugging grade and telangiectatic vessels of the lid margin in MGD patients were significantly decreased after QMR treatment; however, there was no improvement in tear film lipid layer thickness, tear osmolarity, bulbar conjunctival hyperemia, lid margin thickening, and irregularity grade after QMR treatment.

DATA AVAILABILITY

Datasets analyzed in this study are available on reasonable request.

REFERENCES

1. Knop E, Knop N, Millar T, Obata H, Sullivan DA. The international workshop on meibomian gland dysfunction: report of the subcommittee on anatomy, physiology, and pathophysiology of the meibomian gland. Invest Ophthalmol Vis Sci. 2011;52:1938–78.
2. Geerling G, Tauber J, Baudouin C, Goto E, Matsumoto Y, O'Brien T, et al. The international workshop on meibomian gland dysfunction: report of the subcommittee on management and treatment of meibomian gland dysfunction. Invest Ophthalmol Vis Sci. 2011;52:2050–64.
3. Trivli A, Karmiris E, Dalianis G, Ruggeri A, Terzidou C. Evaluating the efficacy of Quantum Molecular Resonance (QMR) electrotherapy in mixed-type dry eye patients. J Optom. 2022;16:128–34.
4. Ferrari G, Colucci A, Barbariga M, Ruggeri A, Rama P. High frequency electrotherapy for the treatment of meibomian gland dysfunction. Cornea. 2019;38:1424–9.
5. Pedrotti E, Bosello F, Fasolo A, Frigo AC, Marchesoni I, Ruggeri A, et al. Transcutaneous periorbital electrical stimulation in the treatment of dry eye. Br J Ophthalmol. 2017;101:814–9.
6. Kavroulaki D, Konstantinidou E, Tsiogka A, Rallis K, Mavrikakis E. Quantum molecular resonance electrical stimulation as a beneficial and safe treatment for multifactorial dry eye disease. Cureus. 2023;15:e39695.
7. Foo VHX, Liu Y-C, Tho B, Tong L. Quantum molecular resonance electrotherapy (Rexon-Eye) for recalcitrant dry eye in an Asian population. Front Med. 2023;10.
8. Piyacomn Y, Kasetsuwan N, Reinprayoon U, Satitpitakul V, Tesapirat L. Efficacy and safety of intense pulsed light in patients with meibomian gland dysfunction-a randomized, double-masked, sham-controlled clinical trial. Cornea. 2020;39:325–32.
9. Altman DG, Bland JM. Treatment allocation by minimisation. BMJ. 2005;330:843.
10. Fraccalvieri M, Salomone M, Di Santo C, Ruka E, Morozzo U, Bruschi S. Quantum molecular resonance technology in hard-to-heal extremity wounds: histological and clinical results. Int Wound J. 2017;14:1313–22.
11. Yao G, Kang L, Li C, Chen S, Wang Q, Yang J, et al. A self-powered implantable and bioresorbable electrostimulation device for biofeedback bone fracture healing. Proc Natl Acad Sci USA. 2021;118.
12. Yoo YS, Park S, Eun P, Park YM, Lim DH, Chung TY. Corneal neuro-regenerative effect of transcutaneous electrical stimulation in rabbit lamellar keratectomy model. Transl Vis Sci Technol. 2022;11:17.
13. Sanie-Jahromi F, Azizi A, Shariat S, Johari M. Effect of electrical stimulation on ocular cells: a means for improving ocular tissue engineering and treatments of eye diseases. Biomed Res Int. 2021;2021:6548554.
14. Arita R, Suehiro J, Haraguchi T, Maeda S, Maeda K, Tokoro H, et al. Topical diquafosol for patients with obstructive meibomian gland dysfunction. Br J Ophthalmol. 2013;97:725–9.

15. Maskin SL, Testa WR. Growth of meibomian gland tissue after intraductal meibomian gland probing in patients with obstructive meibomian gland dysfunction. Br J Ophthalmol. 2018;102:59–68.
16. Yin Y, Gong L. Reversibility of gland dropout and significance of eyelid hygiene treatment in meibomian gland dysfunction. Cornea. 2017;36:332–7.
17. Han G, Lim DH, Yoo YS, Shin EH, Park JY, Kim D, et al. Transcutaneous electrical stimulation for the prevention of dry eye disease after photorefractive keratectomy: randomized controlled trial. Ophthalmol Sci. 2023;3:100242.
18. Cai MM, Zhang J. Effectiveness of transcutaneous electrical stimulation combined with artificial tears for the treatment of dry eye: a randomized controlled trial. Exp Ther Med. 2020;20:175.
19. Wolffsohn JS, Arita R, Chalmers R, Djalilian A, Dogru M, Dumbleton K, et al. TFOS DEWS II diagnostic methodology report. Ocul Surf. 2017;15:539–74.
20. Feng J, Wang J, Wu B, Shao Q, Zang Y, Cao K, et al. Association of meibomian gland morphology with orifice plugging and lid margin thickening in meibomian gland dysfunction patients. Int Ophthalmol. 2023;43:3207–18.
21. Bründl M, Garreis F, Schicht M, Dietrich J, Paulsen F. Characterization of the innervation of the meibomian glands in humans, rats and mice. Ann Anat. 2021;233:151609.
22. Sella S, Adami V, Amati E, Bernardi M, Chieregato K, Gatto P, et al. In-vitro analysis of quantum molecular resonance effects on human mesenchymal stromal cells. PLoS ONE. 2018;13:e0190082.
23. Yang S, Lee HJ, Kim DY, Shin S, Barabino S, Chung SH. The use of conjunctival staining to measure ocular surface inflammation in patients with dry eye. Cornea. 2019;38:698–705.
24. Xiao J, Adil MY, Chen X, Utheim ØA, Ræder S, Tønseth KA, et al. Functional and morphological evaluation of meibomian glands in the assessment of meibomian gland dysfunction subtype and severity. Am J Ophthalmol. 2020;209:160–7.
25. Xiao J, Adil MY, Olafsson J, Chen X, Utheim ØA, Ræder S, et al. Diagnostic test efficacy of meibomian gland morphology and function. Sci Rep. 2019;9:17345.
26. Bartlett JD, Keith MS, Sudharshan L, Snedecor SJ. Associations between signs and symptoms of dry eye disease: a systematic review. Clinical Ophthalmol. 2015;9:1719–30.
27. Kyei S, Dzasimatu SK, Asiedu K, Ayerakwah PA. Association between dry eye symptoms and signs. J Curr Ophthalmol. 2018;30:321–5.
28. Onwubiko SN, Eze BI, Udeh NN, Onwasigwe EN, Umeh RE. Dry eye disease: concordance between the diagnostic tests in African eyes. Eye Contact Lens. 2016;42:395–400.
29. Unlu C, Guney E, Akcay BI, Akcali G, Erdogan G, Bayramlar H. Comparison of ocular-surface disease index questionnaire, tearfilm break-up time, and Schirmer tests for the evaluation of the tearfilm in computer users with and without dry-eye symptomatology. Clinical Ophthalmol. 2012;6:1303–6.
30. Wu X, Chen X, Ma Y, Lin X, Yu X, He S, et al. Analysis of tear inflammatory molecules and clinical correlations in evaporative dry eye disease caused by meibomian gland dysfunction. Int Ophthalmol. 2020;40:3049–58.
31. Enríquez-de-Salamanca A, Castellanos E, Stern ME, Fernández I, Carreño E, García-Vázquez C, et al. Tear cytokine and chemokine analysis and clinical correlations in evaporative-type dry eye disease. Mol Vis. 2010;16:862–73.
32. Chotikavanich S, de Paiva CS, Li de Q, Chen JJ, Bian F, Farley WJ, et al. Production and activity of matrix metalloproteinase-9 on the ocular surface increase in dysfunctional tear syndrome. Invest Ophthalmol Vis Sci. 2009;50:3203–9.
33. Bron AJ, de Paiva CS, Chauhan SK, Bonini S, Gabison EE, Jain S, et al. TFOS DEWS II pathophysiology report. Ocul Surf. 2017;15:438–510.
34. Baudouin C, Messmer EM, Aragona P, Geerling G, Akova YA, Benítez-del-Castillo J, et al. Revisiting the vicious circle of dry eye disease: a focus on the pathophysiology of meibomian gland dysfunction. Br J Ophthalmol. 2016;100:300–6.
35. Zhao H, Li Q, Ye M, Yu J. Tear Luminex analysis in dry eye patients. Med Sci Monit. 2018;24:7595–602.
36. Solomon A, Dursun D, Liu Z, Xie Y, Macri A, Pflugfelder SC. Pro- and anti-inflammatory forms of interleukin-1 in the tear fluid and conjunctiva of patients with dry-eye disease. Invest Ophthalmol Vis Sci. 2001;42:2283–92.
37. Begley C, Caffery B, Chalmers R, Situ P, Simpson T, Nelson JD. Review and analysis of grading scales for ocular surface staining. Ocul Surf. 2019;17:208–20.
38. Tomlinson A, Bron AJ, Korb DR, Amano S, Paugh JR, Pearce EI, et al. The international workshop on meibomian gland dysfunction: report of the diagnosis subcommittee. Invest Ophthalmol Vis Sci. 2011;52:2006–49.
39. Jiang X, Wang Y, Lv H, Liu Y, Zhang M, Li X. Efficacy of intra-meibomian gland injection of the anti-VEGF agent bevacizumab for the treatment of meibomian gland dysfunction with lid-margin vascularity. Drug Des Dev Ther. 2018;12:1269–79.
40. Brinton M, Kossler AL, Patel ZM, Loudin J, Franke M, Ta CN, et al. Enhanced tearing by electrical stimulation of the anterior ethmoid nerve. Invest Ophthalmol Vis Sci. 2017;58:2341–8.
41. Arita R, Minoura I, Morishige N, Shirakawa R, Fukuoka S, Asai K, et al. Development of definitive and reliable grading scales for meibomian gland dysfunction. Am J Ophthalmol. 2016;169:125–37.
42. Ha M, Kim JS, Hong SY, Chang DJ, Whang WJ, Na KS, et al. Relationship between eyelid margin irregularity and meibomian gland dropout. Ocul Surf. 2021;19:31–37.
43. Lam PY, Shih KC, Fong PY, Chan TCY, Ng AL, Jhanji V, et al. A review on evidence-based treatments for meibomian gland dysfunction. Eye Contact Lens. 2020;46:3–16.
44. Butovich IA, Millar TJ, Ham BM. Understanding and analyzing meibomian lipids-a review. Curr Eye Res. 2008;33:405–20.

AUTHOR CONTRIBUTIONS

All authors made a significant contribution to this research. Conceptualization: LU, NK, and UR. Data collection: LU, YP, WQ, and PD. Data analysis: LU and YP. Writing: LU Review and editing: LU, NK, and UR.

FUNDING

This study was supported by the Quality Improvement Fund, King Chulalongkorn Memorial Hospital. The funding agency has no role in conducting this research.

COMPETING INTERESTS

None declared.

ADDITIONAL INFORMATION

Supplementary information The online version contains supplementary material available at https://doi.org/10.1038/s41433-025-03890-3.

Correspondence and requests for materials should be addressed to Ngamjit Kasetsuwan.

Reprints and permission information is available at http://www.nature.com/reprints

Publisher's note Springer Nature remains neutral with regard to jurisdictional claims in published maps and institutional affiliations.

Open Access This article is licensed under a Creative Commons Attribution 4.0 International License, which permits use, sharing, adaptation, distribution and reproduction in any medium or format, as long as you give appropriate credit to the original author(s) and the source, provide a link to the Creative Commons licence, and indicate if changes were made. The images or other third party material in this article are included in the article's Creative Commons licence, unless indicated otherwise in a credit line to the material. If material is not included in the article's Creative Commons licence and your intended use is not permitted by statutory regulation or exceeds the permitted use, you will need to obtain permission directly from the copyright holder. To view a copy of this licence, visit http://creativecommons.org/licenses/by/4.0/.

© The Author(s) 2025

03

Transcutaneous periorbital electrical stimulation in the treatment of dry eye

E. Pedrotti, F. Bosello, A. Fasolo, A. C. Frigo, I. Marchesoni, A. Ruggeri, G. Marchini

Downloaded from http://bjo.bmj.com/ on May 30, 2017 - Published by group.bmj.com

Transcutaneous periorbital electrical stimulation in the treatment of dry eye

Emilio Pedrotti,[1] Francesca Bosello,[1] Adriano Fasolo,[1,2] Anna C Frigo,[3] Ivan Marchesoni,[1] Alfredo Ruggeri,[4] Giorgio Marchini[1]

[1]Department of Neurosciences, Biomedicine, and Movement Sciences, Eye Clinic, AOUI—University of Verona, Verona, Italy
[2]Fondazione Banca degli Occhi del Veneto (The Veneto Eye Bank Foundation), Venezia Zelarino, Italy
[3]Department of Cardiac, Thoracic and Vascular Sciences, University of Padova, Padova, Italy
[4]Department of Information Engineering, University of Padova, Padova, Italy

Correspondence to
Dr Emilio Pedrotti, Eye Clinic, Ospedale Maggiore, P.le A. Stefani, 1, Verona 37126, Italy; emilio.pedrotti@univr.it

Received 7 March 2016
Revised 30 August 2016
Accepted 4 September 2016
Published Online First 22 September 2016

ABSTRACT

Purpose To evaluate efficacy and safety of transcutaneous application of electrical current on symptoms and clinical signs of dry eye (DE).

Methods 27 patients with DE underwent transcutaneous electrostimulation with electrodes placed onto the periorbital region of both eyes and manual stimulation with a hand-piece conductor moved by the operator. Each patient underwent 12 sessions of 22 min spread over 2 months, two sessions per week in the first month and one session per week in the second month. Ocular Surface Disease Index (OSDI) questionnaire, tear break-up time (TBUT), fluorescein staining of the cornea, Schirmer I test and adverse events were evaluated at baseline, at end of treatment and at 6 and 12 months.

Results OSDI improved from 43.0±19.2 at baseline to 25.3±22.1 at end of treatment (mean±SD, p=0.001). These effects were substantially maintained at 6-month and 12-month follow-up evaluations. Improvement of the values of TBUT was recorded for the right eye at the end of treatment (p=0.003) and found in the left eye after 12 months (p=0.02). The Oxford scores changed in both eyes at the end of treatment and at the 6-month evaluation (p<0.001), and in the right eye at the 12-month evaluation (p=0.035). Schirmer I improved significantly at the end of treatment in the left eye (p=0.001) and in both eyes at the 12-month evaluation (p=0.004 and p=0.039 for the left and right eye, respectively). A significant reduction of the use of tear substitutes was found at the end of treatment (p=0.003), and was maintained during the follow-up (p<0.001).

No complications occurred and patients found the treatment satisfying.

Conclusions Transcutaneous electrical stimulation was shown to improve DE, both subjectively and objectively, without any adverse effects and has the potential to enlarge the armamentarium for treating DE.

INTRODUCTION

Aetiology and management of dry eye (DE) challenge ophthalmologists. The International Dry Eye WorkShop in 2007 defined DE as 'a multifactorial disease of the tears and ocular surface that results in symptoms of discomfort, visual disturbances and tears film instability with potential damage to the ocular surface … accompanied by increased osmolarity of tear film and inflammation of the ocular surface'.[1]

Tear dysfunctions leading to DE include primary tear deficiency, tear deficiency associated with systemic connective tissue disorders (eg, Sjögren syndrome), and evaporative loss of water from the tear film in subjects with normal lacrimal secretory function.[2]

All these conditions can lead to the alteration of the tear aqueous, mucin and lipid components that results in the hyperosmolarity of the tear film, a key step in the vicious circle of DE pathology evolving in a chronic inflammatory disease.[3]

Despite the causative mechanisms, tear substitutes to moisten the ocular surface and improve ocular comfort represent the first line in patients with DE. Symptoms rarely completely disappear, while their reduction positively affects patients' quality of life and improves sleep and mood disorders.[4 5]

Since current treatments are substantially palliative, as no one are capable of restoring the physiological lacrimal secretion,[6] a more reliable therapeutic approach could be obtained by the dynamic adaptation of treatment to address every single ocular surface structure involved in the tear film dysfunction.[7]

Consequently, emerging treatments to enlarge the therapeutic armamentarium are currently focused on new drugs that stimulate tear secretion, or on the mechanical stimulation of eyelid and periocular region, by vibration, massage and thermotherapy, or that specifically address the recovering of the meibomian gland function with the thermal pulsation system.[8–10]

No studies have considered the use of electrotherapy to treat DE, although transcutaneous electrical stimulation of nerves and muscles through adhesive pads showed efficacy in different fields of medicine, for example, physiotherapy, pain management, urogenital disorders and obstructive sleep apnoea.[11–13]

Recently, the transpalpebral microcurrent stimulation showed potential efficacy in the treatment of macular degeneration.[14 15]

The application of a frequency-specific electrical current in the range of 4–64 MHz, patented as quantum molecular resonance (QMR) technology by Telea Electronic Engineering (Sandrigo, Italy), showed to be effective in reducing joint effusion in patients undergoing total knee arthroplasty[16] and in skin antiageing treatment (unpublished results).

The QMR was originally employed in an electrosurgical device (VESALIUS, Telea Electronic Engineering, Italy) to achieve both precise cut and coagulation functions, without increasing temperature and damaging the surrounding tissue.[17] According to QMR, the energy is transmitted to the tissue packed into quanta, the energy of each quantum being proportional to the frequency of the current provided. The spectrum of frequencies

To cite: Pedrotti E, Bosello F, Fasolo A, et al. Br J Ophthalmol 2017;101:814–819.

Downloaded from http://bjo.bmj.com/ on May 30, 2017 - Published by group.bmj.com

used by QMR produces an amount of energy adequate to break the molecular bonds in the biological tissue, and to obtain a non-traumatic incision of the tissue, without pressure or crashing of the cells, always keep a temperature lower than 50°C, as coagulation results from protein denaturation instead of tissue warming.

In a subsequent and distinct application of QMR at lower current intensities, the effect of incision of the tissue has been replaced by a stimulation effect that leads to a structural and functional improvement, particularly evident in skin, muscles and joints. Again, the electrical field applied through large plate electrodes has no thermal effects, and improvements appear following applications repeated at intervals of one or a few days.

In vitro studies in cultured murine muscle fibres showed that QMR produces (1) a mechanical stimulation, (2) an electrical interaction with the cellular membrane and (3) a biochemical interaction that involves the internal structures of the cells, particularly the sarcoplasmic reticulum.[18] The series of contractions and relaxations that the cells undergo trigger intercellular and intracellular metabolism. Moreover, the increase in the concentration of calcium ions within the cell constitutes an effective activation signal of intracellular calcium-dependent metabolic pathways. We believe that through the series of contractions and relaxations during this peculiar '*cellular massage*', some biochemical stimulation of cellular structures is obtained that can explain the positive effects achieved by QMR in physiotherapy and aesthetic medicine.

In the case of DE, our hypothesis is that QMR can stimulate the lacrimal system, reactivating the lacrimal and meibomian gland tissue and benefit the ocular annexes.

An initial study was performed by J. Schroeter, at the Charité Augenklinik in Berlin, on seven patients with moderate to severe DE and blepharitis. Data from this case series showed that the stimulation with QMR by means of adhesive electrodes on the periorbital area of both eyes improves DE clinically and subjectively in about half of the patients, without side effects (unpublished results).

Based on these encouraging results, the present study was designed to assess QMR in a larger group of patients with DE, with the aim to evaluate safety and potential efficacy, early after treatment and in the long term.

MATERIALS AND METHODS

A prospective, open-label, single-arm pilot study was conducted at the Eye Clinic of the University of Verona, from December 2012 to September 2014, in agreement with the tenets of the Declaration of Helsinki. Institutional Ethical Committee approval and written patients' informed consent were obtained.

Patient selection

We included adult patients with diagnosis of DE in both eyes, regular use of tear substitutes eye drops, complete eyelids occlusion, Ocular Surface Disease Index (OSDI) score >12, Schirmer I test (without anaesthetic) <10 mm/5 min in both eyes and tear break-up time (TBUT) <10 s in both eyes.

We excluded patients requiring anti-inflammatory, antibiotic or glaucoma eye drops; history of ocular surgery in the previous 3 months; who suffered from ocular infection in the previous 6 months; holding a non-removable electrical device (eg, cardiac pacemaker); or with dermatological skin problems (eg, rosacea, acne). We assessed meibomian gland dysfunction (MGD) by slit-lamp evaluation of lid debris and telangiectasias, and collected patients' medical and personal history to evaluate the presence of risk factors for DE.

Patients were allowed to adjust their current tear substitutes during the study period, and other eye drops were not allowed.

Application of electrical stimulation

Electrical stimuli were applied by means of electrodes placed in the periorbital area of both eyes using the REXON-EYE (Telea Electronic Engineering, Sandrigo, Italy; patent pending), a device that generates QMR by high-frequency (4–64 MHz) and low-power (60–120 mJ/cm^2/s) electrical currents. Its function is based on the resonance effect, which is the possibility of maximising the delivery of energy to biological tissues by oscillating electric fields without increasing the temperature and eliciting biological responses, both pathophysiological and potentially therapeutic.[18–20]

Each session of stimulation consisted in two sequential phases: in the first phase, we applied two electrodes close to each eye, one over the temporal area and one under the lower lid, and activated each of them for 60 s in sequence. The cycle was repeated 4 times, for a total stimulation length of 16 min, at a nominal power of 80 mJ/cm^2/s. In the second phase, the operator moved a hand-piece conductor around the periorbital areas of both eyes during two sequential phases of 3 min each, with a 1 min rest, for a total stimulation time of 6 min, at a nominal power of 80 mJ/cm^2/s.

Each patient underwent 12 sessions of stimulation during a 2-month period: two sessions per week in the first month, and one session per week in the second month. Nominal power and number of sessions were chosen based on previous experiences that showed that 80 mJ/cm^2/s is effective without inducing any patients' discomfort, for example, excessive heat. A repetition of treatment every 3 days in the first month appeared adequate to induce an effect, as well as the repetition of treatment every week in the following month to maintain such effect.

Patients laid down on a bed with head elevated and a passive electrode applied under their back (figure 1). Electrical stimulation was perceived as a pleasant sensation, as a mild warmth under the electrodes. In the case of excessive or absence of the warm sensation, the operator could modify the intensity from the nominal value of 80 mJ/cm^2/s to lower or higher values, respectively, in the range of power allowed by the device.

Outcome assessment

We evaluated all patients at baseline, at 1 week after the last treatment session (end of treatment), and at 6 and 12 months after treatment. The following were assessed: (1) OSDI score (primary endpoint),[14] (2) TBUT, (3) corneal staining with fluorescein dye (Oxford grading system)[21] and (4) Schirmer I test.

During the treatment period, patients recorded daily on a diary (1) type and frequency of tear substitutes, (2) additional eye drops or systemic drugs used for DE or any condition other than DE, and (3) ocular symptoms. We assessed safety before and after each session of treatment, and during a further visit 1 week after the end of treatment. Before starting each session, the treating physician examined the occurrence of adverse events, general health status and eye complaints arisen from the previous visit. Recordings in the diary were also examined.

Safety evaluation after each session of treatment included (1) potential side effects, (2) biomicroscopy of the anterior segment, (3) corneal sensitivity (cotton tip) and (4) intraocular pressure (Goldman tonometry). We measured uncorrected and best-corrected visual acuity at baseline and at the end of treatment.

Downloaded from http://bjo.bmj.com/ on May 30, 2017 - Published by group.bmj.com

Figure 1 Patient receiving microcurrent treatment. (A) During the first phase of each session of treatment, we applied two adhesive electrodes close to each eye, one over the temporal area and one under the lower lid. (B) During the second phase of each session of treatment, the operator moved a hand-piece conductor around the periorbital areas of both eyes.

Statistical analysis

A sample size of 26 patients achieves 80% power to detect a mean standardised difference (mean of the change of OSDI measured at baseline and at the end of treatment over the SD of the change between baseline and end of treatment) of at least 0.6 at a significant level of 5% using the Wilcoxon test for paired observations. To take into account a dropout rate of 15% we sought to enrol at least 31 patients.

We expressed results of descriptive analyses as a means and SD, median and range for quantitative variables, and as a count and percentage for categorical variables. All observations were analysed together or per eye. The primary endpoint and the clinical outcomes were also analysed with respect to the type of DE. Differences of measurements between two time points were assessed with the Wilcoxon signed rank test, and between groups with Wilcoxon rank sum test. A p value <0.05 was considered statistically significant.

Since the pilot nature of the study, we did not make adjustments for taking into account multiple comparisons. Spearman correlation analysis was performed to investigate the possible correlation between response to treatment and baseline values of OSDI scores. A positive Spearman correlation coefficient (rho) indicates positive correlation between severity of OSDI score and effective response to treatment. Statistical analyses were performed with R 3.2.3 for Windows and with SAS statistical software V.9.4 (SAS Institute, Cary, North Carolina, USA).

RESULTS

Thirty-two patients who met the inclusion criteria were recruited and 27, with a mean age of 57.3 (14.9) years (median 58.0; range 23–82), were included in the analyses (table 1). Five patients were not included because they missed to attend to one or more treatment sessions due to professional or personal reasons.

Table 1 Patients' demographics and baseline characteristics (N=27)

	N (%)
Sex	
Female	21 (77.8)
Male	6 (22.2)
Systemic risk factors for DE	
No	19 (70.4)
Yes	8 (29.6)
Sjögren syndrome	4
Rheumatoid arthritis	2
Sarcoidosis	1
Use of antidepressant drugs	1
Lid margins	
Normal	20 (74.1)
Meibomian gland dysfunction	7 (25.9)
Duration of DE (years)	
Mean (SD)	11.8 (13.4)
Median	10
Range	1–55
Type of DE*	
Evaporative	18 (66.7)
Hyposecretive	9 (33.3)
Ocular Surface Disease Index score	
Mean (SD)	43.0 (19.2)
0–12 normal	0
13–22 mild	3 (11.1)
23–32 moderate	6 (22.2)
33–100 severe	18 (66.7)
Schirmer I test (mm)	
Mean (SD)	6.4 (3.5)
>10	0
5–10	21 (77.8)
<5	6 (22.2)
Tear film break-up time (seconds)	
Mean (SD)	4.7 (2.3)
>10	0
10–5	12 (44.4)
<5	15 (55.6)
Oxford test	
Mean (SD)	1.2 (0.9)
0	2 (7.4)
1–2	21 (77.8)
3–5	4 (14.8)
Tear substitutes (no. of drops/day)	
Mean (SD)	6.0 (3.6)
1–3	8 (29.6)
4–6	10 (37.0)
≥7	9 (33.3)

*Two patients have both hyposecretive and evaporative DE.
DE, dry eye.

Downloaded from http://bjo.bmj.com/ on May 30, 2017 - Published by group.bmj.com

Before treatment, 16 (59%) patients showed superficial punctate keratopathy in both eyes, 7 (26%) MGD and 4 (15%) anterior blepharitis. None of the patients had undergone prior refractive surgery or used to wear contact lenses.

Type of DE was differentiated into evaporative or hyposecretive based on the presence of aetiological risk factors (ie, autoimmune diseases, use of medications known to reduce tear production, reduced blinking activity during visual display terminal work, previous refractive surgery or blepharoplasty) and on clinical evaluation of MGD.

Among the patients with evaporative DE, seven had MGD, eight had a reduced blinking, two had undergone blepharoplasty 5 years before and one had undergone various post-traumatic maxillofacial surgeries. Seven patients suffering from hyposecretive DE were affected by an autoimmune disease and one assumed antidepressant drug (paroxetine).

OSDI score

The primary efficacy variable significantly improved from 43.0 ±19.2 at baseline to 25.3±22.1 at the end of treatment (mean ±SD, p=0.001). These effects were substantially maintained at 6-month and 12-month follow-up evaluations. Compared with baseline, OSDI scores showed significant (p<0.01) mean (SD) differences of −17.7 (24.6) at the end of treatment, −15.0 (19.0) at 6 months and of −13.1 (17.6) at 12 months. No statistically significant differences were found in between end of treatment and 6-month and 12-month follow-up (figure 2).

The OSDI scores improved at the end of treatment in 17 (63%) patients, and were unaffected in 10 (37%). In 11 out of 17 patients it improved from severe to normal (N=7), moderate (N=3) and mild (N=1) scores, respectively, and in five out of 17 from moderate to normal (N=3) and mild (N=2) scores, respectively. In one patient, the OSDI score improved from mild to normal. Seven out of 10 unresponsive patients persisted in the category of severe OSDI scores (two of these patients significantly worsened the OSDI scores from 32.2 to 41.7 and from 47.5 to 85.0), one patient in that of moderate and two in that of mild.

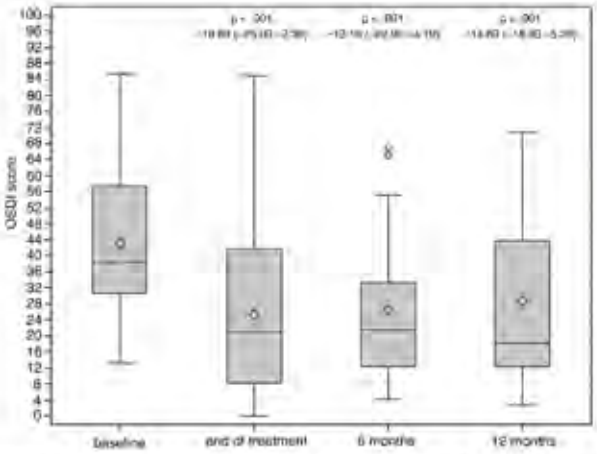

Figure 2 Differences in the Ocular Surface Disease Index (OSDI) scores showed statistically significant reduction from baseline to each evaluation during follow-up, in all patients (N=27). The boxes represent the 25th and 75th percentiles; whiskers are lines extending from each end of the box to the minimum or maximum or the lowest datum within 1.5-fold IQR of the lower quartile or the highest datum within 1.5-fold IQR of the upper quartile. The median value is the line that bisects the boxes, diamond represents the mean and the circles are the outlier values. Data accompanying p values are median and SD.

Patients with evaporative DE reported 31% reduction of OSDI score, from the mean value of 40.5±18.9 at baseline to the 27.7±25.3 value at the end of treatment (− 12.7±24.1; p=0.027).

Patients with hyposecretive DE reported 58% reduction of mean OSDI score, from 48.1±19.8 at baseline (mean±SD) to 20.4±13.8 at the end of treatment (−27.7±23.5; p=0.012).

Compared with baseline, a differential response between evaporative and hyposecretive DE was not significant at all evaluation times (end of treatment p=0.131, 6 months p=0.397, 12 months p=0.066).

Treatment response was unaffected by OSDI severity in patients with evaporative DE at all evaluations, while it was influenced in patients with hyposecretive DE, at the end of treatment and at 6 months (r=−0.63, p=0.067; r=−0.83, p=0.010, respectively).

Tear film break-up time

Significant improvements of the TBUT values were found in the right eye at the end of treatment and in the left eye at 12-month evaluation (table 2). Compared with baseline, 6 (22%) patients worsened TBUT at the end of treatment, in one or both eyes.

Patients with evaporative DE showed higher improvement of TBUT (mean difference±SD) in the right eye than patients with hyposecretive DE, at the end of treatment compared with baseline, 3.7±3.4 and 0.02±3.4 (p=0.007), respectively.

Corneal fluorescein staining

Oxford scores showed statistically significant changes from baseline in both eyes at all evaluations, without statistically differences between end of treatment and the evaluations during follow-up (table 3). Only one patient showed worsened Oxford score value, from 0 to 1 in the left eye, at the end of treatment compared with baseline.

Patients with evaporative DE showed a higher improvement than patients with hyposecretive DE, at the end of treatment compared with baseline, in the right eye (mean difference±SD: −1.0±0.5 and −0.4±0.5, p=0.014).

Schirmer I test

Scores in the Schirmer I test improved significantly after treatment in the left eye and in both eyes at 12 months of evaluation (table 4), while 8 (30%) patients worsened their Schirmer scores

Table 2 TBUT at baseline, end of treatment, and follow-up (N=27)

TBUT (seconds)	Baseline	End of treatment	6 months	12 months
In the left eye				
Mean±SD	4.6±1.8	6.0±4.2	5.3±2.6	7.0±3.8
Median	5.0	4.0	5.0	7.0
Min–max	1.0–8.0	1.0–18.0	1.0–12.0	2.0–15.0
p Value*		n.s.	n.s.	0.01
In the right eye				
Mean (SD)	4.7±2.3	7.1±4.0	5.9±3.2	6.6±2.9
Median	4.5	8.0	5.0	6.0
Min–max	1.0–8.0	1.0–14.0	1.0–13.0	1.0–12.0
p Value*		0.001	n.s.	n.s.

*Between baseline and each evaluation during follow-up.
TBUT, tear break-up time.

Downloaded from http://bjo.bmj.com/ on May 30, 2017 - Published by group.bmj.com

Table 3 Corneal fluorescein staining—Oxford score (N=27)

Oxford score	Baseline	End of treatment	6 months	12 months
In the left eye				
Mean±SD	1.2±0.8	0.4±0.9	0.2±0.5	0.8±1.1
Median	1.0	0.0	0.0	0.0
Min–max	0.0–4.0	0.0–4.0	0.0–2.0	0.0–4.0
p Value*		<0.001	<0.001	n.s.
In the right eye				
Mean (SD)	1.2±0.9	0.4±0.9	0.2±0.5	0.6±1.0
Median	1.0	0.0	0.0	0.0
Min–max	0.0–4.0	0.0–4.0	0.0–2.0	0.0–4.0
p Value*		<0.001	<0.001	0.035

*Between baseline and each evaluation during follow-up.

in one or both eyes, at the end of treatment compared with baseline.

Patients with evaporative DE significantly improved Schirmer I scores (mean difference±SD) at the end of treatment compared with baseline in the left eye, 4.1±5.4 (p=0.009), and in both eyes at 12 months, 3.5±4.3 (p=0.007) and 4.4±7.3 (p=0.035), in the left and right eye, respectively. Improvements of Schirmer scores in patients with hyposecretive DE (4.0±5.0 and 0.6±4.2 in the left and right eye at the end of treatment, respectively; 4.4±8.2 and 1.8±7.0 in the left and right eye at 12 months, respectively) did not reach statistical significance (p>0.05).

Use of tear substitutes and long-term subjective evaluation

A significant reduction of the use of tear substitutes was found at the end of treatment, and such a reduction was almost maintained during the follow-up (table 5).

Compared with baseline, at the end of treatment, 19 (70%) patients reduced the daily number of tear substitutes eye drops, 4 (15%) patients completely halted the use of eye drops and 4 (15%) patients increased this number.

Significant reduction in the use of tear substitutes was observed at the end of treatment, compared with baseline, in both evaporative and hyposecretive patients (mean difference ±SD: −1.3±1.2, p=0.021 and −2.6±2.3, p=0.001).

After 12 months, 15 (56%) patients maintained the number of daily tear substitutes eye drops achieved at the end of treatment, 12 were using tear substitutes less than twice daily as rescue therapy and three did not use tear substitutes at all. The

Table 4 Schirmer I measured at baseline, end of treatment, and follow-up (N=27)

Schirmer test (mm)	Baseline	End of treatment	6 months	12 months
In the left eye				
Mean±SD	5.8±3.1	9.9±6.2	7.3±4.6	10.1±7.0
Median	6.0	11.0	7.5	9.0
Min–max	1.0–10.0	0.0–21.0	0.0–15.0	1.0–27.0
p Value*		<0.001	n.s.	0.002
In the right eye				
Mean (SD)	6.7±3.2	8.0±5.8	9.1±7.5	10.4±8.0
Median	7.0	9.0	8.0	9.0
Min–max	1.0–9.5	0.0–20.0	0.0–30.0	0.0–26.0
p Value*		n.s.	n.s.	0.034

*Between baseline and each evaluation during follow-up.

Table 5 Daily use of tear substitutes (N=27)

No. of drops/day	Baseline	End of treatment	6 months	12 months
Mean±SD	5.5±3.8	3.8±2.8	3.1±2.6	4.0±2.5
Median	4.5	3.0	3.0	3.0
Min–max	1.0–14.5	0.0–12.0	0.0–12.0	0.0–12.0
p Value*		0.003	<0.001	<0.001

*Between baseline and each evaluation during follow-up.

remaining 12 (44%) patients reported to use tear substitute eye drops from 3 to 8 times per day.

Patients provided a subjective evaluation on the maintenance or loss of the result obtained at the end of treatment in the subsequent months. Eight (30%) patients reported that the results of treatment were maintained up to 12 months, 7 (26%) patients that results decreased in the following months and 12 (44%) patients stated that DE was not affected by treatment or that the improvements were quickly lost within the first 2 months after the end of treatment.

Electrical stimulation power applied during study

All patients started both phases of treatment at the nominal power 80 mJ/cm^2/s, as per protocol criteria. Following the first application of QMR during the first phase of treatment (the adhesive electrodes application), we reduced the power to 75 mJ/cm^2/s in two patients, increased it to 90 mJ/cm^2/s in 24 patients, while in one patient the power was not modified. In the second phase of treatment (the hand-piece conductor application), following the first application the power was increased to 100 mJ/cm^2/s in 25 patients and in two patients it was not modified. These powers were then applied unchanged during all the subsequent application sessions.

Safety evaluation

All patients were compliant with the study procedures and underwent all sessions of treatment scheduled by the study protocol.

Adverse effects related to the use of the REXON-EYE occurred in three cases, two patients showed mild cutaneous transitory erythema following the first application of the treatment and one patient generically felt uncomfortable during the first session of treatment. None of these effects was judged as serious. Erythema resolved spontaneously, without recurrences during the following sessions of treatment.

All patients found the treatment very pleasant and none of them asked to stop treatment during stimulation.

Three patients reported blepharitis, conjunctivitis and anterior uveitis (one event each) within the second month of treatment and one patient suffered from a seasonal allergy during the last 2 weeks of treatment. All these effects were mild in severity and not considered related to the treatment.

Intraocular pressure and corneal sensibility, measured after each session of treatment, and uncorrected and best-corrected visual acuity, measured at baseline and at the end of treatment, showed no changes.

DISCUSSION

DE is a chronic disorder and its management is often inadequate, as no established proper cure is available. Patients need to find the better treatment that suits their own condition, must learn how to prevent triggers, and have to refer to doctors in the case of the condition worsening. Tear substitutes, traditional

Downloaded from http://bjo.bmj.com/ on May 30, 2017 - Published by group.bmj.com

warm compresses and heating devices can only help patients to control symptoms to some extent.

In the present study, we show that the periorbital transcutaneous electrical stimulation, with high-frequency low-power microcurrents, significantly affect subjective outcomes and objective measures in patients with DE.

Studies that have investigated the response of cells and tissues to oscillating electrical fields showed that the direct effects of these fields may be attributed to dielectric dispersion, that is, to the variations of the permittivity of a dielectric material in relation to the frequency of the applied electric field.

Although the mechanisms by which the stimulation obtained with high-frequency electrical fields can benefit DE are still unknown, we may offer two possible hypotheses to explain the positive results obtained in the present study, as regards the biological effects induced by this electrical stimulation.

The first hypothesis is that high-frequency low-power microcurrents generated by REXON-EYE could stimulate the self-renewal processes of tissues. A study on cultured muscle fibres[18] showed that QMR determines a change in the membrane potential and increases intracellular free calcium. Therefore, the biological effects of this electric field are strictly related to the cells' biochemistry and the activation of intracellular metabolic pathways.

The second hypothesis is based on the deformation of the cell membranes induced by QMR, which could lead to a cascade of reactions at cellular level capable of increasing the normal metabolism.

It is important to underline that none of these potential mechanisms involves an increase of the tissue temperature to produce a cellular stimulation.

We chose the OSDI score as primary outcome of our study because the main goal of treatment of DE is to improve the symptoms. Moreover, Shiffman[22] showed that OSDI score provides a quantifiable assessment of the frequency of DE symptoms and of their impact on the vision-related function, without the need of a strict correlation between OSDI score and clinical signs. With respect to this, we observed a significant reduction of the OSDI scores at the end of treatment, with a more marked effect on patients with hyposecretive DE.

However, the differential effect in favour of evaporative patients we have found for TBUT, corneal staining and Schirmer test seems to indicate that the evaporative group obtained better objective results.

Whether or not patients with evaporative or hyposecretive DE could differently benefit from the REXON-EYE treatment, and the overall positive effects we have found as well, cannot be proved without a carefully designed randomised clinical trial. Moreover, the difficulties of implementing a placebo group in which the electrodes were placed but not activated, with the risk that patients could easily unmask the mild hear sensation due to the QMR, are another limitation.

However, an important key strength of this study is the long-term follow-up, which allows us to monitor all patients for up to 12 months after the end of treatment and thus appreciate how they were able to basically maintain the improvements over such an extended period of time.

Finally, based on the favourable results provided by this study, scheduling of sessions and the overall duration of treatment should be further evaluated and optimised, in order to shorten and simplify the treatment protocol without affecting its overall efficacy.

In conclusion, this study shows that 2-month treatment with the REXON-EYE is a safe and effective treatment option to improve subjective and objective symptoms in patients with DE, and to reduce the number of applications of rear substitutes eye drops.

Correction notice This article has been corrected since it was published Online First. The in-text citation numbering for Tables 2–4 has been corrected.

Contributors Study design: AF, AR, EP, GM. Research conduction: EP, FB, IM. Data collection and analysis: AF, ACF, FB. Manuscript writing: AF, EP, FB. Manuscript approval: AR, GM.

Funding TELEA Electronic Engineering (Sandrigo, Italy) funded this research.

Disclaimer Results from this study were showed at the 'EUCORNEA annual meeting' 2015.

Data sharing There are no additional unpublished data from the study.

Competing interests None declared.

Patient consent Obtained.

Ethics approval Institutional Ethics Committee Protocol No. TELEA RE, Prog. No. 2223, 24th October 2012.

Provenance and peer review Not commissioned; externally peer reviewed.

REFERENCES

1 No authors listed. Methodologies to diagnose and monitor dry eye disease: report of the diagnostic methodology subcommittee of the international dry eye workshop (2007). *Ocul Surf* 2007;5:108–23.
2 Rolando M, Geerling G, Dua HS, *et al*. Emerging treatment paradigms of ocular surface disease: proceedings of the Ocular Surface Workshop. *Br J Ophthalmol* 2010;94(Suppl 1):i1–9.
3 Baudouin C, Aragona P, Messmer EM, *et al*. Role of hyperosmolarity in the pathogenesis and management of dry eye disease: proceedings of the OCEAN group meeting. *Ocul Surf* 2013;11:246–58.
4 Koffler BH, McDonald M, Nelinson DS, LAC-07-01 Study Group. Improved signs, symptoms, and quality of life associated with dry eye syndrome: hydroxypropyl cellulose ophthalmic insert patient registry. *Eye Contact Lens* 2010;36:170–6.
5 Ayaki M, Toda I, Tachi N, *et al*. Preliminary report of improved sleep quality in patients with dry eye disease after initiation of topical therapy. *Neuropsychiatr Dis Treat* 2016;12:329–37.
6 Gicquel JJ, Bremond-Gignac D. Emerging treatments for dry eye: some like it hot, while others may prefer a cold stimulation. *Br J Ophthalmol* 2013;97:539–40.
7 Aragona P, Rolando M. Towards a dynamic customised therapy for ocular surface dysfunctions. *Br J Ophthalmol* 2013;97:955–60.
8 Bremond-Gignac D, Gicquel JJ, Chiambaretta F. Pharmacokinetic evaluation of diquafosol tetrasodium for the treatment of Sjögren's syndrome. *Expert Opin Drug Metab Toxicol* 2014;10:905–13.
9 Lee IE, Kim NM, Yang JW, *et al*. A randomised controlled trial comparing a thermal massager with artificial teardrops for the treatment of dry eye. *Br J Ophthalmol* 2014;98:46–51.
10 Benitez Del Castillo JM, Kaercher T, Mansour K, *et al*. Evaluation of the efficacy, safety, and acceptability of an eyelid warming device for the treatment of meibomian gland dysfunction. *Clin Ophthalmol* 2014;8:2019–27.
11 Robinson AJ, Snyder-Mackler L. *Clinical electrophysiology: electrotherapy and electrophysiologic testing*. 3rd edn. Baltimore: Lippincott Williams and Wilkins, 2008.
12 Radziszewski K. Outcomes of electrical stimulation of the neurogenic bladder: results of a two year follow up study. *NeuroRehabilitation* 2013;32:867–73.
13 Fergo MF, Steier J. Emerging technology: electrical stimulation in obstructive sleep apnoea. *J Thorac Dis* 2015;7:1286–97.
14 Anastassiou G, Schneegans AL, Selbach M, *et al*. Transpalpebral electrotherapy for dry age-related macular degeneration (AMD): an exploratory trial. *Restor Neurol Neurosci* 2013;31:571–8.
15 Chaikin L, Kashiwa K, Bennet M, *et al*. Microcurrent stimulation in the treatment of dry and wet macular degeneration. *Clin Ophthalmol* 2015;9:2345–53.
16 Lopresti M, Tomba A, Caserta A, *et al*. Studio clinico sull'efficacia della risonanza quantica molecolare nel trattamento dell'edema post-chirurgico in pazienti sottoposti a intervento di artroprotesi di ginocchio. *Archivio di Ortopedia e Reumatologia* 2011;122:34–5. http://link.springer.com/journal/volumesAndIssues/10261
17 Schiavon M, Calabrese F, Nicotra S, *et al*. Favorable tissue effects of quantum molecular resonance device (VESALIUS) compared with standard electrocautery: a novel paradigm in lung surgery. *Eur Surg Res* 2007;39:222–8.
18 Dal Maschio M, Canato M, Pigozzo FM, *et al*. Biophysical effects of high frequency electrical field (4–64 MHz) on muscle fibers in culture. *Basic Applied Myology* 2009;19 (49–56).
19 Mcmakin C. *Frequency specific microcurrent in pain management*. Edinburgh: Churchill/Livingstone/Elsevier, 2011.
20 Pall ML. Electromagnetic fields act via activation of voltage-gated calcium channels to produce beneficial or adverse effects. *J Cell Mol Med* 2013;17:958–65.
21 Bron AJ, Evans VE, Smith JA. Grading of corneal and conjunctival staining in the context of other dry eye tests. *Cornea* 2003;22:640–50.
22 Schiffman RM, Christianson MD, Jacobsen G, *et al*. Reliability and validity of the ocular surface disease index. *Arch Ophthalmol* 2000;118:615–21.

Verona trial results
TBUT 18 MONTH EOT

V0-V1 = baseline
V8 = 1 month into treatment
V13 = end of treatment
V14 = 6 months after treatment
V15 = 18 months after treatment

TBUT
ALL SUBJECT

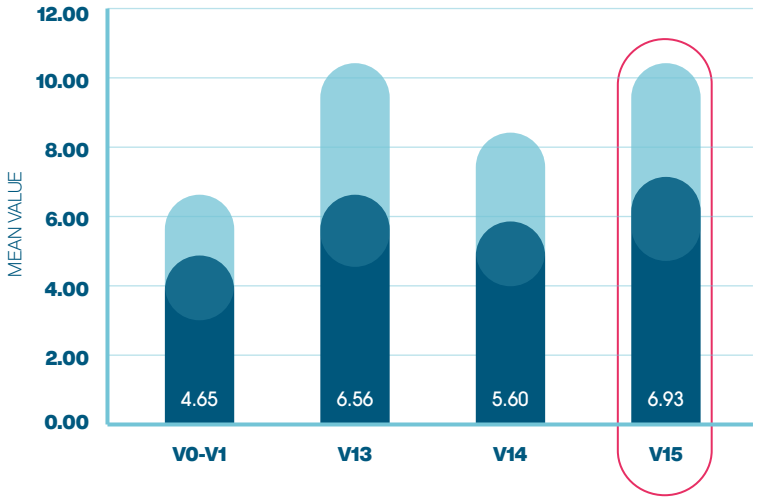

TBUT
EVAPORATIVE

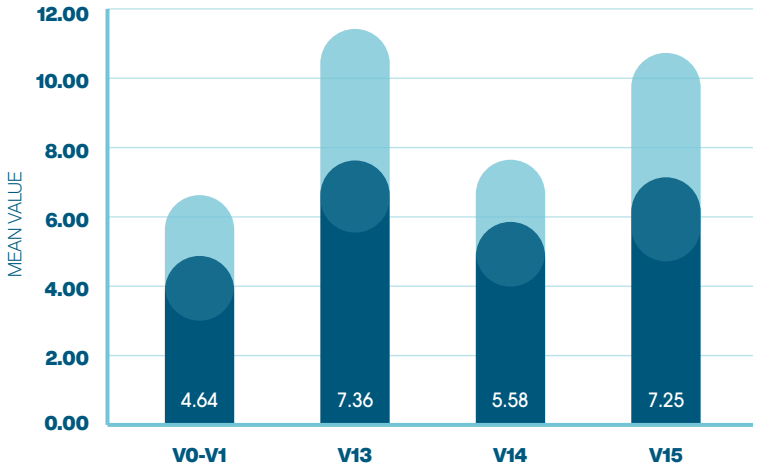

TBUT
HYPOSECRETIVE

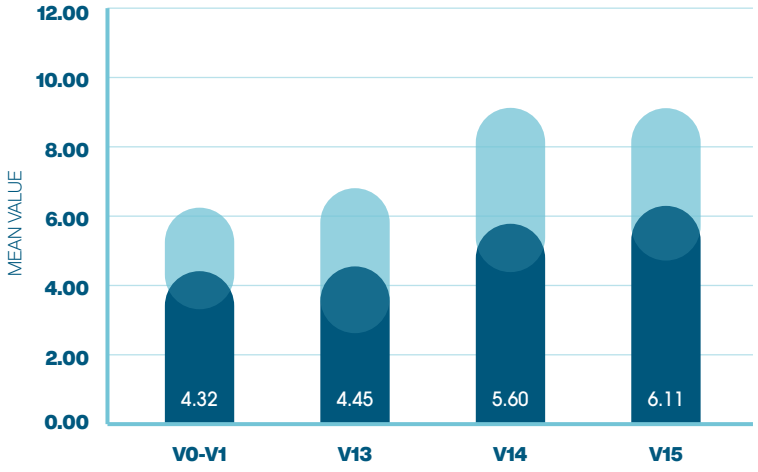

Verona trial results
SCHIRMER'S TEST 18 EOT

V0-V1 = baseline
V8 = 1 month into treatment
V13 = end of treatment
V14 = 6 months after treatment
V15 = 18 months after treatment

SCHIRMER
ALL SUBJECT

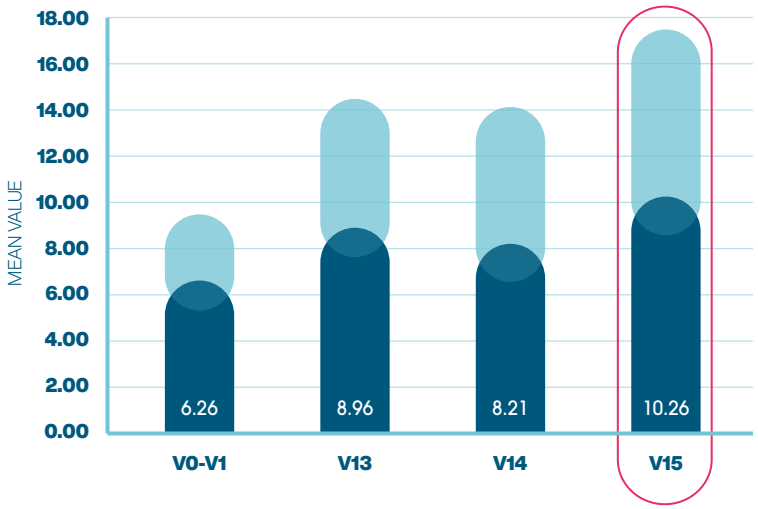

SCHIRMER
EVAPORATIVE

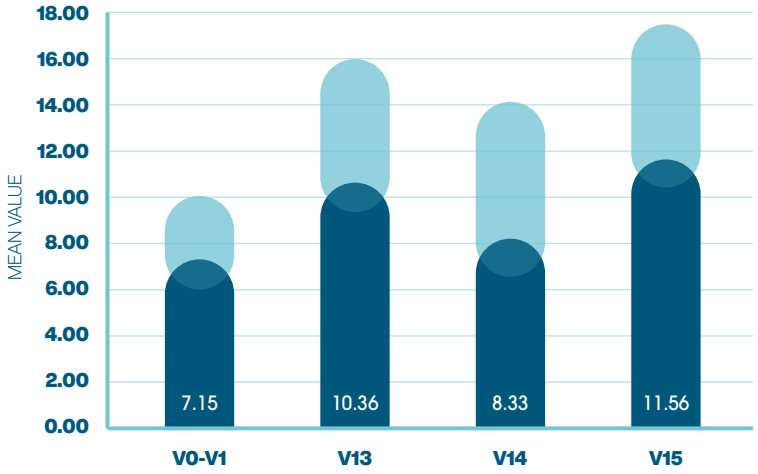

SCHIRMER
HYPOSECRETIVE

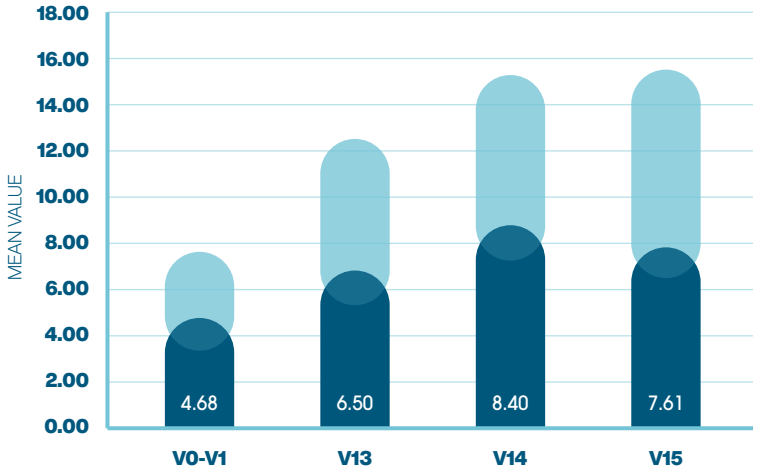

Verona trial results
OSDI 18 MONTHS EOT

V0-V1 = baseline
V8 = 1 month into treatment
V13 = end of treatment
V14 = 6 months after treatment
V15 = 18 months after treatment

OSDI
ALL SUBJECT

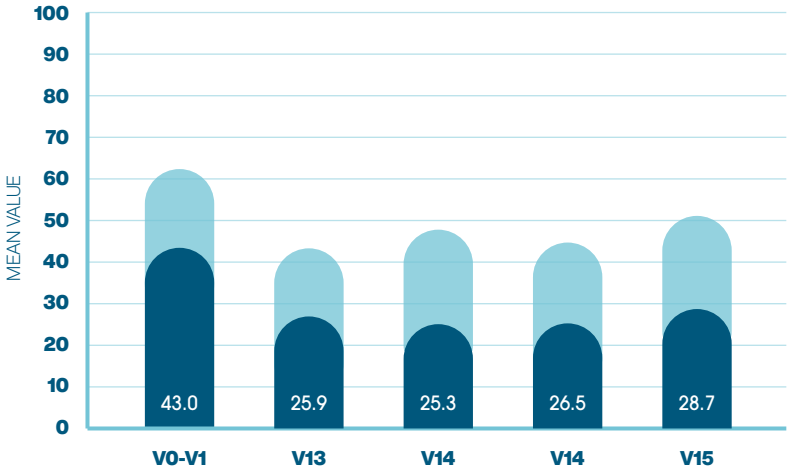

OSDI
EVAPORATIVE

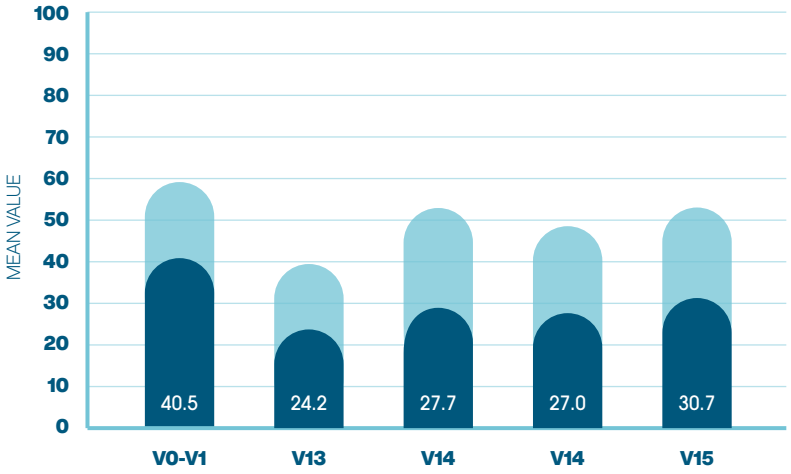

OSDI
HYPOSECRETIVE

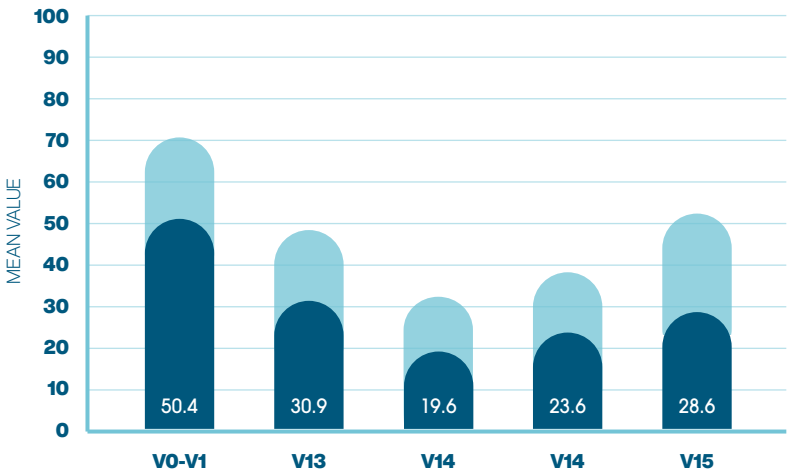

Verona trial results
CS 18 MONTH EOT

V0-V1 = baseline
V8 = 1 month into treatment
V13 = end of treatment
V14 = 6 months after treatment
V15 = 18 months after treatment

OXFORD
ALL SUBJECT

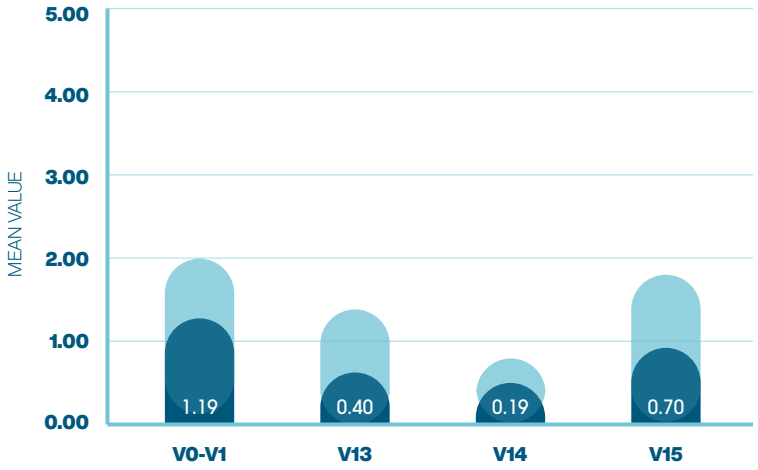

OXFORD
EVAPORATIVE

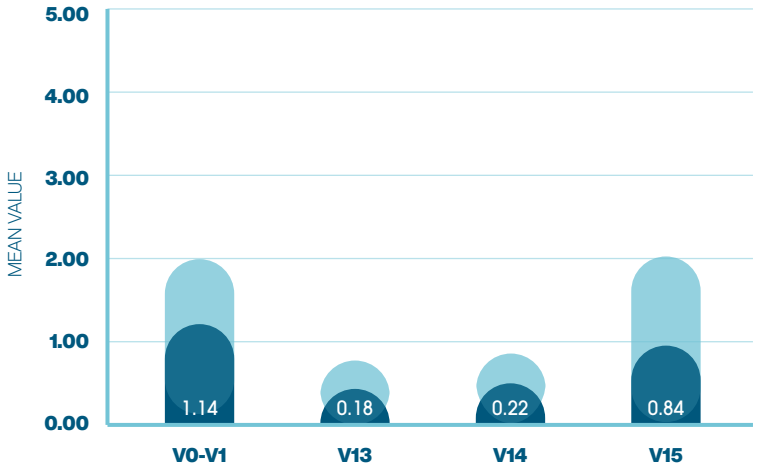

OXFORD
HYPOSECRETIVE

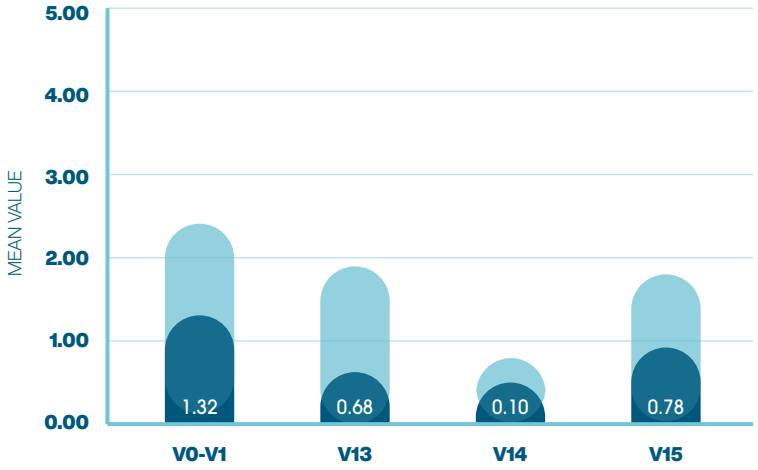

04

High Frequency Electrotherapy for the Treatment of Meibomian Gland Dysfunction

G. Ferrari, A. Colucci, M. Barbariga, A. Ruggeri, P. Rama

High Frequency Electrotherapy for the Treatment of Meibomian Gland Dysfunction

Giulio Ferrari, MD, PhD, Annalisa Colucci, MD,* Marco Barbariga, PhD,* Alfredo Ruggeri, PhD,†‡ and Paolo Rama, MD**

Downloaded from https://journals.lww.com/corneajrnl by BhDMf5ePHKav1zEoum1tQfN4a+kJLhEZgbsIHo4XMi0hCywCX1AWnYQp/IlQrHD3i3D0OdRyi7TvSFl4Cf3VC1y0abggQZXdgGj2MwlZLeI= on 04/09/2020

Purpose: To test the safety and efficacy of high frequency electrotherapy (ET) on the clinical signs and symptoms of patients affected by dry eye and meibomian gland dysfunction (MGD).

Methods: Twenty-five patients affected by MGD were enrolled. Quantum Molecular Resonance ET was administered by means of the Rexon-Eye device 4 times, once per week for 4 weeks. Patients were reexamined 1 month after the last treatment. The primary endpoint was reduction in corneal fluorescein staining. Additional endpoints were tear break-up time, Ocular Surface Disease Index score, meibomian gland secretion score, and the number of expressible meibomian glands. Safety endpoints were Logarithm of the Minimum Angle of Resolution (LogMar) best spectacle-corrected visual acuity and intraocular pressure.

Results: Corneal fluorescein staining improved by 62.5% ($P < 0.0001$), tear breakup time increased by 30.9% ($P < 0.0001$), and the Ocular Surface Disease Index score improved by 37% ($P < 0.001$). The meibum quality and the number of expressible meibomian glands also increased (35.7% and 12%, $P < 0.001$ and $P < 0.0001$, respectively). Schirmer test scores increased after treatment by 16.5% ($P = 0.01$). No adverse events were observed.

Conclusions: Quantum Molecular Resonance ET appears to be safe and significantly reduces symptoms and signs associated with MGD. It may have a relevant role in the treatment of evaporative dry eye disease.

Key Words: meibomian gland disease, dry eye, electrotherapy

(*Cornea* 2019;38:1424–1429)

Dry eye disease (DED) is a highly prevalent and disabling disorder, which affects 9 million persons in the United States alone.[1] Meibomian gland dysfunction (MGD) is a chronic abnormality of the meibomian glands, characterized by duct obstruction and/or qualitative/quantitative changes in gland secretion. As a consequence, the tear film may be altered and clinically apparent ocular surface inflammation can occur.[2] There is no consensus on the exact prevalence of MGD, although it has been reported to be higher than 60% in Asian populations.[3–5] In white populations, the prevalence reached 19.9%.[6] It is generally accepted that when MGD reaches a sufficient degree, it induces evaporative dry eye, although clinical features and symptoms often overlap with aqueous-deficient dry eye, and the 2 clinical conditions are not mutually exclusive.

Available treatments for MGD aim to control inflammation of the ocular surface and/or target the meibomian glands by improving their secretion through physical manipulation and/or by locally increasing the temperature, which is thought to ameliorate the fluidity of the secretion.[7] However, despite the vast armamentarium of drugs and device-based treatments available, MGD still remains an area of unmet medical need.

Quantum Molecular Resonance (QMR) is a technique in which low-intensity, high-frequency (a spectrum of frequencies ranging from 4 MHz to 64 MHz) electric currents are administered to a biological tissue through contact electrodes. Previous data show that this specific stimulation is able to significantly accelerate healing in chronic wounds[8] and to effectively and safely treat symptoms and clinical signs of DED.[9] Although its mechanism of action is still not completely understood, it is known that QMR induces mechanical contraction of the cell surface and downstream activation of intracytoplasmic calcium-dependent pathways.[10] As a result, increased expression of genes involved in tissue regeneration has been observed, possibly through extracellular matrix remodeling.[11] In addition, the expression of matrix metalloproteinase and the infiltration of leukocytes were reduced by cutaneous application of QMR,[8] which supports an anti-inflammatory effect.

Because MGD is an inflammatory ocular disease that affects a large proportion of those diagnosed with DED, we aimed to study the effect of QMR in a cohort of patients with MGD and to quantify its effects by measuring markers specific to the meibomian glands, such as meibum quality and gland expressibility, in addition to ocular symptoms. We administered treatment by using the Rexon-Eye device (Resono Ophthalmic, Trieste, Italy; patented), a new and improved version of the device used in the previous QMR study on DED.[9] Specifically, the new device applies stimulation

Received for publication March 7, 2019; revision received May 27, 2019; accepted May 31, 2019. Published online ahead of print July 23, 2019.
From the *Cornea and Ocular Surface Disease Unit, Eye Repair Lab, IRCCS San Raffaele Scientific Institute, Milan, Italy; †Resono Ophthalmic, Trieste, Italy; and ‡Department of Information Engineering, University of Padova, Padova, Italy.
This study has been funded by Resono Ophthalmic
A. Ruggeri has a financial interest in the company Resono Ophthalmic. The remaining authors have no conflicts of interest to disclose.
Correspondence: Giulio Ferrari, Cornea and Ocular Surface Disease Unit, Eye Repair Lab, IRCCS San Raffaele Scientific Institute, Via Olgettina 60 20132 Milan, Italy (e-mail: ferrari.giulio@hsr.it).
Copyright © 2019 Wolters Kluwer Health, Inc. All rights reserved.

Copyright © 2019 Wolters Kluwer Health, Inc. Unauthorized reproduction of this article is prohibited.

FIGURE 1. Rexon-Eye device. Top panel: An exploded view of the Rexon-Eye goggle electrode, with electronic board (1), temperature sensors (2), active electrodes (3), external plastic shell (4), internal rubber layer (5), internal sponge filling (6). Bottom panel: The Rexon-Eye device, with electrical generator (left side) and goggle electrode (right side).

on the epidermis of closed eyelids up to the lid border by means of ad hoc-designed goggles (Fig. 1). In this way, the treatment is applied by placing the goggles directly onto the target area (MG), thereby making the treatment operator independent and comfortable.

In this study, we present the results of a nonrandomized interventional clinical trial designed to test the safety and efficacy of the treatment using Rexon-Eye in a cohort of patients affected with mild or moderate MGD.

MATERIALS AND METHODS

Study approval was obtained from the local ethics committee. Informed consent was obtained from all the patients enrolled in the study, and potential risks and benefits were discussed before enrollment. This protocol was compliant with the requirements of the Health Insurance Portability and Accountability Act and the tenets of the Declaration of Helsinki.

In this prospective, open-label, single-center, single-group study, we have tested patients affected by mild or moderate MGD the safety and efficacy of the QMR treatment administered with the new Rexon-Eye device.

Patient Selection

Eligible participants were 18 years of age or older, with a clinical diagnosis of DED and MGD in both eyes, positive corneal or conjunctival staining (score included between 1 and 10 on the Oxford Grading Scale). Additional inclusion criteria were a tear breakup time (TBUT) score less than 10 seconds, meibomian gland expressibility score between 1 and 2 (as per the International Workshop on the MGD grading scale[2]), meibomian gland secretion quality between 4 and 13 (as per the International Workshop on MGD[2]), and quantifiable ocular discomfort score measurable on the Ocular Surface Disease Index (OSDI) higher than 12. In addition, included patients did not present anomalies in eyelid position and closure, and, if women, they were not pregnant. Patients affected with active ocular infections were excluded.

Treatment

Twenty-five patients were enrolled in this study. One patient's follow-up was missed because of job relocation. The protocol provided four 20-minute sessions of QMR treatment using Rexon-Eye, once per week, followed by 4 weeks of washout. Treatment was administered using the ad hoc-designed goggles, applied on the closed eyelids (Fig. 1). The intensity was set at 5 (custom unit), corresponding on average to a power of 12 W, with 60 V voltage and 200 mA current between the goggle electrode and the neutral plate electrode. The device interface displays the applied power using a custom unit scale, marked from 0 to 10, where 0 corresponds to no power applied and 10 corresponds to maximum power. This latter value depends on the specific patient electrical impedance and is on average 24 W. Patients were instructed to report any discomfort experienced during or after the sessions. Study visits were performed at weeks 1, 2, 3,

Copyright © 2019 Wolters Kluwer Health, Inc. All rights reserved.

Copyright © 2019 Wolters Kluwer Health, Inc. Unauthorized reproduction of this article is prohibited.

and 4 and before treatment administration. The final evaluation was performed 1 month after the last treatment (ie, 2 months after enrollment). Enrolled patients were allowed to maintain only application of artificial tears as needed and warm compresses twice a day. All other medications used to treat MGD (ie, tetracyclines or other antibiotics), supplements, topical antibiotics or corticosteroids, or cyclosporine were washed out for 2 weeks before enrollment. Patients were asked to report the frequency of the application of artificial tears at the enrollment and last visit.

Clinical Endpoints

The primary end point was reduction in corneal fluorescein staining (CFS). This was measured 3 minutes after the instillation of moistened 1% fluorescein strips (Fluostrips), at the slit lamp under cobalt blue light. Secondary endpoints included the following: 1) change in the TBUT (measured 3 minutes after the instillation of fluorescein), 2) change in the quality of meibomian gland secretion, 3) change in the number of expressible meibomian glands, 4) change in the OSDI score, 5) Schirmer test without anesthesia (as per the TFOS DEWS II report-Diagnostic Methodology-Schirmer Test), 6) visual acuity, 7) intraocular pressure measurements, and 8) frequency of artificial tears use.

Safety endpoints were ocular or systemic side effects related to the treatment.

Statistical Analysis

To obtain the study power, we considered—based on preliminary results—a type 1 error equal to 0.05, a type 2 error of 0.2, a standard deviation in the primary endpoint equal to 1.3. This led us to consider that 25 patients should be enrolled, considering a 10% loss at the follow-up, to test our hypothesis.

We averaged the scores from both eyes for all measured variables with the exception of the OSDI, where only 1 score per subject was obtained.

To assess the effect of treatment, we compared the distribution of scores for each outcome measure before and after treatment using the t test for continuous and ordinal variables. Nonparametric tests were used in other cases. Two-sided $P < 0.05$ was considered statistically significant for all comparisons. The statistical analysis was performed with GraphPad Prism (GraphPad Software, La Jolla, CA).

RESULTS

The mean age was 54 years ± 13.4. The M:F ratio was 5:20. Twenty-five patients were enrolled in this study. One patient's follow-up was missed because of job relocation; hence, the analysis was performed on 24 patients.

Primary Endpoint

CFS

One month after treatment, CFS decreased on average by 62.5%, from 1.29 ± 0.38 to 0.52 ± 0.49 ($P < 0.0001$, Fig. 2A).

Nonprimary Endpoints

TBUT

One month after treatment, the TBUT increased on average by 30.9%, from 5.96 ± 1.01 to 7.71 ± 1.21 after treatment ($P < 0.0001$, Fig. 2B).

Patient Symptoms (OSDI Score)

The treatment reduced the OSDI scores reduced on average by 37.0%, from 47.19 ± 20.20 to 31.96 ± 24.21 ($P = 0.0003$, Fig. 2C).

Meibomian Gland Expressibility

Expressibility of the glands was ameliorated by the treatment. Specifically, the score decreased on average by 12.5%, from 2.00 to 1.75 ± 0.42 ($P < 0.0001$, Fig. 2D). Reduction of this score stands for more expressible glands and, hence, improvement of blepharitis.

Meibum Quality

One month after treatment, the score decreased (ie, improved quality) on average by 35.7%, from 9.44 ± 1.78 to 6.00 ± 1.48 ($P < 0.0001$, Fig. 2E).

Schirmer Test

One month after treatment, it increased on average by 16.5%, from 12.42 ± 4.98 to 13.90 ± 5.01 ($P = 0.01$ Fig. 2F).

Other Endpoints

The frequency of artificial tears use dropped on average by 51.2%, from 4.96 ± 3.37 to 2.52 ± 2.65, before and after treatment, respectively ($P < 0.0001$, Fig. 2G).

Visual acuity was not affected by the treatment (0.1416 ± 0.1393 Logarithm of the Minimum Angle of Resolution (LogMAR) before vs. 0.1267 ± 0.1432 LogMAR after treatment, $P = 0.129$, Fig. 3A).

Intraocular pressure was 14.30 ± 1.46 mm Hg before and 13.98 ± 1.14 mm Hg after treatment, which was not statistically significant ($P = 0.17$, Fig. 3B).

Safety Evaluation

No adverse events related to the use of Rexon-Eye were reported.

DISCUSSION

In this article, we provide evidence of the safety and efficacy of the QMR-based electrotherapy (ET) for MGD-related DED. We observed improvement in a number of clinical parameters, including CFS, TBUT, expressibility of meibomian glands, and meibum quality. Patient-reported symptoms were significantly alleviated, and the frequency of lubricant application was significantly reduced.

QMR-based ET has been used for years in the treatment of cutaneous ulcers, where its postulated mechanism of action includes reduced tissue infiltration of leukocytes and modulation of metalloproteinase expression.[8] On a broader perspective, ET was shown to increase the secretion of salivary glands.[12–14] In the ocular field, electrical stimulation of the

Copyright © 2019 Wolters Kluwer Health, Inc. All rights reserved.

Copyright © 2019 Wolters Kluwer Health, Inc. Unauthorized reproduction of this article is prohibited.

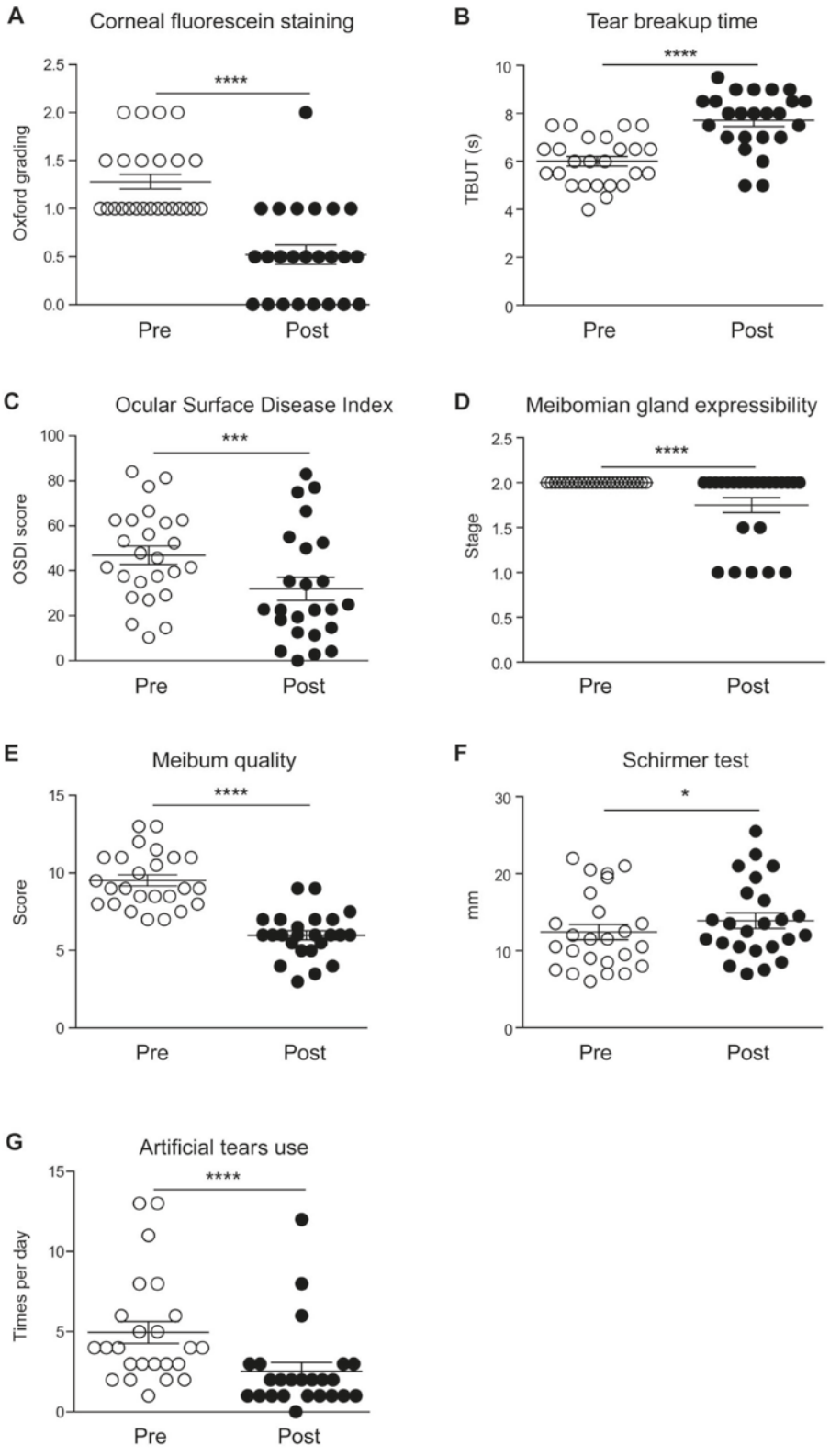

FIGURE 2. Clinical outcomes of Rexon-eye ET. A, ET treatment significantly reduced CFS ($P < 0.0001$). B, TBUT was increased by ET ($P < 0.0001$). C, The Ocular Surface Disease Index was reduced by ET ($P = 0.0003$). D and E, The number of expressible meibomian glands and meibum quality were also improved by ET ($P < 0.0001$). F, Tear secretion, measured with the Schirmer test, improved after ET ($P = 0.01$). G, The frequency of self-administered artificial tears use decreased after ET ($P < 0.0001$). The graphs represent mean values ± Standard Error of the Mean (SEM). Statistics were performed with paired *t* test analysis or the Wilcoxon signed-rank test, as appropriate (*$P < 0.05$, **$P < 0.01$, ***$P < 0.001$, ****$P < 0.0001$).

Copyright © 2019 Wolters Kluwer Health, Inc. All rights reserved.

Copyright © 2019 Wolters Kluwer Health, Inc. Unauthorized reproduction of this article is prohibited.

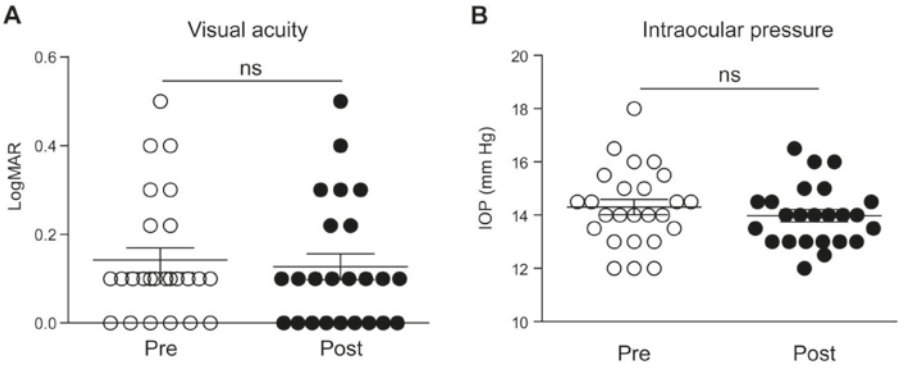

FIGURE 3. Rexon-Eye ET does not significantly alter visual acuity or intraocular pressure. A, Measurements of best spectacle-corrected visual acuity (expressed as LogMAR) did not significantly change after treatment. B, Intraocular pressure (measured in mm Hg) did not significantly change before and after treatment. IOP = intraocular pressure.

ethmoidal nerve successfully increased tear secretion.[15] In this vein, the fact that meibomian glands are richly innervated by the autonomic and sensory nervous system[16] makes ET an attractive tool to modulate their activity in the setting of MGD.

Notably, the treatment was apparently safe, with no reported adverse events and an excellent patient tolerability. Specifically, visual acuity remained stable after treatment, and so did intraocular pressure. This is relevant because the standard treatment of DED includes chronic use of topical corticosteroids, which are associated with a significant risk of intraocular pressure elevation.

No side effects were reported, including minor complications, which is encouraging because the previous version of the device induced cutaneous transitory erythema in 2 patients and 1 patient was uncomfortable during the first session.[9] In addition, no discomfort was reported by any patient after treatment.

The primary outcome, CFS, did not improve in 3 patients. Of these, 1 was the oldest patient recruited (patient no. 23, who was 83 years old). Although it is difficult to draw conclusions from these limited numbers, it may be that ET is less effective in patients of advanced age and/or with long-term disease. The other 2 nonresponders (patient no. 9 and no. 15) did not seem to share any characteristics that may explain the absence of improvement in CFS. Anyway, it should be noted that 71% of patients (17 of 24) showed complete corneal fluorescein clearing in at least 1 eye. Thirty percent of patients (8 of 24) had bilateral complete resolution of CFS.

We cannot fully elucidate the mechanism(s) through which the QMR stimulation exerted its action in patients with MGD, although we hypothesize that an antiinflammatory effect may be involved. In this vein, it is known[8] that QMR significantly reduces the expression of proinflammatory molecules, such as matrix metalloproteinases, which is increased in MGD.[17]

Treatment administration also results in a modest increase in local temperature, 3 to 4°C in all the subjects, as measured with an infrared camera (data not shown). Because local delivery of heat is known to improve meibomian gland function, it is possible that the local temperature increase associated with QMR could also have a role in clinical improvement, although only for a limited time. In any case, it should be noted that heat-based treatments for MGD are normally effective when the temperature is more elevated, approximately 45°C.[18]

Our data corroborate those of the previous study by Pedrotti et al,[9] where Rexon-Eye showed efficacy in a cohort of 27 patients by allowing a significant clinical improvement in signs of DED. However, differently from our trial, the number of patients with MGD was limited (only 7 patients), and no direct measure of meibomian gland function was collected, which makes it difficult to draw definitive conclusions in that specific patient subset. Interestingly, we found that 1 month of treatment (4 treatment sessions), followed by a 1-month washout, was already effective in inducing an increase in Schirmer test scores. In this vein, patients with evaporative DE enrolled by Pedrotti et al[9] also showed increased tear secretion, although with a longer treatment duration (2 months, 12 treatment sessions). It is noteworthy that our treatment protocol was able to ameliorate tear secretion after such a short treatment course because it is known that clinical endpoints used to evaluate the ocular surface and tear production are generally poorly correlated, as reported by many others.[19–21]

QMR was previously[9] administered through periorbital skin electrodes and by an operator using a skin probe, twice a week for 1 month, followed by once per week treatment for 1 additional month, for a total of 12 sessions. In our study, treatment duration was reduced to 4 sessions, once per week, was operator independent because eyelid goggles were used, and efficacy was maintained 1 month after the last treatment.

We acknowledge that our study population was composed of patients with mild or moderate MGD and that the follow-up was limited to 1 month, which may be considered short-term given the chronic nature of the disease. This study was the first to test the goggle-based, operator-independent device, which was different from the one used in a previous trial.[9] This study was designed to preliminarily test the safety and efficacy of such a novel apparatus. Clearly, a randomized clinical trial, and longer-term follow-up, would strengthen our findings, although masking may prove difficult because of the mild heat sensation provided by the active treatment. Further studies are in the pipeline to address these shortcomings.

Regardless of these observations, our results show that the Rexon-Eye ET is effective in the treatment of mild or moderate MGD, is apparently safe and well tolerated, and can significantly reduce the need to use artificial tears.

Copyright © 2019 Wolters Kluwer Health, Inc. All rights reserved.

Copyright © 2019 Wolters Kluwer Health, Inc. Unauthorized reproduction of this article is prohibited.

ACKNOWLEDGMENT

QMR is a registered trademark by Telea Electronic Engineering, Italy.

REFERENCES

1. Novack GD, Asbell P, Barabino S, et al. TFOS DEWS II report. *Ocul Surf.* 2017;15:629–649.
2. Nichols KK, Foulks GN, Bron AJ, et al. The international workshop on meibomian gland dysfunction: executive summary. *Invest Ophthalmol Vis Sci.* 2011;52:1922–1929.
3. Lin PY, Tsai SY, Cheng CY, et al. Prevalence of dry eye among an elderly Chinese population in Taiwan: the Shihpai Eye Study. *Ophthalmology.* 2003;110:1096–1101.
4. Uchino M, Dogru M, Yagi Y, et al. The features of dry eye disease in a Japanese elderly population. *Optom Vis Sci.* 2006;83:797–802.
5. Jie Y, Xu L, Wu YY, et al. Prevalence of dry eye among adult Chinese in the Beijing Eye Study. *Eye (Lond).* 2009;23:688–693.
6. McCarty CA, Bansal AK, Livingston PM, et al. The epidemiology of dry eye in Melbourne, Australia. *Ophthalmology.* 1998;105:1114–1119.
7. Mandal P, Khan MI, Shah S. Drugs—do we need them? Applications of non-pharmaceutical therapy in anterior eye disease: a review. *Cont Lens Anterior Eye.* 2017;40:360–366.
8. Fraccalvieri M, Salomone M, Di Santo C, et al. Quantum molecular resonance technology in hard-to-heal extremity wounds: histological and clinical results. *Int Wound J.* 2017;14:1313–1322.
9. Pedrotti E, Bosello F, Fasolo A, et al. Transcutaneous periorbital electrical stimulation in the treatment of dry eye. *Br J Ophthalmol.* 2017;101:814–819.
10. Dal Maschio M, Canato M, Pigozzo FM, et al. Biophysical effects of high frequency electrical field (4–64 MHz) on muscle fibers in culture. *Basic Appl Myology.* 2009;19:49–56.
11. Sella S, Adami V, Amati E, et al. In-vitro analysis of Quantum Molecular Resonance effects on human mesenchymal stromal cells. *PLoS One.* 2018;13:e0190082.
12. Konidena A, Sharma D, Puri G, et al. Effect of TENS stimulation of saliva in postmenopausal women with or without oral dryness: an interventional study. *J Oral Biol Craniofac Res.* 2016;6(suppl 1):S44–S50.
13. Hasegawa Y, Sugahara K, Sano S, et al. Enhanced salivary secretion by interferential current stimulation in patients with dry mouth: a pilot study. *Oral Surg Oral Med Oral Pathol Oral Radiol.* 2016;121:481–489.
14. Zadik Y, Zeevi I, Luboshitz-Shon N, et al. Safety and efficacy of an intra-oral electrostimulator for the relief of dry mouth in patients with chronic graft versus host disease: case series. *Med Oral Patol Oral Cir Bucal.* 2014;19:e212–e219.
15. Brinton M, Kossler AL, Patel ZM, et al. Enhanced tearing by electrical stimulation of the anterior ethmoid nerve. *Invest Ophthalmol Vis Sci.* 2017;58:2341–2348.
16. Knop E, Knop N, Millar T, et al. International workshop on meibomian gland dysfunction: report of the subcommittee on anatomy, physiology, and pathophysiology of the meibomian gland. *Invest Ophthalmol Vis Sci.* 2011;52:1938–1978.
17. Luo L, Li DQ, Corrales RM, et al. Hyperosmolar saline is a proinflammatory stress on the mouse ocular surface. *Eye Contact Lens.* 2005;31:186–193.
18. Borchman D, Foulks GN, Yappert MC, et al. Human meibum lipid conformation and thermodynamic changes with meibomian-gland dysfunction. *Invest Ophthalmol Vis Sci.* 2011;52:3805–3817.
19. Perry HD, Solomon R, Donnenfeld ED, et al. Evaluation of topical cyclosporine for the treatment of dry eye disease. *Arch Ophthalmol.* 2008;126:1046–1050.
20. Sall K, Stevenson OD, Mundorf TK, et al. Two multicenter, randomized studies of the efficacy and safety of cyclosporine ophthalmic emulsion in moderate to severe dry eye disease. CsA Phase 3 Study Group. *Ophthalmology.* 2000;107:631–639.
21. Goyal S, Chauhan SK, Zhang Q, et al. Amelioration of murine dry eye disease by topical antagonist to chemokine receptor 2. *Arch Ophthalmol.* 2009;127:882–887.

Copyright © 2019 Wolters Kluwer Health, Inc. All rights reserved.

Copyright © 2019 Wolters Kluwer Health, Inc. Unauthorized reproduction of this article is prohibited.

05

Evaluating the efficacy of Quantum Molecular Resonance (QMR) electrotherapy in mixed-type dry eye patients

A. Trivli, E. Karmiris, G. Dalianis, A. Ruggeri, C. Terzidou

Journal of Optometry 000 (xxxx) 1 - 7

Journal of Optometry
www.journalofoptometry.org

ORIGINAL ARTICLE

Evaluating the efficacy of Quantum Molecular Resonance (QMR) electrotherapy in mixed-type dry eye patients

Alexandra Trivli[a], Efthymios Karmiris[b,*], Georgios Dalianis[a], Alfredo Ruggeri[c], Chryssa Terzidou[a]

[a] *Department of Ophthalmology, Konstantopouleio-Patission General Hospital, Athens, Greece*
[b] *Department of Ophthalmology, Hellenic Air Force General Hospital, P. Kanellopoulou Av. 3, 11525 Athens, Greece*
[c] *Resono Ophthalmic, Sandrigo, Italy*

Received 21 December 2021; accepted 16 June 2022
Available online xxx

KEYWORDS
Tear dysfunction;
Ocular surface disease;
MMP-9;
Therapeutic device;
QMR

Abstract
Purpose: To evaluate the efficacy and safety of the low-power, high-frequency electrical current treatment administered by the Rexon-Eye device, in a cohort of patients affected by mixed-type dry eye disease (DED) of medium to severe level.
Patients and methods: In this prospective, non-randomized, interventional clinical study, eighteen mixed type DED patients were treated. Treatment was a specific type of electrotherapy, Quantum Molecular Resonance (QMR®), administered by means of the Rexon-Eye® device (Resono Ophthalmic, Sandrigo, Italy) with a protocol of one 20-min session per week, for 4 weeks. Patients were examined at baseline and one month after the last treatment, utilizing the Ocular Surface Disease Index (OSDI) questionnaire and clinical signs: non-invasive tear break-up time (NIBUT), Oxford staining, meibum quality, meibography, meibomian gland expressibility, tear meniscus height (TMH), Schirmer's test, ocular inflammation expressed by MMP-9 concentration.
Results: Subjective benefit in OSDI was reported ($p = 0.013$). Improvement was also observed in NIBUT ($p < 0.001$), Oxford staining ($p = 0.002$), expressible meibomian glands number ($p = 0.001$) and meibum quality ($p < 0.001$). A remarkable benefit was present in inflammation, as evidenced by the reduction of MMP-9 ($p = 0.003$). Changes, although not statistically significant, were also present in TMH ($p = 0.076$) and Schirmer's test ($p = 0.675$), whereas no change was observed in meibography score. No adverse event was reported.
Conclusion: In this mixed-type DED patients' cohort, Rexon-Eye proved to be effective and safe in improving subjective and objective ocular parameters, as well as capable to normalize inflammatory markers.
© 2022 Spanish General Council of Optometry. Published by Elsevier España, S.L.U. This is an open access article under the CC BY-NC-ND license (http://creativecommons.org/licenses/by-nc-nd/4.0/).

* Corresponding author.
E-mail address: tkarmiris@yahoo.com (E. Karmiris).

https://doi.org/10.1016/j.optom.2022.06.003
1888-4296/© 2022 Spanish General Council of Optometry. Published by Elsevier España, S.L.U. This is an open access article under the CC BY-NC-ND license (http://creativecommons.org/licenses/by-nc-nd/4.0/).

Please cite this article in press as: A. Trivli, E. Karmiris, G. Dalianis et al., Evaluating the efficacy of Quantum Molecular Resonance (QMR) electrotherapy in mixed-type dry eye patients, *Journal of Optometry* (2022), https://doi.org/10.1016/j.optom.2022.06.003

Introduction

Dry eye disease (DED), more broadly defined as tear dysfunction, is a common ocular condition that needs prompt diagnosis and careful treatment intervention.[1,2] It is a multifactorial disease of the ocular surface characterized by loss of homeostasis of the tear film, with a potential discordance between dry eye signs and symptoms.[1,2] The reported prevalence of DED varies widely, from 5% to 33%, depending on both population and diagnostic criteria; however, there is a consensus that is higher among women as compared to men and increases with age.[2] The total estimated burden of DED has been placed at 9.3% of adult Americans with the prevalence being 11.3% among all adults greater than 50 years of age and as high as 22.8% among women greater than 75 years of age.[2] Evaporative and aqueous deficient are recognized as the two main subtypes of DED with potential overlap in their presentation. Meibomian gland dysfunction (MGD), leading to an abnormality in the tear lipid layer, is the leading cause of evaporative dry eye disease.[3]

Tear film instability, hyperosmolarity, inflammation, and cellular damage, which are the main mechanisms contributing to the physio-pathological process, are regarded as triggers of the vicious cycle occurring in DED.[3] Multiple inflammatory markers, including matrix metalloproteinase 9 (MMP-9), have been isolated from the tear film of patients with DED.[4-6] MMPs secreted into tears in DED can destroy tight junctions in the ocular surface epithelium reflecting the loss of ocular surface barrier function.[7,8] Tear film hyperosmolarity in DED triggers the stress-activated protein kinase, signaling a cascade which, in turn, leads to the release of MMP-9 from corneal epithelial cells. This cascade initiates a progressive inflammation cycle.[7,8]

Proper diagnosis of ocular surface diseases requires the careful observation of a patient's symptoms and the measurement of signs through various tests.[1] There is, therefore, considerable interest in finding methods that can measure ocular surface, tear film and Meibomian glands parameters objectively, reproducibly, and noninvasively. The TFOS DEWS II recommended using automated noninvasive measurement techniques that allow for an objective assessment of the DED signs.[9]

The goal of DED treatment is to restore homeostasis of the ocular surface and tear film by breaking this vicious cycle.[1,10] The TFOS DEWS II management and therapy report presents a stepwise approach to the treatment of DED, which ranges from education, environmental or dietary modifications, artificial tear substitutes, punctal plugs, topical and/or systemic anti-inflammatory medications up to surgery.[1] However, alternative therapies, especially for MGD, are emerging on the market, namely the use of vibration, massage, thermotherapy or thermal pulsation.[11]

Our study employed a specific type of electrotherapy device, Rexon-Eye® by Resono Ophthalmic, based on the QMR® stimulation. This technology produces and delivers, through electrical fields, an electrical stimulation with specific high-frequencies (from 4 to 64 MHz) and low intensity, which appears to be in resonance, i.e., has the same frequency, with the molecular bonds in biological tissue, and is thus able to maximize the transfer of power from the electrical stimulus signal to the biological tissue, with a minimum heat dissipation. This signal was also shown to obtain an important effect, i.e., the stimulation of the metabolism and natural regeneration of biological tissue and cells. It is possible to explain this effect by considering several phenomena generated by QMR and experimentally observed, such as a mechanical deformation of the cell membrane and an increase of calcium release and metabolism.[12] Furthermore, using sophisticated micro-array techniques to evaluate gene expression, a more recent in-vitro study on mesenchymal stromal cells has shown that QMR is able to up-regulate genes involved in the extracellular matrix (ECM) remodeling, embryogenesis, wound healing and angiogenesis.[13] It is of interest to note, for the possible application to the healing of corneal wounds, the positive results obtained by the QMR-based therapy in the healing of deep wounds in the limbs.[14]

Rexon-Eye was successfully employed to treat DED patients[15] as well as MGD patients[16] but was not clinically tested yet on mixed type DED patients. Our working hypothesis is that QMR can stimulate also in these patients the metabolism and natural regeneration of cells, resulting in the reactivation of the lacrimal and Meibomian gland tissue and benefit of the ocular annexes.[15,16]

The present study was therefore designed to assess efficacy and safety of QMR-based electrotherapy in a group of moderate to severe mixed type DED patients, utilizing objective diagnostic tools to evaluate symptoms, clinical signs as well as the inflammatory component.

Material and methods

This prospective, non-randomized, interventional clinical study was conducted in the Ophthalmology Department of Konstantopouleio-Patission General Hospital, Athens, Greece. The study was in accordance with the tenets of the Declaration of Helsinki and the study protocol was approved by the hospital ethics committee (29,931/05.12.2019). All patients received oral and written information about the study and signed an informed consent form before receiving the examinations.

Patient selection

The study population consisted of eighteen mixed type DED patients (17 female and 1 male; age range 42–81 years) that were randomly recruited. Patients were enrolled from the external diseases' outpatient clinic, presenting for their first appointment and were quasi-randomly allocated to treatment, by utilizing the last digit (odd or even) of their hospital number. The initial screening was performed with the OSDI questionnaire. Patients that reported an OSDI (Ocular Surface Disease Index) larger or equal to 13 were evaluated further with the DEWS II homeostasis markers of NIBUT (tear Non-Invasive Break Up Time) and corneal staining by Oxford scale. The ones with a NIBUT less than 10 s and/or corneal staining of more than 1 in Oxford scale were considered as DED cases according to DEWS II criteria and evaluated further in order to document the components of the mixed type of disease. A detailed ophthalmic history was evaluated, and a complete eye examination was carried out,

including best corrected visual acuity (BCVA) assessment, intraocular pressure (IOP) measurement by Goldman applanation tonometry, slit lamp biomicroscopy and fundus examination. Participants with a history of ocular surgery, trauma, inflammation other than that attributed to DED, contact lens use, current or prior long-term topical ocular medication or other ocular pathology were excluded from the study. Patients with occasional usage of lubricant eye drops were included in the study, however a washout period of one week before commencement of treatment with Rexon-Eye was established by the study protocol, in order to avoid any confounding factors. Patients were advised against usage of any lubricant drops during the period of treatment.

Treatment

Treatment was delivered with the Rexon-Eye device (Resono Ophthalmic, Sandrigo, Italy), with a protocol of one 20-minute session per week, for four weeks. Treatment is administered by placing a custom designed mask over closed eyelids and closing the electrical circuit with a neutral plate the patient sits on. Special disposable facial tissues are worn between the mask and the eyelid surface, to evenly spread the electrical stimulation in the affected area and protect the eyes from potential transmission of bacteria and other pathogens. A custom unit scale is used by the device interface to display the applied power; the scale goes from 0 to 10, with 0 corresponding to no power applied. Intensity was set at 5 in our protocol, corresponding to an average power of 12 W, with 60 V voltage and 200 mA current between the mask electrodes and the neutral plate electrode. Patients were instructed to report any discomfort experienced during or after the sessions.

Patient evaluation

Our primary endpoint was change in OSDI, a 12-item patient-reported outcome questionnaire designed to provide rapid assessment of the range of ocular surface symptoms related to chronic dry eye disease, their severity, and their effect on the patient's ability to function.[9]

Our secondary endpoints included changes in NIBUT, TMH (Tear Meniscus Height), meibography score, number of expressible Meibomian glands on lower eyelid, quality of meibum, corneal staining by Oxford scale grading, Schirmer's test, and MMP-9.

NIBUT, TMH, and infrared meibography for the measurement of meibography score were assessed with the IDRA® ocular surface analyzer (SBM Sistemi, Turin, Italy). For the detection of expressible Meibomian glands, we used the Meibomian Gland Evaluator (MGE, TearScience Inc., Morrisville, USA), a tool that applies constant pressure analogous to that of a blink for 10–15 s and leads to the expression of approximately 8 meibomian glands, provided the secretion is liquid in consistency, in three positions: nasal, central and temporal.[17] For the glands with a normal appearance that did not yield liquid secretion using the MGE, forceful expression was performed with digital pressure.

Corneal staining by Oxford scale was then assessed, since it requires fluorescein. Corneal staining was divided into six groups according to severity, from 0 (absent) to 5 (severe).[18] We compared the overall appearance of the patient's corneal staining with a reference figure, simulating the pattern of staining encountered in dry eye disease. Schirmer's test with anesthetic was performed 10 min after the evaluation of corneal staining.

The inflammatory component of DED was evaluated with the MMP-9 test (InflammaDry, Quidel Co., San Diego, CA, USA), which assays tear MMP-9 levels producing a dichotomous, positive or negative, outcome.[19] The eye with the worse symptoms was selected and documented for MMP-9 sampling at first visit, and at the last visit, the same eye was used for comparison.

Evaluation of Meibomian gland secretion quality is one of the most informative parameters, despite being a difficult one to evaluate. Based on previous publications,[17] we followed a semiquantitative quality evaluation scale of 1 = clear, 2 = cloudy, 3 = granular and 4 = toothpaste. The evaluation of meibum quality was performed after all diagnostic procedures, in order to avoid any effect of the expressed secretions on the tear film.

Patients were evaluated at baseline and one month after the end of the treatment. All measurements in all visits were performed by the same investigator (AT).

Statistical analysis

Since the applied treatment affected both eyes equally and intraclass correlation coefficient between the two eyes was high (close to unity), scores from both eyes were averaged for all the measured variables except for our primary outcome OSDI and MMP-9, where only 1 score per subject was obtained. All statistical analyses were performed using the SPSS software version 25 (SPSS Inc, Chicago, USA). Shapiro-Wilk test was used to test parameters for normality. Descriptive statistics were used to calculate mean, average and standard deviation of all data. Paired t-tests and Wilcoxon signed ranks test were used to compare the average values of measurements for each outcome before and after treatment. Values were considered statistically significant at $p < 0.05$. Graphs were generated using GraphPad Prism (GraphPad Software, La Jolla, CA).

Results

Patient characteristics and parameter values before and after treatment are presented in Table 1. Of a total of 22 patients initially enrolled in the study, 18 patients completed the protocol, 17 women and one man, due to lost follow-up as they lived in rural areas and were not able to follow protocol intervals. Mean age was 59.66 ± 13.02 years.

Primary endpoint

A statistically significant change in OSDI score was detected, from 45.46 ± 21.86 at the initial visit to 34.45 ± 23.79 ($p = 0.013$) at last visit, eight weeks after enrollment, which represents a 25% improvement. A monotonic decreasing trend was noticed during treatment (Figs. 1 and 2).

Table 1 Values of the measured parameters, (mean, SD, 95% confidence interval) at baseline (Before) and one month after the end of the treatment (After), with statistical significance of the difference.

	Before (mean±SD) 95% CI (min to max)	After (mean±SD) 95% CI (min to max)	*p* value
Total Patients	18		
Male/female	1/17		
Age (years)	59.66 ± 13.02 (53.19-66.14)		
OSDI	45.46 ± 21.86 (34.59-56.34)	34.45 ± 23.79 (22.61-46.28)	0.013
MG number	9.63 ± 3.27 (8.01-11.26)	12.83 ± 2.26 (11.70-13.96)	0.001
Meibum quality	3.33 ± 0.90 (2.88-3.78)	1.66 ± 0.76 (1.28-2.04)	<0.001
Oxford staining	1.41 ± 0.98 (0.92-1.90)	0.55 ± 0.66 (0.22-0.88)	0.002
NIBUT	6.71 ± 1.40 (6.01-7.41)	9.53 ± 2.28 (8.40-10.67)	<0.001
TMH	0.52 ± 0.25 (0.40-0.65)	0.36 ± 0.20 (0.26-0.46)	0.076
Schirmer's	8.75 ± 4.98 (6.27-11.22)	9.19 ± 5.63 (6.39-11.99)	0.675
Meibography	15.05 ± 7.95 (11.09-19.01)	14.88 ± 7.21 (11.30-18.47)	0.926
Positive MMP-9	12	3	0.003

Notes: All parameters follow normal distribution tested by Shapiro-Wilk test for normality. *P* values exported by paired *t*-test and Wilcoxon signed rank test, as appropriate.
Abbreviations: OSDI, Ocular Surface Disease Index; MG, meibomian glands; NIBUT, non-invasive tear break-up time; TMH, tear meniscus height; MMP-9, Matrix metalloproteinase 9; SD, standard deviation.

Secondary endpoints

NIBUT

After treatment, NIBUT increased by 42%, from 6.71 ± 1.40 to 9.53 ± 2.28 s ($p < 0.001$, Fig. 2).

TMH

Tear meniscus height values were normalized, decreasing by 31% from 0.52 ± 0.25 to 0.36 ± 0.20 mm ($p = 0.076$).

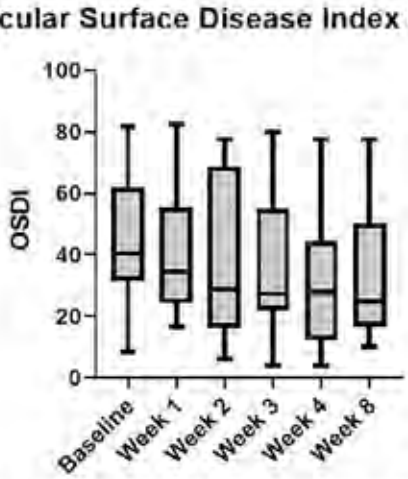

Fig. 1 Time course of the OSDI parameter (mean value and SD bars).

Meibography

Meibomian gland score as recovered by IR meibography did not show any significant change, from 15.05 ± 7.95 to 14.88 ± 7.21 percent ($p = 0.926$).

Meibomian gland expressibility

The number of expressible Meibomian glands on lower lid improved after treatment by 33%, from 9.63 ± 3.27 to 12.83 ± 2.26 ($p = 0.001$, Fig. 2).

Meibum quality

A significant improvement, by 50%, was noticed in meibum quality at the end of treatment, from grade 3.33 ± 0.90 to grade 1.66 ± 0.76 ($p < 0.001$, Fig. 2).

Staining by oxford scale

At the end of treatment, a significant decrease, by 61%, in corneal staining was detected, with Oxford grade decreasing from 1.41 ± 0.98 to 0.55 ± 0.66 ($p = 0.002$, Fig. 2).

MMP-9

At baseline, twelve out of eighteen patients had positive MMP-9. One month after treatment, only three patients had positive MMP-9, a 75% improvement ($p = 0.003$, Fig. 2).

Schirmer's

One month after treatment, there was a slight but not statistically significant improvement in Schirmer's values, from 8.75 ± 4.98 to 9.19 ± 5.63 mm ($p = 0.675$).

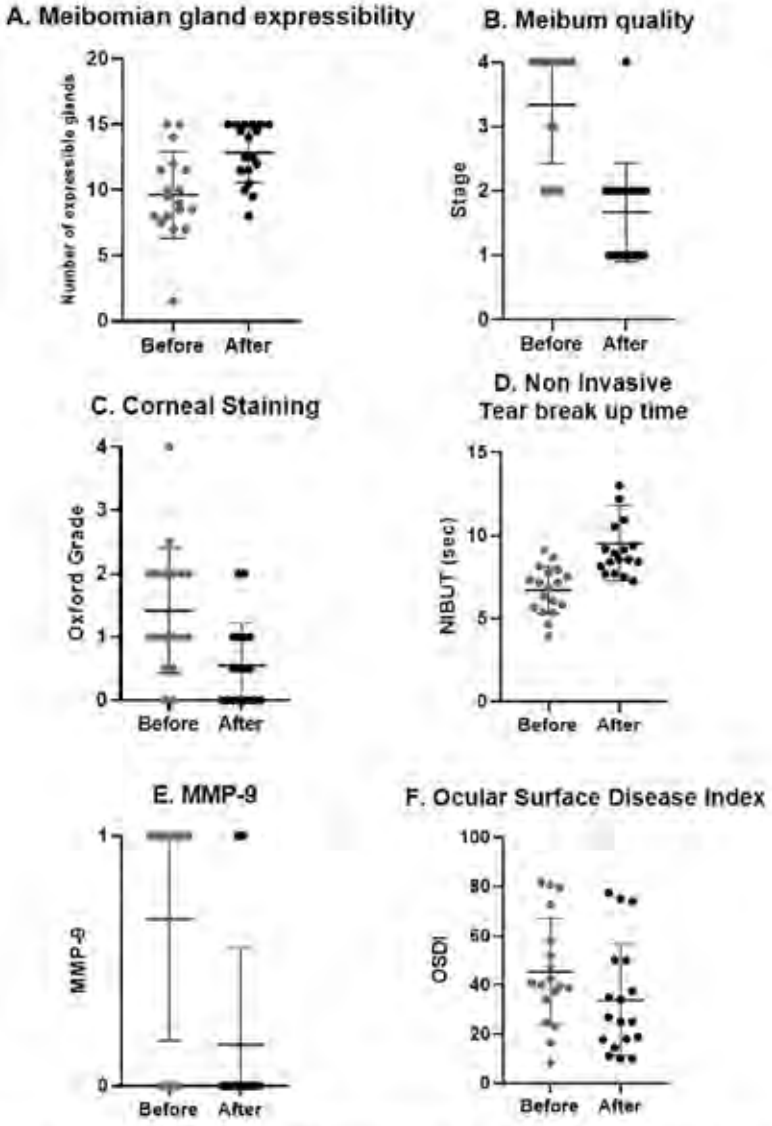

Fig. 2 Clinical outcomes after treatment. A, number of expressible meibomian glands significantly increased ($p = 0.001$). B, meibum quality significantly improved ($p < 0.001$). C, corneal staining significantly decreased ($p = 0.002$). D, NIBUT significantly increased ($p < 0.001$). E, number of patients with positive MMP-9 test significantly decreased ($p = 0.003$). F, OSDI significantly decreased ($p = 0.013$).

Safety evaluation

Compliance was observed in all study patients regarding sessions of treatment scheduled by the study protocol. All patients reported a pleasant feeling during treatment and none of them asked for interruption during stimulation. At the end of each session, a routine eye check was performed, and no adverse events were reported.

Discussion and conclusion

Our study evaluated the safety and efficacy of the treatment with the QMR-based electrotherapy administered by Rexon-Eye in a mixed-type cohort of medium to severe DED patients.

Electromagnetic fields play an essential role in cellular functions, interacting with cellular pathways and tissue physiology. Cells interact with the surrounding environment through receptors and ion channels that transmit chemical, mechanical, and electrical signals.[10]

In this context, the Quantum Molecular Resonance (QMR) produces and delivers, through electrical fields, an electrical stimulation with specific high-frequencies (4–64 MHz) and low intensity. This unique stimulation can obtain an important effect, i.e., the stimulation of the metabolism and natural regeneration of biological tissue and cells.

As regards the specific application of QMR to ophthalmology, previous results showed that this technology is able to effectively and safely treat symptoms and signs of DED.[15,16] Our results confirm those of these two previous studies and extend them to the specific case of mixed DED.

In case of DED, the available severity criteria are confounded by complex disease subtypes and a lack of standardization. Therefore, the selection of single criteria for assessment of disease severity is fraught with difficulties.[12] In the DEWS II diagnosis report, several diagnostic tests are listed, including questionnaires, tear film tests, epithelial abnormalities assessment strategies, and other approaches.[9] The report indicated that the most appropriate and efficacious protocol to diagnose and monitor DED is based on a combination of symptoms, signs, and clinical tests, since any one of these alone would miss some patients.[9]

Considering these guidelines, several subjective and objective clinical parameters have been considered in our study. Patient-reported symptoms reflected by OSDI, our primary outcome, were significantly alleviated. What is more interesting, a gradual improvement in OSDI scores in each one of the four session visits of our therapeutic protocol reflects the effect of each session as well as the additive effect of the whole four-sessions treatment. From our secondary outcomes, both NIBUT and corneal staining, which according to DEWS II are two of the critical diagnostic signs of DED, were statistically significantly improved. There was also a significant improvement in the quality of MG expression, which is clinically translated into a better quality of tear film. In addition, a significant improvement was also observed in inflammation, as documented by the marked reduction in MMP-9.

Control of inflammation seems to play a pivotal role in improving symptomatology, since it is a major component in the pathophysiology underlying the long-standing and more severe types of DED.[4,5] Our purpose was to evaluate the efficacy of treatment protocol not only in symptoms and signs but also regarding the response to the existent inflammation. In this test, levels above 40 ng/ml produce a positive result, however it is a nonspecific marker as regards the source of ocular surface inflammation.[17] Our results document an improvement by 75% (p = 0.003), with only three patients producing a positive MMP-9 test after treatment, compared to twelve out of eighteen patients before treatment. To the authors' knowledge, this is the first study to evaluate the effect of Rexon-Eye treatment in inflammation.

The improvement in the quality of MG production and the reduction of inflammation allowed an overall improvement in tear film homeostasis, which is eventually what one requests from a DED treatment. Reduction of MMP-9 accompanied by improvement of patient-reported symptoms and objective clinical signs confirms the anti-inflammatory effect of Rexon-Eye, as well as the correlation between inflammation and clinical outcomes. The probable mechanism behind the relationship between improvement of meibum quality and tear inflammatory component could be explained by the pathogenesis of MGD. Increased meibum viscosity may arise from the changes in meibum composition.[13] Ocular surface inflammation and quality of Meibomian gland secretions are interactively involved in the cascade of the pathophysiologic mechanism of MGD. Increase in MG viscosity promotes to meibum stasis that can in turn promote bacterial growth, which potentially could lead to the increased release of esterases and lipid-degrading lipases.[10] It has been shown that increased enzyme activity increases meibum melting temperature, generating also free fatty acids that can lead to hyper-keratinization and inflammation.[10] These changes in lipid composition lead to further Meibomian gland obstruction, ocular surface instability, and increased tear evaporation, contributing to the development of DED and patient discomfort.[10] In our patients, the number of expressible glands on lower lid improved after treatment by 33%, alongside meibum quality, which improved from a mean granular composition to a mean clear to cloudy composition, supporting this hypothesis.

From our results there is a suggestion that the improvement in inflammation in conjunction with improvement in MG quality might be important therapeutic targets in patients with MGD. The QMR treatment significantly reduces the expression of proinflammatory molecules, such as matrix metalloproteinases, which is increased in MGD.[14,21] This improvement is related to the stabilization of the ocular surface, also supported by the normalization in the tear meniscus height, whose average decreased from 0.52 to 0.36 mm, possibly attributed to control of inflammation.

The limitations of this study include a relatively small sample size and lack of a control group. Potential risks of placebo effect and investigator bias were greatly reduced by the objective tools used to assess clinical outcomes. By implementing IDRA, InflammaDry, MGE, and the strict guidelines of DEWS II criteria, our effort aimed at standardizing treatment outcomes to ensure that the measurement quality of the acquired data is less likely to be compromised.

The follow-up period after treatment termination was indeed short. Although a previous study showed that clinical benefits from Rexon-Eye therapy are basically maintained one year after the treatment,[11] further investigations are needed to confirm these long-term results also in the specific population of mixed-type DED patients. In addition, since Rexon-Eye is a fairly new technology in dry eye disease treatment, different protocols should be examined in the future, depending potentially on the severity of disease. It would also be of interest to examine the changes in dry eye parameters in the course of treatment in order to investigate future amendments in treatment protocols.

Future studies with larger sample sizes and longer follow-up times might be helpful in replicating and extending our findings, which however established Rexon-Eye as a significant therapeutic option that effectively widens our armamentarium in the treatment of DED.

Declaration of Competing Interest

Author AR has financial interest in Resono Ophthalmic. All other authors report no conflict of interest in this work.

Acknowledgments

We would like to thank Resono Ophthalmic, Sandrigo, Italy for providing us the Rexon-Eye device used in this study.

References

1. Stapleton F, Alves M, Bunya VY, et al. TFOS DEWS II epidemiology report. *Ocul Surf*. 2017;15(3):334–365.
2. Geerling G, Baudouin C, Aragona P, et al. Emerging strategies for the diagnosis and treatment of meibomian gland dysfunction: proceedings of the OCEAN group meeting. *Ocul Surf*. 2017;15(2):179–192.
3. Willcox MDP, Argüeso P, Georgiev GA, et al. TFOS DEWS II tear film report. *Ocul Surf*. 2017;15:366–403.
4. Acera A, Rocha G, Vecino E, et al. Inflammatory markers in the tears of patients with ocular surface disease. *Ophthalmic Res*. 2008;40:315–321.
5. Chotikavanich S, de Paiva CS, Li de Q, et al. Production and activity of matrix metalloproteinase-9 on the ocular surface increase in dysfunctional tear syndrome. *Invest Ophthalmol Vis Sci*. 2009;50:3203–3209.
6. Aragona P, Aguennouz M, Rania L, et al. Matrix metalloproteinase 9 and transglutaminase 2 expression at the ocular surface in patients with different forms of dry eye disease. *Ophthalmology*. 2015;122(1):62–71.
7. Hessen M, Akpek EK. Dry eye: an inflammatory ocular disease. *J Ophthalmic Vis Res*. 2014;2:240–250.
8. Sambursky R, Davitt 3rd WF, Latkany R, et al. Sensitivity and specificity of a point-of-care matrix metalloproteinase 9 immunoassay for diagnosing inflammation related to dry eye. *JAMA Ophthalmol*. 2013;131:24–28.
9. Lee JM, Jeon YJ, Kim KY, et al. Ocular surface analysis: a comparison between the LipiView® II and IDRA®. *Eur J Ophthalmol*. 2020:1120672120969035.
10. O'Neil EC, Henderson M, Massaro-Giordano M, et al. Advances in dry eye disease treatment. *Curr Opin Ophthalmol*. 2019;30(3):166–178.
11. Ferrari G, Colucci A, Barbariga M, et al. High frequency electrotherapy for the treatment of meibomian gland dysfunction. *Cornea*. 2019;38(11):1424–1429.
12. Sella S, Adami V, Amati E, et al. In-vitro analysis of Quantum Molecular Resonance effects on human mesenchymal stromal cells. *PLoS One*. 2018;13(1).
13. Fraccalvieri M, Salomone M, Di Santo C, et al. Quantum molecular resonance technology in hard-to-heal extremity wounds: histological and clinical results. *Int Wound J*. 2017;14:1313–1322.
14. Sullivan BD, Whitmer D, Nichols KK, et al. An objective approach to dry eye disease severity. *Invest Ophthalmol Vis Sci*. 2010;51:6125–6130.
15. Pedrotti E, Bosello F, Fasolo A, et al. Transcutaneous periorbital electrical stimulation in the treatment of dry eye. *Br J Ophthalmol*. 2017;101(6):814–819.
16. Miller KL, Walt JG, Mink DR, et al. Minimal clinically important difference for the ocular surface disease index. *Arch Ophthalmol*. 2010;128(1):94–101.
17. Tomlinson A, Bron AJ, Korb DR, et al. The international workshop on meibomian gland dysfunction: report of the diagnosis subcommittee. *Invest Ophthalmol Vis Sci*. 2011;52(4):2006–2049.
18. Korb DR, Blackie CA. Meibomian gland diagnostic expressibility: correlation with dry eye symptoms and gland location. *Cornea*. 2008;27:1142–1147.
19. Wolffsohn JS, Arita R, Chalmers R, et al. TFOS DEWS II diagnostic methodology report. *Ocul Surf*. 2017;15:539–574.
20. Costin GE, Birlea SA, Norris DA. Trends in wound repair: cellular and molecular basis of regenerative therapy using electromagnetic fields. *Curr Mol Med*. 2012;12(1):14–26.
21. Nelson JD, Shimazaki J, Benitez-del-Castillo JM, et al. The international workshop on meibomian gland dysfunction: report of the definition and classification subcommittee. *Invest Ophthalmol Vis Sci*. 2011;52(4):1930–1937.

06

Quantum Molecular Resonance Electrical Stimulation as a Beneficial and Safe Treatment for Multifactorial Dry Eye Disease

D. Kavroulaki, E. Konstantinidou, A. Tsiogka, K. Rallis, E. Mavrikakis

Cureus

Open Access Original Article

DOI: 10.7759/cureus.39695

Quantum Molecular Resonance Electrical Stimulation as a Beneficial and Safe Treatment for Multifactorial Dry Eye Disease

Dimitra Kavroulaki [1], Elena Konstantinidou [1], Anastasia Tsiogka [2], Konstantinos Rallis [1], Emmanuel Mavrikakis [1]

1. Ophthalmology, General Hospital of Athens G. Gennimatas, Athens, GRC 2. Opthalmology, General Hospital of Athens G. Gennimatas, Athens, GRC

Corresponding author: Dimitra Kavroulaki, dimitrakavroulaki@gmail.com

Review began 05/18/2023
Review ended 05/28/2023
Published 05/30/2023

© **Copyright** 2023
Kavroulaki et al. This is an open access article distributed under the terms of the Creative Commons Attribution License CC-BY 4.0., which permits unrestricted use, distribution, and reproduction in any medium, provided the original author and source are credited.

Abstract

Introduction: To assess the clinical benefits obtained with transcutaneous low-power, high-frequency quantum molecular resonance (QMR) electrotherapy in a group of multifactorial dry eye patients.

Methods: Fifty-one patients (total of 102 eyes) with dry eye symptoms were enrolled in the study. Included clinical conditions were meibomian gland dysfunction, glaucoma, cataract surgery within the past six months, and autoimmune disease-related superficial punctuate keratitis. The QMR treatment was administered using the Rexon-Eye device (Resono Ophthalmic, Sandrigo, Italy) for four consecutive weeks, with one 20-minute treatment session per week. The measured ocular parameters included non-invasive tear break-up time (NIBUT), corneal interferometry, lower eyelid meibography, and tear meniscus height, all measured at baseline, at the end of treatment, and two months after the end of treatment. The Ocular Surface Disease Index (OSDI) questionnaire was gathered at the same time. The study has received approval from our institution's ethics committee.

Results: At the end of treatment, interferometry, tear meniscus height, and OSDI score improved at a statistically significant level. No statistically significant change was observed in NIBUT or meibography. At two months after the end of treatment, all parameters showed a statistically significant improvement, namely NIBUT, meibography, interferometry, tear meniscus, and OSDI score. No adverse events or side effects were reported.

Conclusions: The QMR electrotherapy by the Rexon-Eye device shows statistically significant improvement of dry eye clinical signs and symptoms with a duration of at least two months.

Categories: Ophthalmology, Healthcare Technology
Keywords: ocular surface disease, meibomian gland disease, quantum molecular resonance, transcutaneous electrical stimulation, dry eye

Introduction

The significant increment at all ages of symptoms of dry eye disease (DED), due to air pollution, overuse of beauty products, and excessive screen time, has prompted the development of new, more effective treatment strategies for dry eye. A recent promising approach is electrical stimulation based on quantum molecular resonance (QMR). This innovative technology is based on the transcutaneous delivery of low-intensity, high-frequency alternating electrical current producing high-frequency non-ionizing waves (4 MHz to 64 MHz). The electromagnetic fields produced have been shown to be capable of stimulating the metabolism and natural regeneration of biological tissue and cells. It is possible to explain this effect based on various phenomena generated by the QMR stimulation and experimentally observed: mechanical deformation of the cell membrane, increase in calcium release, and activation of signaling pathways [1]. Using sophisticated microarray techniques to evaluate gene expression, a more recent in vitro study on mesenchymal stromal cells has shown that QMR is able to up-regulate genes involved in extracellular matrix (ECM) remodeling, embryogenesis, wound healing, and angiogenesis [2]. This technology has been shown to provide excellent results in wound healing in human patients [3] and, more recently, in animal studies related to very severe corneal inflammation [4]. QMR was then applied with the Rexon-Eye device (Resono Ophthalmic, Sandrigo, Italy) in the treatment of DED [5]. Several studies have provided evidence that it stimulates and reactivates all aspects of the lacrimal system, improving tear and lipid secretion and providing significant benefits to patients [5-8]. The aim of this study is to assess the effect of this treatment in a cohort of patients suffering from multifactorial dry eye disease, including meibomian gland dysfunction, cataract surgery, glaucoma, and keratitis related to autoimmune disease.

Materials And Methods

Fifty-one patients (102 eyes) randomly selected from the outpatient clinic of our tertiary hospital were

How to cite this article
Kavroulaki D, Konstantinidou E, Tsiogka A, et al. (May 30, 2023) Quantum Molecular Resonance Electrical Stimulation as a Beneficial and Safe Treatment for Multifactorial Dry Eye Disease. Cureus 15(5): e39695. DOI 10.7759/cureus.39695

enrolled in the study. The median age was 57.4 years ± 15.67 (SD) (range, 21 to 84 years). 12 (23.53%) were male, and 39 (76.47%) were female. Inclusion criteria were dry eye symptoms with a value higher than 18 as quantified by the Ocular Surface Disease Index (OSDI) questionnaire, caused by meibomian gland dysfunction (27 patients), glaucoma (two patients), cataract surgery within the past six months (four patients), and superficial punctuate keratitis related to autoimmune disease, specifically primary Sjogren, thyroid eye disease, and rheumatoid arthritis (18 patients). Treatment was performed with the Rexon-Eye device, which consists of a generator transmitting a low-power, high-frequency alternating electrical current to a specially designed mask containing two electrodes, one for each eye. The mask was placed over the patient's closed eyelids, and the current was applied to the eyelids and periocular skin for 20 minutes, with a 30-second alternation between eyes. The session was repeated once per week for a total of four consecutive weeks, according to manufacturer guidelines. The IDRA device (SBM Sistemi, Turin, Italy) was used to objectively quantify dry eye ocular parameters, specifically non-invasive tear break-up time (NIBUT), corneal interferometry, lower eyelid meibography, and tear meniscus height. This ocular surface analyzer provides a personalized measurement of the three layers of the tear film and the meibomian glands of the upper and lower eyelids. Interferometry evaluates the lipid layer thickness, the tear meniscus, and the thickness of the tears on the eyelid margin, providing information on the tear volume. NIBUT evaluates the stability of the mucin layer between blinking and meibography, which is the visualization of the glands through the illumination of the eyelid with infrared light, measuring meibomian gland loss. All ocular parameters were measured before the initiation of treatment (baseline), at the end of the fourth and last session, and two months after the end of treatment. Patients' satisfaction was recorded at the same time with the Speed II Ocular Surface Disease Index questionnaire. Subjective evaluation of symptoms and satisfaction was documented on a scale from zero to four and was all added up to a final number. The study has received approval from our institution's ethics committee. Informed consent was obtained from all patients. Recruitment of patients, treatment protocols, and measurements were conducted by the same physicians. All 51 patients (a total of 102 eyes) were analyzed as one group. At the two-month follow-up, only 32 patients managed to attend. Data analysis was performed with STATA version 13 (StataCorp LLC, Texas, USA), comparisons of score values were performed with the paired t-test for normally distributed differences, and all reported p-values were based on two-sided tests and compared to a significance level of 5%.

Results

At the end of the treatment (EoT), interferometry ($p=0.021$), tear meniscus height ($p = 0.002$), and OSDI score ($p<0.001$) improved to a statistically significant level compared to baseline values. There was no statistically significant change in the values of NIBUT ($p=0.891$) and lower eyelid meibography ($p=0.962$). At the two-month follow-up, a total of 32 patients were analyzed. With respect to baseline, NIBUT showed a statistically significant increase ($p = 0.002$), and lower eyelid meibography showed a statistically significant decrease in glands loss ($p=0.003$) when compared to baseline values. The scores remained significantly improved in the interferometry values ($p<0.001$), tear meniscus ($p<0.001$), and OSDI scores ($p<0.001$). No adverse events or side effects were recorded. No thermal or electrical burns were noted (Table 1 and Figure 1).

	NIBUT	Interferometry	Meibography	Tear meniscus	OSDI score
Baseline	7.50± 0.18	53.32± 1.8	25.28±2.57	0.81±0.04	10.83±0.57
EoT	7.53±0.19	58.13±2.2	25.46±2.52	0.94±0.04	7.63±0.62
p-value	0.891	0.021	0.962	0.002	<0.001
Two months after EoT	7.59±0.18	59.77±2.60	23.98±2.89	0.74±0.04	6.38±0.63
p-value	0.002	<0.001	0.003	<0.001	<0.001

TABLE 1: Statistical analysis of results at baseline, end of treatment, and two months after the end of treatment

EoT: end of treatment, NIBUT: non-invasive tear break-up-time, OSDI: Ocular Surface Disease Index

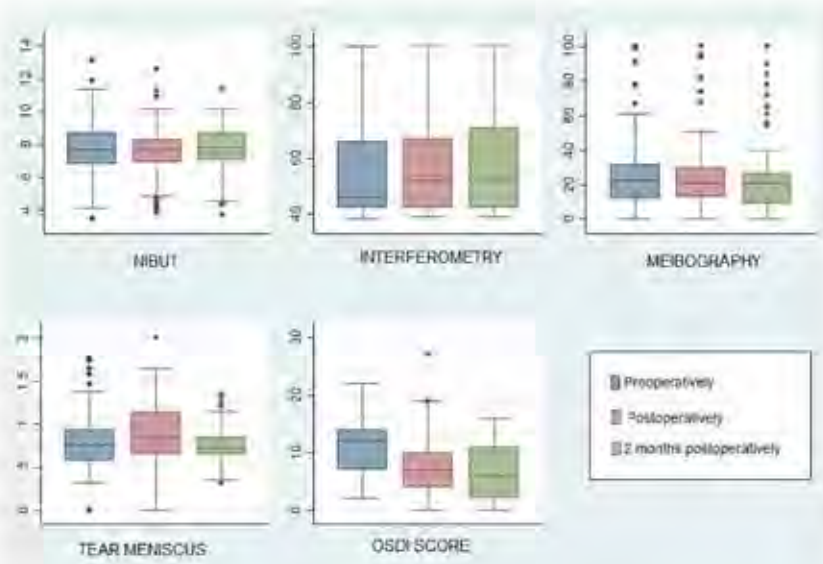

FIGURE 1: Box plots of each examined variable baseline (pre-operatively), end of treatment (post-operatively), and two months after the end of treatment (two months post-operatively)

Discussion

This larger-scale study supports and confirms the safety and efficacy of the QMR technology in the treatment of DED, as shown in previous studies [3-5] and also in our cohort of multifactorial dry eye patients. The different etiology of the dry eye signs and symptoms in our patients might have hampered the outcome of the treatment, but on the other hand, it shows promising results not only in patients with meibomian gland dysfunction but also in patients with autoimmune diseases like rheumatoid arthritis, primary Sjogren syndrome, and thyroid eye disease. All objectively measured ocular parameters showed significant improvement post-treatment, as did patients' subjective symptoms of irritation, itching, ocular redness, and discomfort for a period of two months. The treatment appears to reactivate the lacrimal system, supposedly through the regeneration of goblet and lacrimal gland cells, improving tear secretion early in the course of treatment. Meibomian glands appear to regenerate later in time with an increase in their number, affecting lipid layer secretion and tear break-up time around two months post-therapy. There are few studies related to electrotherapy for DED. The study by Cai and Zhang [9] tested the efficacy and safety of the combination of transcutaneous electrical stimulation, with a current at 20 Hz and therefore not based on the QMR effect, with artificial tears on 44 eyes. The electrodes were placed on the periorbital skin, and treatment was administered for 20 sessions (five sessions per week for four weeks). They reported a statistically significant improvement in OSDI scores, tear break up time (TBUT), Schirmer's I test, and corneal fluorescein staining at four weeks after treatment, with no adverse events. As regards the studies specifically related to QMR electrotherapy in DED, Pedrotti et al. [5] applied periorbital stimulation using skin electrodes and manually with a handpiece conductor moved by the operator in 12 sessions over a period of two months. They reported statistically significant improvements in OSDI scores, TBUT, Schirmer's I test, and fluorescein staining at the six- and twelve-month follow-ups, with a reduced need for artificial tears. Ferrari et al. [6] tested the effects of the Rexon-Eye treatment on 25 patients with meibomian gland dysfunction, showing significant reductions in all the signs and symptoms of DED associated with gland dysfunction taken into account in their study. Trivli et al. [7] have applied QMR technology to the treatment of mixed-type DED, with remarkable improvements in signs and symptoms, in particular as regards lipid layer composition and corneal inflammation. More recently, Shemer et al. [8] presented the preliminary results obtained in a subset of patients from their randomized controlled trial with the Rexon-Eye, where significant improvements were obtained in OSDI, meibomian gland disease score, and corneal staining in treated subjects versus controls.

Conclusions

This study has confirmed in our cohort of multifactorial DED patients the significant improvement of dry eye clinical signs and symptoms observed in other clinical studies employing QMR electrotherapy with the Rexon-Eye device with a duration of at least two months. Further investigations with a longer follow-up period may be needed to fully elucidate the expected duration of the benefits for the patients and the

improved range of clinical conditions.

Additional Information

Disclosures

Human subjects: Consent was obtained or waived by all participants in this study. Ethics Committee General Hospital of Athens G. Gennimatas issued approval 2021-1234. The study has received approval from our institution's ethics committee . **Animal subjects:** All authors have confirmed that this study did not involve animal subjects or tissue. **Conflicts of interest:** In compliance with the ICMJE uniform disclosure form, all authors declare the following: **Payment/services info:** All authors have declared that no financial support was received from any organization for the submitted work. **Financial relationships:** All authors have declared that they have no financial relationships at present or within the previous three years with any organizations that might have an interest in the submitted work. **Other relationships:** All authors have declared that there are no other relationships or activities that could appear to have influenced the submitted work.

References

1. Dal Maschio M, Carnato M, Pigozzo FM, Cipullo A, Pozzato G, Reggiani C: Biophysical effects of high frequency electrical field (4-64 MHz) on muscle fibers in culture. Basic Appl Myol. 2009, 19:49-56.
2. Sella S, Adami V, Amati E, et al.: In-vitro analysis of quantum molecular resonance effects on human mesenchymal stromal cells. PLoS One. 2018, 13:e0190082. 10.1371/journal.pone.0190082
3. Fraccalvieri M, Salomone M, Di Santo C, Ruka E, Morozzo U, Bruschi S: Quantum molecular resonance technology in hard-to-heal extremity wounds: histological and clinical results. Int Wound J. 2017, 14:1313-22. 10.1111/iwj.12803
4. Ruggeri A, Dyrdin T, Barbariga M, Rama P, Ferrari G: Innovative radiofrequency electrotherapy significantly reduces cornea perforation in an alkali burn murine model. Invest Ophthalmol Vis Sci. 2018, 59:4350.
5. Pedrotti E, Bosello F, Fasolo A, Frigo AC, Marchesoni I, Ruggeri A, Marchini G: Transcutaneous periorbital electrical stimulation in the treatment of dry eye. Br J Ophthalmol. 2017, 101:814-9. 10.1136/bjophthalmol-2016-308478
6. Ferrari G, Colucci A, Barbariga M, Ruggeri A, Rama P: High frequency electrotherapy for the treatment of meibomian gland dysfunction. Cornea. 2019, 38:1424-9. 10.1097/ICO.0000000000002065
7. Trivli A, Karmiris E, Dalianis G, Ruggeri A, Terzidou C: Evaluating the efficacy of quantum molecular resonance (QMR) electrotherapy in mixed-type dry eye patients. J Optom. 2023, 16:128-34. 10.1016/j.optom.2022.06.003
8. Quantum molecular resonance effects on patients with dry eye disease . (2020). Accessed: May 30, 2025: https://clinicaltrials.gov/ct2/show/record/NCT05469932.
9. Cai MM, Zhang J: Effectiveness of transcutaneous electrical stimulation combined with artificial tears for the treatment of dry eye: a randomized controlled trial. Exp Ther Med. 2020, 20:175. 10.3892/etm.2020.9301

07

Quantum molecular resonance electrotherapy (Rexon-Eye) for recalcitrant dry eye in an Asian population

V. Hui Xian Foo, Y. Liu, B. Tho, L. Tong

frontiers | Frontiers in Medicine

TYPE Original Research
PUBLISHED 12 September 2023
DOI 10.3389/fmed.2023.1209886

Check for updates

OPEN ACCESS

EDITED BY
Dario Rusciano,
Consultant, Catania, Italy

REVIEWED BY
Luca Gualdi,
Independent Researcher, Rome, Italy
Swaminathan Sethu,
Narayana Nethralaya Foundation, India

*CORRESPONDENCE
Louis Tong
louis.tong.h.t@singhealth.com.sg

RECEIVED 21 April 2023
ACCEPTED 28 August 2023
PUBLISHED 12 September 2023

CITATION
Foo VHX, Liu Y-C, Tho B and Tong L (2023) Quantum molecular resonance electrotherapy (Rexon-Eye) for recalcitrant dry eye in an Asian population. *Front. Med.* 10:1209886. doi: 10.3389/fmed.2023.1209886

COPYRIGHT
© 2023 Foo, Liu, Tho and Tong. This is an open-access article distributed under the terms of the Creative Commons Attribution License (CC BY). The use, distribution or reproduction in other forums is permitted, provided the original author(s) and the copyright owner(s) are credited and that the original publication in this journal is cited, in accordance with accepted academic practice. No use, distribution or reproduction is permitted which does not comply with these terms.

Quantum molecular resonance electrotherapy (Rexon-Eye) for recalcitrant dry eye in an Asian population

Valencia Hui Xian Foo[1,2], Yu-Chi Liu[2,3], Bryan Tho[1] and Louis Tong[1,2,3,4]*

[1]Ocular Surface Research Group, Singapore Eye Research Institute, Singapore, Singapore, [2]Cornea and External Eye Disease Service, Singapore National Eye Centre, Singapore, Singapore, [3]Eye Academic Clinical Programme, Duke-NUS Medical School, Singapore, Singapore, [4]Department of Ophthalmology, Yong Loo Lin School of Medicine, National University of Singapore, Singapore, Singapore

Objectives: To assess the safety, efficacy, patients' satisfaction and acceptability of Rexon-Eye electrotherapy in treating Asian severe dry eye disease (DED) patients.

Methods: Prospective parallel-arm pilot study recruiting 40 DED Chinese patients with >moderate recalcitrant DED (Contact Lens Research Unit [CCLRU] > grade 2). Subjects were randomized into 2 groups, undergoing four weekly treatment sessions each: group 1 received full treatment power; group 2 received control treatment (power 1 treatment). Non-invasive tear break-up time (NIBUT), cornea fluorescein staining graded via CCLRU and Schirmer's I test were compared pre- and 2 months post-treatment. The SPEED and QUEST questionnaires that evaluated subjective symptoms and treatment satisfaction, respectively, at baseline and 2 weeks post-treatment were carried out. Tear cytokine levels in both groups were examined at 2 weeks post-treatment.

Results: The amount of improvement in post-treatment corneal staining in the inferior corneal zone was significant in Group 1 (p = 0.038) but not in Group 2 (p = 0.832). Group 1 eyes with worse baseline staining (total score >9.8) had a significantly greater reduction of corneal staining than those with better baseline staining (-11.7 ± 1.98 vs. -4.6 ± 2.89, $p < 0.001$). There were no other significant differences in NIBUT, Schirmer's 1 and cornea fluorescein staining grading within or between the groups. Group 1 (n = 24) had improved subjective dryness scores compared to Group 2 (n = 16) (SPEED score: 6.38 + 4.16 vs. 10.0 + 6.36, p = 0.04). No significant differences were seen in 11 tear cytokine levels at 2 weeks post-treatment between the 2 groups.

Conclusion: In Asian DED patients treated with Rexon-Eye, inferior cornea staining showed significant improvement compared to placebo, and eyes with greater cornea staining at baseline achieved a greater improvement in staining. There were no other significant improvements in NIBUT and Schirmer's 1. Rexon-Eye also improved subjective DED scores in 41.7% of eyes without any adverse effects.

KEYWORDS
tear disorder, ocular disease, dry eye, therapeutics, clinical trial

10.3389/fmed.2023.1209886

Highlights

- **What is already known on this topic** - Earlier case studies on Rexon-Eye have shown encouraging improvement in subjective and objective dry eye parameters, but they were mostly conducted small scale in Western populations targeting mild to moderate dry eye disease.
- **What this study adds** - In Asian moderate to severe recalcitrant dry eyes treated with Rexon-Eye, inferior cornea staining showed significant improvement compared to placebo, and eyes with worse corneal staining had the greatest improvement in their ocular surface. Rexon-Eye showed subjective improvement in dry eye symptoms in 40%.
- **How this study might affect research, practice or policy** - Rexon-Eye could be a potential adjunctive treatment option for patients with moderate to severe dry eye disease that is poorly responsive to current treatments.
- **Synopsis/Precis** - In Asian moderate to severe recalcitrant dry eyes treated with Rexon-Eye, inferior cornea staining showed significant improvement compared to placebo, and eyes with worse corneal staining had the greatest improvement in their ocular surface. Rexon-Eye showed subjective improvement in dry eye symptoms in 40%.

Introduction

Dry eye disease (DED) as defined by the International Dry Eye Workshop (DEWS 2017), is a multifactorial disease of the ocular surface characterized by a loss of homeostasis of the tear film that leads to ocular symptoms due to tear film instability, ocular surface inflammation and neurosensory abnormalities (1). It can be contributed by various factors such as aqueous deficiency or increased tear film evaporation. The available treatments for DED aim to supplement patient's natural tears or improve the residing time of the tears present (2). Theses include topical artificial tears, ciclosporine, corticosteroids, lifitegrast, punctal occlusion, Microblepharoexfoliation, Thermal Pulsation System and Intense Pulsed Light (IPL) therapy (3). However, these treatments may have various side effects with their use (4); hence low-risk adjunctive DED treatments are often of interest.

Quantum Molecular Resonance (QMR) is a technique in which low-intensity, high-frequency electric currents are administered to a target biological tissue through contact electrodes (5). Earlier studies have proposed several mechanisms of QMR stimulation (6), including mechanical deformation of cellular membrane, transient membrane potential modification and calcium ion release from the sarcoplasmic reticulum. *In vivo* studies showed that a series of cellular contractions and relaxation are then invoked, which triggers cellular metabolism and stimulates tissues downstream. In addition, the expression of matrix metalloproteinase and the infiltration of leukocytes were reduced, supporting an anti-inflammatory effect (5). Electrical stimulation has been hypothesized to affect cell migration and proliferation (7–10), and accelerate nerve regeneration via the promotion of neurotrophic factors such as brain-derived neurotrophic factor and nerve growth factor with the influx of calcium into neurons (11).

Rexon-Eye® (Resono Ophthalmic, Sandrigo, Italy) was developed and patented since 2014 with the basis of stimulating cellular regeneration and reactivating the lacrimal system and tear secretion in DED (6, 12). It uses a broad waveform of 4 to 64 MHz, but with intensities of wavelength within this range optimized for effect on membrane potential and cell regeneration (12). Earlier case studies have been encouraging, reporting improvement in subjective and objective ocular parameters in mixed dry eye patients without adverse effects (6, 13). Other studies also showed its effectiveness in reducing meibomian gland dysfunction (MGD)-induced ocular signs and symptoms (14). Furthermore, previous studies have shown that QMR can accelerate healing in chronic skin wounds (15), reduce pain and muscle injury in inflammatory musculoskeletal diseases (16), and reduce post-operative joint effusion in osteoarthritic knees (17).

However, earlier studies looking at DED-recovery with Rexon-Eye are small scale, targeting mild to moderate DED and conducted mainly in the Western population. Thus, our randomized, masked, comparative interventional study aims to evaluate the safety and efficacy of the Rexon-Eye device in improving recalcitrant DED in an Asian population, while determining patient satisfaction and acceptability of this device.

Materials and methods

Design and patient recruitment

This is a randomized comparative, single-center, masked, parallel group, interventional study conducted at the Singapore National Eye Centre from June 2021 to June 2022. Asian patients that attended the Cornea clinic with moderate or worse and recalcitrant DED and met the study inclusion criteria were recruited and randomized into either the full treatment (Group 1) or the control treatment group (Group 2). The study (Clinical trial no: NCT04320563) was approved by the SingHealth Centralized Institutional Review Board (CIRB number: 2019/2446) and complied with the tenets of the Declaration of Helsinki for human research. Informed written consent was obtained from all participants.

Eligibility

The inclusion criteria were as follows: subjects 21 years of age or older, had at least moderate DED based on grade 2 or worse corneal fluorescein staining graded on the Cornea and Contact Lens Research Unit Grading Scale (CCLRU) grading scale (18) in the central interpalpebral region, had been treated for DED and shown to have no further improvement on maximal therapy (defined as using topical corticosteroids or cyclosporin if medically not contraindicated, and punctal plugs) with no further improvement of symptoms and corneal staining on consecutive visits at least 6 months apart, were already on other topical eye drops (including artificial tears, topical ciclosporin or steroids), lid cleansers or lid warming solely for dry eyes, and with no recent change in topical medications in the last 1 month. Patients were continued on their existing dry-eye medications and were not

allowed to change their medication regimen, with the duration of topical medications extending throughout the study period. The exclusion criteria were as follows: contact lens wearers, pregnant women, had active implantable devices (e.g., pacemakers), were oncologic patients undergoing treatment, vegetarian, on topical antibiotic or anti-glaucoma drops, had active ocular infections or eyelid position anomalies.

Randomization

Consecutive eligible patients were enrolled in this study and were randomly allocated to the study or control group, with a randomization of 3:2, respectively, in order to assess factors of treatment response in the study group. The randomization was conducted by computer-generated random number allocation and applied to sequentially enrolled patients. The randomization schedule was pre-determined, prior to commencing participant recruitment, such that the investigator involved in the baseline participant assessment were not involved in the treatment allocation.

Study treatment

The treatment is delivered by a device that applies stimulation on the epidermis of closed eyelids up to the lid border via goggles placed directly over the patient's eyes simultaneously, making the treatment operator-independent. Both groups underwent a session of either the full treatment or comparative treatment per week for 4 weeks, with each session lasting 20 min. Group 1 was assigned to undergo the full treatment power 4, while Group 2 was assigned to undergo the control treatment (low energy, selected as power 1) on the Rexon-Eye device. In order to maximize patient masking, the participants in both groups observed the machine being switched on, but once the mask had been worn, the power setting in the comparative treatment group was reduced to 1.

Patient evaluation

A questionnaire including demographic and ocular data was completed by all patients at baseline, including age, gender, type and frequency of tear substitutes, additional eye drops or systemic drugs used for DED, any other ocular conditions other than DED or surgeries, and systemic diseases. Dry eye signs and symptoms were evaluated pre- and post-intervention month 2. DED symptoms were assessed using the Standard patient Evaluation for Eye Dryness (SPEED) questionnaire (19).

Study procedures

Dry eye signs were assessed using Schirmer's 1 test without anesthesia, non-invasive tear break-up time (NIBUT) (20) and total corneal fluorescein staining via Oculus Keratograph 5 M. The cornea fluorescein staining was scored in 5 corneal zones, central, superior, inferior, nasal and temporal, as in the CCLRU system. In each zone, the grade was assigned 0 to 4, with a greater number indicating a more intense or greater area of staining. The change in corneal staining is calculated as the sum of staining scores in the 5 cornea zones after treatment minus the sum of staining scores in the 5 zones before treatment.

Right at the end of the intervention, the QUEST and Acceptability and Satisfaction Questionnaire (Supplementary Appendix 1) was completed by each subject.

Tear cytokine elution and analysis

Our tear cytokine procedure has been published and is summarized in Supplementary material (21). Tears were collected from all subjects in the study 2 months after the end of the intervention, in order to assess persistence of any treatment effect 2 months post-treatment.

Data analysis and sample size calculation

As this therapy has not been evaluated in recalcitrant dry eyes before in a randomized controlled trial, we are unable to base the expected treatment effect on any previous available studies. Based on clincalc.com, assuming the comparative group's SPEED score to be 10, of the full power treatment group to be 7 or lower, detecting a minimum SPEED difference of 3, with the alpha of 0.05 and power of 80%, we would need 32 subjects overall (or 16 subjects per group). We recruited more (40 subjects) in the event of loss to follow up. Statistical analysis were performed using SPSS version 24. The primary outcomes were the changes in the SPEED questionnaire, and secondary outcomes being Schirmer's 1 test, NIBUT, corneal fluorescein staining and tear cytokine concentrations pre- and post-intervention. The Wilcoxon signed-rank test was used for intra-group comparisons and the Wilcoxon rank-sum test was used for inter-group comparisons. Data are presented as the mean ± standard deviation (SD) unless otherwise stated. All tests were two-tailed, and $p < 0.05$ was considered significant.

Results

Forty Chinese patients who met the inclusion criteria were included in the study, with 24 participants in the study group and 16 participants in the control group. Overall mean age was 66.55 ± 10.45 years. There were no significant differences in age or gender between the two groups. Before treatment, 40% had undergone previous refractive or cataract surgery. Baseline SPEED questionnaire scores were not significantly different between both groups. There were also no significant differences in the baseline Schirmer's 1 test, NIBUT and corneal fluorescein staining in all 5 zones. Schirmer's 1 test results were slightly worse in the left than right eye of the subjects, (2.64 ± 4.71 vs. 3.33 ± 5.51), while NIBUT was slightly worse in the right than the left eye of the subjects (5.05 ± 3.04 vs. 5.63 ± 4.24). The inferior corneal zone had the highest grade of corneal staining amongst all 5 quadrants in both groups (Table 1).

10.3389/fmed.2023.1209886

TABLE 1 Clinical and demographic characteristics and baseline DED parameters of participants.

	Overall Mean ± SD/n (%)	Group 1 full power Mean ± SD/n (%)	Group 2 comparative Mean ± SD/n (%)	p-value*
Total number	40	24	16	
Female	36 (90.0)	21 (87.5)	15 (93.8)	0.67
Age (years)	66.55 ± 10.45	64.08 ± 11.0	70.25 ± 8.49	0.07
Current medications				
Topical Ciclosporin	16 (40.0)	8 (33.3)	8 (50.0)	0.87
Topical steroids	13 (32.5)	6 (25.0)	7 (43.8)	0.79
Topical Diquafosol	11 (27.5)	6 (25.0)	5 (31.3)	0.65
Schirmer (mm), right eye	3.33 ± 5.51	3.41U5.8	3.21 ± 5.25	0.70
Schirmer (mm), left eye	2.64 ± 4.71	2.45 ± 4.62	2.93 ± 5.0	0.57
NIBUT†† (s), right eye	5.05 ± 3.04	5.43 ± 3.49	4.46 ± 2.18	0.12
NIBUT†† (s), left eye	5.63 ± 4.24	5.98 ± 4.92	5.09 ± 2.99	0.29
Fluorescein staining†††, right eye				
Superior	0.86 ± 1.27	0.83 ± 1.21	0.91 ± 1.39	0.67
Inferior	3.00 ± 1.08	3.06 ± 1.14	3.06 ± 1.03	0.67
Nasal	2.50 ± 1.34	2.58 ± 1.25	2.38 ± 1.50	0.26
Temporal	1.94 ± 1.26	1.83 ± 1.38	2.09 ± 1.20	0.64
Central	1.44 ± 1.29	1.58 ± 1.25	1.34 ± 1.40	0.43
Fluorescein staining†††, left eye				
Superior	0.91 ± 1.56	0.67 ± 1.20	1.28 ± 1.53	0.09
Inferior	3.14 ± 1.23	3.13 ± 1.36	3.16 ± 1.04	0.25
Nasal	2.66 ± 1.38	2.62 ± 1.42	2.72 ± 1.35	0.78
Temporal	1.66 ± 1.55	1.58 ± 1.49	1.78 ± 1.68	0.31
Central	1.45 ± 1.51	1.47 ± 1.51	1.50 ± 1.56	0.80
SPEED questionnaire	9.03 ± 5.19	8.13 ± 4.12	10.31 ± 8.30	0.24

†Participants are classified under dry eye if they demonstrated dry eye symptoms and one of the clinical signs (Staining, Schirmer's test, or NIBUT). Since participants in the dry eye group tend not to have abnormal results in all the tests: staining, Schirmer's test and NIBUT; these parameters are individually not lower than the control group and the values had a large SD. ††Non-invasive tear break up times. †††The staining were mild in the zones when present, with no cases of above 10 fluorescein spots in any single corneal zone. Control and dry eye groups were not significantly different in any of the parameters above ($p > 0.05$). *Based on independent sample t-tests or Wilcoxon rank-sum test, comparing characteristics between the two groups.

Because this study was conducted on participants on maximal DED standard therapy, and participants continued their use of topical therapy during the study period, we report the use of concurrent medications in each of the two study groups (Table 1). There were no significant differences in the number of subjects on topical ciclosporin, Diquafosol or steroids between the 2 groups at baseline ($p > 0.05$).

On the study visit 2 weeks after the last treatment, the SPEED questionnaire scores significantly improved from baseline in both groups 1 and 2 (Table 3), with group 1 having significantly lower scores than the group 2, (6.38 + 4.16 vs. 10.0 + 6.36, $p = 0.04$) (Table 2). Within group 1, majority of the subjects (58.3%) had maintained scores, while 41.7% had improved scores. Within group 2, interestingly, 64.3% had improved scores, while 35.7% had maintained scores. None had worsened scores in either groups (Table 4).

The overall post-treatment mean Schirmer's 1 test improved compared to pre-treatment, however, they were not significantly different between or within each group pre- and post-treatment in either eye (Table 3). We also observed that a greater proportion of left eyes in group 1 had stable or improved Schirmer's 1 compared to the left eyes in group 2 post-treatment (87.5 vs. 75.0%, $p = 0.43$), although this difference was not statistically significant. In the right eyes, there were similar proportions of stable or improved Schirmer's 1 between both groups (81.8 vs. 83.4%, $p = 0.84$) (Table 4).

Overall NIBUT also improved in both groups post- compared to pre-treatment, and group 1 had greater NIBUT than the group 2, although this differences between and within each group pre- and post-intervention were not statistically significant (Table 3). However, we noted the right eyes had a lower proportion of stable or improved NIBUT in group 1 compared to group 2 (right eye: 58.2 vs. 68.8%, $p = 0.75$), and the left eyes had a greater proportion of stable or improved NIBUT in group 1 compared to group 2 (left eye: 58.3 vs. 50%, $p = 0.83$) (Table 4).

In terms of corneal staining, the overall mean grades improved post- compared to pre-treatment. The inferior zone of group 1 (right eye) had a significant reduction in staining compared to baseline ($p = 0.038$) whereas the temporal zone of group 2 had a significant reduction in staining compared to baseline (Table 3). Group 1 also had lower staining grading than the Group 2 in the inferior corneal zones for both right and left eyes (right eye:

10.3389/fmed.2023.1209886

TABLE 2 Main outcomes post-treatment.

	Overall Mean ± SD/*n* (%)	Group 1 full power Mean ± SD/*n* (%)	Group 2 comparative† Mean ± SD/*n* (%)	*p*-value*
Total number	40	24	16	
Schirmer (mm), right eye	3.49 ± 4.26	3.22 ± 5.21	4.0 ± 5.56	0.68
Schirmer (mm), left eye	2.77 ± 4.15	3.13 ± 4.62	2.08 ± 3.12	0.49
NIBUT†† (s), right eye	6.01 ± 4.23	6.54 ± 5.01	5.15 ± 2.39	0.26
NIBUT†† (s), LE	5.72 ± 4.38	5.96 ± 3.73	5.33 ± 5.41	0.67
Fluorescein staining†††, right eye				
Superior	0.75 ± 1.21	0.75 ± 1.18	0.71 ± 1.28	0.93
Inferior	2.57 ± 1.43	2.42 ± 1.54	2.82 ± 1.23	0.41
Nasal	2.14 ± 1.55	2.29 ± 1.54	1.89 ± 1.58	0.45
Temporal	1.33 ± 1.37	1.46 ± 1.41	1.11 ± 1.32	0.45
Central	1.26 ± 1.41	1.38 ± 1.48	1.07 ± 1.31	0.53
Fluorescein staining, †††, left eye				
Superior	0.81 ± 1.56	0.69 ± 0.98	1.18 ± 1.51	0.23
Inferior	2.87 ± 1.23	2.75 ± 1.35	3.07 ± 1.22	0.47
Nasal	2.61 ± 1.65	2.69 ± 1.41	2.57 ± 1.40	0.81
Temporal	1.71 ± 1.31	1.54 ± 1.46	1.86 ± 1.40	0.52
Central	1.36 ± 1.31	1.48 ± 1.31	1.68 ± 1.50	0.67
SPEED questionnaire	**7.65 ± 5.21**	**6.38 ± 4.16**	**10.0 ± 6.36**	**0.04**

†Participants are classified under dry eye if they demonstrated dry eye symptoms and one of the clinical signs (Staining, Schirmer's test, or NIBUT). Since participants in the dry eye group tend not to have abnormal results in all the tests: staining, Schirmer's test and NIBUT, these parameters are individually not lower than the control group, and the values had a large SD. ††Non-invasive tear break up times. †††The staining were mild in the zones when present, with no cases of above 10 fluorescein spots in any single corneal zone. *Based on the independent sample *t*-test, comparing characteristics between the two groups. Bolded values are those with significant *p* values.

TABLE 3 Pre- vs. post-treatment paired T-test *P*-values within each group.

		Pre vs. post paired T-test *p*-values	
		Group 1 full power	Group 2 comparative
Speed		**0.031***	**0.008***
NIBUT	Right eye	0.259	0.353
	Left eye	0.905	0.978
Schirmers	Right eye	0.789	0.407
	Left eye	0.497	0.638
Staining right	Superior	0.505	0.067
	Inferior	**0.038***	0.832
	Nasal	0.252	0.927
	Temporal	0.310	**0.005***
	Central	0.703	0.551
Left	Superior	0.448	0.823
	Inferior	0.333	0.713
	Nasal	0.414	0.608
	Temporal	0.918	0.820
	Central	0.449	0.111

Bolded values are those with significant *p* values.

2.42 + 1.54 vs. 2.82 + 1.23, $p = 0.41$, left eye: 2.75 + 1.35 vs. 3.07 + 1.22, $p = 0.47$) (Table 4), although this difference was not statistically significant. Majority of both right and left eyes had improved or maintained staining in their inferior zones in both groups 1 and 2 (right eye: 83.3 vs. 81.3%, $p = 0.82$, left eye: 79.1 vs. 87.6%, $p = 0.78$) (Table 4).

When we divided group 1 according to their pre-treatment severity of corneal staining, the eyes with more severe staining (total score >9.8 or mean) resulted in significantly greater reduction of corneal staining than the eyes starting with less severe staining (total score <9.8 or mean) (-11.7 ± 1.98 and -4.6 ± 2.89, $p < 0.001$) (Results not shown in Tables).

Analysis of 11 different cytokine tear levels showed no significant differences between groups 1 and 2 at baseline (all $p > 0.05$, Table 5). Analysis of the cytokine tear levels post-treatment also showed no statistically significant differences in all tear cytokine levels between groups 1 and 2, and in all tear cytokine levels pre- and post- treatment (all $p > 0.05$, Table 5). Pre- and post-treatment cytokine tear levels within either groups were also not significantly different (all $p > 0.05$, not shown).

Majority found the treatment pleasant compared to the comparative treatment (83.3 vs. 57.1%, $p = 0.045$). The rest of the results were not statistically significant between both groups (Table 6). A total of 37.5% of subjects felt the treatment was effective in group 1 compared to 21.4% in group 2, and 29.2% in group 1 felt the treatment was durable compared to 14.3% in group 2. A total of 41.7% also felt the treatment was better than other DED treatments in group 1 compared to 21.4% in group 2. Overall, 41.2% had felt that their DED situation was improved in group 1 compared to 35.7% in group 2. However no significant difference in the frequency of tear substitutes usage were observed between the groups, and close to 100% still had dry eye symptoms and maintained the same number of daily tear substitutes eye

10.3389/fmed.2023.1209886

TABLE 4 Change in outcomes post treatment.

	Group 1 full power (*n* = 24) *n* (%)	Group 2 comparative (*n* = 16) *n* (%)	*P*-value*
Schirmer (mm), right eye			0.84
Improved	7 (29.2)	7 (43.8)	
Same	13 (54.2)	7 (43.8)	
Worse	4 (16.6)	2 (12.4)	
Schirmer (mm), left eye			0.43
Improved	8 (33.3)	4 (25.0)	
Same	13 (54.2)	8 (50.0)	
Worse	3 (12.5)	4 (25.0)	
NIBUT†† (s), right eye			0.73
Improved	10 (41.6)	8 (50.0)	
Same	4 (16.4)	3 (18.8)	
Worse	10 (41.8)	5 (31.3)	
NIBUT†† (s), left eye			0.83
Improved	11 (45.8)	6 (37.5)	
Same	3 (12.5)	2 (12.5)	
Worse	10 (41.7)	8 (50.0)	
Fluorescein staining to inferior corneal zone††† right eye			0.82
Improved	9 (37.5)	7 (43.8)	
Same	11 (45.8)	6 (37.5)	
Worse	4 (16.7)	3 (18.8)	
Fluorescein staining to inferior corneal zone†††, left eye			0.78
Improved	8 (33.3)	5 (31.3)	
Same	11 (45.8)	9 (56.3)	
Worse	5 (20.8)	2 (12.5)	
SPEED questionnaire			0.12
Improved	10 (41.7)	10 (62.5)	
Same	14 (58.3)	6 (37.5)	
Worse	0	0	

††Non-invasive tear break up times. †††The staining were mild in the zones when present, with no cases of above 10 fluorescein spots in any single corneal zone. *Based on independent sample *t*-test, comparing characteristics between the two groups.

drops at the end of treatment in both groups (Table 5). No adverse effects related to the use of Rexon-eye occurred, such as increased intraocular pressure, worsened visual acuity, or increased discomfort after the intervention.

Discussion

In our prospective study of Asian recalcitrant dry eye patients treated with Rexon-Eye, inferior cornea staining showed significant improvement compared to placebo, and eyes with greater cornea staining at baseline achieved a greater improvement in staining. There were no other significant improvements in NIBUT and Schirmer's 1. Rexon-Eye also improved subjective DED scores in 41.7% of eyes without any adverse effects. There were no significant differences in the other DED measures between both groups. There were also no significant differences seen in the tear cytokine profile between both groups 2 months after treatment.

We found that there was significant improvement in the inferior cornea staining in the eyes treated with Rexon-Eye, compared to placebo. In our sub-analysis of corneal fluorescein staining outcomes in the full power treatment group, we observed that the participants with more severe baseline staining (CCLRU total score of >9.8) had a significantly greater reduction of corneal staining than the participants starting with less severe staining. This novel observation could suggest that the amount of benefit in improvement of corneal staining derived from this treatment may be correlated to the severity of initial corneal staining. Overall, it was encouraging to see that patients were more severe DED benefited more with Rexon-Eye compared to those with better cornea staining, suggesting that epithelial disease may be improved with such treatment. More future work would still be needed to confirm such a finding. However, did not find significant differences in the other objective DED parameters of NIBUT, Schirmer's 1 and corneal fluorescein staining between the treatment and control groups (all with moderate to severe DED).

Our results that Rexon-Eye could improve subjective DED measures are supported by earlier studies. Trivli et al. (13) and Pedrotti (5) both showed in non-randomized interventional cohort studies that DED patients experienced a subjective benefit in the Ocular Surface Disease Index (OSDI) score post-Rexon, where Ferrari et al. (14) reported that in patients affected by Meibomian gland dysfunction, Rexon-Eye improved total OSDI scores by 37%.

Although these studies did not use a parallel control group, other different forms of transcutaneous electrical stimulation (TES) therapy did show similar positive results. For instance, Cai et al. reported in a randomized controlled trial of 104 eyes in 52 DED patients that those treated with both TES therapy via the Huatuo SDZ-II electrical stimulator and sodium hyaluronate eyedrops had significantly better OSDI scores compared with patients treated with sodium hyaluronate eyedrops alone (22). Han et al. demonstrated in a prospective randomized clinical trial of 24 patients for prevention of dry eye after PRK, that patients who had TES via a goggle-like device called Nu Eyne 01 (Nu Eyne Co., Ltd., Seoul, Republic of Korea) had significantly lower eye pain intensity compared to control group by 65% at the first week post-PRK due to an improvement in DED-related corneal nerve damage, although OSDI and SPEED II questionnaire scores were similar between the 2 groups at 3 months post-surgery (23). Sivanesan et al. found in a small pilot study that the use of TES in the stimulation of the trigeminal nerve achieved a short-term reduction in DED-related chronic ocular pain by 57% and photophobia by 28% (24). Friedman et al. revealed an improvement in OSDI scores in a non-randomized clinical trial, using neurostimulation of the nasal sensory nerves via the nasolacrimal pathway, however, there were concerns of hygiene and patient discomfort (25).

In our study, we found that both full treatment and control arms had improvement in SPEED scores. Unlike other studies, all participants were continued on the pre-existing treatment

TABLE 5 Tear cytokines concentration pre- and post- therapy between groups (pg/ml).

		Group 1 full power		Group 2 comparison		
		Mean	SD	Mean	SD	p-value*
GM-CSF	Pre	4.85	5.34	5.05	4.42	0.91
	Post	4.36	4.96	4.00	3.27	0.80
IFNg	Pre	60.36	78.53	66.94	81.29	0.83
	Post	58.43	57.55	50.16	64.45	0.71
IL-1B	Pre	47.31	99.59	69.17	111.45	0.58
	Post	67.40	123.77	61.68	146.16	0.91
IL-2	Pre	6.00	7.01	4.69	4.21	0.51
	Post	7.50	12.96	5.39	4.97	0.30
IL-4	Pre	5.57	5.34	5.20	3.55	0.82
	Post	5.20	3.22	4.96	3.05	0.83
IL-5	Pre	27.49	25.25	24.30	17.87	0.68
	Post	19.28	16.28	19.06	16.48	0.97
IL-6	Pre	132.11	148.87	263.64	278.22	0.19
	Post	418.60	595.26	213.90	277.36	0.19
IL-8	Pre	1667.97	2877.72	2160.64	1842.07	0.59
	Post	6593.51	11688.54	4291.61	9006.89	0.53
IL-10	Pre	6.57	6.69	7.02	6.72	0.86
	Post	5.90	6.20	5.58	4.63	0.78
IL-12p70	Pre	13.25	17.39	10.29	8.58	0.52
	Post	15.96	30.08	9.17	7.35	0.32
TNF-a	Pre	14.97	18.99	26.98	31.81	0.25
	Post	16.10	17.38	21.73	32.70	0.59

*Based on independent sample t-test, comparing characteristics between the two groups.

including immunosuppressive eyedrops, so it would be harder to demonstrate improvement of SPEED and objective clinical parameters. A total of 62% of eyes in the control group also had improvement in SPEED scores too; we are uncertain if the improvement in the control group is related to better medication compliance and outcomes, since clinical trial patients are monitored more closely than routine clinic patients. Nonetheless, our results lend support to the potential adjunctive use of the Rexon- Eye in treating and improving subjective DED in our moderate to severe Asian DED patients in the armamentarium of treatment for dry eyes, especially those with recalcitrant symptoms.

In DED, the degree of ocular surface inflammation is an important quantifiable parameter for diagnosis and monitoring of the disease before and after treatments. Tear collection followed by cytokine determination if a less invasive measure of documenting inflammation compared to other methods such as impression cytology or tissue biopsy (26–28). Earlier studies have shown that alterations of the tear cytokine profiles occur in DED patient, with elevated proinflammatory cytokine levels such as IL-1, IL-6, IL-8, and TNF-α shown to be strongly correlated with dry eye markers (29), leading to ocular surface damage and goblet cell reduction (30). Topical anti-inflammatory treatments such as ciclosporin (31) or methylprednisolone (32) are effective in reducing the levels of inflammatory cytokine levels in tears. In our study, we found that 11 different tear cytokine levels did not differ significantly pre- and post-Rexon-Eye treatment. To the best of our knowledge, this study is the first to analyze tear cytokine changes with Rexon-Eye treatment. However, we postulate that the possible reason for our observation of the tear film cytokine levels could be attributed to the time-frame that the subjects' tear secretion was measured at; which was at 2 months after cessation of Rexon-Eye therapy. We are unsure if the effect of Rexon-Eye on the tear film and ocular surface inflammation may be more transient than expected and not last beyond 2 months. Trivli et al. reported earlier that Rexon-Eye treatment was able to show a 75% reduction in tear MMP-9-positive patients compared to pre-treatment levels (13).

The exact mechanisms underlying the benefits of Rexon-Eye on DED remain unclear. Previous studies have hypothesized that in transcutaneous application of electrical stimulation, electric fields can hasten cell migration during the wound healing process by improving cell directionality (33). Different groups of cells, including neural crest cells (34, 35), fibroblasts (33), neurons (36, 37), and CECs (38–40), respond to electric fields by directed migration or directed growth *in vitro*. This has been shown to increase the rate of cornea healing in cornea abrasions in a vivo model of corneal wound healing in rabbits (10). It is also hypothesized that QMR can stimulate the lacrimal system, reactivate the lacrimal and meibomian gland tissue and benefit the ocular annexes (5).

10.3389/fmed.2023.1209886

TABLE 6 Change in satisfaction and acceptability post-treatment at 2 months.

n (%)	Group 1 full power	Group 2 comparative	P-value*
Situation compared to before treatment			0.46
Better	12 (50)	9 (64.0)	
Same	10 (41.7)	5 (35.7)	
Worse	2 (8.3)	2 (14.3)	
Situation compared to end of treatment			0.38
Better	11 (45.8)	9 (64.0)	
Same	11 (45.8)	5 (35.7)	
Worse	2 (8.3)	2 (14.3)	
Situation compared to 1 month after treatment			0.46
Better	10 (41.7)	5 (35.7)	
Same	12 (50.0)	9 (64.0)	
Worse	2 (8.3)	2 (14.3)	
Dry eye symptoms during last week			0.90
Yes	22 (91.7)	13 (92.9)	
No	2 (8.3)	1 (7.1)	
Used lubricants in last 1 week during day			0.60
Yes	24 (100.0)	14 (100.0)	
No	0	0	
Used lubricants in last 1 week during night			0.58
Yes	21 (87.5)	13 (92.9)	
No	3 (12.5)	1 (7.1)	
In last 2 months had other eye problems			0.19
Yes	0	1 (7.1)	
No	24 (100.0)	13 (92.9)	
Last 2 months used lubricants			
Yes	24 (100.0)	14 (100.0)	
No	0	0	
Last 2 months tried to suspend lubricants			0.44
Yes	1 (4.2)	0	
No	23 (95.8)	14 (100.0)	
Eyes now have more tears			0.97
Yes	7 (29.2)	4 (28.6)	
No	17 (70.8)	10 (71.4)	
Eyes now more wet			
Yes	7 (29.2)	6 (42.9)	0.74
No	17 (70.8)	9 (64.3)	

(Continued)

TABLE 6 (Continued)

n (%)	Group 1 full power	Group 2 comparative	P-value*
Eyes feel better than before treatment			
Yes	14 (58.3)	8 (57.1)	0.94
No	10 (41.7)	6 (42.9)	
Use less lubricants now than before Treatment			0.15
Yes	4 (16.7)	1 (7.1)	
No	20 (83.3)	13 (92.9)	
Pleasant			**0.045**
Yes	**20 (83.3)**	**8 (57.1)**	
No	0	0	
Neutral	4 (16.7)	6 (42.9)	
Effective			0.09
Yes	9 (37.5)	3 (21.4)	
No	7 (29.2)	2 (8.3)	
Neutral	8 (33.3)	9 (64.3)	
Durable			0.22
Yes	7 (29.7)	2 (14.3)	
No	7 (29.7)	4 (28.6)	
Neutral	10 (41.7)	8 (58.7)	
With respect to other treatments			0.29
Better	10 (41.7)	3 (21.4)	
Same	13 (54.2)	11 (78.6)	
Worse	1 (4.1)	0	

*Based on the independent sample *t*-tests, comparing characteristics between the 2 groups. Bolded values are those with significant *p* values.

Our study has several limitations. First, our study has a relatively small sample size and did not have true observer masking because some participants that underwent QMR with the full treatment power may experience a heating sensation. We did not categorize the different subtypes of DED in our subjects, although Trivli et al. suggested that Rexon-Eye could improve both inflammation and meibomian gland quality (13). We also did not have any immediate or intermediate visits 1 month or longer-term after the treatment, and did not measure tear film lipid layer or osmolarity at our timepoints. Furthermore, single timepoints differences across the various DED parameters between the 2 groups are difficult to account for, and could be due to individual differences within each group at baseline.

Our study's strengths include the use of detailed subjective and objective parameters, including the SPEED and QUEST questionnaires, the first use of the multiplex cytokine assay to evaluate the effects of Rexon-Eye on DED. A total of 83% of subjects found the Rexon-Eye treatment pleasant, compared to 50% in the control treatment group, and 41.2% felt that the Rexon-Eye treatment was more effective than other DED treatments and had improved DED symptoms compared to before treatment. Future studies with larger sample sizes and longer follow-up times would

be useful in confirming our findings. Because of the apparent greater efficacy of corneal epithelial healing in cases with greater staining, it is also worth evaluating the use of Rexon-Eye in persistent corneal epithelial defects.

In conclusion, in Asian recalcitrant dry eyes treated with Rexon-Eye, inferior cornea staining showed significant improvement compared to placebo, and eyes with greater cornea staining at baseline achieved a greater improvement in staining. There were no other significant improvements in NIBUT and Schirmer's I. Rexon-Eye also improved subjective DED scores in 41.7% of eyes without any adverse effects. Other objective DED markers were not significantly altered after therapy. The tear cytokine levels were not significantly different between both treatment and control groups 2 months after the use of Rexon-Eye. Rexon-Eye as an adjunctive therapy in Asian recalcitrant moderate to severe DED is promising especially for a specific subgroup of more advanced DED subjects, but the characterization of this subgroup needs further evaluation. In future, we could focus on patients with severe and poorly responsive DED and evaluate changes in DED parameters earlier on at 1-month from the treatment.

Data availability statement

The raw data supporting the conclusions of this article will be made available by the authors, without undue reservation.

Author contributions

LT, VF, and Y-CL have made a substantial contribution to the concept or design of the article, and the acquisition, analysis, or interpretation of data for the article. All authors drafted the article or revised it critically for important intellectual content.

Funding

This project was supported in part by the National Medical Research Council, Singapore (NMRC\CSA\017\2017).

Acknowledgments

We would like to acknowledge Ms. Cynthia Boo and Ms. Sharon Yeo for their help in facilitating the study visits of the subjects throughout the study. We would also like to acknowledge the loan of the equipment by our study sponsor (Mandarin Optomedics, Resono).

Conflict of interest

The authors declare that the research was conducted in the absence of any commercial or financial relationships that could be construed as a potential conflict of interest.

Publisher's note

All claims expressed in this article are solely those of the authors and do not necessarily represent those of their affiliated organizations, or those of the publisher, the editors and the reviewers. Any product that may be evaluated in this article, or claim that may be made by its manufacturer, is not guaranteed or endorsed by the publisher.

Supplementary material

The Supplementary Material for this article can be found online at: https://www.frontiersin.org/articles/10.3389/fmed.2023.1209886/full#supplementary-material

References

1. Craig J, Nichols K, Akpek E, Caffery B, Dua H, Joo C, et al. Definition and classification report. *Ocul Surf.* (2017) 15:276–83. doi: 10.1016/j.jtos.2017.05.008

2. Agarwal P, Craig J, Rupenthal I. Formulation considerations for the management of dry eye disease. *Pharmaceutics.* (2021) 13:207. doi: 10.3390/pharmaceutics13020207

3. O'Neil E, Henderson M, Massaro-Giordano M, Bunya V. Advances in dry eye disease treatment. *Curr Opin Ophthalmol.* (2019) 30:166. doi: 10.1097/ICU.0000000000000569

4. Shen Lee B, Toyos M, Karpecki P, Schiffbauer J, Sheppard J. Selective pharmacologic therapies for dry eye disease treatment: efficacy, tolerability, and safety data review from preclinical studies and pivotal trials. *Ophthalmol Ther.* (2022) 11:1333–69. doi: 10.1007/s40123-022-00516-9

5. Pedrotti E, Bosello F, Fasolo A, Frigo A, Marchesoni I, Ruggeri A, et al. Transcutaneous periorbital electrical stimulation in the treatment of dry eye. *Br J Ophthalmol.* (2017) 101:814–9. doi: 10.1136/bjophthalmol-2016-308678

6. Maschio M, Canato M, Pigozzo F. Biophysical effects of high frequency electrical field (4 MHz) on muscle fibers in culture. *Basic Appl Myol.* (2009) 19:49–56.

7. Song B, Gu Y, Pu J, Reid B, Zhao Z, Zhao M. Application of direct current electric fields to cells and tissues in vitro and modulation of wound electric field in vivo. *Nat Protoc.* (2007) 2:1479–89. doi: 10.1038/nprot.2007.205

8. Haastert-Talini K, Grothe C. Electrical stimulation for promoting peripheral nerve regeneration. *Int Rev Neurobiol.* (2013) 109:111–24. doi: 10.1016/B978-0-12-420045-6.00005-5

9. Song B, Zhao M, Forrester J, McCaig C. Nerve regeneration and wound healing are stimulated and directed by an endogenous electrical field in vivo. *J Cell Sci.* (2004) 117:4681–90. doi: 10.1242/jcs.01341

10. Ghaffarieh A, Ghaffarpasand F, Dehghankhalili M, Honarpisheh N, Nirumanda S, Tanideh N. Effect of transcutaneous electrical stimulation on rabbit corneal epithelial cell migration. *Cornea.* (2012) 31:559–63. doi: 10.1097/ICO.0b013e31823f8b2a

11. Wenjin W, Wenchao L, Hao Z, Feng L, Yan W, Wodong S, et al. Electrical stimulation promotes BDNF expression in spinal cord neurons through Ca(2+)- and Erk-dependent signaling pathways. *Cell Mol Neurobiol.* (2011) 31:459–67. doi: 10.1007/s10571-010-9639-0

12. Sella S, Adami V, Amati E, Bernardi M, Chieregato K, Gatto P, et al. In-vitro analysis of quantum molecular resonance effects on human mesenchymal stromal cells. *PLoS One.* (2018) 13:e0190082. doi: 10.1371/journal.pone.0190082

13. Trivli A, Karmiris E, Dalianis G, Ruggeri A, Terzidou C. Evaluating the efficacy of quantum molecular resonance (QMR) electrotherapy in mixed-type dry eye patients. *J Opt.* (2022) 16:128–34. doi: 10.1016/j.optom.2022.06.003

14. Ferrari G, Colucci A, Barbariga M, Ruggeri A, Rama P. High frequency electrotherapy for the treatment of meibomian gland dysfunction. *Cornea.* (2019) 38:1424–9. doi: 10.1097/ICO.0000000000002063

15. Fraccalvieri M, Salomone M, Di Santo C, Ruka E, Morozzo U, Bruschi S. Quantum molecular resonance technology in hard-to-heal extremity wounds: histological and clinical results. *Int Wound J.* (2017) 14:1313–22. doi: 10.1111/iwj.12805

16. Frobinger V. *Esperienze cliniche nell'impiego del dispositivo Rexon-Age.* (2009). Available online at: [illegible] (accessed March 13, 2023).

17. Lopresti M, Tomba A, Caserta A, Di Domenica F. Studio clinico sull'efficacia della risonanza quantica molecolare nel trattamento dell'edema post-chirurgico in pazienti sottoposti a intervento di artroprotesi di ginocchio. *Arch Ortop Reumatol.* (2011) 122:34–5. doi: 10.1007/s10261-011-0013-7

18. Terry R, Schnider C, Holden B, Cornish R, Grant T, Sweeney D, et al. CCLRU standards for success of daily and extended wear contact lenses. *Opt Vis Sci.* (1993) 70:234–43. doi: 10.1097/00006324-199303000-00011

19. Ngo W, Situ P, Keir N, Korb D, Blackie C, Simpson T. Psychometric properties and validation of the standard patient evaluation of eye dryness questionnaire. *Cornea.* (2013) 32:1204–10. doi: 10.1097/ICO.0b013e318294b0c0

20. Lee R, Yeo S, Aung H, Tong L. Agreement of noninvasive tear break-up time measurement between Tomey RT-7000 auto refractor-Keratometer and oculus Keratograph 5M. *Clin Ophthalmol.* (2016) 10:1785–90. doi: 10.2147/OPTH.S110180

21. Willems B, Tong L, Minh T, Pham N, Nguyen X, Zumbansen M. Novel cytokine multiplex assay for tear fluid analysis in Sjogren's syndrome. *Ocul Immunol Inflamm.* (2021) 29:1639–44. doi: 10.1080/09273948.2020.1767793

22. Cai M, Zhang J. Effectiveness of transcutaneous electrical stimulation combined with artificial tears for the treatment of dry eye: a randomized controlled trial. *Exp Ther Med.* (2020) 20:175. doi: 10.3892/etm.2020.9305

23. Han G, Yoo Y, Shin E, Park J, Park Y, Kim P, et al. Transcutaneous electrical stimulation for the prevention of dry eye disease after photorefractive keratectomy: randomized controlled trial. *Ophthalmol Sci.* (2022) 3:100242. doi: 10.1016/j.xops.2022.100242

24. Sivanesan E, Levitt R, Sarantopoulos C, Patin D, Galor A. Noninvasive electrical stimulation for the treatment of chronic ocular pain and photophobia. *Neuromodulation.* (2018) 21:727–34. doi: 10.1111/ner.12742

25. Friedman N, Butron K, Robledo N, Loudin J, Baba S, Chayet A. A nonrandomized, open-label study to evaluate the effect of nasal stimulation on tear production in subjects with dry eye disease. *Clin Ophthalmol.* (2016) 10:795–804. doi: 10.2147/OPTH.S101716

26. Tong L, Beuerman R, Simonyi S, Hollander D, Stern M. Effects of punctal occlusion on clinical signs and symptoms and on tear cytokine levels in patients with dry eye. *Ocul Surf.* (2016) 14:233–41. doi: 10.1016/j.jtos.2015.12.004

27. Tong L, Wong T, Cheng C. Level of tear cytokines in population-level participants and correlation with clinical features. *Cytokine.* (2018) 110:452–8. doi: 10.1016/j.cyto.2018.05.013

28. Le Guezennec X, Quah J, Tong L, Kim N. Human tear analysis with miniaturized multiplex cytokine assay on "wall-less" 96-well plate. *Mol Vis.* (2015) 21:1151–61.

29. Roda M, Corazza I, Bacchi Reggiani M, Pellegrini M, Taroni L, Giannaccare G, et al. Dry eye disease and tear cytokine levels-a meta-analysis. *Int J Mol Sci.* (2020) 21:3111. doi: 10.3390/ijms21093111

30. Yamaguchi T. Inflammatory response in dry eye. *Invest Ophthalmol Vis Sci.* (2018) 59:DES192–9. doi: 10.1167/iovs.17-23651

31. Periman L, Mah F, Karpecki PMA. Review of the mechanism of action of cyclosporine a: the role of cyclosporine a in dry eye disease and recent formulation developments. *Clin Ophthalmol.* (2020) 14:4187–200. doi: 10.2147/OPTH.S279051

32. Lee J, Min K, Kim S, Kim E, Kim T. Inflammatory cytokine and osmolarity changes in the tears of dry eye patients treated with topical 1% methylprednisolone. *Yonsei Med J.* (2014) 55:203–8. doi: 10.3349/ymj.2014.55.1.203

33. Stump R, Robinson K. Xenopus neural crest cell migration in an applied electrical field. *J Cell Biol.* (1983) 97:1226–33. doi: 10.1083/jcb.97.4.1226

34. Zhao M, Penninger J, Isseroff R. Electrical activation of wound-healing pathways. *Adv Skin Wound Care.* (2010) 1:567–73.

35. Nuccitelli R, Erickson C. Embryonic cell motility can be guided by physiological electric fields. *Exp Cell Res.* (1983) 147:195–210. doi: 10.1016/0014-4827(83)90284-7

36. Erickson C, Nuccitelli R. Embryonic fibroblast motility and orientation can be influenced by physiological electric fields. *J Cell Biol.* (1984) 98:296–307. doi: 10.1083/jcb.98.1.296

37. Hinkle L, McCaig C, Robinson K. The direction of growth of differentiating neurones and myoblasts from frog embryos in an applied electric field. *J Physiol.* (1981) 314:121–35. doi: 10.1113/jphysiol.1981.sp013695

38. Jaffe L, Poo M. Neurites grow faster towards the cathode than the anode in a steady field. *J Exp Zool.* (1979) 209:115–28. doi: 10.1002/jez.1402090114

39. Soong H, Parkinson W, Bafna S, Sulik G, Huang S. Movements of cultured corneal epithelial cells and stromal fibroblasts in electric fields. *Invest Ophthalmol Vis Sci.* (1990) 31:2278–82.

40. Zhao M, Agius-Fernandez A, Forrester J, McCaig C. Orientation and directed migration of cultured corneal epithelial cells in small electric fields are serum dependent. *J Cell Sci.* (1996) 109:1405–14. doi: 10.1242/jcs.109.6.1405

08

Quantum Molecular Resonance Effects on Patients With Dry Eye Disease: A Randomized Controlled Trial

A. Shemer, A. Altarescu, L. Nusbaum, M. Vardi, B. Dubinsky-Pertzov, I. Hecht, L. Or, A. Einan-Lifshitz, E. Pras

Quantum Molecular Resonance Effects on Patients With Dry Eye Disease: A Randomized Controlled Trial

Asaf Shemer, MD,† Aya Altarescu, MD,*† Lee Nusbaum, MD,*† Maya Vardi, MD,*† Biana Dubinsky-Pertzov, MD, MPH,*† Idan Hecht, MD,*† Lior Or, MD,*† Adi Einan-Lifshitz, MD,*† and Eran Pras, MD*†‡*

Downloaded from http://journals.lww.com/corneajrnl by BhDMf5ePHKav1zEoum1tQfN4a+kJLhEZgbsIHo4XMi0hCywCX1AWnYQp/IlQrHD3i3D0OdRyi7TvSFl4Cf3VC4/OAVpDDa8KKGKV0Ymy+78= on 01/08/2024

Purpose: The aim of the study was to evaluate the efficacy and safety of quantum molecular resonance in the treatment of dry eye disease.

Methods: This study was a double-blind randomized control trial in 1 academic medical center, for 2 years. Participants received treatment or a placebo with the Rexon-Eye device, once per week for 4 weeks. The primary outcome was the change in dry eye symptoms assessed by the Ocular Surface Disease Index (OSDI). Secondary outcomes were clinical findings associated with the dry eye such as meibomian gland dysfunction (MGD) score, tear break-up time (TBUT), corneal fluorescein staining, Schirmer test, and best-corrected visual acuity (BCVA).

Results: Forty patients were recruited, 20 in each arm. The mean age was 63.5 ± 15.1 years and 27 (67.5%) were female. The mean OSDI score significantly improved in the intervention group from 19.15 ± 10.3 to 10.5 ± 7.0 ($P < 0.001$), whereas the control group showed no significant change (14.4 ± 8.4 to 15.5 ± 8.6, $P = 0.830$). MGD scores significantly improved in the intervention group (1.57 ± 1.2 to 0.8 ± 0.9, $P = 0.006$), whereas showing no significant change in the control group (1.60 ± 0.9 to 1.99 ± 1.0, $P = 0.244$). The corneal staining score also showed significant improvement in the intervention group ($P = 0.045$) and a non-significant decline in the placebo group ($P = 0.50$). No significant difference was seen in TBUT, visual acuity, and Schirmer scores between groups. No harm resulting from treatment was reported during the duration of the trial.

Conclusions: High-frequency electrotherapy may have a positive effect on symptoms and signs of dry eye. This emerging technology may become part of the arsenal of therapeutic modalities for this condition.

Key Words: dry eye, dry eye disease, quantum molecular resonance, Rexon, Ocular Surface Disease Index

(*Cornea* 2023;00:1–6)

Dry eye disease (DED) is a highly prevalent and disabling disorder, which affects approximately 9 million persons in the United States alone.[1] Affected individuals can have a considerable reduction in quality of life and suffer from decreased visual function, social and physical functioning, and workplace productivity.[2] Available treatments include the administration of artificial tear substitutes, suppression of ocular inflammation, eyelid hygiene, and targeted treatment for improving meibomian gland function. However, these therapeutic modalities have limited efficacy and the dry eye remains a chronic and debilitating disorder and an area of unmet medical need.[3]

The Rexon-Eye device (Resono Ophthalmic Inc, Sandrigo, Italy) is a new device based on quantum molecular resonance (QMR) technology. QMR is a technique in which low-intensity, high-frequency electric currents are administered to a biological tissue through contact electrodes.[4] The Rexon-Eye device applies stimulation to the epidermis of closed eyelids up to the lid margin through specially designed goggles. Previous studies have shown a favorable safety profile with high patient satisfaction for several QMR devices. Results of several studies suggested that the Rexon device can be an effective tool for accelerating healing in systemic chronic wounds and tissue regeneration.[5,6] In addition, 2 recent observational, nonrandomized studies reported the device to be both subjectively and objectively effective for treating symptoms of dry eye; however, no control group was evaluated.[6,7]

Given these results, we set out to evaluate whether the QMR technology is effective for the treatment of dry eye disorder. The purpose of this study was to evaluate the efficacy and safety of the Rexon-Eye device in a randomized, placebo-controlled, double-blind fashion.

Received for publication August 6, 2023; revision received September 19, 2023; accepted October 29, 2023.

From the *Department of Ophthalmology, Shamir Medical Center (formerly Assaf-Harofeh), Tzrifin, Israel; †Faculty of Medicine, Tel Aviv University, Tel Aviv, Israel; and ‡The Matlow's Ophthalmo-Genetics Laboratory, Department of Ophthalmology, Shamir Medical Center (formerly Assaf-Harofeh), Tzrifin, Israel.

The authors have no funding or conflicts of interest to disclose.

Supplemental digital content is available for this article. Direct URL citations appear in the printed text and are provided in the HTML and PDF versions of this article on the journal's Web site (wwwcorneajrnl.com).

This study was approved by the institutional research committee (Reference number: 0194-20-ASF) and was performed in accordance with the ethical standards of the 1964 Declaration of Helsinki and its later amendments. This study involves human participants and was approved by Shamir Medical Center Helsinki Ethics Committee. Reference number: 0194-20-ASF.

Correspondence: Asaf Shemer, MD, Department of Ophthalmology, Shamir Medical Center, Be'er Ya'akov 70300, Israel (e-mail: ShemerAsafMD@gmail.com).

Copyright © 2023 Wolters Kluwer Health, Inc. All rights reserved.

Copyright © 2023 Wolters Kluwer Health, Inc. Unauthorized reproduction of this article is prohibited.

METHODS

This study adhered to the tenets of the Declaration of Helsinki and was approved by the Institutional Review Board (IRB) of the Shamir Medical Center. Informed written consent was granted before enrollment.

Design and Patient Population

The study was conducted at Shamir Medical Center (Assaf-Harofeh), an academic tertiary medical center in central Israel. This was a double-masked, randomized control trial (ClinicalTrials.gov Identifier: NCT05469932).

We included male or female subjects 18 years or older who have the full legal capacity to volunteer on the date the informed consent document is signed. Additional inclusion criteria were subjects who agreed to participate in the study, subjects who can follow the instructions of the clinical staff at the clinical site, can attend examinations on the scheduled examination date, and subjects who meet the applicable criteria for patients suspected of having DED. A diagnosis of DED was obtained after a corneal specialist examination. The definition of DED was defined as having each of the following in OU: 1) Ocular Surface Disease Index (OSDI) score <13, 2) tear break-up time (TBUT) ≤ 10, and 3) corneal staining ≥ 1. We excluded subjects who routinely use contact lenses, have active intraocular inflammation, female subjects of childbearing potential who are currently pregnant or nursing, experienced ocular trauma, or subjects who underwent any ophthalmic intervention (surgery, refractive laser surgery, etc) within 6 months before the trial.

Study Protocol

Participants were randomized into 2 groups: intervention and placebo groups. Patients in the intervention group were treated with the Rexon-Eye device 4 times, once per week for a total of 4 weeks at the manufacturer's recommended power setting (power 4). Patients in the control group were treated at identical treatment sessions with the Rexon-Eye device (4 times, once per week for a total of 4 weeks) at identical locations and duration. They were connected to the device; however, the device was set at zero power during treatment. Throughout the trial, we took all measures to ensure that patients had a consistent experience in both groups, making it difficult for them to discern whether they were receiving active treatment or placebo. Treatment sessions were scheduled at varying times, effectively preventing communication between participants in the 2 groups.

All patients were examined by an experienced ophthalmologist before the first treatment and after the last treatment.

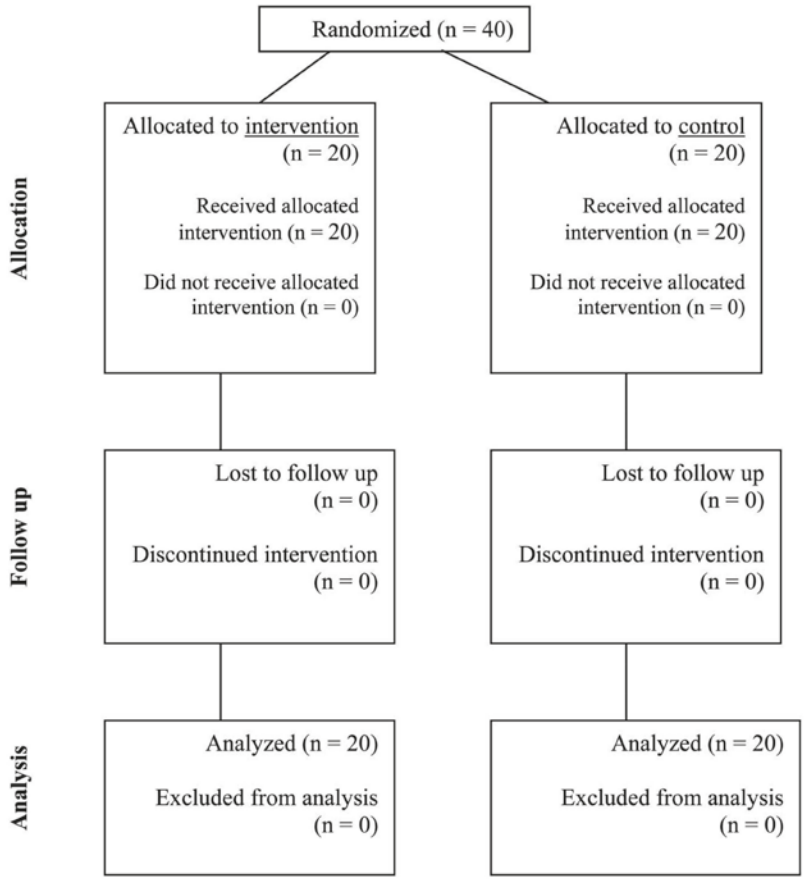

FIGURE 1. Diagram showing the flow of participants through each stage of the trial (CONSORT).

Copyright © 2023 Wolters Kluwer Health, Inc. All rights reserved.

Copyright © 2023 Wolters Kluwer Health, Inc. Unauthorized reproduction of this article is prohibited.

Downloaded from http://journals.lww.com/corneajrnl by BhDMf5ePHKav1zEoum1tQfN4a+kJLhEZgbsIHo4XMi0hCywCX1AWnYQp/IlQrHD3i3D0OdRyi7TvSFl4Cf3VC4/OAVpDDa8KKGKV0Ymy+78= on 01/08/2024

Downloaded from http://journals.lww.com/corneajrnl by BhDMf5ePHKav1zEoum1tQfN4a+kJLhEZgbsIHo4XMi0hCywCX1AWnYQp/IlQrHD3i3D0OdRyi7TvSFl4Cf3VC4/OAVpDDa8KKGKV0Ymy+78= on 01/08/2024

TABLE 1. Clinical Characteristics of the Intervention and Control Groups at Baseline

Variable	Intervention Group N (%)	Intervention Group SD	Control Group N (%)	Control Group SD	*P*
No. of patients	20		20		
Age, mean	62.8	16.5	64.3	14.1	0.769
Female sex	13 (65)		14 (70)		0.736
BMI, kg/m^2	26.6	7.2	26.2	6.0	0.867
Medical history					
Smoking	4 (20)		3 (15)		0.677
Asthma	0 (0)		2 (10)		0.136
Diabetes mellitus	3 (15)		7 (35)		0.118
Hypertension	4 (20)		7 (35)		0.243
History of malignancy*	1 (5)		0 (0)		0.323
Ocular history					
Refractive surgery - LASIK	2 (10)		1 (5)		0.720
Refractive surgery - PRK	3 (15)		2 (10)		0.652
Cataract surgery	6 (30)		9 (45)		0.484
Pars plana vitrectomy	1 (5)		1 (5)		1.0
Anti-VEGF treatment	0 (0)		1 (5)		0.323
Blepharoplasty	4 (20)		3 (15)		0.677
Pterygium	0 (0)		1 (5)		0.323
BCVA (logMAR)	0.141	0.155	0.133	0.11	0.855
Signs and symptoms of dry eye disease (mean ± SD)					
Baseline OSDI score, mean	19.15	10.3	14.4	8.4	0.119
MGD score, mean	1.57	1.2	1.60	0.9	0.943
Tear break-up time, seconds	6.58	3.1	6.65	2.9	0.941
Corneal staining, mean	2.25	2.3	2.30	2.1	0.943
Schirmer score, mm	8.50	7.5	10.6	7.7	0.379

Clinical and demographic characteristics of 40 patients included in the study.
*One individual in the intervention group had thyroid cancer.
BMI, body mass index.

Each examination was composed of a subjective questionnaire (eg, OSDI) filled out by the subject and clinical assessment that included the following for each eye: meibomian gland dysfunction (MGD) score: we used gentle meibomian gland expression for the lower and upper eyelids using a cotton-tipped applicator. Secretions were graded according to the Bron scale (0 = clear, 1 = cloudy, 2 = cloudy with debris, and 3 = inspissated, toothpaste-like). MGD score was calculated as a mean of both upper and lower lids; TBUT was assessed after placing a drop of fluorescein solution into the eye; and corneal staining was evaluated under cobalt blue filter illumination after fluorescein instillation. The cornea was examined for the presence of discrete "dots" of staining, and the number of dots was counted and assigned a grading score (0 = 0 dots, 1 = 1–5 dots, 2 = 6–30 dots, and 3 = >30 dots). Additional extra points are collected for patches of confluent staining (+1 point), staining in the pupillary area (+1 point), and the presence of one or more filaments (+1 point). The total ocular staining score for each eye was determined by adding up the fluorescein score for the cornea. The maximum possible score for each eye was 6. MGD score, TBUTs, and corneal staining were measured using a slit-lamp biomicroscope. Schirmer test was conducted after anesthesia with 1 drop of oxybuprocaine hydrochloride 0.4%. The physician then bend a TearFlo Schirmer test strip (HUB Pharmaceuticals, LLC) and placed it into the lower temporal lid margin of each eye of the participant. Subjects were instructed to close their eyes. After 5 minutes have elapsed, the Schirmer strip was removed. The length of the moistened area was recorded (mm) for each eye separately.

Demographics, medical history, concomitant medication, and artificial tear use data were collected. During the trial, the patients were instructed to continue their regular treatment for dry eye (eg, artificial tears, etc).

Masking

Patients and examiners were masked to the allocation. Patients allocated to the placebo group were given the same number and length of treatments performed identically to the intervention group but with the device set to a power of zero in the duration of treatment. During treatment, the electrical current provided by the device is not felt by the patient and no noise or other indication exists for the power setting used. Patients did not have access to the device control panel or display. Ophthalmologists examining the patients at the beginning and end of the trial were also masked to the treatment.

Outcomes

The primary objective of this study was to evaluate the change in dry eye symptoms assessed by the OSDI between patients treated with the Rexon-Eye device and controls. This index has been previously shown to be a valid and reliable instrument for measuring the severity of DED.[8] It is based on assessing 3 aspects: ocular symptoms, vision-related function, and environmental triggers. The index was assessed twice, at the beginning of the trial and after the last treatment.

Secondary objectives were clinical signs associated with a dry eye disorder, which were assessed by a masked examiner. These included MGD score, TBUT, corneal staining score, Schirmer score, and best-corrected visual acuity (BCVA).

Statistical Analysis

Statistical analysis was performed using SPSS for Windows version 23.0 by IBM (Armonk, NY). For categorical variables, χ^2 tests were used. Clinical parameter distributions were tested for normality by the Shapiro–Wilk test. Independent and paired t-tests were conducted for continuous variables with a normal distribution and the Mann–Whitney U and Wilcoxon tests were for variables with a nonnormal distribution. For TBUT, a cutoff of 10 seconds was used to indicate normal and abnormal values. *P* values less than 0.05 on a 2-sided test were considered statistically significant. To avoid biases arising from between-eye correlation, a single eye (right eye) of each patient was included in the analysis.[9]

Copyright © 2023 Wolters Kluwer Health, Inc. All rights reserved.

Copyright © 2023 Wolters Kluwer Health, Inc. Unauthorized reproduction of this article is prohibited.

Table 2. Clinical Outcomes Between Groups

Variable	Intervention Group Change	Intervention Group SD	Control Group Change	Control Group SD	*IP*
Main outcome					
Overall OSDI score	−8.6	7.8	0.5	9.4	**0.002**
1st part*	−3.2	3.7	0	5.7	**0.036**
2nd part†	−3.0	3.2	0.4	1.9	**0.004**
3rd part‡	−2.6	3.6	0.9	3.4	**0.003**
Secondary outcomes					
MGD score	−0.75	1.1	0.37	1.4	**0.007**
Upper lid	−0.60	1.3	0.35	1.5	**0.037**
Lower lid	−0.90	1.0	0.41	1.6	**0.004**
Tear break-up time, sec	1.6	4.1	−0.45	3.3	0.097
Corneal staining	−1.1	2.3	0.30	1.9	0.044
Schirmer score (mm)	0.90	5.0	1.65	6.7	0.693
BCVA (logMAR)	−0.0074	0.06	0.0049	0.04	0.450

*Symptoms.
†Limitation in activity.
‡Environmental triggers.
Clinical outcomes of the 40 patients included in the study according to the group. The change in each parameter after the trial period is compared between groups.
Data were expressed as mean ± SD.
Significant values are in bold.

We also report the outcomes for the left eye for sensitivity testing.

Sample Size

For sample size calculations, we used the reduction in OSDI as the primary outcome.[8] Power calculations showed that a minimum of 14 participants in each group were required to detect a clinically significant difference of 5 points with a 2-sided significance level of 0.05 and a power of 80% using a paired model. The SD of normal values was estimated to be 6 points. To increase power and take into account unexpected variables, we decided on an additional 30% margin and recruitment was set at 20 participants in each group. Calculations were performed using MedCalc software version 16 (Mariakerke, Belgium).

RESULTS

Participant Flow and Baseline Data

Forty patients were recruited and included in the final analysis (20 were randomly allocated to the intervention group and 20 to the control group; Fig. 1). The mean age was 63.5 ± 15.1 years and 27 (67.5%) were female. Eight patients had previously undergone laser refractive surgery (n = 5 photorefractive keratectomy (PRK), n = 3 laser-assisted in situ keratomileusis (LASIK)), 16 patients had a history of cataract surgery (14 in OU, 2 in either the left or right eye only), and 2 patients had previously undergone pars plana vitrectomy. No statistically significant difference in any baseline characteristic was seen between the 2 groups. All 40 patients had a known diagnosis of DED. Additional baseline characteristics are available in Table 1.

Main Outcome: OSDI Scores

Baseline OSDI scores were similar between groups (Table 1). The mean OSDI score significantly improved in the intervention group from 19.15 ± 10.3 to 10.5 ± 7.0 ($P < 0.001$), whereas the control group showed no statistically significant change (14.4 ± 8.4–15.5 ± 8.6, $P = 0.830$). The difference between groups was statistically significant (−8.6 ± 7.8 vs. 0.5 ± 9.4, intervention and control groups, respectively, $P = 0.002$). A comparison of clinical outcomes between groups is further detailed in Table 2.

Assessing the individual parts of the OSDI showed consistent results. In all 3 parts individually, a significant improvement was seen in the intervention group but not in the control (Fig. 2 and Table 3).

Secondary Outcomes: Clinical Signs Assessment

MGD scores significantly improved in the intervention group (1.57 ± 1.2–0.8 ± 0.9, $P = 0.006$) while showing no significant change in the control group (1.60 ± 0.9–1.97 ± 1.0, $P = 0.244$). The lower eyelids specifically showed the largest amount of improvement (1.50 ± 1.1–0.60 ± 0.8, $P = 0.001$ in the intervention group; 1.60 ± 1.0–2.0 ± 1.1, $P = 0.269$ in the control group; Table 3).

Further secondary outcomes included corneal staining that showed a significant improvement in the intervention group (2.25 ± 2.3–1.1 ± 1.4, $P = 0.045$) while showing a nonsignificant change in the control group (2.3 ± 2.1–2.6 ± 2.1, $P = 0.500$). The difference between groups was also statistically significant (Table 2).

TBUT showed a nonsignificant improvement in the intervention group (6.6 ± 3.1–8.2 ± 2.4 seconds, $P = 0.112$) and a nonsignificant decline in the control group (6.6 ± 2.9–6.2 ± 2.2 seconds, $P = 0.549$). In the intervention group, 7 patients (35%) improved from below 10 seconds to 10 or more seconds, compared with only 1 (5%) in the control group ($P = 0.082$, Table 2).

Schirmer scores showed no significant change in either group after the study period, and no significant differences between groups were seen (Table 2). To further assess sensitivity scores, we also analyzed the left eye scores, which demonstrated similar results between groups (Supplemental Table 1, Supplemental Digital Content 1, hiip://links.lww.com/ICO/B608).

Safety and Side Effects

Visual acuity was assessed for safety monitoring. Visual acuity did not change significantly in the duration of the trial (0.141 ± 0.155 logarithm of the minimum angle of resolution (logMAR) [Snellen equivalent: 20/27.67] to 0.133 ±0.12 logMAR [Snellen equivalent: 20/27.16], $P = 0.578$ in the intervention group; 0.133 ± 0.11 logMAR [Snellen equivalent: 20/27.16] to 0.137 ±0.11 logMAR [Snellen equivalent: 20/27.41], $P = 0.609$ in the control group). No further adverse events were reported during the trial.

Copyright © 2023 Wolters Kluwer Health, Inc. All rights reserved.

Copyright © 2023 Wolters Kluwer Health, Inc. Unauthorized reproduction of this article is prohibited.

Downloaded from http://journals.lww.com/corneajrnl by BhDMf5ePHKav1zEoum1tQfN4a+kJLhEZgbsIHo4XMi0hCywCX1AWnYQp/IlQrHD3i3D0OdRyi7TvSFl4Cf3VC4/OAVpDDa8KKGKV0Ymy+78= on 01/08/2024

subjective and objective parameters. OSDI scores improve from 43.0 to 25.3 ($P = 0.001$), TBUT increased from 4.7 to 7.1 in the right eyes ($P = 0.001$) and from 4.6 to 6 in the left eyes ($P > 0.05$), fluorescein staining decreased from 1.2 to 0.4 in OU ($P < 0.001$), and Schirmer test score increased from 5.8 to 9.9 in the left eyes ($P < 0.001$) and from 6.7 to 8 in the right eyes ($P > 0.05$). However, the study was limited by the lack of a control group. Furthermore, results were significant only in part of the parameters, and sometimes for 1 eye only.[6] A different study specifically addressed a population of 25 patients with evaporative DED and also reported positive outcomes of the QMR high-frequency electrotherapy, with no adverse events.[7]

Recently, Trivli et al tested the effects of QMR on 18 patients with DED. In that study, OSDI improved from 45.46 to 34.45 ($P = 0.013$), corneal staining (by the Oxford scale) decreased from 1.41 to 0.55 ($P = 0.002$), TBUT increased from 6.71 to 9.53 ($P < 0.001$), and Schirmer test results increased from 8.75 to 9.91 ($P = 0.675$).[14]

Yet, while presenting significant improvement in most parameters, all of the above studies did not include a control group and thus are prone to biases. Our results correspond with these of previous studies. They demonstrate an improvement in symptoms and some clinical signs.

This study has limitations. First, we evaluated only 40 patients in 1 center. Our results should be confirmed in a larger multicenterd trial. Second, we included all types of DED, with no subclassification including postrefractive patients. Finally, we mainly assess short-term results, and long-term follow-up data are not yet available.

To conclude, among 40 patients randomly treated with the Rexon-Eye device or placebo treatments, a positive therapeutic effect was seen in the intervention group. This modality can be considered an adjunct option in the arsenal of therapeutic agents for patients with DED.

REFERENCES

1. Novack GD, Asbell P, Barabino S, et al. TFOS DEWS II clinical trial design report. *Ocul Surf.* 2017;15:629–649.
2. Miljanović B, Dana R, Sullivan DA, et al. Impact of dry eye syndrome on vision-related quality of life. *Am J Ophthalmol.* 2007; 143:409–415.
3. O'Neil EC, Henderson M, Massaro-Giordano M, et al. Advances in dry eye disease treatment. *Curr Opin Ophthalmol.* 2019;30:166–178.
4. Sella S, Adami V, Amati E, et al. In-vitro analysis of quantum molecular resonance effects on human mesenchymal stromal cells. *PLoS One.* 2018;13:e0190082.
5. Fraccalvieri M, Salomone M, Di Santo C, et al. Quantum molecular resonance technology in hard-to-heal extremity wounds: histological and clinical results. *Int Wound J.* 2017;14:1313–1322.
6. Pedrotti E, Bosello F, Fasolo A, et al. Transcutaneous periorbital electrical stimulation in the treatment of dry eye. *Br J Ophthalmol.* 2017;101:814–819.
7. Ferrari G, Colucci A, Barbariga M, et al. High frequency electrotherapy for the treatment of meibomian gland dysfunction. *Cornea.* 2019;38: 1424–1429.
8. Özcura F, Aydin S, Helvaci MR. Ocular surface disease index for the diagnosis of dry eye syndrome. *Ocul Immunol Inflamm.* 2007;15: 389–393.
9. Karakosta A, Vassilaki M, Plainis S, et al. Choice of analytic approach for eye-specific outcomes: one eye or two? *Am J Ophthalmol.* 2012;153: 571–579.e1.
10. Maschio MD, Canato M, Pigozzo FM, et al. Biophysical effects of high frequency electrical field (4-64 MHz) on muscle fibers in culture. *Basic Appl Myology.* 2009;19:49–56.
11. Gulotta F, Grazzi L, Allais GB, et al. P031. An observational study on chronic tension-type headache treatment with Quantum Molecular Resonance according to I.A.R.A. model®. *J Headache Pain.* 2015; 16(suppl 1):A176.
12. Demirhan E, Çukurova I, Arslan IB, et al. Quantum molecular resonance-assisted phonomicrosurgery: preliminary experience. *Otolaryngol Head Neck Surg.* 2015;152:189–192.
13. Ahn TH, Kim DY, Kim HM, et al. Use of quantum molecular resonance energy for managing postrhinoseptoplasty perilesional edema and ecchymosis. *J Cosmet Dermatol.* 2022;21:3530–3536.
14. Trivli A, Karmiris E, Dalianis G, et al. Evaluating the efficacy of Quantum Molecular Resonance (QMR) electrotherapy in mixed-type dry eye patients. *J Optom.* 2023;16:128–134.

Downloaded from http://journals.lww.com/corneajrnl by BhDMf5ePHKav1zEoum1tQfN4a+kJLhEZgbsIHo4XMi0hCywCX1AWnYQp/IlQrHD3i3D0OdRyi7TvSFl4Cf3VC4/OAVpDDa8KKGKV0Ymy+78= on 01/08/2024

Copyright © 2023 Wolters Kluwer Health, Inc. All rights reserved.

Copyright © 2023 Wolters Kluwer Health, Inc. Unauthorized reproduction of this article is prohibited.

09

Efficacy and Safety of Quantum Molecular Resonance Electrotherapy in Patients with Aqueous-Deficient, Evaporative and Mixed-Type Dry Eye: A Randomized Interventional Study

A. Ballesteros-Sánchez, J.M. Sánchez-González, G.R. Tedesco, C. Rocha-De-Lossada, F. Russo, A. Spinelli, I. Ingrande, D. Borroni

Ophthalmol Ther
https://doi.org/10.1007/s40123-023-00868-w

ORIGINAL RESEARCH

Efficacy and Safety of Quantum Molecular Resonance Electrotherapy in Patients with Aqueous-Deficient, Evaporative and Mixed-Type Dry Eye: A Randomized Interventional Study

Antonio Ballesteros-Sánchez · José-María Sánchez-González · Giovanni Roberto Tedesco · Carlos Rocha-De-Lossada · Fedele Russo · Antonio Spinelli · Irene Ingrande · Davide Borroni

Received: October 17, 2023 / Accepted: November 24, 2023
© The Author(s) 2023

ABSTRACT

Introduction: To evaluate the efficacy and safety of Quantum Molecular Resonance (QMR) treatment in patients with severe dry eye disease (DED), as well as its effects on aqueous-deficient (ADDE), evaporative (EDE), and mixed (MDE) dry eye.

Methods: In this prospective, interventional study, 81 patients were randomly allocated to received four treatment sessions of QMR at 1-week intervals (Rexon-Eye®, Resono Ophthalmic, Trieste, Italy) (QRM group) or tear substitute four times daily, containing 0.15% sodium hyaluronate and 3% trehalose (Thealoz Duo®, Thea Pharma, France) (SH-TH group). Outcome measures included ocular surface disease index (OSDI) questionnaire, tear meniscus height (TMH), tear breakup time (TBUT), non-invasive breakup time (NIBUT), corneal fluorescein staining (CFS), lipid layer thickness

A. Ballesteros-Sánchez · J.-M. Sánchez-González
Department of Physics of Condensed Matter, Optics Area, University of Seville, 41004 Seville, Spain

J.-M. Sánchez-González
e-mail: jsanchez88@us.es

A. Ballesteros-Sánchez
Department of Ophthalmology, Clínica Novovisión, 30008 Murcia, Spain
e-mail: antbasan@alum.us.es

G. R. Tedesco · F. Russo
Studio Oculistica Tedesco, 88024 Girifalco, Italy

G. R. Tedesco
e-mail: j.tedesco@libero.it

C. Rocha-De-Lossada
Qvision, Ophthalmology Department, VITHAS Almería Hospital, 04120 Almería, Spain

C. Rocha-De-Lossada
Ophthalmology Department, VITHAS Malaga, 29016 Malaga, Spain

C. Rocha-De-Lossada
Regional University Hospital of Malaga, Hospital Civil Square, 29009 Malaga, Spain

C. Rocha-De-Lossada
Department of Surgery, Ophthalmology Area, University of Seville, 41009 Seville, Spain
e-mail: carlosrochadelossada5@gmail.com

A. Spinelli
Biomeeting, Reggio Calabria, Italy

I. Ingrande
University of Messina, Messina, Italy

D. Borroni (✉)
Riga Stradins University, Riga 1007, Latvia
e-mail: info.borroni@gmail.com

D. Borroni
Centro Oculistico Borroni, Gallarate, Italy

D. Borroni
Eyemetagenomics Ltd., 71–75, Shelton Street, Covent Garden, London WC2H 9JQ, UK

Published online: 19 December 2023

(LLT), tear film osmolarity (OSM), and meibomian gland dysfunction (MGD) grade, which were assessed at baseline and 1-month and 3-month follow-up.

Results: The QMR group achieved better improvements than the SH-TH group in OSDI and SANDE questionnaires, NIBUT, LLT, and CFS. The mean differences between the groups were as follows: OSDI (− 12.4 ± 0.25 points, $P = 0.01$), SANDE (10.6 ± 1.7 points, $P = 0.01$), NIBUT (2 ± 0.25 s, $P = 0.01$), LLT (18.7 ± 0.7 nm, $P = 0.01$), and CFS (1.2 ± 0.1 points, $P = 0.02$). In subgroups analysis, QMR treatment demonstrated a beneficial role to improve DED symptoms and signs in ADDE, EDE, and MDE.

Conclusion: QMR is an effective and well-tolerated treatment that seems to improve DED symptoms and signs in patients with severe DED. However, further studies are needed to confirm this.

Trial Registration: ClinicalTrials.gov identifier NCT06119386.

Keywords: Quantum Molecular Resonance electrotherapy; Dry eye disease; Aqueous-deficient dry eye; Evaporative dry eye; Mixed dry eye; Meibomian gland dysfunction

Key Summary Points

Why carry out this study?

Current treatments for dry eye disease (DED) require chronic use with possible side effects in some of them. Therefore, there is an unmet need for novel treatments that target the specific mechanism involved in the pathogenesis of DED.

This study evaluates the efficacy and safety of Quantum Molecular Resonance (QMR) treatment in patients with severe DED.

What was learned from the study?

Four sessions of QMR treatment seems to improve symptoms and signs in aqueous-deficient dry eye (ADDE), evaporative dry eye (EDE), and mixed dry eye (MDE), which suggests that this treatment could be an effective and safe option to address DED. However, further studies are needed.

INTRODUCTION

Dry eye disease (DED) is a multifactorial, chronic disease of the ocular surface that affects up to 30% of adults over the age of 50, it is more frequent in women, and its prevalence increases with age [1, 2]. According to the recent definition provided by The Tear Film and Ocular Surface Society (TFOS) Dry Eye Workshop (DEWS) II, DED is characterized by loss of homeostasis and tear film instability, where hyperosmolarity and inflammation play a key role in its pathogenesis [1, 3]. In addition, corneal and conjunctival epithelial cell damage, apoptosis, and metaplasia as well as inflammation and imbalance of cytokines on the ocular surface are also key factors of DED [1, 3–5], which may lead to a wide variety of ocular symptoms, such as foreign body sensation, burning, and visual disturbances, affecting patients' quality of life [6–8].

Dry eye diagnosis could be established by a combination of objective and subjective tests [9]. Regarding DED symptoms assessment, the ocular surface disease index (OSDI) and the symptom assessment in dry eye (SANDE) questionnaires are the most commonly used in clinical studies [9–12]. Both questionnaires determine the severity of DED symptoms with a score from 0 to 100. However, the OSDI questionnaire requires the patient to read, understand, and answer 12 questions, whereas the SANDE questionnaire only includes two questions on a visual analog scale and provides clinicians with a quick and reliable assessment of DED symptoms [13, 14]. Regarding DED signs

assessment, classic methods, such as tear film breakup time (TBUT), Schirmer test (ST), and corneal fluorescein staining (CFS), have been widely used, but these depend on the skill of the examiner and influence tear film stability [9, 15, 16]. Therefore, objective, non-invasive tests, such as non-invasive tear film breakup time (NIBUT), tear meniscus height (TMH), and lipid layer thickness (LLT), are preferred in the assessment of patients with DED [9, 17]. In addition, new devices that automatically perform objective, non-invasive tests have been developed, which reduce observer bias in some tests, such as meibography, and do not alter tear film stability, resulting in a potential screening tool for DED [18, 19].

Although DED may be classified in aqueous-deficient dry eye (ADDE), evaporative dry eye (EDE), and mixed dry eye (MDE), the evidence suggests that all forms of DED have an evaporative component since ocular surface hyperosmolarity only can arise in response to evaporation [3]. Meibomian gland dysfunction (MGD) is the most common form of EDE and its first line of treatment usually includes warm compresses, eyelid hygiene, oral antibiotics, and preservative-free tear substitutes containing lipid supplements [20–22]. However, these treatments require chronic instillations with possible side effects related to some of them [23, 24]. Therefore, novel treatments that target the specific mechanism involved in the pathogenesis of DED have emerged, such as microblepharoexfoliation (MBE) [25], vectoral thermal pulsation (VTP) [26], intense pulse light (IPL) [27], and low-level light therapy (LLLT) [28]. Recently, Quantum Molecular Resonance (QMR) has been proposed as a novel therapy for DED, demonstrating promising results [29–33]. QMR involves passing an electric current at a low intensity and high frequency (4–64 MHz) through contact electrodes [30, 32]. Previous studies have demonstrated the wound healing properties and anti-inflammatory effects of QMR on the ocular surface [29–33]. However, most of these studies evaluated only patients with mild to moderate DED with a short-term follow-up period [29–32].

Therefore, this study aims to evaluate the efficacy and safety of QMR treatment in patients with severe DED after 3-month follow-up, as well as to analyze its effects on ADDE, EDE, and MDE.

METHODS

Study Design

This prospective, randomized interventional study was carried out at the Tedesco Eye Center (Girifalco, CZ, Italy) between November 2022 and February 2023. This study fulfilled all the requirements of the Declaration of Helsinki and was approved by the center's internal review board (Approval Nr. DB13385-2568932022, ClinicalTrials.gov identifier NCT06119386). Before initiating the study, informed and written consent was obtained from each patient. Patient consent was received for Fig. 2.

Patients

Eligible patients were adults > 18 years old with a self-reported history of DED in both eyes for ≥ 6 months who met the following inclusion criteria in ≥ 1 eye at screening and randomization: OSDI score ≥ 33 points and TBUT < 10 s [9]. In addition, patients were divided into ADDE, EDE, and MDE subgroups according to the following criteria: TMH < 0.20 mm and ST 1 < 10 mm/5 min for ADDE; meibomian gland expressibility score between 1 and 2 points, meibum quality between 4 and 13 points, and LLT < 40 nm for EDE; and both sets of criteria were considered for MDE [9, 34].

Patients were excluded from participation if they met any of the following criteria: skin pathologies that prevent QRM treatment; all corneal disorders that affect diagnostic test, such as active corneal infection and corneal dystrophies; active ocular allergies; intraocular surgery or laser ocular surgery within the previous 6 months; use of topical antibiotics and anti-inflammatory treatments, including steroids and non-steroidal anti-inflammatory drugs; contact lens wearers; pregnant or lactating women; and patients who did not understand or comprehend the informed consent. A

washout period of 1 week was considered before QMR treatment.

Treatments

Eligible patients were randomized in a 1:1 ratio to received either four treatment sessions of QMR treatment at 1-week intervals (Rexon-Eye®, Resono Ophthalmic, Trieste, Italy) (QMR group) (Figs. 1 and 2) or four times daily tear substitute containing 0.15% sodium hyaluronate and 3% trehalose (Thealoz Duo®, Thea Pharma, France) (SH-TH group). QMR treatment was performed using specific contact electrodes built into a mask, which is worn by the patient over closed eyes. In addition, a disposable waterproof facial strip, worn between the mask and the eyelid surface, was used to uniformly spread the electric current over the whole ocular surface, and also ensuring personal hygiene. The device provides an interface showing the applied power with a custom unit scale, marked from 0 to 10, and the duration of the treatment. The duration of each treatment session was 20 min, using an intensity of 5 units, which correspond to an average power of 12 W, with 60 V voltage and 200 mA current between the goggle electrode and the neutral plate electrode.

Clinical Endpoints

Clinical endpoints were assessed at baseline (1 day) and two follow-up visits: month 1 (4 ± 0.5 weeks) and month 3 (12 ± 1 weeks). All clinical endpoints were performed in the sequence proposed by Ballesteros et al. [19] to best preserve the integrity of the tear film to avoid affecting test results. In addition, they were obtained in standard environmental conditions in the same room by a trained optometrist.

Fig. 1 Rexon-Eye® suite

Fig. 2 Real-time Rexon-Eye® procedure

Dry Eye Symptoms

The OSDI and SANDE questionnaires were used to evaluate DED symptoms severity, ranging from 0 (no ocular surface disease) to 100 (severe ocular surface disease) points [10, 12]. Both questionnaires were completed in consultation at all follow-up visits.

Tear Film Stability and Volume

Tear film stability was automatically evaluated with NIBUT (expressed in seconds, s) by projecting the Keratograph 5M® (Oculus Optikgeräte GmbH, Wetzlar, Germany) Placido rings onto the corneal surface, recording the time between the last blink and the initial distortion of the ring pattern. Fluorescein TBUT (expressed in seconds, s) was also evaluated. Patients were instructed to blink and then stare without blinking, recording the time

between the blink and the initial appearance of a dark spot. Three consecutive measurements of NIBUT and TBUT were averaged for statistical analysis. In addition, the Lipiview II® ocular surface interferometer (Johnson & Johnson, NJ, USA) and the TearLab® osmolarity system (TearLab corporation, CA, USA) were used to assess LLT (expressed in nanometers, nm) and tear film osmolarity (OSM, expressed in milliosmole, mOsm), respectively. Regarding tear volume, TMH was evaluated using the tear film scanning function of the Keratograph 5M® device, which allows for capturing images of the lower tear film meniscus determining its height.

Ocular Surface Staining

CFS was subjectively and invasively evaluated with the modified Oxford scale, ranging from grade 0 (no epithelial staining) to grade 5 (severe epithelial staining) [35]. Prior to assessing CFS, a single drop of unit dose saline was instilled onto a fluorescein impregnated strip. The lower right lid was then pulled down and the strip was tapped onto the lower tarsal conjunctiva. The same procedure was performed on the left eye. A cobalt-blue filter with yellow Kodak Wratten 12 barrier filter was used for better detection of CFS.

Meibomian Gland Analysis

Meibography was performed on the upper and lower eyelids to evaluate MGD. The loss area of meibomian glands was automatically assessed with the Keratograph 5M® device, which incorporates the JENVIS Grading Scale software, classifying MGD in four grades: grade 0 (no gland loss), grade 1 (loss in an area smaller than 1/3), grade 2 (loss in an area between 1/3 and 2/3), and grade 3 (loss in an area greater than 2/3).

Safety Assessment

Safety assessment included adverse events (AEs), best-corrected visual acuity (BCVA), intraocular pressure (IOP), slit-lamp biomicroscopy, and dilated funduscopy.

Statistical Analysis

Statistical analyses were performed with SPSS statistics software, version 28.0 (IBM Corporation, NY, USA). A total sample size of 62 patients was estimated using the GRANMO calculator, version 7.12 (Municipal Institute of Medical Research, Barcelona, Spain). Estimation was based on a statistically significant paired difference at 95% confidence and with 80% power of 6.45 ± 0.77 s in NIBUT based on previous studies [31–33].

Continuous variables were displayed as the mean ± standard deviation (SD), while ordinal categorical variables were expressed as frequencies (n) and percentages (%). Before the analyses, one eye was randomly selected. The randomization scheme was generated using an online randomizer program (https://www.randomization.com). After testing for normality with Kolmogorov–Smirnov test, we performed the paired Student's t test (parametric) or Wilcoxon's signed-rank test (nonparametric) to compare intra-group clinical outcomes. Within each group, the increment (Δ) was calculated. It was defined as the change from the last visit (LV) to baseline (B): $\Delta = LV - B$. Inter-group clinical outcomes were analyzed with the unpaired Student's t test (parametric) or Mann–Whitney's U test (nonparametric). Between each group, the differences were calculated as $\Delta_{IQM8\ group} - \Delta_{SH\text{-}TH\ group}$. Categorical variables were compared using the χ^2 test. A P value of less than 0.05 is considered to be statistically significant.

RESULTS

Baseline characteristics of the study populations are shown in Table 1. Eighty-one eyes of 81 patients, 23 (28.3%) men and 58 (71.6%) women with a mean age of 60.7 ± 7.9 years, were enrolled in the study. No significant differences in demographic characteristics or parameters related to DED were detected between both groups at baseline. In addition, all patients completed the study.

Table 1 Baseline characteristics of the study populations

Characteristics	QMR group (n = 43)	SH-TH group (n = 38)	P value
Demographics, mean ± SD or n (%)			
Age, years	60.2 ± 8.1	61.1 ± 7.6	0.46
Sex, male/female	11 (25.5)/32 (74.5)	12 (31.5)/26 (68.5)	0.24
Related to DED, mean ± SD			
SANDE, points	44.8 ± 27.4	45.2 ± 24.5	0.76
OSDI, points	55.8 ± 18.7	53.2 ± 21.4	0.79
NIBUT, s	8.7 ± 5.2	7.3 ± 7.1	0.89
TMH, mm	0.2 ± 0.2	0.3 ± 0.1	0.8
LLT, nm	54.6 ± 18.2	63.5 ± 13.5	0.76
TBUT, s	3.4 ± 1.4	3.2 ± 1.5	0.56
CFS, points*	3.1 ± 0.8	3.2 ± 0.6	0.59
OSM, mOsm/L	316.9 ± 9.4		
MGD, grade	1.8 ± 0.6	1.5 ± 0.6	0.43

CFS corneal fluorescein staining, *LLT* lipid layer thickness, *MGD* meibomian gland dysfunction, *NIBUT* non-invasive tear film breakup time, *OSDI* ocular surface disease index, *OSM* osmolarity, *QMR* Quantum Molecular Resonance, *SANDE* symptom assessment in dry eye, *SD* standard deviation, *SH* sodium hyaluronate, *TBUT* tear film breakup time, *TH* trehalose, *TMH* tear meniscus height
*Modified Oxford grading scale

Efficacy Endpoints

The efficacy of QMR treatment on DED symptoms and ocular surface parameters during follow-up visits in both groups is shown in Table 2.

Dry Eye Symptoms

After 3 months of follow-up, QMR treatment achieved significant ΔOSDI and ΔSANDE questionnaire reductions of − 23.3 ± 2.2 (P = 0.02) and − 22.7 ± 7.1 points (P = 0.01), respectively. However, only SH-TH treatment led to significant improvement in ΔSANDE questionnaire with a reduction of − 12.1 ± 2.7 points (P = 0.04).

Comparing both groups, the results were in favor QMR treatment with a difference in OSDI and SANDE questionnaire scores of − 12.4 ± 0.25 (P = 0.01) and − 10.6 ± 1.7 points (P = 0.01), respectively.

Tear Film, Ocular Surface Staining, and Meibomian Gland Analysis

After 3 months of follow-up, QMR treatment achieved significant improvements in ΔTBUT and ΔNIBUT of 1.7 ± 0.1 (P = 0.01) and 4.8 ± 0.6 s (P < 0.001), respectively. In addition, ΔTMH, ΔLLT, ΔCFS, and ΔOSM also showed significant improvements of 0.05 ± 0.04 mm (P < 0.001), 10.8 ± 2.4 nm (P = 0.002), − 1.6 ± 0.2 points (P = 0.01), and − 17.4 ± 2.5 mOsm/L (P < 0.001), respectively. Regarding SH-TH treatment, ΔTBUT and ΔNIBUT also achieved significant improvements of 3 ± 0.1 (P = 0.01) and 2.8 ± 0.1 s (P = 0.03) after 3 months of follow-up, respectively. Similar results were reported in ΔCFS and ΔOSS with values of − 0.4 ± 0.05 points and − 10.2 ± 2.3 mOsm/L, respectively. However, ΔLLT showed a significant worsening of − 7.9 ± 3.8 nm (P = 0.002).

Comparing both groups, the differences in NIBUT, LLT, and CFS were in favor of QMR treatment with values of 2 ± 0.25 s (P = 0.01), 18.7 ± 0.7 nm (P = 0.01), and − 1.2 ± 0.1 points (P = 0.02), respectively. The remaining outcomes were not in favor of any treatment group. In addition, no significant improvement in MGD grade was observed within and between groups.

Subgroups Analysis

The effects of QMR treatment on symptoms and ocular surface parameters of patients with ADDE, EDE, and MDE are shown in Tables 3, 4, and 5, respectively. Regarding the ADDE subgroup, significant improvement in ΔOSDI questionnaire, ΔNIBUT, ΔTMH, ΔLLT, and ΔOSM were reported, with values of

Table 2 Changes in symptoms and ocular surface parameters during follow-up visits in both groups

Parameters, mean ± SD	Baseline	1 Month	3 Months	*P* value
QMR group (n = 43)				
SANDE, points	44.8 ± 27.4	21.3 ± 11.3	22.1 ± 13.2	0.01*
OSDI, points	55.8 ± 18.7	31.7 ± 16.5	32.5 ± 14.3	0.02*
NIBUT, s	8.7 ± 5.2	13.9 ± 6.7	13.5 ± 6.4	< 0.001*
TMH, mm	0.23 ± 0.18	0.28 ± 0.1	0.28 ± 0.1	< 0.001*
LLT, nm	54.6 ± 18.2	64.8 ± 22	65.4 ± 23	0.002*
TBUT, s	3.4 ± 1.4	5.3 ± 1.5	5.1 ± 1.6	0.01*
CFS, points	3.1 ± 0.8	1.4 ± 0.4	1.5 ± 0.4	0.01*
OSM, mOsm/L	316.9 ± 9.4	299.1 ± 4.4	299.5 ± 4.5	< 0.001*
MGD, grade	1.8 ± 0.6	1.9 ± 0.6	1.9 ± 0.5	0.9
SH-TH group (n = 38)				
SANDE, points	45.2 ± 24.5	39.2 ± 20.2	33.1 ± 17.2	0.04*
OSDI, points	53.2 ± 21.4	47.3 ± 14.5	42.3 ± 16.1	0.06
NIBUT, s	7.3 ± 7.1	9.4 ± 6.3	10.1 ± 7.3	0.03*
TMH, mm	0.3 ± 0.1	0.24 ± 0.13	0.24 ± 0.12	0.08
LLT, nm	63.5 ± 13.5	55.2 ± 21.1	55.6 ± 21.2	0.002*
TBUT, s	3.2 ± 1.5	3.6 ± 1.6	6.2 ± 1.7	0.01*
CFS, points	3.2 ± 0.6	3.1 ± 0.6	2.8 ± 0.5	0.04*
OSM, mOsm/L	316.7 ± 9.3	309.6 ± 5.4	306.5 ± 4.8	< 0.001*
MGD, grade	1.5 ± 0.6	1.9 ± 0.6	1.9 ± 0.5	0.9

CFS corneal fluorescein staining, *LLT* lipid layer thickness, *MGD* meibomian gland dysfunction, *NIBUT* non-invasive tear film breakup time, *OSDI* ocular surface disease index, *OSM* osmolarity, *QMR* Quantum Molecular Resonance, *SANDE* symptom assessment in dry eye, *SD* standard deviation, *SH* sodium hyaluronate, *TBUT* tear film breakup time, *TH* trehalose, *TMH* tear meniscus height

*$P < 0.05$

− 31.3 ± 4.1 points ($P < 0.001$), 6.4 ± 0.9 s ($P < 0.001$), 0.09 ± 0.04 mm ($P < 0.001$), 10.6 ± 2.3 nm ($P = 0.02$), and − 19.4 ± 2.5 mOsm/L ($P < 0.001$) after 3 months of follow-up, respectively. Similar results were achieved in the EDE subgroup with significant ΔOSDI, ΔNIBUT, ΔLLT, and ΔOSM improvements of − 17.4 ± 0.75 points ($P < 0.001$), 4.2 ± 0.4 s ($P = 0.01$), 14 ± 4.6 nm ($P < 0.001$), and − 17.6 ± 3.2 mOsm/L ($P < 0.001$), respectively. However, the MDE subgroup only showed significant improvements in ΔOSDI, ΔNIBUT, and ΔOSM with values of − 35.4 ± 6.4 points ($P < 0.001$), 6.1 ± 1.2 s ($P < 0.001$), and − 17.5 ± 1.4 mOsm/L ($P < 0.001$), respectively.

Safety Endpoints

No significant changes of BCVA, IOP, slit-lamp biomicroscopy, and dilated funduscopy were observed after QMR treatment (data not shown). In addition, no AEs were documented

Table 3 Changes in symptoms and ocular surface parameters between baseline and 3-month follow-up in the aqueous-deficient dry eye subgroup after QMR treatment

Parameters, mean ± SD	Baseline	3 Months	*P* value
OSDI, points	51.1 ± 18.2	19.8 ± 10.1	< 0.001*
NIBUT, *s*	8.1 ± 4.7	14.5 ± 6.6	< 0.001*
TMH, mm	0.16 ± 0.02	0.25 ± 0.1	< 0.001*
LLT, nm	57.8 ± 17.8	68.4 ± 22.4	0.02*
OSM, mOsm/L	317 ± 10.1	297.6 ± 5.2	< 0.001*

LLT lipid layer thickness, *NIBUT* non-invasive tear film breakup time, *OSDI* ocular surface disease index, *OSM* osmolarity, *QMR* Quantum Molecular Resonance, *SD* standard deviation, *TMH* tear meniscus height
*$P < 0.05$

during treatment sessions with QMR, and throughout the follow-up period.

DISCUSSION

Tear film hyperosmolarity is considered the trigger for the ocular surface inflammatory mechanism resulting in DED symptoms and signs [3, 36]. Therefore, new treatments that target the specific mechanism involved in the pathogenesis of DED and improve the tear film stability and restore the homeostasis of the ocular surface are under research [37, 38]. The aim of this study is to evaluate the efficacy and safety of QMR treatment in patients with severe DED, as well as its effects on ADDE, EDE, and MDE.

Table 4 Changes in symptoms and ocular surface parameters between baseline and 3-month follow-up in the evaporative dry eye subgroup after QMR treatment

Parameters, mean ± SD	Baseline	3 Months	*P* value
OSDI, points	56.1 ± 17.4	38.7 ± 18.9	< 0.001*
NIBUT, *s*	8.6 ± 5.8	12.8 ± 6.6	0.01*
TMH, mm	0.24 ± 0.18	0.26 ± 0.1	0.19
LLT, nm	42.4 ± 8.4	56.4 ± 17.6	< 0.001*
OSM, mOsm/L	317.9 ± 9.9	300.3 ± 3.5	< 0.001*
MGD, grade	1.6 ± 0.6	1.6 ± 0.7	0.9

LLT lipid layer thickness, *MGD* meibomian gland dysfunction, *NIBUT* non-invasive tear film breakup time, *OSDI* ocular surface disease index, *OSM* osmolarity, *QMR* Quantum Molecular Resonance, *SD* standard deviation, *TMH* tear meniscus height
*$P < 0.05$

Table 5 Changes in symptoms and ocular surface parameters between baseline and 3-month follow-up in the mixed dry eye subgroup after QMR treatment

Parameters, mean ± SD	Baseline	3 Months	*P* value
OSDI, points	54.5 ± 20.4	19.1 ± 7.7	< 0.001*
NIBUT, *s*	9.1 ± 4.2	15.2 ± 6.6	< 0.001*
TMH, mm	0.23 ± 0.18	0.29 ± 0.1	0.16
LLT, nm	72.9 ± 12.9	78.2 ± 22.6	0.37
OSM, mOsm/L	315.1 ± 7.9	297.6 ± 5.2	< 0.001*
MGD, grade	1.9 ± 0.6	1.9 ± 0.7	0.9

LLT lipid layer thickness, *MGD* meibomian gland dysfunction, *mOsm* osmolarity expressed in milliosmole, *NIBUT* non-invasive tear film breakup time, *OSDI* ocular surface disease index, *OSM* osmolarity, *QMR* Quantum Molecular Resonance, *SD* standard deviation, *TMH* tear meniscus height
*$P < 0.05$

Quantum Molecular Resonance Efficacy

In this study, QMR treatment achieved significant improvements in OSDI and SANDE questionnaires, NIBUT, LLT, and CFS compared to SH-TH treatment after 3 months of follow-up. In addition, QMR treatment was beneficial for ADDE, EDE, and MDE, with similar result between the subgroups.

Several studies have evaluated the effects of QMR treatment on DED symptoms and signs [29–33]. Pedrotti et al. [29] reported that 12 sessions of QMR treatment significantly improved OSDI questionnaire, TBUT, CFS, and ST after 1 year of follow-up in patients with ADDE. Although ST was performed during the screening stage in our study, it was not used as a clinical endpoint because of its invasiveness and association with CFS, which could affect our results [39, 40]. For this reason, tear volume was evaluated by TMH, showing a significant improvement after 3 months of follow-up. Ferrari et al. [30] reported similar results in OSDI questionnaire, NIBUT, and CFS after four treatment sessions of QMR. In addition, this study also reported significant improvements in meibum quality and the number of expressible meibomian glands after 1 month of follow-up. Although meibomian gland secretion was not assessed in our study, a significant LLT improvement was reported in patients with EDE, which is consistent with the results reported by Ferrari et al. [30] In addition, Trivli et al. [32] reported significant improvements in DED symptoms and signs after 1 month of follow-up in patients with MDE, which is also in harmony with the results reported in our study.

Although the mechanism underlying QMR treatment remains unclear, it is hypothesized that electrical stimulation of the ethmoidal nerve may modulate the activity of lacrimal and meibomian gland, thereby improving tear film stability [20, 41]. In addition, similarly to Corneal Cross Linking [4], QMR treatment also seems to produce anti-inflammatory effects by reducing tissue infiltration of leukocytes and modulating metalloproteinase (MMP) expression [42]. It is well known that MMPs may be an indicator for tear film OSM, playing a key role in the initiation and maintenance of ocular surface damage [3, 43]. In particular, MMP-9 contributes to corneal epithelial barrier instability, with increased corneal epithelial desquamation and corneal surface irregularity [44, 45]. Recently, Trivli et al. [32] demonstrated a significant reduction of MMP-9 expression on the ocular surface in patients with DED after treatment with QMR, which was associated with a significant reduction in CFS. Although our study did not analyze MMP levels, tear film OSM was evaluated, showing a significant reduction after 3 months of follow-up. Overall, these hypotheses support the results reported in this study. However, further studies are needed to confirm this.

Quantum Molecular Resonance Safety

In this study, the absence of reported AEs after QMR treatment aligns with the findings from other studies conducted by Ferrari et al. [30], Trivli et al. [32], Kavroulaki et al. [31], and Foo et al. [33]. This consistent pattern of safety across multiple studies underscores the robustness of QMR as a safe therapeutic option for DED. In addition, the safety profile of QMR treatment becomes even more significant when compared to alternative novel therapies, such as IPL, whose main AEs may include blistering, cheek swelling, and loss of eyelashes [46].

Strengths and Limitations

To the best of our knowledge this is the first randomized, interventional study that analyzes the efficacy and safety of QMR treatment in patients with severe DED, as well as its effects on different types of dry eye. However, there are some limitations that need to be addressed. First, masking was not possible because both groups received quite different treatments. Second, since the QMR group did not receive treatment with SH-TH tear substitutes, it may be difficult to specifically determine the beneficial effects in the QMR group over the SH-TH group. Similarly, multiple previous treatments and a 1-week washout might have influenced the outcomes. In addition, it would have been interesting to have a third group receiving both

treatments, which would allow a more solid comparison between the QMR and SH-TH treatments, as well as to evaluate whether the combination of both treatments has a synergistic effect. Changes in the expressibility and quality of meibum secretions after treatments could be evaluated as well in future studies. Therefore, there is a need for larger, well-designed, strictly blinded randomized controlled trials evaluating the long-term efficacy and safety of QMR treatment in patients with DED, as well as its effects on different types of dry eye, identifying the minimum number of effective sessions. In addition, it would also be interesting to compare the effects of QMR treatment with other novel therapies, such as MBE, VTP, LLLT, and IPL, as well as their combinations. This would be of special interest in patients with Sjögren's syndrome and MGD, which are the main cause of ADDE and EDE, respectively.

CONCLUSIONS

This study seems to demonstrated that four treatment sessions of QMR treatments improves DED symptoms and signs, with no adverse effects reported. In addition, this treatment also appears to be beneficial for ADDE, EDE, and MDE. These findings suggest that QMR treatment could be an effective and safe option to address DED and its different subtypes. However, further research and well-designed clinical trials are needed to confirm these results and to better understand the underlying mechanisms of QMR treatment in the context of DED.

Author Contributions. Drafting the paper: Antonio Ballesteros-Sánchez and José-María Sánchez-González; Data collection: Giovanni Roberto Tedesco, Carlos Rocha-De-Lossada, Fedele Russo and Antonio Spinelli; Statistical analysis: Irene Ingrande; Data collection, concept and design, supervision and drafting the paper: Davide Borroni.

Funding. No funding or sponsorship was received for this study or publication of this article.

Data Availability. The datasets generated during and/or analyzed during the current study are available from the corresponding author on reasonable request.

Declarations

Conflict of Interest. Antonio Ballesteros-Sánchez, José-María Sánchez-González, Giovanni Roberto Tedesco, Carlos Rocha-De-Lossada, Fedele Russo, Antonio Spinelli, Irene Ingrande, and Davide Borroni have nothing to disclose.

Ethical Approval. This study fulfilled all the requirements of the Declaration of Helsinki and was approved by the internal review board for Tedesco Eye Center (Approval Nr. DB13385-2568932022). Before initiating the study, informed and written consent was obtained from each patient. Patient consent was received for Fig. 2.

Open Access. This article is licensed under a Creative Commons Attribution-NonCommercial 4.0 International License, which permits any non-commercial use, sharing, adaptation, distribution and reproduction in any medium or format, as long as you give appropriate credit to the original author(s) and the source, provide a link to the Creative Commons licence, and indicate if changes were made. The images or other third party material in this article are included in the article's Creative Commons licence, unless indicated otherwise in a credit line to the material. If material is not included in the article's Creative Commons licence and your intended use is not permitted by statutory regulation or exceeds the permitted use, you will need to obtain permission directly from the copyright holder. To view a copy of this licence, visit http://creativecommons.org/licenses/by-nc/4.0/.

REFERENCES

1. Craig JP, Nichols KK, Akpek EK, et al. TFOS DEWS II definition and classification report. Ocul Surf.

2017;15(3):276–83. https://doi.org/10.1016/J.JTOS.2017.05.008.

2. Su P, Chen T, Xie J, et al. Corneal nerve tortuosity grading via ordered weighted averaging-based feature extraction. Med Phys. 2020;47(10):4983–96. https://doi.org/10.1002/mp.14431.

3. Bron AJ, de Paiva CS, Chauhan SK, et al. TFOS DEWS II pathophysiology report. Ocul Surf. 2017;15(3):438–510. https://doi.org/10.1016/J.JTOS.2017.05.011.

4. Acar Eser N, Dikmetas O, Kocabeyoglu S, et al. Evaluation of keratoconus disease with tear cytokine and chemokine levels before and after corneal cross-linking treatment. Ocul Immunol Inflamm. 2023;6:1–7. https://doi.org/10.1080/09273948.2023.2165950.

5. Azzolini C, Pagani IS, Pirrone C, et al. Expression of VEGF-A, Otx homeobox and p53 family genes in proliferative vitreoretinopathy. Mediators Inflamm. 2013;2013:857380. https://doi.org/10.1155/2013/857380.

6. Uchino M, Schaumberg DA. Dry eye disease: impact on quality of life and vision. Curr Ophthalmol Rep. 2013;1(2):51–7. https://doi.org/10.1007/S40135-013-0009-1.

7. Friedman NJ. Impact of dry eye disease and treatment on quality of life. Curr Opin Ophthalmol. 2010;21(4):310–6. https://doi.org/10.1097/ICU.0B013E32833A8C15.

8. Barabino S, Labetoulle M, Rolando M, Messmer EM. Understanding symptoms and quality of life in patients with dry eye syndrome. Ocul Surf. 2016;14(3):365–76. https://doi.org/10.1016/J.JTOS.2016.04.005.

9. Wolffsohn JS, Arita R, Chalmers R, et al. TFOS DEWS II diagnostic methodology report. Ocul Surf. 2017;15(3):539–74. https://doi.org/10.1016/j.jtos.2017.05.001.

10. Dougherty BE, Nichols JJ, Nichols KK. Rasch analysis of the Ocular Surface Disease Index (OSDI). Invest Ophthalmol Vis Sci. 2011;52(12):8630–5. https://doi.org/10.1167/IOVS.11-8027.

11. Özcura F, Aydin S, Helvaci MR. Ocular surface disease index for the diagnosis of dry eye syndrome. Ocul Immunol Inflamm. 2007;15(5):389–93. https://doi.org/10.1080/09273940701486803.

12. Schaumberg DA, Gulati A, Mathers WD, et al. Development and validation of a short global dry eye symptom index. Ocul Surf. 2007;5(1):50–7. https://doi.org/10.1016/S1542-0124(12)70053-8.

13. Amparo F, Schaumberg DA, Dana R. Comparison of two questionnaires for dry eye symptom assessment: the ocular surface disease index and the symptom assessment in dry eye. Ophthalmology. 2015;122(7):1498–503. https://doi.org/10.1016/J.OPHTHA.2015.02.037.

14. Rodriguez-Garcia A, Ruiz-Lozano RE, Bustamante-Arias A, Pantaleon-Garcia J, Hernandez-Quintela E, Navas A. Reply to Letter to the Editor: Correlation and level of agreement between the ocular surface disease index and the symptom assessment in dry eye questionnaires: a survey-based study. Curr Eye Res. 2023;48(11):1086–8. https://doi.org/10.1080/02713683.2023.2255397.

15. Pflugfelder SC, Solomon A, Stern ME. The diagnosis and management of dry eye: a twenty-five-year review. Cornea. 2000;19(5):644–9. https://doi.org/10.1097/00003226-200009000-00009.

16. Sullivan BD, Whitmer D, Nichols KK, et al. An objective approach to dry eye disease severity. Invest Ophthalmol Vis Sci. 2010;51(12):6125–30. https://doi.org/10.1167/IOVS.10-5390.

17. Ozulken K, Aksoy Aydemir G, Tekin K, Mumcuoğlu T. Correlation of non-invasive tear break-up time with tear osmolarity and other invasive tear function tests. Semin Ophthalmol. 2020;35(1):78–85. https://doi.org/10.1080/08820538.2020.1730916.

18. Sánchez-González MC, Capote-Puente R, García-Romera MC, et al. Dry eye disease and tear film assessment through a novel non-invasive ocular surface analyzer: the OSA protocol. Front Med (Lausanne). 2022. https://doi.org/10.3389/FMED.2022.938484.

19. Ballesteros-Sánchez A, Gargallo-Martínez B, Gutiérrez-Ortega R, Sánchez-González JM. Intra-observer repeatability assessment of the S390L Firefly WDR slit lamp in patients with dry eye disease: objective, automated and non-invasive measures. Eye Contact Lens. 2023;49(7):283–91.

20. Knop E, Knop N, Millar T, Obata H, Sullivan DA. The international workshop on meibomian gland dysfunction: report of the subcommittee on anatomy, physiology, and pathophysiology of the meibomian gland. Invest Ophthalmol Vis Sci. 2011;52(4):1938–78. https://doi.org/10.1167/IOVS.10-6997C.

21. Geerling G, Tauber J, Baudouin C, et al. The international workshop on meibomian gland dysfunction: report of the subcommittee on management and treatment of meibomian gland dysfunction. Invest Ophthalmol Vis Sci. 2011;52(4):2050–64. https://doi.org/10.1167/IOVS.10-6997G.

22. Bonzano C, Borroni D, Lancia A, Bonzano E. Doxycycline: from ocular rosacea to COVID-19 anosmia. New insight into the coronavirus outbreak. Front Med (Lausanne). 2020. https://doi.org/10.3389/FMED.2020.00200.

23. Jones L, Downie LE, Korb D, et al. TFOS DEWS II management and therapy report. Ocul Surf. 2017;15(3):575–628. https://doi.org/10.1016/J.JTOS.2017.05.006.

24. O'Neil EC, Henderson M, Massaro-Giordano M, Bunya VY. Advances in dry eye disease treatment. Curr Opin Ophthalmol. 2019;30(3):166–78. https://doi.org/10.1097/ICU.0000000000000569.

25. Ballesteros-Sánchez A, Gargallo-Martínez B, Gutiérrez-Ortega R, Sánchez-González JM. Eyelid exfoliation treatment efficacy and safety in dry eye disease, blepharitis, and contact lens discomfort patients: a systematic review. Asia-Pac J Ophthalmol. 2023;12(3):315–25. https://doi.org/10.1097/APO.0000000000000607.

26. Blackie CA, Coleman CA, Holland EJ. The sustained effect (12 months) of a single-dose vectored thermal pulsation procedure for meibomian gland dysfunction and evaporative dry eye. Clin Ophthalmol. 2016;10:1385–96. https://doi.org/10.2147/OPTH.S109663.

27. Karaca EE, Evren Kemer Ö, Özek D. Intense regulated pulse light for the meibomian gland dysfunction. Eur J Ophthalmol. 2020;30(2):289–92. https://doi.org/10.1177/1120672118817687.

28. Park Y, Kim H, Kim S, Cho KJ. Effect of low-level light therapy in patients with dry eye: a prospective, randomized, observer-masked trial. Sci Rep. 2022;12(1):3575. https://doi.org/10.1038/s41598-022-07427-6.

29. Pedrotti E, Bosello F, Fasolo A, et al. Transcutaneous periorbital electrical stimulation in the treatment of dry eye. Br J Ophthalmol. 2017;101(6):814–9. https://doi.org/10.1136/BJOPHTHALMOL-2016-308678.

30. Ferrari G, Colucci A, Barbariga M, Ruggeri A, Rama P. High frequency electrotherapy for the treatment of meibomian gland dysfunction. Cornea. 2019;38(11):1424–9. https://doi.org/10.1097/ICO.0000000000002063.

31. Kavroulaki D, Konstantinidou E, Tsiogka A, Rallis K, Mavrikakis E. Quantum molecular resonance electrical stimulation as a beneficial and safe treatment for multifactorial dry eye disease. Cureus. 2023. https://doi.org/10.7759/CUREUS.39695.

32. Trivli A, Karmiris E, Dalianis G, Ruggeri A, Terzidou C. Evaluating the efficacy of Quantum Molecular Resonance (QMR) electrotherapy in mixed-type dry eye patients. J Optom. 2023;16(2):128–34. https://doi.org/10.1016/J.OPTOM.2022.06.003.

33. Foo VHX, Liu YC, Tho B, Tong L. Quantum molecular resonance electrotherapy (Rexon-Eye) for recalcitrant dry eye in an Asian population. Front Med (Lausanne). 2023. https://doi.org/10.3389/FMED.2023.1209886.

34. Tomlinson A, Bron AJ, Korb DR, et al. The international workshop on meibomian gland dysfunction: report of the diagnosis subcommittee. Invest Ophthalmol Vis Sci. 2011;52(4):2006–49. https://doi.org/10.1167/IOVS.10-6997F.

35. Bron AJ, Evans VE, Smith JA. Grading of corneal and conjunctival staining in the context of other dry eye tests. Cornea. 2003;22(7):640–50. https://doi.org/10.1097/00003226-200310000-00008.

36. Baudouin C, Aragona P, Messmer EM, et al. Role of hyperosmolarity in the pathogenesis and management of dry eye disease: proceedings of the OCEAN group meeting. Ocul Surf. 2013;11(4):246–58. https://doi.org/10.1016/J.JTOS.2013.07.003.

37. Barabino S, Benitez-Del-Castillo JM, Fuchsluger T, et al. Dry eye disease treatment: the role of tear substitutes, their future, and an updated classification. Eur Rev Med Pharmacol Sci. 2020;24(17):8642–52. https://doi.org/10.26355/EURREV_202009_22801.

38. Zeng J, Lin C, Zhang S, et al. Isolation and identification of a novel anti-dry eye peptide from tilapia skin peptides based on in silico, in vitro, and in vivo approaches. Int J Mol Sci. 2023;24(16):12772. https://doi.org/10.3390/ijms241612772.

39. Li N, Deng XG, He MF. Comparison of the Schirmer I test with and without topical anesthesia for diagnosing dry eye. Int J Ophthalmol. 2012;5(4):478–81. https://doi.org/10.3980/J.ISSN.2222-3959.2012.04.14.

40. Afonso AA, Monroy D, Stern ME, Feuer WJ, Tseng SC, Pflugfelder SC. Correlation of tear fluorescein clearance and Schirmer test scores with ocular irritation symptoms. Ophthalmology. 1999;106(4):803–10. https://doi.org/10.1016/S0161-6420(99)90170-7.

41. Brinton M, Kossler AL, Patel ZM, et al. Enhanced tearing by electrical stimulation of the anterior ethmoid nerve. Invest Ophthalmol Vis Sci. 2017;58(4):2341–8. https://doi.org/10.1167/IOVS.16-21362.

42. Fraccalvieri M, Salomone M, Di Santo C, Ruka E, Morozzo U, Bruschi S. Quantum molecular resonance technology in hard-to-heal extremity

wounds: histological and clinical results. Int Wound J. 2017;14(6):1313–22. https://doi.org/10.1111/IWJ.12805.

43. Willcox MDP, Argüeso P, Georgiev GA, et al. TFOS DEWS II tear film report. Ocul Surf. 2017;15(3):366–403. https://doi.org/10.1016/J.JTOS.2017.03.006.

44. Messmer EM, von Lindenfels V, Garbe A, Kampik A. Matrix metalloproteinase 9 testing in dry eye disease using a commercially available point-of-care immunoassay. Ophthalmology. 2016;123(11):2300–8. https://doi.org/10.1016/J.OPHTHA.2016.07.028.

45. Lanza NL, Valenzuela F, Perez VL, Galor A. The matrix metalloproteinase 9 point-of-care test in dry eye. Ocul Surf. 2016;14(2):189–95. https://doi.org/10.1016/J.JTOS.2015.10.004.

46. Toyos R, Toyos M, Willcox J, Mulliniks H, Hoover J. Evaluation of the safety and efficacy of intense pulsed light treatment with meibomian gland expression of the upper eyelids for dry eye disease. Photobiomodul Photomed Laser Surg. 2019;37(9):527–31. https://doi.org/10.1089/photob.2018.4599.

10

Mixed dry eye patients successfully treated by the innovative high-frequency electrotherapy device Rexon-Eye®

A. Ruggeri, E. Fatigati, L. Vigo

June 2020
Volume 61, Issue 7
ISSUE

OPEN ACCESS

ARVO Annual Meeting Abstract | June 2020

Mixed dry eye patients successfully treated by the innovative high-frequency electrotherapy device Rexon-Eye®

Alfredo Ruggeri; Eleonora Fatigati; Luca Vigo

— Author Affiliations & Notes

Alfredo Ruggeri
Resono Ophthalmic, Sandrigo, Italy

Eleonora Fatigati
Carones Vision, Milan, Italy

Luca Vigo
Carones Vision, Milan, Italy

Footnotes

Commercial Relationships **Alfredo Ruggeri**, Resono Ophthalmic (I), Resono Ophthalmic (P); **Eleonora Fatigati**, None; **Luca Vigo**, Resono Ophthalmic (C)

Support None

Investigative Ophthalmology & Visual Science June 2020, Vol.61, 114. doi:

SHARE ▾ TOOLS ▾

Abstract

Purpose : We investigated the efficacy of an innovative treatment in a small cohort of nine patients affected by mixed dry eye disease (MDED), i.e., both aqueous deficient and evaporative type. The treatment consists in the administration of a specific low-power, high-frequency electric current using the Rexon-Eye® device.

Methods : Nine consecutive MDED patients were recruited and all treated. Therapy was administered with the Rexon-Eye® device (Resono Ophthalmic, Sandrigo, Italy, patented), which applies a low-power electric current with a specific spectrum of frequencies (4-64 MHz, Quantum Molecular Resonance, QMR®, patented). Patients were administered one 20 min treatment per week, for 4 weeks, and were examined at baseline and two month after the last treatment, by measuring: lipid layer thickness, tear meniscus, and non-invasive tear break-up time (NIBUT), all measured with IDRA (SBM Sistemi, Turin, Italy); Ocular Surface Disease Index (OSDI) score; tear osmolarity (TearLab, Escondido (CA), USA); ocular inflammation (InflammaDry; Quidel, San Diego (CA), USA).

Results : Results are reported in Table 1 and 2. The clinical endpoints improved significantly in most of the patients and no adverse events nor side effects were observed in any of them.

Conclusions : The innovative therapeutic device Rexon-Eye®, based on the QMR® patented electric stimulation, proved to be very effective in improving subjective and objective ocular parameters in most of the mixed dry eye patients of this study.

This is a 2020 ARVO Annual Meeting abstract.

11

Innovative radiofrequency electrotherapy significantly reduces cornea perforation in an alkali burn murine model

A. Ruggeri, T. Dyrdin, M. Barbariga, P. Rama, G. Ferrari

OPEN ACCESS

ARVO Annual Meeting Abstract | July 2018

Innovative radiofrequency electrotherapy significantly reduces cornea perforation in an alkali burn murine model

Alfredo Ruggeri; Timur Dyrdin; Marco Barbariga; Paolo Rama; Giulio Ferrari

+ Author Affiliations & Notes

Investigative Ophthalmology & Visual Science July 2018, Vol.59, 4350. doi:

SHARE TOOLS

Abstract

Purpose : An innovative treatment for ocular surface diseases, based on the administration of a radiofrequency electrical current containing a specific spectrum of frequencies (QMR), was recently shown to be effective in the dry eye syndrome. We investigated the effectiveness of this treament in reducing the perforation rate in alkali burn corneas.

Methods : Forty 6-week old C57Bl/6 mice underwent 1N alkali burn to induce a severe cornea inflammation. The QMR treatment (Rexon-Eye, Resono Ophthalmic, Italy) was started immediately after the model induction and consisted in 2 sessions per week for 3 weeks. Each session included a 20 min treatment, where the QMR radiofrequency current was applied (following a 30 seconds ON/30 seconds OFF protocol) to one eye of the 20 treated animals, using a small metal electrode touching the cornea. The remaining 20 animals underwent a fake treatment, where the electrode was also positioned over the cornea but no current was administered. All the animals were monitored during the 3-week treatment and for 1 additional week, and the presence of cornea perforations was assessed clinically with a slit-lamp by an ophthalmologist.

Results : The time course of the percentage of corneas without perforations over the four weeks of the experiment, for both treated and control animals, is reported in Fig. 1. The Gehan-Breslow-Wilcoxon test was performed to assess the difference between the two curves, which was statistically significant (P value <0.0001).

Conclusions : The use of the QMR treatment to reduce the incidence of corneal perforations in alkali burn mice was highly effective, supporting the use of this technology in the treatment of severe corneal inflammation.

This is an abstract that was submitted for the 2018 ARVO Annual Meeting, held in Honolulu, Hawaii, April 29 - May 3, 2018.

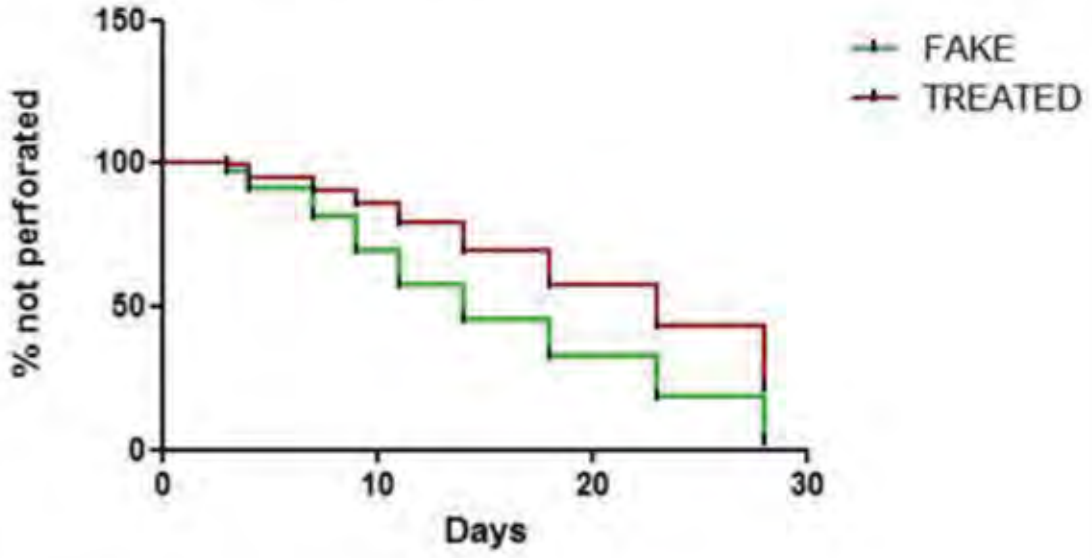

View Original | Download Slide

Fig 1: Percentage of corneas without perforation as a function of time, for treated (green line) and control (red line) mice.

12

Quantum Molecular Resonance Inhibits NLRP3 Inflammasome/Nitrosative Stress and Promotes M1 to M2 Macrophage Polarization: Potential Therapeutic Effect in Osteoarthritis Model In Vitro

T. Paolucci, V. Pino, O. Elsallabi, M. Gallorini, G. Pozzato, A. Pozzato, P. Lanuti, V. Machado Reis, M. Pesce, A. Pantalone, R. Buda, and A. Patruno

antioxidants

MDPI

Article

Quantum Molecular Resonance Inhibits NLRP3 Inflammasome/Nitrosative Stress and Promotes M1 to M2 Macrophage Polarization: Potential Therapeutic Effect in Osteoarthritis Model In Vitro

Teresa Paolucci [1], Vanessa Pino [2], Osama Elsallabi [2,3], Marialucia Gallorini [4], Gianantonio Pozzato [5], Alessandro Pozzato [5], Paola Lanuti [2], Victor Machado Reis [6], Mirko Pesce [2,*], Andrea Pantalone [2], Roberto Buda [2] and Antonia Patruno [2]

1 Department of Oral, Medical and Biotechnological Sciences, Physical Medicine and Rehabilitation, University G. D'Annunzio, 66100 Chieti, Italy; teresa.paolucci@unich.it
2 Department of Medicine and Aging Sciences, University "G. d'Annunzio" of Chieti-Pescara, 66100 Chieti, Italy; pivassa1@gmail.com (V.P.); osama.elsallabi@unich.it (O.E.); paola.lanuti@unich.it (P.L.); andrea.pantalone@unich.it (A.P.); roberto.buda@unich.it (R.B.); antonia.patruno@unich.it (A.P.)
3 Institute on the Biology of Aging and Metabolism and Department of Biochemistry, Molecular Biology and Biophysics, University of Minnesota, Minneapolis, MN 55455, USA
4 Department of Pharmacy, University "G. d'Annunzio" of Chieti-Pescara, 66100 Chieti, Italy; marialucia.gallorini@unich.it
5 Telea Electronic Engineering srl, 36066 Sandrigo, Italy; gianantonio.pozzato@teleamedical.com (G.P.); alessandro.pozzato@teleamedical.com (A.P.)
6 Research Centre in Sport Sciences, Health Sciences and Human Development, 5001-801 Vila Real, Portugal; vreis@utad.pt
* Correspondence: mirko.pesce@unich.it

check for updates

Citation: Paolucci, T.; Pino, V.; Elsallabi, O.; Gallorini, M.; Pozzato, G.; Pozzato, A.; Lanuti, P.; Reis, V.M.; Pesce, M.; Pantalone, A.; et al. Quantum Molecular Resonance Inhibits NLRP3 Inflammasome/Nitrosative Stress and Promotes M1 to M2 Macrophage Polarization: Potential Therapeutic Effect in Osteoarthritis Model In Vitro. *Antioxidants* **2023**, *12*, 1358. https://doi.org/10.3390/antiox12071358

Academic Editors: Serge P. Bottari and Maria-Jose Alcaraz

Received: 18 April 2023
Revised: 22 June 2023
Accepted: 23 June 2023
Published: 28 June 2023

Copyright: © 2023 by the authors. Licensee MDPI, Basel, Switzerland. This article is an open access article distributed under the terms and conditions of the Creative Commons Attribution (CC BY) license (https://creativecommons.org/licenses/by/4.0/).

Abstract: This study aimed to investigate the anti-inflammatory effects of Quantum Molecular Resonance (QMR) technology in an in vitro model of osteoarthritis-related inflammation. The study used THP-1-derived macrophages stimulated with lipopolysaccharide and hyaluronic acid fragments to induce the expression of inflammatory cytokines and nitrosative stress. QMR treatment inhibited COX-2 and iNOS protein expression and activity and reduced NF-κB activity. Furthermore, QMR treatment led to a significant reduction in peroxynitrite levels, reactive nitrogen species that can form during inflammatory conditions, and restored tyrosine nitration values to those similar to sham-exposed control cells. We also investigated the effect of QMR treatment on inflammasome activation and macrophage polarization in THP-1-derived macrophages. Results showed that QMR treatment significantly decreased NLRP3 and activated caspase-1 protein expression levels and downregulated IL-18 and IL-1β protein expression and secretion. Finally, our findings indicate that QMR treatment induces a switch in macrophage polarization from the M1 phenotype to the M2 phenotype.

Keywords: osteoarthritis; inflammation; macrophages; DAMP; QMR; rehabilitation

1. Introduction

In the pathogenesis and progression of osteoarthritis (OA), a complex multi-tissue pathology, low-grade and chronic inflammation play a key role as evidenced by sensitive imaging methods (magnetic resonance imaging (MRI) and ultrasound) [1,2].

It has been established that in addition to the production of proinflammatory and destructive mediators, the cellular component and in particular the macrophages in the OA synovium are responsible for maintaining synovial inflammation. Studies have demonstrated that OA synovial macrophages can make up around 30–40% of the cellular content exhibiting an activated phenotype and producing proinflammatory cytokines like TNFα

and IL-l and matrix metalloproteinases and expressing aggrecanases involved in driving the inflammatory response and joint destruction [3].

In the immune system, macrophages are antigen-presenting cells (APCs) with effective phagocytic activity responsive to cytokines released by lymphocytes. We know that macrophages evoke responses that can be variable and dependent on the tissue environment that influences their polarization. The pro-inflammatory phenotype, classically activated M1 macrophage, produces high levels of TNFα, IL-1, IL-6, IL-12, IL-23, reactive oxygen species (ROS), and low levels of IL-10. The anti-inflammatory phenotype or alternatively activated macrophage (M2), of which there are three subsets [4], produces high levels of IL-10, IL-1 receptor antagonist, decoy IL-1RII, TGFβ, and low levels of IL-12. Both phenotypes are necessary for the correct resolution of inflammation. The inflammatory signals in some pathological situations, such as AO, are activated both in the presence and in the absence of infection. Then, the mechanism by which macrophages monitor an inflamed environment is by sensing pathogen-associated molecular patterns (PAMPs) and endogenous danger-associated molecular patterns (DAMPs) leading to the assembly and activation of the inflammasome. Emerging evidence suggests that DAMPs-induced inflammation plays an important role in the pathogenesis of OA [5]. DAMPs or endogenous pattern recognition receptors (PRRs)-ligands are a group of molecules derived from host tissues or cells, either components of cells or induced gene products in specific conditions. The majority are extracellular matrix components such as fibronectin, heparan sulfate, biglycan, fibrinogen, oligosaccharides of hyaluronan, and hyaluronan breakdown fragments [6].

Extensive in vitro and in vivo data reported in the literature show the use of biophysical stimulation techniques to treat various diseases in human beings. Biophysical stimulation refers to the use of physical stimuli, such as electromagnetic fields, ultrasound, and mechanical vibrations, to promote healing and tissue regeneration. For example, electromagnetic field therapy has been used to treat conditions such as bone fractures, chronic pain, and OA [7]. Ultrasound has been used to treat soft tissue injuries, promote bone healing, and improve blood flow [8]. Mechanical vibrations, such as those used in whole-body vibration therapy, have been studied for their potential to improve muscle strength, bone density, and balance in elderly individuals [9]. Specifically, in rehabilitation, instrumental physical therapies can be classified according to the energy source: (i) electromagnetic (such as electric current and electromagnetic fields); (ii) mechanical (mechanical sound waves and vibratory energy); (iii) thermal (micro-waves and short waves). Each different instrumental physical therapy induces peculiar effects on biological tissues, some being more suitable for pain control, others for inflammation and for regeneration. Also, the most used methods for administrating physical energy to a biological system can be divided into (a) electrical energy applied directly to the tissue using adhesive electrodes (capacitively coupled electrical field), (b) electromagnetic energy applied using coils (pulsed electromagnetic fields, PEMFs), and (c) ultrasound energy applied directly to the tissue in the form of mechanical forces (low-intensity pulsed ultrasound system). The understanding of the interaction between physical agents and biological systems is particularly complex and depends on waveform, frequency, duration, and energy, on the identification of the dose–response effects, and on the characteristics of the targeted cell/tissue types. Obviously, the identification of the effects of physical agents in terms of how these can modulate a particular cellular function constitutes the basis for its possible clinical application. Electromagnetic fields are outlined as a potential alternative or in association with pharmacological treatments in several inflammatory-related pathologies [10–15]. Several papers have demonstrated the anti-inflammatory effect of PEMFs exposure in human synoviocytes, chondrocytes, and osteoblasts with a significant reduction in some of the most relevant pro-inflammatory cytokines [16,17].

In this study, the in vitro anti-inflammatory activity of Quantum Molecular Resonance (QMR) technology was investigated. Nowadays, applied mainly in bipolar coagulators and electrosurgery devices [18–20], QMR is a non-ionizing, low-potency technology that uses high-frequency waves in the range between 4 and 64 MHz delivered through al

ternating electric fields. QMR develops quanta of energy capable of breaking molecular bonds without increasing the kinetic energy of the affected molecules. This prevents the temperature from rising and limits damage to the surrounding tissue. Unlike medical devices with ELF technology, QMR produces nanosecond pulses that could penetrate through the plasma membrane and interact with cytoplasmic organelles [21]. To evaluate the potential mechanisms of action of QMR-therapeutic intervention for OA, in this study, we have used a physiologically relevant in vitro model of OA-related inflammation based on induction inflammatory cytokine expression in response to the combination of a PAMPs (lipopolysaccharide (LPS)) and a DAMPs (hyaluronan (HA) fragments) exposure.

In a previous study, it was demonstrated that small HA fragments (<289 kDa) can induce a macrophage-related inflammatory response in THP-1 cells when the cells are primed with the TLR4 agonist LPS, in a physiologically relevant concentration. This is important because the presence of LPS in the synovial fluid of OA patients has been associated with the presence of activated macrophages within the synovium and radiographic OA severity [22].

We examined the QMR effect, assessing the impact on inducible nitric oxide synthase (iNOS) and cyclooxygenase-2 (COX-2) expression/activity and peroxynitrite generation on differentiated (macrophages) human immortalized monocyte-like cell line (THP-1), a well-established cell model for the immune-modulation study. Considering the fact that the key response in vitro of macrophages to the stimulus by PAMPs and/or DAMPs, respectively, is the activation of the inflammasome formed by a pattern recognition receptor called NOD-like receptor pyrin domain containing three (NLRP3), we sought to determine the QMR anti-inflammatory responses through the NLRP3 signaling pathway.

Finally, we also tested whether QMR exposure could promote changes in the macrophage phenotypes related to M1/M2 macrophage polarization.

2. Materials and Methods

2.1. QMR Exposure System

Exposure was performed using a QMR generator supplied by Telea (Telea Electronic Engineering, Sandrigo, VI, Italy). The device generates alternating electric currents characterized by high-frequency (4–64 MHz) and low-intensity waves [23]. The QMR generator setup was with the following parameters: power supply, 230 V, ~50/60 Hz; maximum power input, 250 VA; and power output, 5 W/400 Ω. QMR was supplied using a pair of custom-made electrodes placed directly on the edge of a 100 mm Petri dish and connected to the QMR generator (Figure 1). No significant temperature changes were observed to be associated with the application of the QMR generator ($\Delta T = 0.1$ °C).

2.2. Cell Culture and Stimulation Protocol

The THP-1 cell line (ATCC, Rockville, MD, USA) was grown in RPMI (Roswell Park Memorial Institute) 1640 (Merck, Milan, Italy) supplemented with fetal bovine serum (10%) (Merck, Milan, Italy), L-glutamine (2 mM), and 10 mM HEPES (4-(2-hydroxy-ethyl)-1-piperazineethanesulfonic acid) (10 mM) in a humidified 5% CO_2 incubator at 37 °C. The induction to THP-1 cell differentiation into mature monocyte-derived macrophages was carried out with 20 ng/mL of phorbol myristate acetate (PMA) (Merck, Milan, Italy) for 72 h [24,25].

For TLR pathways activation, differentiated (macrophage) THP-1 cells were incubated with a physiologically relevant concentration of LPS (10 ng/mL) from E. coli, Serotype R515 (Enzo Life Sciences), and ultra-low molecular weight (ULMW, 7.5 KDa) HA (10 mg/mL) (R&D Systems). After treatment with LPS/HA for 24 h, the planned experiments considered two modalities of temporal: (a) 24 h; (b) 4 days. The cells were then subjected to QMR (Quantum Magnetic Resonance) stimulation for 10 min per day, for 4 consecutive days, with a rest period of 24 h between treatments. One QMR setting was used, corresponding to nominal powers of 30.

Overall, the goal of the experiment was to recreate therapeutic conditions in vitro, in order to investigate the effects of QMR stimulation on macrophage cells. By testing different time settings and comparing them to sham-exposed controls, we assessed the potential benefits of QMR stimulation on cell cultures.

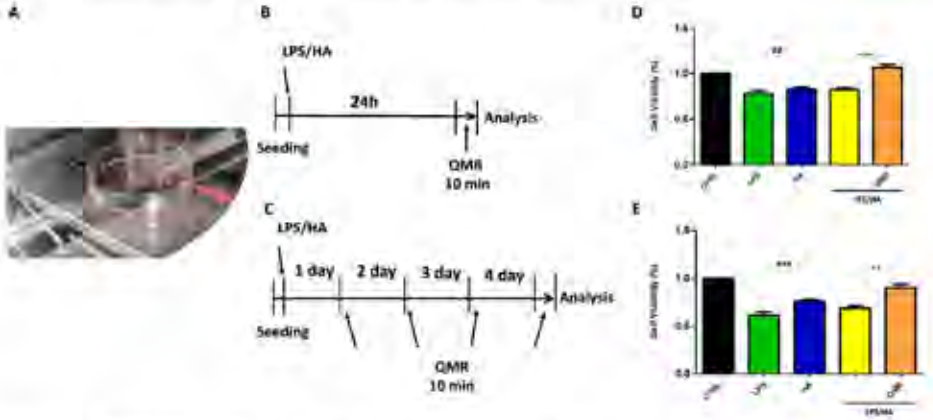

Figure 1. QMR stimulation protocol. (**A**) Image of the exposure system. (**B**,**C**) Schematic figure describing the timelines of the experiments. PMA differentiate THP-1 human monocytic cells were stimulated with LPS (10 ng/mL) and HA (10 µg/mL). In panel B, after 24 h, cells were treated with QMR for 10 min. In panel (**C**), cells were treated with QMR 10 min/day for 4 consecutive days at 30 nominal powers. (**D**,**E**) Cellular viability after QMR treatment. Histograms represent the % of cellular viability determined using MTS assay after QMR treatment (10 min) at the two different settings (D: 24 h and E: 4 days). Sham-exposed controls (CTRL) were kept in parallel. Data were represented as mean ± SD of $n = 6$ independent experiments. $^{\#\#}$ $p < 0.01$ vs. control cells; $^{\#\#\#}$ $p < 0.001$ vs. control cells; ** $p < 0.01$ vs. LPS/HA-treated cells; *** $p < 0.001$ vs. LPS/HA-treated cells.

2.3. MTS Assay for Viability and Metabolic Cellular

The MTS assay is a colorimetric assay that measures the metabolic activity of cells. The assay is based on the ability of metabolically active cells to convert MTS into a colored formazan product, which is measured at 490 nm using a spectrophotometer.

MTS assay was used to measure the metabolic activity of THP-1-differentiated cells in response to an activating stimulus (LPS/HA) and treatment with QMR at two-time points (24 h and 4 days).

To perform the assay, cells were plated in 96-well plates, incubated with the activating stimulus alone, and exposed to QMR for the desired time period. After incubation, MTS was added to each well, and the cells were incubated for an additional 4 h. The absorbance of the formazan product was measured at 490 nm using a spectrophotometer, and the percentage of metabolically active cells was calculated based on the absorbance of treated samples relative to control cells. All assays were performed in triplicate to ensure the reproducibility of results.

2.4. Western Blot

Western blot analysis was performed to detect the protein expression levels of iNOS, nitrotyrosine, COX-2, p-NF-kB (p65), NF-kB (p65), IL-18, IL-1β, NLRP3, caspase-1 in macrophage cells. The cells were incubated at two-time points (24 h and 4 days) and were lysed in RIPA buffer. The protein concentration was determined by a bicinchoninic acid assay [26]. Briefly, total protein extracts were separated by sodium dodecyl sulfate-polyacrylamide gel electrophoresis (SDS-PAGE) on a 10% gel and then transferred to nitrocellulose membranes. The blots were probed with primary antibodies against the target proteins and incubated overnight. The primary antibodies used were anti-iNOS (NOS2 (N-20), sc-651), anti-COX-2 (ab52237), p-NF-kB (p65) (sc-166748), NF-kB (p65) (sc-8008), IL-18 (10663-1-AP), IL-1β (sc-32294), NLRP3 (D2P5E) (#13158), caspase-1 (AB_2016691). After

washing, the blots were incubated with secondary antibodies conjugated with horseradish peroxidase. The protein expression levels were detected using Super Signal Ultra chemiluminescence detection reagents. β-actin was used as a loading control, and the densitometry analysis of the blots was performed using a gel analysis software package (Gel Doc 1000; Bio-Rad, Milan, Italy). The results were presented as mean values ± standard deviations (S.D.) of normalized densitometric values on the loading control.

2.5. Analysis of Peroxynitrite Generation

The cells were grown and treated with LPS/HA with or without exposure to QMR at two-time points (24 h and 4 days), in 6-well plates. The production of peroxynitrite was detected using a DAX-J2™ PON Green probe (Cell 205 MeterTM Fluorimetric Intracellular Peroxynitrite Assay Kit, AAT Bioquest, Pleasanton, CA, USA) and flow cytometry at 24 and 48 h. To perform the analysis, the exposure medium was removed, and a fresh medium containing 1 µL/mL of DAX-J2™ PON Green 500 X was added to the cells. The cells were then incubated at 37 °C and 5% CO_2 in the dark for 1 h before processing according to the manufacturer's instructions. The analysis was performed using a CytoFLEX Flow Cytometer equipped with a 488 nm laser and an FL1 (FITC) detector in a linear mode. The cells were gated based on their forward and side scatter properties (FSC/SSC), and the relative fluorescence emissions were analyzed using the CytExpert software (version 2.5). The results were expressed as mean fluorescence intensity (MFI) ratios on the unstained control.

2.6. NOS Activity

Oxyhemoglobin assay was used to monitor the intracellular NOS enzyme activity [27]. The assay was initiated with enzyme in a total volume of 1 mL. NO reacts with oxyhemoglobin to yield methemoglobin that is detected at 576 nm (ε = 12,000 M^{-1} cm^{-1}) using a Perkin-Elmer LamdaBIO UV–Vis spectrophotometer.

2.7. Prostaglandin PGE_2 Measurement

The concentration of PGE_2 was measured using a colorimetric detection method, specifically an enzyme-linked immunosorbent assay (ELISA) according to the instructions provided by the manufacturer of the assay kit (ADI-901-001). THP-1 cells were seeded onto six-well tissue culture plates at concentrations of 5×10^4 mL^{-1} and cultured in the presence or absence of LPS/HA with or without QMR treatment. Aliquots of cell culture supernatants, human anti-PGE_2, and PGE_2 conjugate were added to the 96-well plates coated with anti-human antibody and incubated for 1 h at room temperature. Then, the reaction mixture was aspirated and 3,3′,5,5′-tetramethylbenzidine (TMB) enzyme substrate (150 µL) was added and incubated for 30 min at room temperature. The reaction was stopped by adding sulphuric acid (1 M), and the absorbance was measured at 405 nm.

2.8. Immunophenotyping In Vitro

The expression of surface markers (CDs) in macrophages was analyzed using flow cytometry. After differentiation, macrophages were stimulated with LPS and exposed to treatments for 4 days. After that, cells were harvested with Stem Pro™ Accutase™ cell dissociation reagent (ThermoFisher Scientific, Waltham, MA, USA), collected by centrifugation in the cold, and washed once with FACS buffer prepared with 10 mM 4-(2-hydroxyethyl)-1-piperazineethanesulfonic acid (HEPES) buffer at pH 7.4, 140 mM sodium chloride (NaCl), and 2.5 mM calcium chloride ($CaCl_2$). Cells were incubated with fluorochrome-conjugated antibodies (1:50 dilutions) in 50 µL of FACS buffer for 15 min in the dark. Cells were stained separately in each single screening tube with a cluster of differentiation (CD)80-PE and CD163-PE (all purchased by BD Biosciences, MA, USA) Then, the excess antibodies were removed by adding fresh FACS buffer and centrifugation. After that, 20,000 events were run in a Beckman Coulter CytoFLEX flow cytometer (Brea, CA, USA). Relative fluorescence emissions of gated cells by forward and side scatter properties (FSC/SSC) were analyzed using the CytExpert Software (Beckman Coulter) and expressed as the MFI ratio on the

isotype control. Individual values obtained from three independent experiments ($n = 3$) were summarized as means and standard deviations.

2.9. ELISA

The concentrations of IL-1β, IL-10, TNF-α, and IL-18 in cell culture supernatants were measured using the commercial ELISA kit (Thermofisher Scientific) according to the instructions of the producer. Plates were scanned using a specialized Charge Coupled Device cooled tool. The integrated density values of the spots of known standards were used to generate a standard curve. Density values for unknown samples were determined using the standard curve for each analysis to calculate the real values in pg/mL. All steps were performed twice and at room temperature. The intra- and inter-assay reproducibility was >90%. Duplicate values that differed from the mean by more than 10% were considered suspect and therefore repeated. We did not report missing values [28].

2.10. Statistical Analyses

Each assay was replicated at least three times. Data are expressed as mean ± SD (standard deviation), and statistical significance was determined using the XLStat software, version 2.2 (New York, NY, USA). Statistical analyses for data obtained from monocytes/macrophages were performed by one-way analysis of variance (ANOVA) followed by Tukey's multiple comparison tests by means of the Prism 5.0 software (GraphPad, San Diego, CA, USA). All results were expressed as mean values ± standard deviations. Values of $p < 0.05$ were considered statistically significant.

3. Results

3.1. Effect of QMR Treatment on Cell Viability

In order to determine the best exposure time and nominal powers for QMR stimulation, an MTS test was performed at 24 h on both undifferentiated (monocyte) and differentiated (macrophages) THP-1 cell cultures stimulated for 5, 10, and 30 min. The results were compared to non-exposed cells set at 100% cell viability. We found that 10 min of QMF stimulation and 30 nominal power was the optimal culture condition. At higher QMR doses, the cell viability of both cells was lower compared to the controls.

Based on previous results, all subsequent experiments were carried out by exposing the cells to QMR for 10 min, setting up two experimental sets: after 24 h, and repeating 4 times over a period of 4 days (Figure 1). To evaluate the potential cytoprotective effect of QMR exposure, we used an LPS/HA-induced inflammatory cell model. The data presented in Figure 1D,E show that QMR treatment alone did not have a significant effect on cellular viability in the differentiated (macrophages) THP-1 cell being studied. The stimulation with LPS/HA reduced the cell metabolic activity compared to the sham-exposed control cell. QMR treatment was able to restore the metabolic activity to values similar to sham-exposed control cells at both experimental sets (after 24 h (D) and 4 days (E)).

3.2. QMR Inhibits Activity and Protein Expression of COX-2 and iNOS

We investigated the effect of QMR treatment on the activity and protein expression of the well-known proinflammatory mediators COX-2 and iNOS after LPS/HA stimulation in differentiated THP-1 cells (Figures 2 and 3). To determine whether QMR can inhibit the COX-2 activity, macrophages THP-1 cells were stimulated with LPS/HA, and the amount of PGE_2 release was assessed using anti-PGE_2-coated ELISA plates. Cells stimulated with LPS/HA exhibited a significant increment in PGE_2 release compared with sham-exposed control cells (CTRL). This induction was significantly reduced ($p < 0.05$) by treatment with QMR at both experimental sets (after 24 h and 4 days) (Figure 2A,B). To confirm the inhibitory effects of QMR treatment on COX-2, LPS/HA-treated macrophage cells were assessed for their protein level, using specific antibodies by Western blotting analysis. As shown in Figure 2, LPS/HA stimulation caused an increased COX-2 protein expression at both times 24 h (A) and 4 days (B), as assessed by measuring the relative COX-2 density

compared to sham-exposed cells ($p < 0.05$). The QMR exposure following the LPS/HA stimulation led to a significant reduction in COX-2 protein expression in both experimental sets ($p < 0.05$).

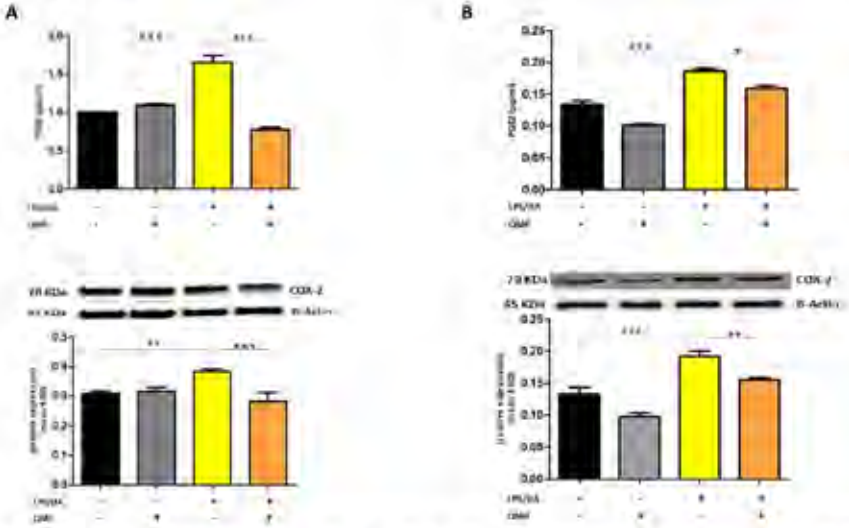

Figure 2. Effect of QMR treatment on PGE_2 levels and COX-2 protein expression in differentiated (macrophages) THP-1 cells. QMR treatment for 10 min at the two different settings (**A**) 24 h and (**B**) 4 days. Prostaglandin (PG) E_2 levels released in the culture medium are expressed as pg/mL (top). At the bottom, a representative image of Western blot experiments performed on cell lysates and averaged band density of relative expression of COX-2 normalized vs. β-actin. The data represented means ± SD ($n = 6$). $^{\#\#}$ $p < 0.01$ vs. control cells; $^{\#\#\#}$ $p < 0.001$ vs. control cells; * $p < 0.05$ vs. LPS/HA-treated cells; ** $p < 0.01$ vs. LPS/HA-treated cells; *** $p < 0.001$ vs. LPS/HA-treated cells.

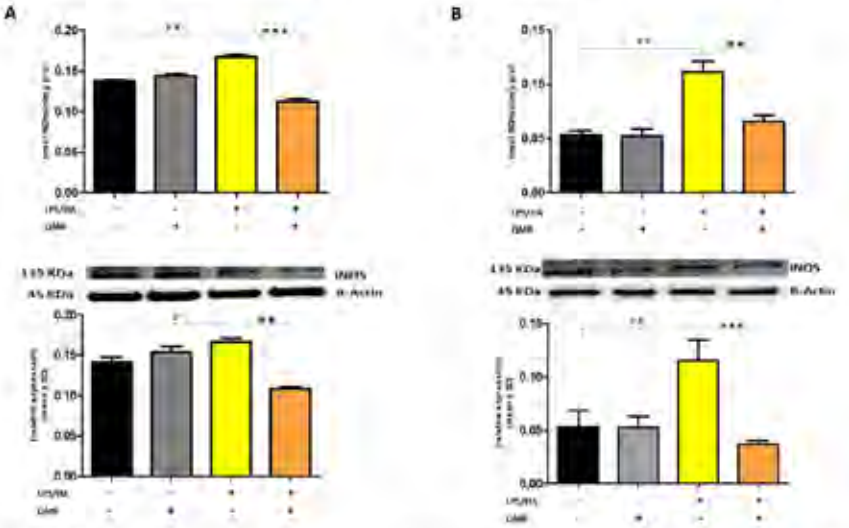

Figure 3. Effect of QMR treatment on iNOS activity and protein expression in differentiated (macrophages) THP-1 cells. QMR treatment for 10 min at the two different settings (**A**) 24 h and (**B**) 4 days. Spectrophotometric evaluation of the enzymatic activity of NOS performed on cell lysates and NOS enzymatic activities are expressed in nmol/min/mg prot. (top). At the bottom, a representative image of Western blot experiments performed on cell lysates and averaged band density of relative expression of iNOS normalized vs. β-actin. The data represented means ± SD ($n = 3$). $^{\#}$ $p < 0.05$ vs. control cells; $^{\#\#}$ $p < 0.01$ vs. control cells; ** $p < 0.01$ vs. LPS/HA-treated cells; *** $p < 0.001$ vs. LPS/HA-treated cells.

Stimulation of cells with LPS/HA resulted in a significant enhancement of the iNOS activity compared with sham-exposed control cells (Figure 3A,B) at 24 h and 4 days. This indicated increased production of NO and release of its stable product into the culture medium. However, cells stimulated with QMR showed a reduction in the iNOS enzyme activity following stimulation with LPS/HA. Western blot analysis applied to identify iNOS protein showed an iNOS up-regulated after LPS/HA stimulation at both times when examined with respect to sham-exposed cells. In accordance with activity results, QMR treatment produced a significant reduction in LPS/HA-induced iNOS protein expression at all time points studied, with a higher action in the experimental set of 4 days (Figure 3A,B). Moreover, the ability of QMR treatment to inhibit iNOS protein expression was much stronger than the ability to inhibit COX-2. Lastly, as COX-2 and iNOS expression is activated by the transcription factor NF-kB, it was assumed that QMR treatment may also inhibit NF-kB (Figure 4). The protein expression level of NF-kB was studied using p65-specific antibodies. LPS/HA stimulation strongly induced NF-κB activity of the macrophage THP-1 cells by monitoring the levels of p-p65 protein in nuclear extracts by Western blot analysis. The QMR treatment 24 h after cell activation by LPS/HA significantly reduced NF-κB activity compared to sham-exposed control cells (Figure 4A). This reduction remained significant after 4 days of QMR treatment as shown in Figure 4B.

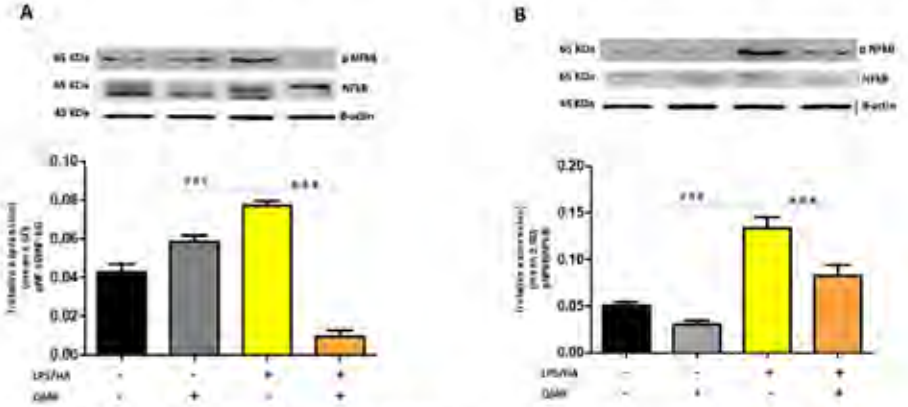

Figure 4. Effect of QMR treatment on NF-kB expression in differentiated (macrophages) THP-1 cells. QMR treatment for 10 min at the two different settings (**A**) 24 h and (**B**) 4 days. Representative image of Western blot experiments performed on cell lysates (top). At the bottom, averaged band density of relative expression of pNF-kB (p65) normalized vs. β-actin. The data represented means ± SD ($n = 3$). ### $p < 0.001$ vs. control cells; *** $p < 0.001$ vs. LPS/HA-treated cells.

3.3. Effect of QMR on Nitrosative Stress

We investigated the effects of QMR treatment on peroxynitrite production and tyrosine nitration in PMA-differentiated THP-1 cells in response to LPS/HA stimulation. Peroxynitrite is a reactive nitrogen species that can form when large amounts of NO and superoxide are present during inflammatory conditions. In this study, intracellular peroxynitrite was detected using fluorescence-based quantitative measurements. Figure 5 showed that peroxynitrite levels were significantly enhanced after the LPS/HA stimulation only 4 days compared to sham-exposed cells. After treatment with QMR, we observed a significant reduction in peroxynitrite levels. Nitration of tyrosine residues as 3-nitrotyrosine is considered a biomarker of peroxynitrite production. In our cellular model, the larger amount of immunoreactive band for 3-nitrotyrosine was present at a molecular weight of about 70–75 kDa. Our results show that after LPS/HA stimulation, nitrated proteins accumulate in a significant manner at 4 days and QMR treatment, in PMA-differentiated THP-1 cells, restored values of tyrosine nitration similar to the sham-exposed control cells at the same time point. No difference was recorded at 24 h (Figure 6). These findings suggest

that QMR treatment may have a beneficial effect in reducing peroxynitrite production and nitrosative stress in immune cells.

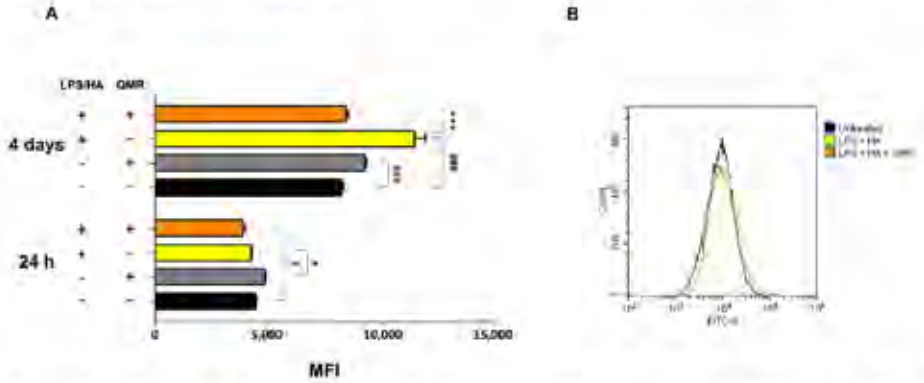

Figure 5. Generation of peroxynitrites in differentiated (macrophages) THP-1 cells after 24 h and 4 days of QMR treatment. (**A**) Bar graphs show the fold increase in the mean fluorescence intensities (MFIs) related to the emissions in the FL-1/FITC channel, which is proportional to the generation of peroxynitrite. Values are the ratios of the MFI generated from each sample on the unstained control (negative). (**B**) Peaks of emission were obtained using flow cytometry and are generated by plotting the cell count (y-axis) and the FITC fluorescence emission (x-axis). $^{\#}$ $p < 0.05$ vs. control cells; $^{\#\#\#}$ $p < 0.001$ vs. control cells; * $p < 0.05$ vs. LPS/HA-treated cells.; *** $p < 0.001$ vs. LPS/HA-treated cells.

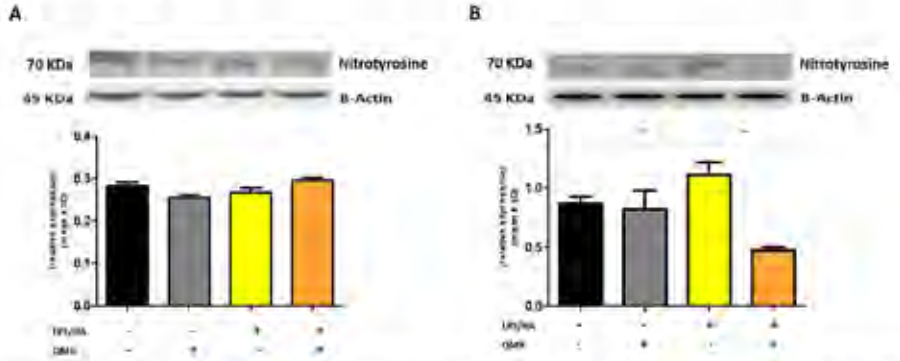

Figure 6. Nitrotyrosine protein expression in differentiated (macrophages) THP-1 cells. Effect of QMR treatment (10 min) after 24 h of incubation cells (**A**) and 4 days (**B**) on the expression of the 3-nitrotyrosine protein in LPS/HA-stimulated cells. Representative image of Western blot experiment (top) and at the bottom averaged band density of protein normalized vs. β-actin. The data represented means ± SD ($n = 3$). $^{\#}$ $p < 0.05$ vs. control cells; ** $p < 0.01$ vs. LPS/HA-treated cells.

3.4. QMR Treatment Attenuates LPS/HA-Induced Activation of NLRP3 Inflammasome

We next investigated whether QMR treatment affects NLRP3 inflammasome signaling.

Inflammasome signaling is a critical component of the innate immune response to environmental danger signals, which can trigger chronic inflammation in various diseases, including OA. Inflammasomes are multiprotein complexes that detect PAMPs or DAMPs and activate caspase-1, which then cleaves and releases pro-inflammatory cytokines such as IL-1β and IL-18 [29].

To further clarify the effect of QMR treatment on inflammasome activation, we examined the protein expression of the inflammasome signaling pathway. Results showed that the protein expression levels of NLRP3 and activated caspase-1 (Figure 7) were significantly increased after the LPS/HA induction compared to sham-exposed cells. However, the high level of proteins induced by LPS/HA was dramatically decreased in the QMR treatment group in both experimental set points.

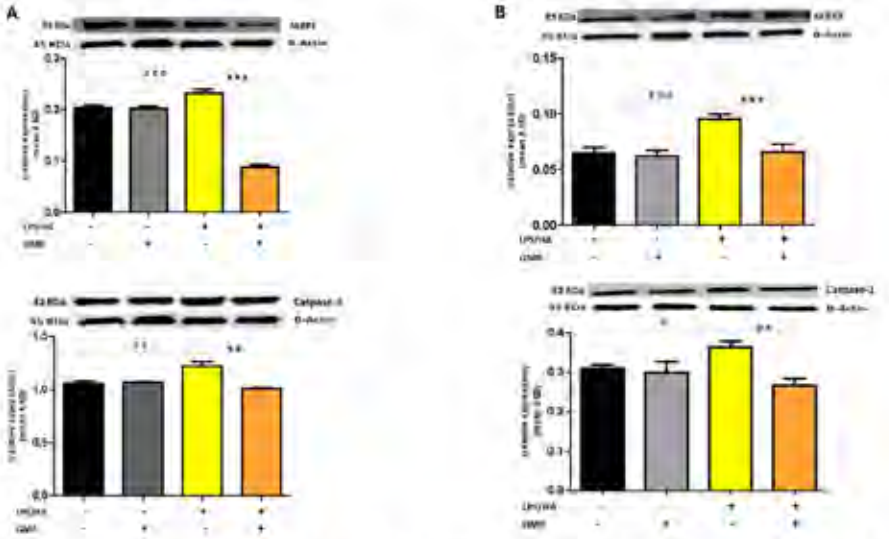

Figure 7. Effect of QMR treatment on NLRP3 and caspase-1 protein expression in differentiated (macrophages) THP-1 cells. QMR treatment for 10 min at the two different settings (**A**) 24 h and (**B**) 4 days. Representative image of Western blot experiments performed on cell lysates (top). At the bottom, averaged band density of relative expression of pNF-kB (p65) normalized vs. β-actin. The data represented means ± SD ($n = 3$). $^{\#}$ $p < 0.05$ vs. control cells; $^{\#\#}$ $p < 0.01$ vs. control cells; $^{\#\#\#}$ $p < 0.001$ vs. control cells; ** $p < 0.01$ vs. LPS/HA-treated cells; *** $p < 0.001$ vs. LPS/HA-treated cells.

The activation of the NLRP3 inflammasome is responsible for the processing and release of pro-inflammatory cytokines IL-18 and IL-1β, which are licensed through caspase-1. In the study, QMR treatment was found to downregulate IL-18 and IL-1β protein expression and secretion induced by LPS/HA at both times in macrophage THP-1 cells (Figure 8). Overall, these findings strongly suggest that QMR inhibits the LPS/HA-triggered activation of the NLRP3 inflammasome in THP-1-derived macrophages.

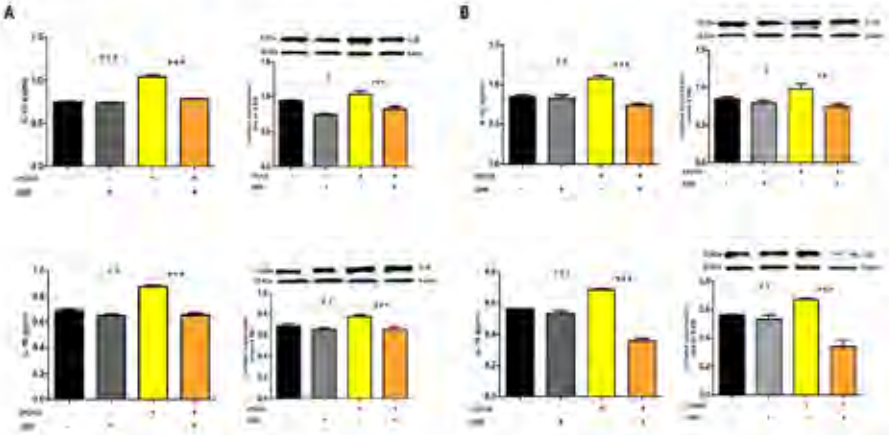

Figure 8. Effect of QMR treatment on IL-1β and IL-18 protein expression and secretion in differentiated (macrophages) THP-1 cells. THP-1-derived macrophages were stimulated with LPS/HA and treated with QMR for 10 min at two different settings (**A**) 24 h and (**B**) 4 days. The cytokines IL-1β (top) and IL-18 (bottom) were determined using ELISA kits (left) and relative protein expression normalized vs. β-actin was detected using a Western blot analysis (right). The data represented means ± SD ($n = 3$). $^{\#}$ $p < 0.05$ vs. control cells; $^{\#\#}$ $p < 0.01$ vs. control cells; $^{\#\#\#}$ $p < 0.001$ vs. control cells; ** $p < 0.01$ vs. LPS/HA-treated cells; *** $p < 0.001$ vs. LPS/HA-treated cells.

3.5. QMR Treatment Affects the Polarization of Macrophages

Recent pieces of evidence suggest that inflammation of the synovium and polarization of macrophages play a role in the pathogenesis of OA [30]. Traditionally, synovial macrophages can be classified into two main subtypes based on their activation state and function. Classically activated M1 macrophages are primarily involved in the inflammatory response and are activated by pro-inflammatory cytokines, such as interferon-gamma (IFN-γ) and LPS. M1 macrophages produce pro-inflammatory cytokines, such as IL-1β, IL-6, IL-12, and TNF-α, which help to activate and recruit other immune cells to the site of infection or tissue injury. Alternately, activated M2 macrophages are activated by anti-inflammatory cytokines, such as IL-4 and IL-13, and produce high levels of anti-inflammatory cytokines, such as IL-10 and transforming growth factor-beta (TGF-β). M2 macrophages are involved in tissue repair and remodeling, and they promote an anti-inflammatory and immunosuppressive environment [31]. Therefore, we investigated the influence of QMR on the polarization of macrophages (Figure 9A,B). The results of the flow cytometry assay showed that the expression of CD80 in LPS/HA-induced macrophage (M1) was remarkably up-regulated at 4 days compared to control cells. We found that QMR treatment of LPS/HA-stimulated macrophage THP-1 cells for 10 min significantly induced the expression of markers of M2 macrophage phenotype (CD163). This significant switching macrophage M1/M2 polarization effect observed was evidenced by the levels of cytokines released in the culture medium. In particular, the up-regulation of TNF-α induced by LPS/HA stimulation and cytokine related to M1-type was attenuated with a simultaneous increase in the anti-inflammatory cytokine (IL-10) associated with the M2 phenotype due to QMR treatment (Figure 9C,D).

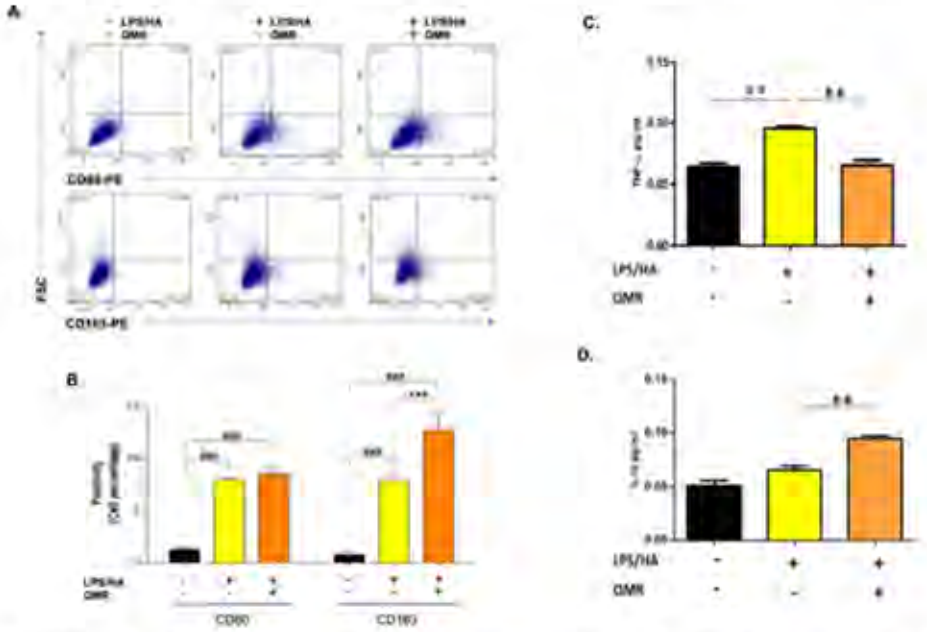

Figure 9. Effect of QMR treatment on polarization-related immunophenotype profile and IL-10 and TNF-α secretions in LPS/HA-stimulated differentiated macrophages. (**A**) Representative dot plots show the distribution of the cell population in response to QMR treatments at 4 days. Dot plots represent the population stained positive for CD80-PE or CD163-PE (x-axis) plotted towards the forward scatter (y-axis: FSC-Width). (**B**) The graph shows the percentages of the cell population stained positive for CD80 or CD163 after 4 days. The cytokines TNF-α (**C**) and IL-10 (**D**) were determined using ELISA kits after 4 days. The data represented means ± SD ($n = 3$). $^{\#\#}$ $p < 0.01$ vs. control cells; $^{\#\#\#}$ $p < 0.001$ vs. control cells; ** $p < 0.01$ vs. LPS/HA-treated cells; *** $p < 0.001$ vs. LPS/HA-treated cells.

4. Discussion

Osteoarthritis is a chronic degenerative joint disease characterized by cartilage breakdown, subchondral bone sclerosis, and synovial inflammation. Inflammation is a key factor in the pathogenesis of OA, and synovial macrophages play a crucial role in mediating this inflammatory response. Inflammation in OA is driven by various factors, including mechanical stress, cartilage degradation products, and cytokines such as IL-1β and TNF-α [32]. Inflammatory cytokines activate synovial macrophages, which are the major producers of pro-inflammatory mediators such as IL-1β, TNF-α, and PGE_2. Synovial macrophages also play a key role in the activation of the NLRP3 inflammasome, which is a multiprotein complex involved in the maturation and secretion of IL-1β. The activation of the inflammasome in synovial macrophages leads to further amplification of the inflammatory response in OA [33]. The use of biophysical stimulation techniques in clinical medicine has become increasingly popular as a method to promote repair and anabolic activity in tissue or to strengthen the activity of drug treatment while lessening side effects [34]. The complexity of the interaction between physical agents and biological systems made research difficult, but recent developments in physics have led to a greater understanding of how physical means can be used clinically. The new pharmacology involves identifying the effects of physical agents on a particular cell function, which forms the basis of its clinical application. The cell membrane has been identified as a target and site of interaction, and the physical signal activates a cascade of intracellular events through which transduction pathways differ depending on the type of energy used [35].

The promotion of cellular energy production is one of the mechanisms by which QMR therapy could exert anti-inflammatory effects. By enhancing mitochondrial function and increasing ATP production, the therapy can help to reduce cellular stress and inflammation. ATP is a key molecule that provides energy for cellular processes, and its production is closely linked to mitochondrial function. When mitochondrial function is impaired, as can occur in inflammatory conditions, there is a decrease in ATP production, which can lead to further cellular stress and inflammation. QMR therapy may help to counteract this by enhancing mitochondrial function and increasing ATP production, which can in turn reduce cellular stress and inflammation.

While the effect observed may be function-specific rather than cell- or tissue-specific, this allows all conditions positively influenced by the activation or modulation of this cell function to be treated with the same physical agent. Furthermore, PEMFs have shown potential therapeutic effects in the treatment of OA. Although studies in animal models have demonstrated that PEMFs based therapy can improve bone and cartilage turnover, the results of clinical trials in humans have been inconclusive. The conflicting results can be attributed to differences in study design, small sample sizes, and various subject-related factors [36].

This study was conducted to assess the anti-inflammatory activity of QMR technology in vitro. Specifically, we used an in vitro model of osteoarthritis-related inflammation to evaluate the potential mechanisms of QMR intervention and directed at improving therapeutic efficacy. This model involved inducing inflammatory cytokine expression using a combination of LPS and HA fragments such as PAMPs and DAMPs in the THP-1 cell line differentiated in macrophages.

A preliminary MTS test was performed to determine the optimal exposure time and nominal power for QMR stimulation on undifferentiated and differentiated THP-1 cell cultures. It was found that 10 min of QMR stimulation and 30 nominal power was the best culture condition. We observed that QMR treatment alone did not have a significant effect on cellular viability, but it was able to restore the metabolic activity to values similar to the sham-exposed control cells in both experimental sets (after 24 h and 4 days), which suggests a potential cytoprotective effect of QMR exposure.

We reported for the first time that QMR treatment has a beneficial effect in reducing proinflammatory mediators and nitrosative stress in immune cells. The results showed the inhibitory effects of QMR treatment on COX-2 and iNOS protein expression and

activity after LPS/HA stimulation. Western blot analysis showed that LPS/HA stimulation caused an increase in COX-2 and iNOS protein expression compared to sham-exposed cells. However, QMR treatment following LPS/HA stimulation led to a significant reduction in COX-2 and iNOS protein expression. Moreover, the study also investigated the effect of QMR treatment on NF-kB, a transcription factor that activates COX-2 and iNOS expression. The results showed that QMR treatment significantly reduced NF-κB activity compared to sham-exposed control cells after both 24 h and 4 days of LPS/HA stimulation. Moreover, QMR treatment led to a significant reduction in peroxynitrite levels, reactive nitrogen species that can form during inflammatory conditions, and restored values of tyrosine nitration similar to sham-exposed control cells.

The main contribution of inflammatory mediators in OA is to promote the breakdown of cartilage. Proinflammatory cytokines such as IL-1β, IL-6, TNF-α, and IL-18 are consistently elevated in OA and participate in chronic and low-grade inflammation, also known as inflammaging. Cartilage breakdown results in the release of cartilage matrix fragments that stimulate chondrocytes, synovial fibroblasts, and immune cells, leading to the release of matrix metalloproteinases and DAMPs, which promote the development of OA [37]. Inflammasomes, multi-protein complexes activated by DAMPs binding to pattern recognition receptors (PPRs), play a critical role in the innate immune response and are a major disruptor of tissue homeostasis in various diseases, including OA. Dysregulation of inflammasome activity promotes the upregulation of proinflammatory cytokines, apoptosis, and inflammation. NLRP3 and NLRP1 are important inflammasome components in OA, triggering pathogenic processes in macrophages. Targeting inflammasomes in chondrocytes and fibroblast-like synoviocytes presents a promising strategy for developing OA disease-modifying therapies [38].

To date, to our best knowledge, there has been no report about the regulation of QMR treatment on IL-1β/NALP3/caspase-1 expression in OA progression. In this study, we compared NALP3/caspase-1 expression in LPS/HA-stimulated human THP-1 monocytes with QMR treatment to the sham group. The findings indicate that the protein expression levels of NLRP3 and activated caspase-1 were significantly increased by LPS/HA induction compared to sham-exposed cells. However, in both experimental set points, the high protein levels induced by LPS/HA were significantly reduced by QMR treatment. The activation of the NLRP3 inflammasome leads to the processing and release of pro-inflammatory cytokines IL-18 and IL-1β, which are licensed via caspase-1. QMR treatment was found to downregulate IL-18 and IL-1β protein expression and secretion induced by LPS/HA at both time points in macrophage THP-1 cells. Overall, these results strongly suggest that QMR inhibits the LPS/HA-triggered activation of the NLRP3 inflammasome in THP-1-derived macrophages.

Recent research has identified inflammasomes as key regulators of macrophage polarization in OA [39]. The infiltration of immune cells, such as macrophages, into the joint space is a hallmark of OA. They can adopt different polarization states, depending on the signals they receive from the local microenvironment. Two main phenotypes have been described: M1 and M2 macrophages [40]. M1 macrophages are classically activated by pro-inflammatory stimuli, such as IFN-γ and LPS, and produce high levels of pro-inflammatory cytokines, such as TNF-α, IL-1β, and IL-6. M1 macrophages also have high levels of iNOS and produce ROS, which can cause tissue damage. In contrast, M2 macrophages are activated by anti-inflammatory cytokines, such as IL-4 and IL-13, and produce high levels of anti-inflammatory cytokines, such as IL-10 and TGF-β. M2 macrophages are also involved in tissue repair and remodeling. In OA, the balance between M1 and M2 macrophages is disrupted, leading to a chronic inflammatory state that contributes to disease progression. Studies have shown that M1 macrophages are more prevalent in the synovial fluid and tissues of OA patients than M2 macrophages. Liu et al. showed that the ratio of M1/M2 macrophages in synovial fluid and peripheral blood was markedly higher in knee OA patients compared to healthy controls and positively correlated with the severity of knee OA based on KL grade [41]. M1 macrophages contribute to joint tissue destruction by pro-

ducing pro-inflammatory cytokines and degrading extracellular matrix components. They also stimulate the production of metalloproteinases, which can cause cartilage degradation. In contrast, M2 macrophages have anti-inflammatory properties and can promote tissue repair by producing growth factors and extracellular matrix components.

The results of a transwell in vitro study investigated the effects of M1- and M2-polarized macrophages on OA chondrocytes. The study found that coculture of M1-polarized macrophages with OA chondrocytes could exacerbate the severity of OA, whereas coculture of M2-polarized macrophages with OA chondrocytes attenuated expression of OA-related proteases but increased matrix gene expression. These findings suggest that M1 and M2 macrophages have different effects on the cartilage in OA. The factors that regulate macrophage polarization in OA are complex and not yet fully understood [42]. However, several studies have identified potential molecular targets that could be used to modulate macrophage polarization in OA. For example, the activation of peroxisome proliferator-activated receptor gamma has been shown to induce M2 polarization and reduce joint inflammation in OA. Similarly, the inhibition of TLR4 signaling has been shown to reduce M1 polarization and inflammation in OA [43].

Our findings indicate that QMR treatment induces a switch in macrophage polarization from the M1 phenotype to the M2 phenotype. We observed a significant increase in CD80 expression in LPS/HA-induced macrophages, indicating the presence of M1 macrophages. However, when these macrophages were treated with QMR for 10 min, we observed a significant upregulation of CD163 expression, a marker of M2 macrophages, after 4 days. This suggests that QMR treatment can promote the polarization of macrophages towards the anti-inflammatory M2 phenotype. Moreover, we found that QMR treatment was associated with changes in cytokine levels. Specifically, we observed a reduction in TNF-α, a pro-inflammatory cytokine associated with M1 macrophages, and an increase in IL-10, an anti-inflammatory cytokine associated with M2 macrophages. These changes in cytokine levels provide further evidence that QMR treatment can induce a switch in macrophage polarization.

5. Conclusions

In summary, our results suggest that QMR treatment in in vitro model of osteoarthritis-related inflammation reduces proinflammatory mediators and nitrosative stress in immune cells by inhibiting COX-2 and iNOS protein expression as well as reducing NF-κB activity and peroxynitrite levels. QMR treatment also downregulates IL-18 and IL-1β protein expression and secretion induced by LPS/HA at both time points in macrophage THP-1 cells. The study provides evidence that QMR technology inhibits the LPS/HA-triggered activation of the NLRP3 inflammasome in THP-1-derived macrophages, suggesting that QMR treatment may have a beneficial effect in reducing inflammation associated with OA.

The study is characterized by common limitations inherent to the use of an in vitro model.

Briefly, the study only examined a limited set of inflammatory markers and pathways affected by QMR technology. Future studies should investigate a broader range of inflammatory markers and pathways to gain a more comprehensive understanding of QMR technology's anti-inflammatory effects. The study only investigated the effects of QMR technology on macrophages stimulated with lipopolysaccharide and hyaluronic acid fragments. While these stimuli are commonly used to induce inflammation in vitro, they may not fully replicate the complex inflammatory processes that occur in osteoarthritis in vivo. Therefore, future studies should investigate the effects of QMR technology on a broader range of cell types and inflammatory stimuli to determine its potential efficacy in the treatment of osteoarthritis and other inflammatory conditions. Therefore, the study's findings should be validated in animal models and human clinical trials.

However, the current study is novel and is our first report of the ability of QMR technology in modulating macrophage polarization towards the anti-inflammatory M2 phenotype. It enriches the knowledge that fills the gap in the current in vitro research

available in the literature that precedes the in vivo application of QMR for alleviating pain associated with osteoarthritis.

These results are promising and have the potential to provide significant opportunities for the clinical rehabilitative treatment of patients with osteoarthritis and other inflammation-correlated diseases. These findings also have important implications for the development of new therapeutic strategies aimed at targeting macrophage polarization in the treatment of inflammatory diseases.

Author Contributions: Conceptualization, T.P., M.P. and A.P. (Antonia Patruno); methodology, V.P., M.G. and O.F.; software, M.P.; validation, A.P. (Antonia Patruno); formal analysis, V.P. and M.G.; resources, G.P. and A.P. (Alessandro Pozzato); data curation, A.P. (Antonia Patruno) and V.M.R.; writing—original draft preparation, A.P. (Antonia Patruno); writing—review and editing, T.P., M.P., and A.P. (Antonia Patruno); supervision, K.B., P.L. and A.P. (Andrea Pantalone); funding acquisition, T.P., M.P. and A.P. (Antonia Patruno). All authors have read and agreed to the published version of the manuscript.

Funding: This research received no external funding.

Institutional Review Board Statement: Not applicable.

Informed Consent Statement: Not applicable.

Data Availability Statement: Data are contained within the article.

Acknowledgments: The authors acknowledge Telea Electronic Engineering for supporting this study with economic donations but did not have any additional role in the study design, data collection and analysis, decision to publish, or preparation of the manuscript.

Conflicts of Interest: The authors declare no conflict of interest.

References

1. Tarhan, S.; Unlu, Z. Magnetic resonance imaging and ultrasonographic evaluation of the patients with knee osteoarthritis: A comparative study. *Clin. Rheumatol.* **2003**, *22*, 181–188. [CrossRef] [PubMed]
2. Boffa, A.; Salerno, M.; Merli, G.; De Girolamo, L.; Laver, L.; Magalon, J.; Sánchez, M.; Tischer, T.; Filardo, G. Platelet-rich plasma injections induce disease-modifying effects in the treatment of osteoarthritis in animal models. *Knee Surg. Sport. Traumatol. Arthrosc.* **2021**, *29*, 4100–4121. [CrossRef] [PubMed]
3. Kraus, V.B.; McDaniel, G.; Huebner, J.L.; Stabler, T.V.; Pieper, C.F.; Shipes, S.W. Direct in vivo evidence of activated macrophages in human osteoarthritis. *Osteoarthr. Cartil.* **2016**, *24*, 1613–1621. [CrossRef]
4. Mantovani, A.; Sica, A.; Sozzani, S.; Allavena, P.; Vecchi, A.; Locati, M. The chemokine system in diverse forms of macrophage activation and polarization. *Trends Immunol.* **2004**, *25*, 677–686. [CrossRef]
5. Sohn, D.H.; Sokolove, J.; Sharpe, O.; Erhart, J.C.; Chandra, P.E.; Lahey, L.J.; Lindstrom, T.M.; Hwang, I.; Boyer, K.A.; Andriacchi, T.P. Plasma proteins present in osteoarthritic synovial fluid can stimulate cytokine production via Toll-like receptor 4. *Arthritis Res. Ther.* **2012**, *14*, R7. [CrossRef]
6. Frevert, C.W.; Felgenhauer, J.; Wygrecka, M.; Nastase, M.V.; Schaefer, L. Danger-Associated Molecular Patterns Derived From the Extracellular Matrix Provide Temporal Control of Innate Immunity. *J. Histochem. Cytochem.* **2018**, *66*, 213–227. [CrossRef] [PubMed]
7. Massari, L.; Benazzo, F.; Falez, F.; Perugia, D.; Pietrogrande, L.; Setti, S.; Osti, R.; Vaien-ti, E.; Ruosi, C.; Cadossi, R. Biophysical Stimulation of Bone and Cartilage: State of the Art and Future Perspectives. *Int. Orthop.* **2019**, *43*, 539–551. [CrossRef] [PubMed]
8. Speed, C.A. Therapeutic ultrasound in soft tissue lesions. *Rheumatology* **2001**, *40*, 1331–1336. [CrossRef]
9. Singh, A.; Varma, A.R. Whole-Body Vibration Therapy as a Modality for Treatment of Senile and Postmeno-pausal Osteoporosis: A Review Article. *Cureus* **2023**, *15*, e33690. [CrossRef]
10. Patruno, A.; Costantini, E.; Ferrone, A.; Pesce, M.; Diomede, F.; Trubiani, O.; Reale, M. Short ELF-EMF Exposure Targets SIRT1/Nrf2/HO-1 Signaling in THP-1 Cells. *Int. J. Mol. Sci.* **2020**, *21*, 7284. [CrossRef]
11. Patruno, A.; Ferrone, A.; Costantini, E.; Franceschelli, S.; Pesce, M.; Speranza, L.; Amerio, P.; D'Angelo, C.; Felaco, M.; Grilli, A.; et al. Extremely low-frequency electromagnetic fields accelerates wound healing modulating MMP-9 and inflammatory cytokines. *Cell. Prolif.* **2018**, *51*, 12432. [CrossRef]
12. Patruno, A.; Tabrez, S.; Pesce, M.; Shakil, S.; Kamal, M.A.; Reale, M. Effects of extremely low frequency electromagnetic field (ELF-EMF) on catalase, cytochrome P450 and nitric oxide synthase in erythro-leukemic cells. *Life Sci.* **2015**, *15*, 117–123. [CrossRef]
13. Patruno, A., Pesce, M.; Marrone, A.; Speranza, L.; Grilli, A.; De Lutiis, M.A.; Felaco, M.; Reale, M. Activity of matrix metallo proteinases (MMPs) and the tissue inhibitor of MMP (TIMP)-1 in electromagnetic field-exposed THP-1 cells. *J. Cell. Physiol.* **2012**, *227*, 2767–2774. [CrossRef]

14. Simko, M.; Mattsson, M.O. Extremely low frequency electromagnetic fields as effectors of cellular responses in vitro: Possible immune cell activation. *J. Cell. Biochem.* **2004**, *9*, 83–92. [CrossRef]
15. Guerriero, F.; Ricevuti, G. Extremely low frequency electromagnetic fields stimulation modulates autoimmunity and immune responses: A possible immuno-modulatory therapeutic effect in neurodegenerative diseases. *Neural Regen. Res.* **2014**, *11*, 1888–1895. [CrossRef]
16. Ongaro, A.; Varani, K.; Masieri, F.F.; Pellati, A.; Massari, L.; Cadossi, R.; Vincenzi, F.; Borea, P.A.; Fini, M.; Caruso, A.; et al. Electromagnetic fields (EMFs) and adenosine receptors modulate prostaglandin F(2) and cytokine release in human osteoarthritic synovial fibroblasts. *J. Cell. Physiol.* **2012**, *227*, 2461–2469. [CrossRef] [PubMed]
17. Vincenzi, F.; Targa, M.; Corciulo, C.; Gessi, S.; Merighi, S.; Setti, S.; Cadossi, R.; Goldring, M.B.; Borea, P.A.; Varani, K. Pulsed electromagnetic fields increased the anti-inflammatory effect of A_2A and A_3 adenosine receptors in human T/C-28a2 chondrocytes and hFOB 1.19 osteoblasts. *PLoS ONE* **2013**, *8*, e65561. [CrossRef]
18. D'Eredità, R.; Bozzola, L. Molecular resonance vs. coblation tonsillectomy in children. *Laryngoscope* **2009**, *119*, 1897–1901. [CrossRef] [PubMed]
19. Chang, H.; Hah, J.H. Comparison of post-tonsillectomy pain with two different types of bipolar forceps: Low-temperature quantum molecular resonance device versus high-temperature conventional electrocautery. *Acta Oto-Laryngol.* **2012**, *132*, S130–S133. [CrossRef] [PubMed]
20. Marzaro, M.; Algeri, M.; Tomao, L.; Tedesco, S.; Caldaro, T.; Balassone, V. Successful muscle regeneration by a homologous microperforated scaffold seeded with autologous mesenchymal stromal cells in a porcine esophageal substitution model. *Ther. Adv. Gastroenterol.* **2020**, *13*, 1756284820923220. [CrossRef] [PubMed]
21. Dal Maschio, M.; Canato, M.; Pigozzo, F.M.; Cipullo, A.; Pozzato, G.; Reggiani, C. Bio-physical effects of the high-frequency electrical field (4 ÷ 64 MHz) on muscle fibers in culture. *Basic. Appl. Miology* **2009**, *19*, 49–56.
22. Sella, S.; Adami, V.; Amati, E.; Bernardi, M.; Chieregato, K.; Gatto, P. In-vitro analysis of quantum molecular resonance effects on human mesenchymal stromal cells. *PLoS ONE* **2018**, *13*, e0190082. [CrossRef] [PubMed]
23. Stabler, T.V.; Huang, Z.; Montell, E.; Verges, J.; Kraus, V.B. Chondroitin sulphate inhibits NF-kappaB activity induced by interaction of pathogenic and damage associated molecules. *Osteoarthr. Cartil.* **2017**, *25*, 166–174. [CrossRef] [PubMed]
24. Kim, Y.K.; Hwang, J.H.; Lee, H.T. Differential susceptibility to lipopolysaccharide affects the activation of toll-like receptor 4 signaling in THP-1 cells and PMA-differentiated THP-1 cells. *Innate Immun.* **2022**, *28*, 122–129. [CrossRef]
25. Pesce, M.; Ferrone, A.; Rizzuto, A.; Tatangelo, R.; Iezzi, I.; Ladu, S.; Franceschelli, S.; Speranza, L.; Patruno, A.; Felaco, M.; et al. The SHP-1 expression is associated with cytokines and psychopathological status in unmedicated first-episode schizophrenia patients. *Brain Behav. Immun.* **2014**, *41*, 251–260. [CrossRef]
26. Maccallini, C.; Patruno, A.; Besker, N.; Ali, J.I.; Ammazzalorso, A.; De Filippis, B.; Franceschelli, S.; Giampietro, L.; Pesce, M.; Reale, M.; et al. Synthesis, biological evaluation, and docking studies of N-substituted acetamidines as selective inhibitors of inducible nitric oxide synthase. *J. Med. Chem.* **2009**, *52*, 1481–1485. [CrossRef] [PubMed]
27. Pantacuzzi, M.; Maccallini, C.; Lannutti, F.; Patruno, A.; Masella, S.; Pesce, M.; Speranza, L.; Ammazzalorso, A.; De Filippis, B.; Giampietro, L.; et al. Selective inhibition of iNOS by benzyl- and dibenzyl derivatives of N-(3-amino benzyl)acetamidine. *ChemMedChem* **2011**, *6*, 1203–1206. [CrossRef]
28. Zhao, C.; Zhao, W. NLRP3 inflammasome—A key player in antiviral responses. *Front. Immunol.* **2020**, *11*, 211. [CrossRef]
29. Pesce, M.; Speranza, L.; Franceschelli, S.; Ialenti, V.; Iezzi, I.; Patruno, A.; Rizzuto, A.; Robazza, C.; De Lutiis, M.A.; Felaco, M.; et al. Positive correlation between serum interleukin-1β and state anger in rugby athletes. *Aggress. Behav.* **2013**, *39*, 141–148. [CrossRef] [PubMed]
30. Chen, Y.; Jiang, W.; Yong, H.; He, M.; Yang, Y.; Deng, Z.; Li, Y. Macrophages in osteoarthritis: Pathophysiology and therapeutics. *Am. J. Transl. Res.* **2020**, *12*, 261–268.
31. Gordon, S.; Martinez, F.O. Alternative activation of macrophages: Mechanism and functions. *Immunity* **2010**, *32*, 593–604. [CrossRef]
32. Goldring, M.B.; Otero, M. Inflammation in osteoarthritis. *Curr. Opin. Rheumatol.* **2011**, *23*, 471–478. [CrossRef] [PubMed]
33. Yang, J.; Liu, W. The Role of AIM2 Inflammasome in Knee Osteoarthritis. *J. Inflamm. Res.* **2022**, *15*, 6453–6461. [CrossRef]
34. Patruno, A.; Amerio, P.; Pesce, M.; Vianale, G.; Di Luzio, S.; Tulli, A.; Franceschelli, S.; Grilli, A.; Muraro, R.; Reale, M. Extremely low frequency electromagnetic fields modulate expression of inducible nitric oxide synthase, endothelial nitric oxide synthase and cyclooxygenase-2 in the human keratinocyte cell line HaCat: Potential therapeutic effects in wound healing. *Br. J. Derm.* **2010**, *162*, 258–266. [CrossRef] [PubMed]
35. Goodman, E.M.; Greenebaum, B.; Marron, M.T. Effects of electromagnetic fields on molecules and cells. *Int. Rev. Cytol.* **1995**, *158*, 279–338. [CrossRef] [PubMed]
36. Tong, J.; Chen, Z.; Sun, G.; Zhou, J.; Zeng, Y.; Zhong, P.; Deng, C.; Chen, X.; Liu, L.; Wang, S.; et al. The Efficacy of Pulsed Electromagnetic Fields on Pain, Stiffness, and Physical Function in Osteoarthritis: A Systematic Review and Meta-Analysis. *Pain. Res. Manag.* **2022**, *9*, 9939891. [CrossRef]
37. Hamasaki, M.; Terkawi, M.A.; Onodera, T.; Homan, K.; Iwasaki, N. A Novel Cartilage Fragments Stimulation Model Revealed that Macrophage Inflammatory Response Causes an Upregulation of Catabolic Factors of Chondrocytes In Vitro. *Cartilage* **2021**, *12*, 354–361. [CrossRef]

38. Ramirez-Perez, S.; Reyes-Perez, I.V.; Martinez-Fernandez, D.E.; Hernandez-Palma, L.A.; Bhattaram, P. Targeting inflammasome-dependent mechanisms as an emerging pharmacological approach for osteoarthritis therapy. *iScience* **2022**, *25*, 105548. [CrossRef]
39. Mushenkova, N.V.; Nikiforov, N.G.; Shakhpazyan, N.K.; Orekhova, V.A.; Sadykhov, N.K.; Orekhov, A.N. Phenotype Diversity of Macrophages in Osteoarthritis: Implications for Development of Macrophage Modulating Therapies. *Int. J. Mol. Sci.* **2022**, *23*, 8381. [CrossRef]
40. Yunna, C.; Mengru, H.; Lei, W.; Weidong, C. Macrophage M1/M2 polarization. *Eur. J. Pharm. Pharmacol.* **2020**, *877*, 173090. [CrossRef]
41. Liu, B.; Zhang, M.; Zhao, J.; Zheng, M.; Yang, H. Imbalance of M1/M2 macrophages is linked to severity level of knee osteoarthritis. *Exp. Ther. Med.* **2018**, *16*, 5009–5014. [CrossRef] [PubMed]
42. Chen, B.; Hong, H.; Sun, Y.; Chen, C.; Wu, C.; Xu, G.; Bao, G.; Cui, Z. Role of macrophage polarization in osteoarthritis (Review). *Exp. Ther. Med.* **2022**, *24*, 757. [CrossRef] [PubMed]
43. Zhu, X.; Lee, C.W.; Xu, H.; Wang, Y.F.; Yung, P.S.H.; Jiang, Y.; Lee, O.K. Phenotypic alteration of macrophages during osteoarthritis: A systematic review. *Arthritis Res. Ther.* **2021**, *23*, 110. [CrossRef] [PubMed]

Disclaimer/Publisher's Note: The statements, opinions and data contained in all publications are solely those of the individual author(s) and contributor(s) and not of MDPI and/or the editor(s). MDPI and/or the editor(s) disclaim responsibility for any injury to people or property resulting from any ideas, methods, instructions or products referred to in the content.

13

In-vitro analysis of Quantum Molecular Resonance effects on human mesenchymal stromal cells

S. Sella, V. Adami, E. Amati, M. Bernardi, K. Chieregato, P. Gatto, M. Menarin, A. Pozzato, G. Pozzato, G. Astori

PLOS ONE

RESEARCH ARTICLE

In-vitro analysis of Quantum Molecular Resonance effects on human mesenchymal stromal cells

Sabrina Sella[1], Valentina Adami[2], Eliana Amati[1], Martina Bernardi[1,3], Katia Chieregato[1,3], Pamela Gatto[2], Martina Menarin[1], Alessandro Pozzato[4], Gianantonio Pozzato[4], Giuseppe Astori[1]*

1 Advanced Cellular Therapy Laboratory, Hematology Unit, Vicenza Hospital, Vicenza, Italy, **2** High Throughput Screening Core Facility, Center for Integrative Biology, University of Trento, Trento, Italy, **3** Hematology Project Foundation, Vicenza, Italy, **4** Telea Electronic Engineering srl, Sandrigo, Italy

* astori@hematology.vcn.it

Check for updates

OPEN ACCESS

Citation: Sella S, Adami V, Amati E, Bernardi M, Chieregato K, Gatto P, et al. (2018) *In-vitro* analysis of Quantum Molecular Resonance effects on human mesenchymal stromal cells. PLoS ONE 13 (1): e0190082. https://doi.org/10.1371/journal.pone.0190082

Editor: Antonio Paolo Beltrami, Universita degli Studi di Udine, ITALY

Received: May 11, 2017

Accepted: December 7, 2017

Published: January 2, 2018

Copyright: © 2018 Sella et al. This is an open access article distributed under the terms of the Creative Commons Attribution License, which permits unrestricted use, distribution, and reproduction in any medium, provided the original author and source are credited.

Data Availability Statement: All relevant data are within the paper and its Supporting Information files. Cluster dendrogram of samples according to similarity of gene expression profile is available publicly in doi: 10.6084/m9.figshare.5702137.

Funding: Telea Electronic Engineering provided support in the form of salaries for SS, AP and GP but did not have any additional role in the study design, data collection and analysis, decision to publish, or preparation of the manuscript. The

Abstract

Electromagnetic fields play an essential role in cellular functions interfering with cellular pathways and tissue physiology. In this context, Quantum Molecular Resonance (QMR) produces waves with a specific form at high-frequencies (4–64 MHz) and low intensity through electric fields. We evaluated the effects of QMR stimulation on bone marrow derived mesenchymal stromal cells (MSC). MSC were treated with QMR for 10 minutes for 4 consecutive days for 2 weeks at different nominal powers. Cell morphology, phenotype, multilineage differentiation, viability and proliferation were investigated. QMR effects were further investigated by cDNA microarray validated by real-time PCR. After 1 and 2 weeks of QMR treatment morphology, phenotype and multilineage differentiation were maintained and no alteration of cellular viability and proliferation were observed between treated MSC samples and controls. cDNA microarray analysis evidenced more transcriptional changes on cells treated at 40 nominal power than 80 ones. The main enrichment lists belonged to development processes, regulation of phosphorylation, regulation of cellular pathways including metabolism, kinase activity and cellular organization. Real-time PCR confirmed significant increased expression of MMP1, PLAT and ARHGAP22 genes while A2M gene showed decreased expression in treated cells compared to controls. Interestingly, differentially regulated MMP1, PLAT and A2M genes are involved in the extracellular matrix (ECM) remodelling through the fibrinolytic system that is also implicated in embryogenesis, wound healing and angiogenesis. In our model QMR-treated MSC maintained unaltered cell phenotype, viability, proliferation and the ability to differentiate into bone, cartilage and adipose tissue. Microarray analysis may suggest an involvement of QMR treatment in angiogenesis and in tissue regeneration probably through ECM remodelling.

specific roles of these authors are articulated in the 'author contributions' section.

Competing interests: I have read the journal's policy and the authors of this manuscript have the following competing interests: GP is the cofounder and AP is an employee of Telea Electronic Engineering srl, Sandrigo, Italy. This does not alter our adherence to PLOS ONE policies on sharing data and materials.

Introduction

Cells interact with the surrounding environment through receptors and ion channels which transmit chemical, mechanical and electrical signals. In this context, electromagnetic fields (EMF) interfere with cellular pathways and tissue physiology [1]. Cell-EMF interaction can occur through charged molecules and proteins in the cell membrane that alters the flow of ions or rearranges the distribution of the membrane receptors, or via direct field penetration inside the cell [2].

There is evidence that the manipulation of the electromagnetic environment on biological systems favours wound healing process, reduction of inflammatory state, angiogenesis and extracellular matrix (ECM) synthesis [3]. In fact, EMF regulate a variety of cell functions including promotion and inhibition of cellular proliferation [4, 5], cellular viability [6, 7], differentiation [8–10], cellular migration and motility [11–13], inflammatory response [14, 15] and gene expression profiles [16, 17]. As a consequence, therapeutic application of EMF has undergone a raising interest in medicine. By contrast, the mechanisms of action of EMF in biological tissues are only partially known [18].

Quantum Molecular Resonance (QMR) stimulation is a technology already applied for surgical and medical purposes. QMR creates quanta of energy able to break the molecular bonds without increasing the kinetic energy of the hit molecules, thus without raising in the temperature and limiting the damage to the surrounding tissue. QMR technology exploits no-ionizing high-frequency waves in the range between 4 and 64 MHz at low intensity delivered through alternating electric fields. The effect of QMR stimulation relies on the induction of more frequencies at the same time, where the fundamental wave is at 4 MHz and the subsequent ones increase in harmonic content until 64 MHz with related decreasing amplitudes.

QMR finds clinical application in bipolar coagulators or electrosurgery devices [19, 20]. For this kind of applications, the molecular resonance generator works on the combination of four frequencies in the range of 4–16 MHz. The first experimental study testing QMR effects described in a rat model of thoracotomy a less severe tissue damage than standard electrocautery [21].

Since now, few data are available on the mechanism of interaction between QMR and cells. Dal Maschio and colleagues [22] provided the description of the behavior of muscle fibers exposed to QMR, where the changes of membrane potential and the variations of free calcium concentration strictly followed the time course of electrical field application and removal. Moreover, the effectiveness of molecular quantum resonance in reducing edema after total knee arthroplasty in a clinical trial has been reported [23].

Our work aimed at understanding how QMR acts on human bone marrow-derived mesenchymal stromal cells (MSC).

The use of MSC for tissue healing and in regenerative medicine was extended in the last decade [24], but current research on MSC aims not only to the development of clinical protocols of cellular therapy or regenerative medicine but also to provide experimental models that can inform about molecular mechanisms such as inflammation, angiogenesis and apoptosis [25].

Three main criteria were proposed by the International Society for Cellular Therapy (ISCT) for MSC definition [26]: adherence to plastic under standard culture conditions; expression of CD105, CD73, CD90 and lack of expression of HLA-DR, together with the lack of hematopoietic and endothelial surface markers CD14, CD45, CD34, CD11b and CD31 [27]; *in vitro* differentiation potential into osteocytes, chondrocytes and adipocytes under appropriate culture conditions [28]. Despite of attempts for establishing generally acceptable minimal criteria for defining human MSC by immunophenotyping, the functional capability to differentiate along

the classical tri-lineage mesodermal pathways remains one fundamental characteristic of this cell type.

MSC represent an ideal model to study the effects of high frequency EMF and electric current. MSC exhibit remarkable plasticity given their ability to transdifferentiate or undergo rapid alteration in phenotype, thereby giving rise to cells possessing the characteristics of different lineages. Moreover, there are evidences that endogenous bone marrow-derived MSC could be recruited and mobilized to sites of injury [29]. As a consequence MSC can be used in various clinical conditions in which tissue repair is needed, or in which these cells are believed to act through their anti-inflammatory and immunomodulatory activities.

In the present study, we used a broad evaluation approach to study the effects of QMR on human MSC at different levels of investigation. Cell cultures were exposed to distinct QMR settings and times of treatment. We assessed the maintenance of MSC identity and then therefore performed viability and cellular proliferation assays to assess additional information about. Finally, we investigated the transcriptional profile of MSC after QMR stimulation.

Materials and methods

MSC isolation and *ex-vivo* expansion

MSC were isolated from cells obtained through the washouts of discarded bone marrow collection bags and filters of healthy donors, 2 male and 4 female (median age: 34.5 years. Range 23–47). After two washing steps with 200 ml saline solution and centrifugation at 2.000 rpm for 10 min, the collected nucleated cells were seeded in toto at the density of $1x10^5$ cells/cm^2 in low-glucose Dulbecco's modified Eagle's medium (DMEM) with GlutaMAX™ and pyruvate (Gibco, Thermo Fisher Scientific, Waltham, MA, USA) supplemented with 10% fetal bovine serum (FBS, Qualified Australian, Gibco, Thermo Fisher Scientific) and 1% penicillin/streptomycin (P/S, Sigma-Aldrich, St Louis, MO, USA). Cultures were incubated at 37˚C in a humidified atmosphere with 5% CO_2. Non-adherent cells were removed after 72 hours and fresh medium was added, then the culture medium was changed every 3–4 days. At 80% confluence, MSC were washed with Dulbecco's phosphate-buffered saline (D-PBS, Sigma-Aldrich), harvested using 10X TrypLE Select (Gibco, Thermo Fisher Scientific) and sub-cultured at a density of 1.500 cells/cm^2. The cultures were observed with an inverted light microscope Axiovert 40 CFL (Carl Zeiss, Oberkochen, Germany) and the images were acquired by using an AxioCam Mrm camera system (Carl Zeiss).

Cellular model and QMR stimulation protocol

MSC cultures were exposed to QMR using an experimental QMR generator supplied by Telea (Telea Electronic Engineering, Sandrigo, VI, Italy). The QMR generator setup was the following: alimentation: 230 V ~ 50/60 Hz; maximum power in input: 250 VA; power in output: 45 W/400 Ω. The prototype enhanced alternating electric currents characterized by high-frequency waves and low intensity. The fundamental wave was at 4 MHz and the subsequent ones increased in harmonic content until 64 MHz with related decreasing amplitudes. The stimulations were delivered through the raise of effective powers in output (4–45 W) corresponded to increase in value to the nominal powers employed as QMR settings.

The cellular model and QMR delivery system were composed of a pair of custom made spheroidal electrodes (anodes) of 35 mm-diameter and by an electrode (cathode) constituted of a metallic plate. The electrodes were placed inside two Petri dishes and supported by a polyvinyl chloride component to allow the direct contact of the electrode with the surface of the culture medium. The cathode was positioned below the Petri dishes (Fig 1A).

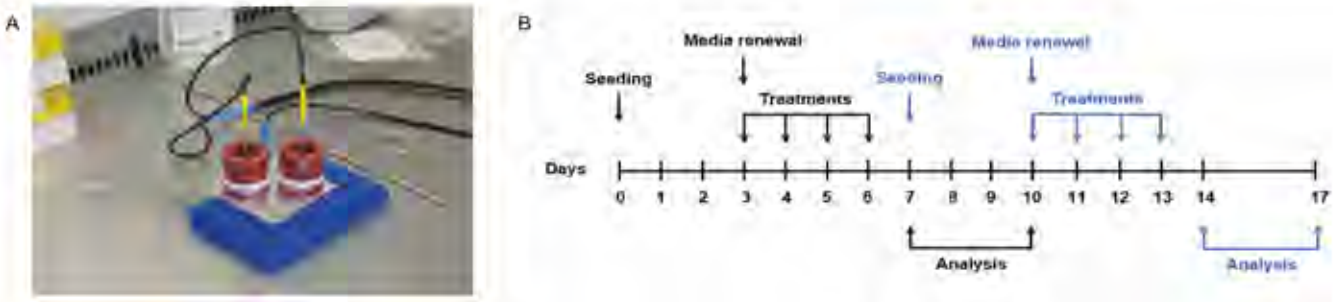

Fig 1. QMR stimulation protocol. A) Image of the exposure system. B) Scheme of QMR treatment. Cells were seeded on day 0, harvested and reseeded on day 7. The first cycle of treatment started after media renewal on day 3 (black arrows) and the second one on day 10 (blue arrows). Cultures were stimulated 10 minutes/day for 4 consecutive days at 40 or 80 nominal powers. Sham-exposed controls were kept in parallel.

https://doi.org/10.1371/journal.pone.0190082.g001

The experimental setup was planned in order to reproduce in-vitro the therapeutic conditions in terms of timing and powers. Based on medical reports and on long company experience, the most effective settings with positive follow-up were selected for MSC cultures experimentation.

MSC at passages 4–6 were seeded in 35 mm-diameter Petri dishes in duplicate per condition (Greiner Bio-One, Kremsmünster, Austria) and after 72 hours from initial seeding, complete medium was changed. Cells were subjected to 10 minutes/day of QMR stimulation for 4 consecutive days with rest period of 24 hours between them. The same MSC cultures exposed to the first QMR cycle of treatment were reseeded for the second one and treated under identical conditions (Fig 1B). Two different QMR settings corresponding to 40 and 80 nominal powers were applied. Controls were kept in parallel as sham-exposed controls with electrodes presence in cell media and without QMR exposition.

MSC phenotype characterization

MSC phenotype was characterized by flow cytometry before and after QMR stimulation. Briefly, $1x10^5$ cells were incubated with the following monoclonal antibodies: CD90-FITC, CD105-PE, CD45-ECD, HLA-DR-APC (all purchased from Beckman Coulter, Brea, CA, USA) and CD73-PC7 (Becton Dickinson, Franklin Lakes, NJ, USA) for 15 minutes at room temperature protected from light. At least 20.000 events were acquired on a CYTOMICS FC500 flow-cytometer and data were analysed by Kaluza software (both Beckman Coulter). The expression of each marker was assessed as percentage (%) of positive cells and as relative median fluorescence intensity (rMFI), this latter defined as the ratio between the median fluorescence intensity of the marker and its specific negative control.

Multilineage differentiation

After two cycles of consecutive stimulations MSC differentiation potential was tested. Samples were harvested and reseeded in 24-well plates (Falcon, Corning Life Sciences, NY, USA) in the presence of circular 13 mm-diameter and 0.2 mm-thickness coverslips (Nunc, Thermo Fisher Scientific) at the density of 4.000 cells/cm^2. Differentiation was induced at semi-confluence with specific differentiation media for 21 days with StemPro Adipogenesis, Osteogenesis and Chondrogenesis kit, (Gibco, Thermo Fisher Scientific). Fresh medium was added every 3 days and the respective controls were maintained in parallel with standard expansion medium.

To detect the formation of lipid droplets, cells were fixed in 10% formalin for 5 minutes and stained with Oil Red O (Diapath, Martinengo, BG, Italy) according to manufacturer's instructions.

The presence of calcium deposit as an expression of osteogenic induction was analysed with Alizarin red staining. The samples were washed with D-PBS and fixed in ice-cold 70% ethanol at 4˚C for 1 hour. Then, they were incubated for 15 minutes with 0.02 g/ml of Alizarin red solution (Sigma-Aldrich) at room temperature. Finally, several washes were performed with deionized water.

To verify chondrogenic differentiation, cells were fixed in 10% formalin for 5 minutes and stained with 1 g/l in 0.1 M HCl of Alcian blue for 2 hours at room temperature. At the end of the staining specific for acidic polysaccharides, the coverslips were rinsed extensively with deionized water.

After each staining, the coverslips were mounted on microscope slides using Kaiser's glycerol gelatine pre-warmed at 37˚C. The acquisition of images was obtained by AxioCam Erc 5s camera system (Carl Zeiss).

Assessment of cellular viability

Cellular viability was determined by flow cytometry using LIVE/DEAD Fixable Far Red Dead Cell Stain kit (Invitrogen™, Thermo Fisher Scientific) according to manufacturer's instructions by samples acquisition on a CYTOMICS FC500 flow-cytometer. Data were analysed as % of dim or bright positive cells by Kaluza software (Beckman Coulter).

Quantification of cellular proliferation

Cellular proliferation was determined by WST-1 assay (Sigma Aldrich). At the end of two consecutive cycles of QMR treatment, cells were harvested and seeded in 96 well-plates (Falcon, Corning Life Sciences) at the density of 2.000 cells/well. After 72 hours WST-1 was added and incubated for 3 hours at 37˚C. Finally, the plates were read at 450 nm with a spectrophotometer (SpectraCount, Packard Instrument Company Inc, Meriden, CT, USA). Data were expressed as percentage (%) of proliferation on the control.

cDNA microarray analysis

The RNA derived from five different MSC samples exposed to one cycle of QMR stimulation and their corresponding MSC controls were extracted using RNeasy plus mini kit (Qiagen, Hilden, Germany) according to the manufacturer's instructions. The total RNA quantification was obtained with NanoDrop UV-VIS Spectrophotometer (Thermo Fisher Scientific). The quality of RNA was determined using Agilent 2100 Bioanalyzer system with Eukaryote Total RNA Nano kit (Agilent Technologies, Santa Clara, CA, USA). The samples were processed according to protocol "Agilent One-Color Microarray-based Gene Expression Analysis (Low Input Quick Amp Labeling)" with Human GE 4x44K V2 Microarray Kit (Agilent Technologies).

Microarray slides were detected with Agilent scanner through ScanControl software. Row data from microarray images were extracted by Agilent Feature Extraction software. Afterward data were subjected to a pre-processing step using open-source program Bioconductor that employs the Limma package with R language [30].

Quantitative real-time PCR

MSC cultures were exposed or not to QMR at 40 nominal power for one cycle and the total RNA was extracted using RNeasy Plus Mini Kit (Qiagen) following the manufacturer's

instructions. Quality and quantity were determined using Nanodrop UV-VIS Spectrophotometer (Thermo Fisher Scientific). cDNA was synthesized starting from 800 ng of total RNA, using the iScript cDNA synthesis kit (Bio-Rad, Hercules, CA, USA) according to the manufacturer's instructions.

The obtained cDNA was diluted 1:10 and the quantitative real-time PCR experiments were performed using SsoFast EvaGreen Supermix with Low Rox (Bio-RAD) on ABI 7500 Real-Time PCR System (Applied Biosystem, Thermo Fisher Scientific). Primers used for the amplification were validated and purchased from Bio-RAD. The protocol consisted of 30 seconds at 95˚C, 40 cycles of 5 seconds at 95˚C and an elongation step of 32 seconds at 60˚C, followed by a final melting step to evaluate the quality of the product. Each gene was tested in three replicates and six independent experiments were performed. Data acquisition was obtained by SDS v1.2 software (Applied Biosystem, Thermo Fisher Scientific) and the relative expression was determined using $2^{-\Delta\Delta Ct}$ method [31] with TBP and YWHAZ as reference genes.

Statistical analysis

To analyse the differences between the experimental settings and the sham-exposed controls after both QMR cycles, data were analysed by one-way ANOVA followed by Dunnett's multiple comparison post-hoc test.

Quantitative real-time PCR data were analysed by paired t-test comparing the ΔCt values. Statistical analysis was performed using GraphPad Prism version 5.01 (GraphPad Software Inc, La Jolla, CA, USA). Differences between samples were considered statistically significant at $p<0.05$.

For the cDNA microarray analysis, differentially expressed genes (DEG) between treated (40 or 80 nominal power) cells and control cells were elaborated using Limma package with Bayes' empirical method, taking into account the provenience of batches (paired test). Differences between conditions (treated cells versus control cells) were considered significant after Benjamini & Hochberg correction at $p<0.05$. To analyse the best enrichment of gene lists, the ToppGene Suite and Ingenuity Pathway Analysis (IPA) computational tools were applied. It was considered a q-value<0.01 with Benjamini & Hochberg's false discovery rate (FDR) correction for ToppGene Suite and a p-value<0.01 with Bonferroni-Hochberg correction for IPA analysis.

Results

Evaluation of MSC identity after QMR stimulation

In order to evaluate modification in MSC identity after the first and second cycle of treatment with QMR, we analysed morphology, expression of surface markers and multi-differentiation potential. MSC morphology was observed daily before and after QMR treatments at the different settings. The cells conserved their canonical fibroblast-like spindle-shaped aspect during all the time of the experiments (Fig 2A and 2B). Typical phenotypic MSC expression of CD90, CD105 and CD73 was constantly >95%, while that of CD45 and HLA-DR constantly lower than 2% (Fig 2C). Moreover each marker showed similar rMFI of expression without statistical significance between treated and untreated samples at the different settings (S2 Fig). To investigate if cell cultures lost their *in vitro* mesenchymal differentiation potential after two cycles of QMR stimulation, we induced cells to differentiate down into osteogenic, adipogenic and chondrogenic lineages by using defined media components and conditions (Fig 3). QMR-treated and sham-exposed MSC samples were able to multi-differentiate after 21 days of induction, being positive to Alizarin Red, Oil Red O and Alcian blue specific staining for osteogenesis (Fig 3A and 3B), adipogenesis (Fig 3C and 3D) and chondrogenesis (Fig 3E and 3F),

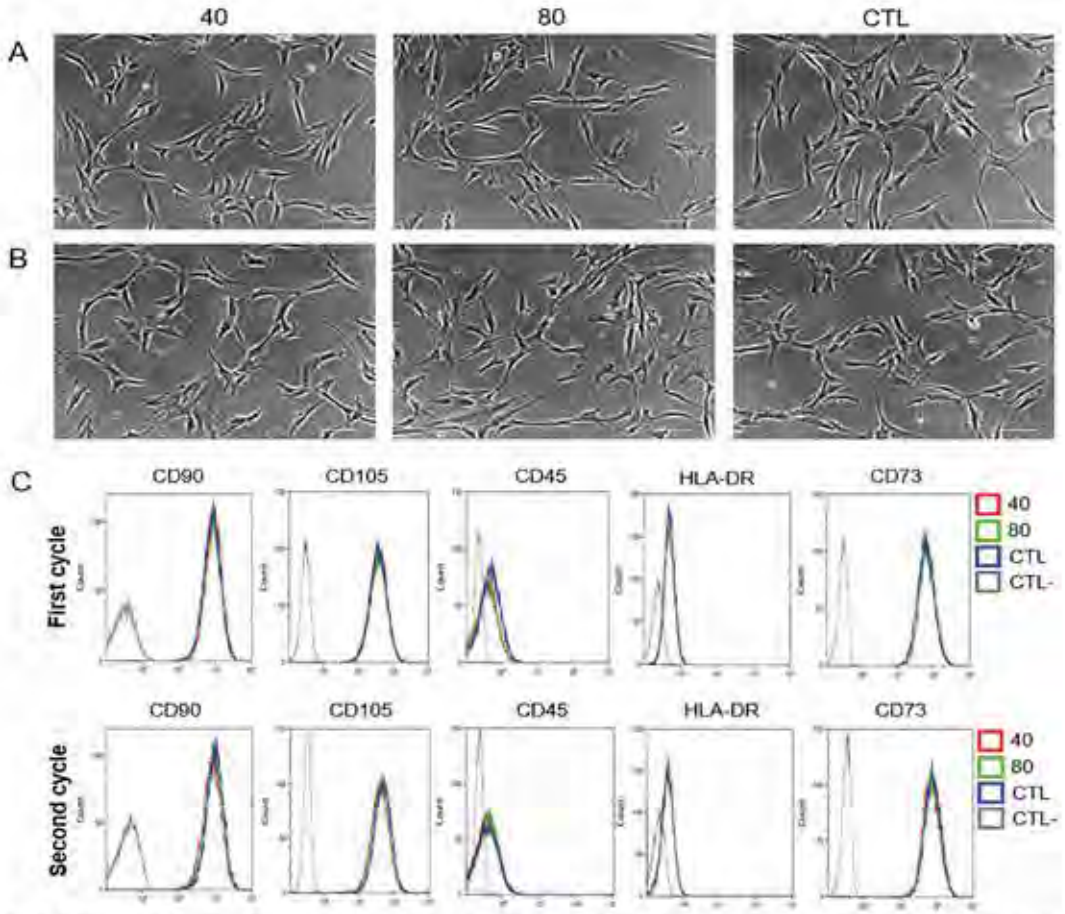

Fig 2. MSC morphology and flow cytometry analysis after QMR stimulation. A) The images were obtained after 10 minutes of QMR stimulation at Day 5 (first cycle of treatment) and at B) Day 12 (second cycle of treatment). Scale bar = 100 μm. Total magnification = 100X. One representative experiment was shown. C) Five colour combination of monoclonal antibodies was used to verify MSC identity according to the above listed surface markers of a representative sample, Grey line = unstained control (CTL-). Blue line = sham-exposed control (CTL). Green line = QMR setting 80. Red line = QMR setting 40.

https://doi.org/10.1371/journal.pone.0190082.g002

respectively. No qualitative differences were observed between different QMR treatments and controls at this level. Similar results were detected between one (Fig 3A, 3C and 3E) and two cycles (Fig 3B, 3D and 3F) of stimulation.

MSC viability and proliferation after QMR stimulation

Cellular viability was quantified by flow cytometry at the end of each cycle (Fig 4A). Viability was not affected by QMR; indeed, more than 95% of cells were alive similarly to the controls, with low variability between the different MSC batches and settings. These results confirmed the morphological observations. MSC proliferation was not affected by QMR showing no significant differences between controls and QMR-treated samples at the different settings and times (Fig 4B).

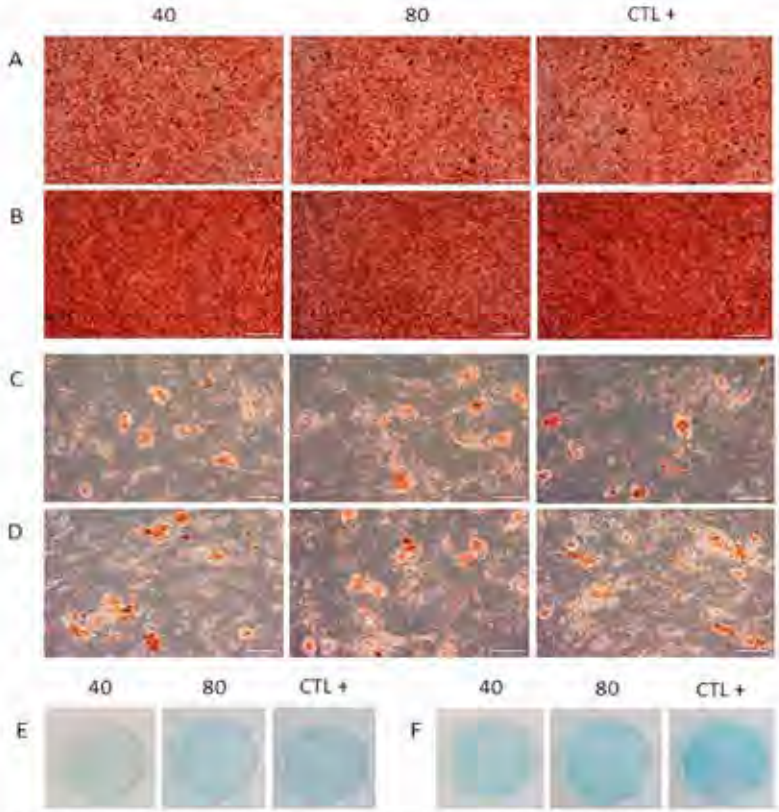

Fig 3. Adipogenic, osteogenic and chondrogenic differentiation after QMR cycles of stimulation. Panels display one representative experiment showing the final outcome in MSC multilineage differentiation after 21 days of induction. QMR-treated (at 40 and 80 nominal powers) and untreated samples (CTL+) were induced to differentiation. Osteogenic differentiation after one cycle (A) and two cycles (B) of QMR stimulation was assessed using Alizarin Red. Adipogenic (C, D) and chondrogenic (E, F) differentiation were detected using Oil Red O and Alcian Blue stainings, respectively. Scale bar = 100 μm. Total magnification = 100x.

https://doi.org/10.1371/journal.pone.0190082.g003

Microarray gene expression analysis after QMR treatment

Based on previous results, we studied the effect of QMR on MSC at transcriptional level by performing cDNA microarray experiments after one cycle of treatment (Day 7). cDNA microarray data pre-processing step reduced the initial number of transcripts from 28,000 to about 12,600. After that, samples were grouped by the similarity of gene expression profiles (doi: 10.6084/m9.figshare.5702137). Not surprisingly, results of clustering showed that samples grouped mainly according to the donor's provenience and not by QMR treatments, as a result of inherent biological variability between analysed MSC batches.

DEG analysis was applied to identify the differences between QMR-treated and sham-exposed MSC samples. Three out of the 16 samples (15 samples + 1 technical replicate) did not meet quality control criteria and therefore were discarded from the subsequent analysis. More transcriptional changes were identified for 40 nominal power than 80 ones. According to a cut-off corrected p-value<0.05, 411 up-regulated and 987 down-regulated genes were found when using 40 as nominal power (Fig 5A). At 80 nominal power, 163 genes were found up-

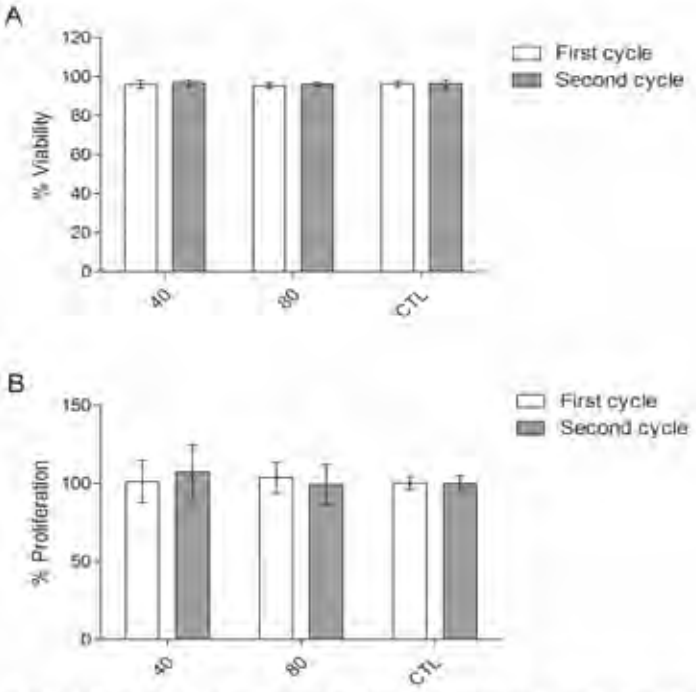

Fig 4. Cellular viability and proliferation after QMR treatment. A) Histograms represent the % of cellular viability after two cycles of QMR treatment at the different settings compared to the sham-exposed controls determined by flow cytometry. Data were shown as mean ± SD of three independent experiments; B) Percentages of cellular proliferation on the controls were obtained by WST-1 assay after 72 hours. Data were represented as mean ± SD of n = 6 independent experiments. No statistical differences were found between conditions.

https://doi.org/10.1371/journal.pone.0190082.g004

regulated while 199 down-regulated (Fig 5B). In both cases, most of the DEGs showed a very low fold change.

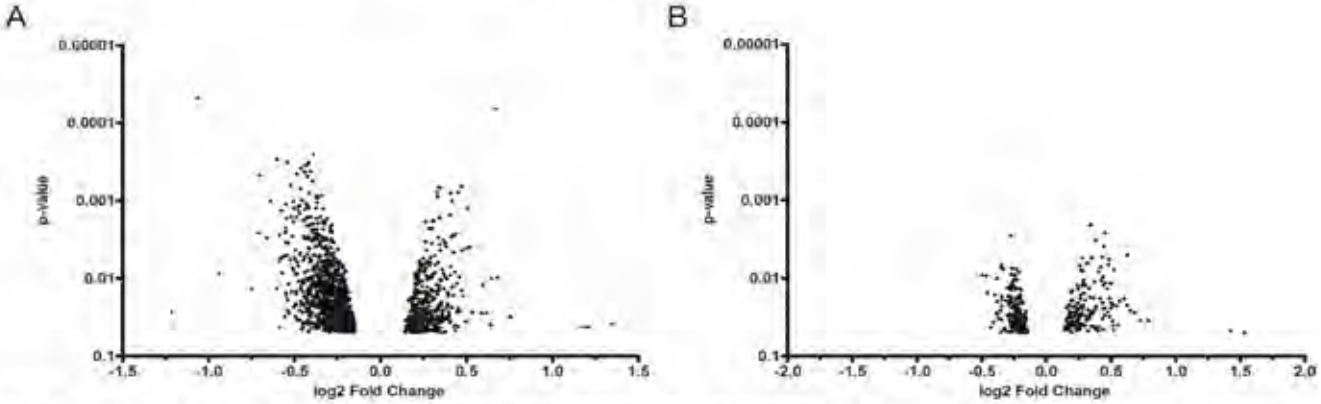

Fig 5. Dot plots of differentially expressed genes associated with QMR treatment at 40 and 80 nominal powers. Images illustrated the distribution of (A) 40 and (B) 80 up- and down-regulated genes (Benjamini & Hochberg correction at $p<0.05$). The results were assessed by comparing QMR-treated MSC (after one cycle of QMR at 40 and 80 nominal powers) with untreated control cultures. The y-axis was in log10 scale.

https://doi.org/10.1371/journal.pone.0190082.g005

To investigate the biological processes and biofunctions in response to QMR stimulation, gene enrichment analysis was performed using ToppGene Suite and IPA tools (Fig 6). The main biological processes up-regulated by 40 nominal power were related to cellular and tissue development, cellular differentiation and vascular system development (Fig 6A and 6C). Positive regulation of protein phosphorylation, vesicle mediated-transport, positive regulation of metabolic processes (Fig 6A), cellular morphology and cell-to-cell interaction biofunctions (Fig 6C) were found down-regulated by the QMR stimulation. Cellular proliferation and movement processes are equally significantly enriched in both gene dataset. The treatment with 80 nominal power showed an enrichment of up-regulated genes related to extracellular matrix organization and down-regulated genes corresponding to membrane protein intracellular domain proteolysis. The latter were identified using ToppGene Suite because IPA did not evidence relevant enrichment lists (S1 Fig).

Assessment of gene expression after 40 QMR stimulation in quantitative real-time PCR

To confirm the gene expression modulation revealed by cDNA microarray analysis, quantitative real-time PCR was carried out in MSC cultures treated at 40 nominal power for one QMR cycle. As shown in Table 1, genes were involved in pathways related to cellular and tissue development, like ECM remodelling, angiogenesis, cellular migration and regulation of actin filaments. Differentially expressed genes obtained by 80 QMR treatment were not further investigated, due to the lower fold change and significance compared to 40 setting.

Our results from six independent experiments, revealed significant increased expression of MMP1, PLAT and ARHGAP22, while A2M gene showed significant decreased expression compared to the controls. By contrast SLIT2, CORO1B, SHC1 and FN1 were not found modulated by QMR treatment, partially confirming cDNA microarray data (Fig 7).

Discussion

We analysed the effects of QMR treatment on MSC *in vitro* at cellular and molecular level.

At the cellular level, we have observed that the treatment with QMR maintained unchanged cell morphology and viability, cell phenotype at least based on cell markers analysis and cell proliferation.

It was evidenced that EMF and electric fields had the capacity to modify cell physiology and signalling pathways altering ion channels, transport protein activation and intracellular ionic concentration [1, 32]. In particular, some authors suggested that EMF affect early stages of differentiation and reduce the time of differentiation [33, 34]. Moreover, Teven and colleagues [35] demonstrated that high-frequency pulsed EMF stimulation augmented osteogenic differentiation. We observed that the ability of MSC exposed to QMR to generate mesodermal tissues *in vitro* was unaltered by the treatment.

To investigate a possible effect of QMR at the transcriptional level, we performed gene expression analysis. As expected for donor-derived cells, cDNA microarray analysis revealed high variability between the different MSC batches. This observation explained the low number of highly significant DEGs between different QMR conditions and controls. DEG analysis also revealed that MSC exposed at 40 QMR setting underwent to more transcriptional changes, suggesting that the treatment at this nominal power is more effective than 80 QMR. In both cases, the relatively low amplitude of the changes confirms the phenotypic observations. The reason because in our experimental setting the 40 stimulation was more effective than 80 remain unclear. In literature there are open questions regarding the mechanism of action of EMF [36]. Since a possible mechanism of action could be related to structural vibrations of

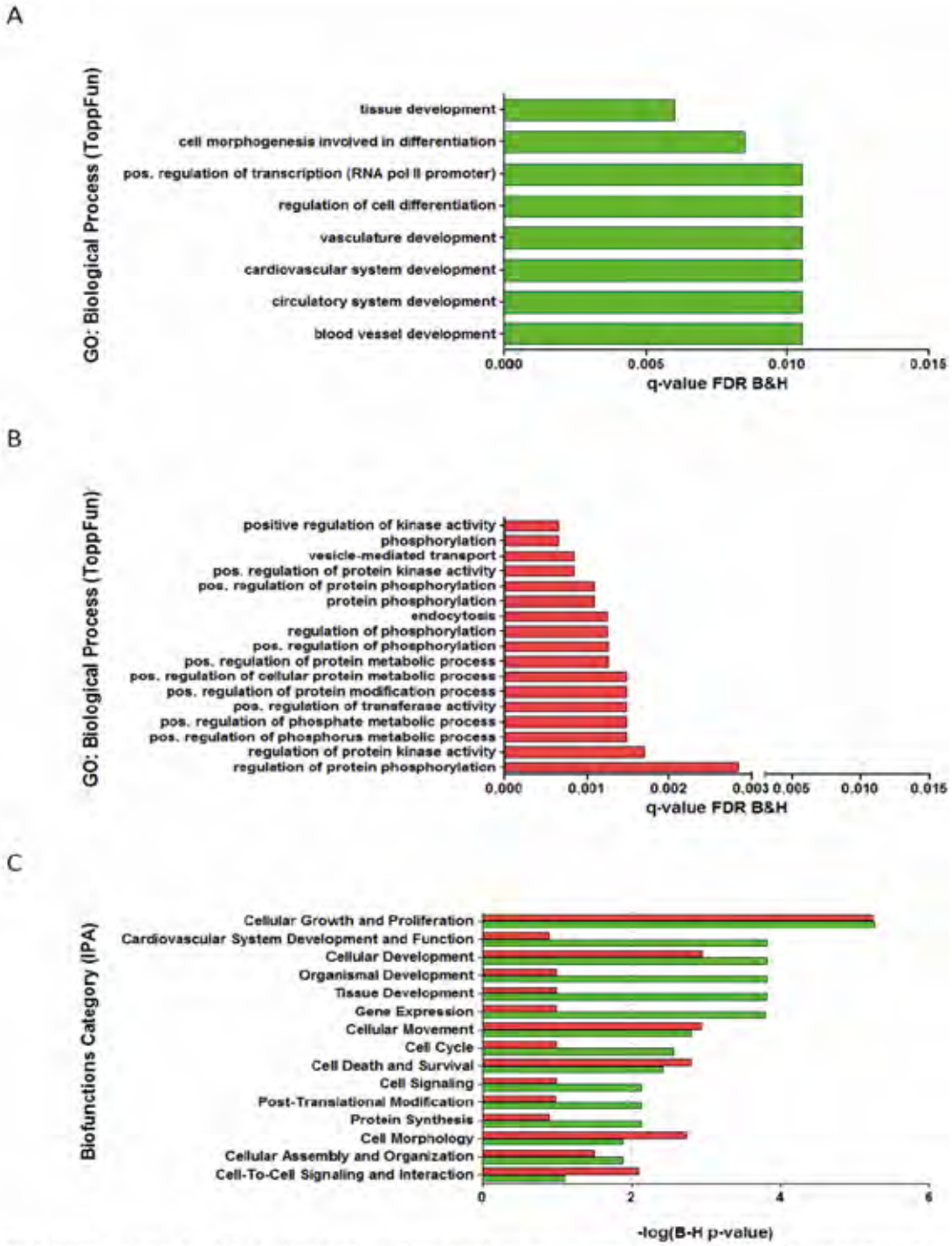

Fig 6. Best enrichment gene lists. Analysis of functional gene enrichment using ToppFun tool (application of ToppGene Suite) for A) up-regulated and B) down-regulated DEG between 40 QMR setting and control with significant enrichment (dotted line) for FDR

B&H q-value <0.01); C) Comparative analysis of up-regulated (green bar) and down-regulated (red bar) functional gene enrichments using IPA software with significant enrichment (dotted line) for -log2 (B-H p-value) >2.

https://doi.org/10.1371/journal.pone.0190082.g006

electrically polar molecules or larger structures, it is likely that a molecule and a biological system could be more responsive to a particular intensity of stimulation in function of its polarity but further studies are necessary to clarify the issue. The gene set enrichment analysis of DEG, performed to understand which main biological processes were involved, revealed that QMR stimulation on MSC cultures affected a lot of different biofunctions. In fact, we found transcriptionally modulated genes related to development processes, regulation of phosphorylation, regulation of cellular pathways including metabolism, kinase activity and cellular organization. The most represented enrichment lists among up-regulated genes were related to cardiovascular system development as also observed by Serena et al [8] with the electrical stimulation of human embryonic stem cells. Sheikh and colleagues [37] showed that electric fields induced the regulation of endothelial antigenic response via MAPK/ERK pathway activation. In particular, our gene by gene analysis also revealed that 40 up- and down-regulated genes were involved in cellular and tissue development processes such as ECM remodelling, angiogenesis, cellular migration and regulation of actin filaments.

The most representative genes for each category were further validated by quantitative real-time PCR on MSC exposed to 40 nominal power after a single QMR cycle. Overall, 50% of them comprising ARHGAP22, MMP1, PLAT and A2M were found significantly modulated compared to controls. ARHGAP22 is a gene expressing a RhoGAP cytoplasmic protein involved in angiogenesis and in the negative regulation of rearrangement of actin filaments through the inhibition of Rac1 [38, 39]. This datum is interesting since some frequencies produced by QMR treatment are inside the endogenous range that affects actin and microtubule filaments [40].

Interestingly, differentially regulated MMP1, PLAT and A2M genes are involved in the ECM remodelling through the fibrinolytic system that is also implicated in embryogenesis, wound healing and angiogenesis [41].

PLAT is a serine protease that converts plasminogen into plasmin where the latter activates other proteases including MMP1 [41]. Neuss and collaborators [42] demonstrated that MSC were able to secrete enzymes involved into this biological pathway and our results showed its promotion by stimulated MSC. In particular, the positive regulation of the two enzymes PLAT (upstream protein) and MMP1 (downstream protein) was in agreement with the negative regulation of the inhibitor of proteases A2M.

Table 1. Selected genes for testing DNA microarray outcomes in quantitative real-time PCR.

Gene name	Systematic name	P-value	Fold change	Protein name	Function
MMP1	NM_002421	0,00007	1,6	Interstitial collagenase	Cleaves collagens of types I, II, and III
PLAT	NM_000930	0,003	1,4	Tissue-type plasminogen activator	Role in tissue remodeling
SLIT2	NM_004787	0,003	1,3	Slit homolog 2 protein	Molecular guidance in cellular migration
ARHGAP22	NM_021226	0,004	1,3	Rho GTPase-activating protein 22	Regulates endothelial cell capillary tube formation
A2M	NM_000014	0,00005	-2,1	Alpha-2-macroglobulin	Inhibitor of proteinases
CORO1B	NM_020441	0,001	-1,4	Coronin-1B	Regulates leading edge dynamics and cell motility
SHC1	NM_183001	0,002	-1,5	SHC-transforming protein 1	Signaling adapter
FN1	NM_054034	0,005	-1,4	Fibronectin	Involved in cell adhesion and motility

The individuated genes took part to biological processes where MSC could have a role in the regenerative support after QMR stimulation.

https://doi.org/10.1371/journal.pone.0190082.t001

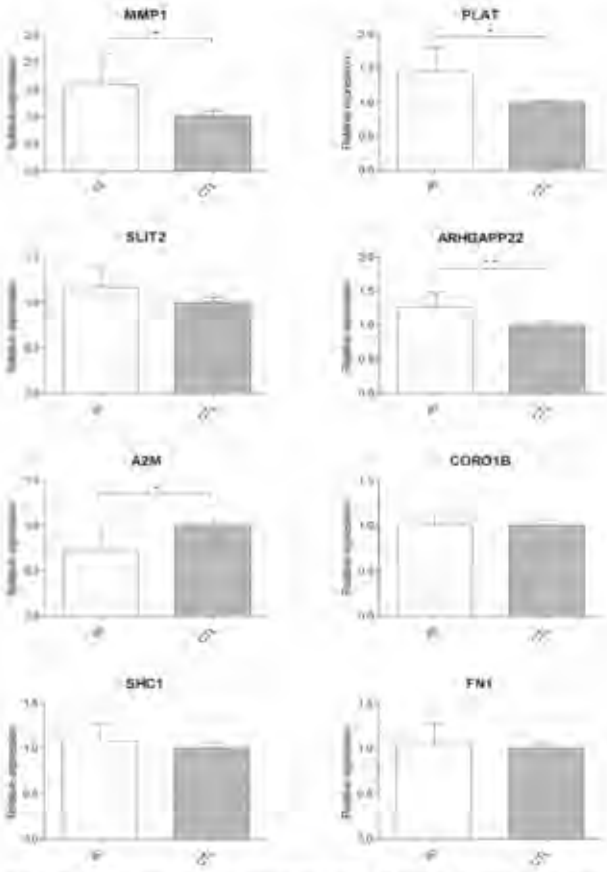

Fig 7. Relative gene expressions using quantitative real-time PCR. Expression of 8 genes selected by cDNA microarray was illustrated after n = 6 independent experiments using TBP as representative reference gene; mean ± SD; * $p<0.05$; ** $p<0.01$.

https://doi.org/10.1371/journal.pone.0190082.g007

Proteases participate in the regulation of angiogenesis through a modulation of an extremely complex process [43] whereas extracellular proteolysis is a requirement for new blood vessel formation. Therefore, matrix metalloproteinases as well as plasminogen activator-plasmin systems play an important role during angiogenesis [44, 45]. Their release allows the bioavailability of factors stored in ECM reservoir [46–48] and PLAT is able to activate PDGF-C [49]. Other studies demonstrated a direct induction of angiogenic factors using electric current [50–52].

In conclusion, our data suggests that in our model QMR-treated MSC maintained unaltered cell phenotype, viability, proliferation and the ability of MSC to differentiate into bone, cartilage and adipose tissue. cDNA microarray analysis may suggest an involvement of some genes after treatment in angiogenesis and in tissue regeneration probably through ECM remodelling. In the present study, donor-to-donor variability may have limited the robustness of microarray data to detect subtle modulation in gene expression profile. However, real-time PCR data validated changes detected in the highly regulated genes in QMR-treated MSC, relatively to the lower setting tested.

Further studies are necessary to confirm our findings both at the protein and at functional level on different cellular models.

Supporting information

S1 Fig. Best enrichment gene lists of up- and down- regulated DEG between 80 QMR setting and control using IPA software. Figure illustrated the comparative analysis of up-regulated (green bar) and down-regulated (red bar) functional gene enrichments using IPA software with significant enrichment (dotted line) for -log2 (B-H p-value) >1.3.
(TIF)

S2 Fig. Relative median fluorescence intensity of MSC markers after QMR stimulation at different settings. A) First cycle of treatment; B) Second cycle of treatment. Bars represented the maximum, median and minimum values of 3 independent experiments. The y-axis was in log10 scale.
(TIF)

Acknowledgments

We are grateful to bone marrow donors for their consent. Thanks also to the physicians and nurses of the Hematology of the S. Bortolo Hospital for bone marrow collection.

We thank Tarcisio Fedrizzi (CIBIO Bioinformatics Core Facility) for helping in the microarray pre-processing analysis. We are also indebted to Davide Pozzato and Alberto Cipullo for the critical discussion of the paper.

Author Contributions

Conceptualization: Sabrina Sella, Giuseppe Astori.

Formal analysis: Sabrina Sella, Valentina Adami, Pamela Gatto.

Funding acquisition: Giuseppe Astori.

Investigation: Sabrina Sella, Valentina Adami, Eliana Amati, Martina Bernardi, Katia Chieregato, Pamela Gatto, Martina Menarin.

Methodology: Sabrina Sella.

Project administration: Giuseppe Astori.

Resources: Sabrina Sella, Alessandro Pozzato, Gianantonio Pozzato.

Supervision: Giuseppe Astori.

Writing – original draft: Sabrina Sella, Giuseppe Astori.

Writing – review & editing: Sabrina Sella, Giuseppe Astori.

References

1. Liu Q, Song B. Electric field regulated signaling pathways. The international journal of biochemistry & cell biology. 2014 Oct; 55:264–8.
2. Taghian T, Narmoneva DA, Kogan AB. Modulation of cell function by electric field: a high-resolution analysis. J R Soc Interface. 2015 Jun; 12(107).
3. Costin GE, Birlea SA, Norris DA. Trends in wound repair: cellular and molecular basis of regenerative therapy using electromagnetic fields. Curr Mol Med. 2012 Jan; 12(1):14–26. PMID: 22082478

4. Fan W, Qian F, Ma Q, Zhang P, Chen T, Chen C, et al. 50 Hz electromagnetic field exposure promotes proliferation and cytokine production of bone marrow mesenchymal stem cells. Int J Clin Exp Med. 2015; 8(5):7394–404. PMID: 26221281
5. Zimmerman JW, Pennison MJ, Brezovich I, Yi N, Yang CT, Ramaker R, et al. Cancer cell proliferation is inhibited by specific modulation frequencies. Br J Cancer. 2012 Jan; 106(2):307–13. https://doi.org/10.1038/bjc.2011.523 PMID: 22134506
6. Stacey M, Fox P, Buescher S, Kolb J. Nanosecond pulsed electric field induced cytoskeleton, nuclear membrane and telomere damage adversely impact cell survival. Bioelectrochemistry. 2011 Oct; 82 (2):131–4. https://doi.org/10.1016/j.bioelechem.2011.06.002 PMID: 21719360
7. Yoon YJ, Li G, Kim GC, Lee HJ, Song K. Effects of 60-Hz time-varying electric fields on DNA damage and cell viability support negligible genotoxicity of the electric fields. JEES. 2015; 15(3):134–41.
8. Serena E, Figallo E, Tandon N, Cannizzaro C, Gerecht S, Elvassore N, et al. Electrical stimulation of human embryonic stem cells: cardiac differentiation and the generation of reactive oxygen species. Exp Cell Res. 2009 Dec; 315(20):3611–9. https://doi.org/10.1016/j.yexcr.2009.08.015 PMID: 19720058
9. Rouabhia M, Park H, Meng S, Derbali H, Zhang Z. Electrical stimulation promotes wound healing by enhancing dermal fibroblast activity and promoting myofibroblast transdifferentiation. PLoS One. 2013; 8(8):e71660. https://doi.org/10.1371/journal.pone.0071660 PMID: 23990967
10. Maioli M, Rinaldi S, Santaniello S, Castagna A, Pigliaru G, Gualini S, et al. Radiofrequency energy loop primes cardiac, neuronal, and skeletal muscle differentiation in mouse embryonic stem cells: a new tool for improving tissue regeneration. Cell Transplant. 2012; 21(6):1225–33. https://doi.org/10.3727/096368911X600966 PMID: 21975035
11. Zhao Z, Watt C, Karystinou A, Roelofs AJ, McCaig CD, Gibson IR, et al. Directed migration of human bone marrow mesenchymal stem cells in a physiological direct current electric field. Eur Cell Mater. 2011 Nov; 22:344–58. PMID: 22125259
12. Tandon N, Goh B, Marsano A, Chao PH, Montouri-Sorrentino C, Gimble J, et al. Alignment and elongation of human adipose-derived stem cells in response to direct-current electrical stimulation. Conf Proc IEEE Eng Med Biol Soc. 2009; 2009:6517–21. https://doi.org/10.1109/IEMBS.2009.5333142 PMID: 19964171
13. Zhang J, Ren R, Luo X, Fan P, Liu X, Liang S, et al. A small physiological electric field mediated responses of extravillous trophoblasts derived from HTR8/SVneo cells: involvement of activation of focal adhesion kinase signaling. PLoS One. 2014; 9(3):e92252. https://doi.org/10.1371/journal.pone.0092252 PMID: 24643246
14. Gómez-Ochoa I, Gómez-Ochoa P, Gómez-Casal F, Cativiela E, Larrad-Mur L. Pulsed electromagnetic fields decrease proinflammatory cytokine secretion (IL-1β and TNF-α) on human fibroblast-like cell culture. Rheumatol Int. 2011 Oct; 31(10):1283–9. https://doi.org/10.1007/s00296-010-1488-0 PMID: 20372910
15. Vianale G, Reale M, Amerio P, Stefanachi M, Di Luzio S, Muraro R. Extremely low frequency electromagnetic field enhances human keratinocyte cell growth and decreases proinflammatory chemokine production. Br J Dermatol. 2008 Jun; 158(6):1189–96. https://doi.org/10.1111/j.1365-2133.2008.08540.x PMID: 18410412
16. Jennings J, Chen D, Feldman D. Transcriptional response of dermal fibroblasts in direct current electric fields. Bioelectromagnetics. 2008 Jul; 29(5):394–405. https://doi.org/10.1002/bem.20408 PMID: 18302142
17. Lee HC, Hong MN, Jung SH, Kim BC, Suh YJ, Ko YG, et al. Effect of extremely low frequency magnetic fields on cell proliferation and gene expression. Bioelectromagnetics. 2015 Oct; 36(7):506–16. https://doi.org/10.1002/bem.21932 PMID: 26239017
18. Messerli MA, Graham DM. Extracellular electrical fields direct wound healing and regeneration. Biol Bull. 2011 Aug; 221(1):79–92. https://doi.org/10.1086/BBLv221n1p79 PMID: 21876112
19. D'Eredità R, Bozzola L. Molecular resonance vs. coblation tonsillectomy in children. Laryngoscope. 2009 Oct; 119(10):1897–901. https://doi.org/10.1002/lary.20210 PMID: 19598217
20. Chang H, Hah JH. Comparison of post-tonsillectomy pain with two different types of bipolar forceps: low temperature quantum molecular resonance device versus high temperature conventional electrocautery. Acta Otolaryngol. 2012 Jun; 132 Suppl 1:S130–3.
21. Schiavon M, Calabrese F, Nicotra S, Marulli G, Pozzato G, Giacometti C, et al. Favorable tissue effects of quantum molecular resonance device (Vesalius) compared with standard electrocautery. A novel paradigm in lung surgery. Eur Surg Res. 2007; 39(4):222–8. https://doi.org/10.1159/000101745 PMID: 17438358
22. Dal Maschio M, Canato M, Pigozzo FM, Cipullo A, Pozzato G, Reggiani C. Biophysical effects of high frequency electrical field (4–64 MHz) on muscle fibers in culture. Basic Applied Miology. 2009; 19 (1):49–56.

23. Lopresti M, Tomba A, Caserta A, Di Dimenica F. Effectiveness of molecular quantum resonance in reducing edema after total knee arthroplasty: a clinical trial. Arch Ortop Reumatol. 2011; 122(1):34–5.
24. Murphy MB, Moncivais K, Caplan AI. Mesenchymal stem cells: environmentally responsive therapeutics for regenerative medicine. Exp Mol Med. 2013 Nov; 45:e54. https://doi.org/10.1038/emm.2013.94 PMID: 24232253
25. Rubio-Azpeitia E, Andia I. Partnership between platelet-rich plasma and mesenchymal stem cells: in vitro experience. Muscles Ligaments Tendons J. 2014 Jan; 4(1):52–62. PMID: 24932448
26. Dominici M, Le Blanc K, Mueller I, Slaper-Cortenbach I, Marini F, Krause D, et al. Minimal criteria for defining multipotent mesenchymal stromal cells. The International Society for Cellular Therapy position statement. Cytotherapy. 2006; 8(4):315–7. https://doi.org/10.1080/14653240600855905 PMID: 16923606
27. Aggarwal S, Pittenger MF. Human mesenchymal stem cells modulate allogeneic immune cell responses. Blood. 2005 Feb 15; 105(4):1815–22. https://doi.org/10.1182/blood-2004-04-1559 PMID: 15494428
28. Uccelli A, Moretta L, Pistoia V. Immunoregulatory function of mesenchymal stem cells. Eur J Immunol. 2006 Oct; 36(10):2566–73. https://doi.org/10.1002/eji.200636416 PMID: 17013987
29. Chen Y, Xiang L- X, Shao J- Z, Pan R- L, Wang Y- X, Dong X- J, et al. Recruitment of endogenous bone marrow mesenchymal stem cells towards injured liver. Journal of Cellular and Molecular Medicine. 2010; 14(6b):1494–508. https://doi.org/10.1111/j.1582-4934.2009.00912.x PMID: 19780871
30. Ritchie ME, Phipson B, Wu D, Hu Y, Law CW, Shi W, et al. limma powers differential expression analyses for RNA-sequencing and microarray studies. Nucleic Acids Res. 2015 Apr; 43(7):e47. https://doi.org/10.1093/nar/gkv007 PMID: 25605792
31. Livak KJ, Schmittgen TD. Analysis of relative gene expression data using real-time quantitative PCR and the 2(-Delta Delta C(T)) Method. Methods. 2001 Dec; 25(4):402–8. https://doi.org/10.1006/meth.2001.1262 PMID: 11846609
32. Sundelacruz S, Levin M, Kaplan DL. Membrane potential controls adipogenic and osteogenic differentiation of mesenchymal stem cells. PLoS One. 2008; 3(11):e3737. https://doi.org/10.1371/journal.pone.0003737 PMID: 19011685
33. Sun LY, Hsieh DK, Lin PC, Chiu HT, Chiou TW. Pulsed electromagnetic fields accelerate proliferation and osteogenic gene expression in human bone marrow mesenchymal stem cells during osteogenic differentiation. Bioelectromagnetics. 2010 Apr; 31(3):209–19. https://doi.org/10.1002/bem.20550 PMID: 19866474
34. Esposito M, Lucanello A, Riccio I, Riccio V, Esposito V, Riccardi G. Differentiation of human osteoprogenitor cells increases after treatment with pulsed electromagnetic fields. In Vivo. 2012 2012 Mar-Apr; 26(2):299–304. PMID: 22351673
35. Teven CM, Greives M, Natale RB, Su Y, Luo Q, He BC, et al. Differentiation of osteoprogenitor cells is induced by high-frequency pulsed electromagnetic fields. J Craniofac Surg. 2012 Mar; 23(2):586–93. https://doi.org/10.1097/SCS.0b013e31824cd6de PMID: 22446422
36. Kučera O, Cifra M. Radiofrequency and microwave interactions between biomolecular systems. Journal of Biological Physics. 2016; 42(1):1–8. https://doi.org/10.1007/s10867-015-9392-1 PMID: 26174548
37. Sheikh AQ, Taghian T, Hemingway B, Cho H, Kogan AB, Narmoneva DA. Regulation of endothelial MAPK/ERK signalling and capillary morphogenesis by low-amplitude electric field. J R Soc Interface. 2013 Jan; 10(78):20120548. https://doi.org/10.1098/rsif.2012.0548 PMID: 22993248
38. Marinković G, Heemskerk N, van Buul JD, de Waard V. The Ins and Outs of Small GTPase Rac1 in the Vasculature. J Pharmacol Exp Ther. 2015 Aug; 354(2):91–102. https://doi.org/10.1124/jpet.115.223610 PMID: 26036474
39. Mori M, Saito K, Ohta Y. ARHGAP22 localizes at endosomes and regulates actin cytoskeleton. PLoS One. 2014; 9(6):e100271. https://doi.org/10.1371/journal.pone.0100271 PMID: 24933155
40. Cifra M, Fields JZ, Farhadi A. Electromagnetic cellular interactions. Prog Biophys Mol Biol. 2011 May; 105(3):223–46. https://doi.org/10.1016/j.pbiomolbio.2010.07.003 PMID: 20674588
41. Heissig B, Dhahri D, Eiamboonsert S, Salama Y, Shimazu H, Munakata S, et al. Role of mesenchymal stem cell-derived fibrinolytic factor in tissue regeneration and cancer progression. Cell Mol Life Sci. 2015 Dec; 72(24):4759–70. https://doi.org/10.1007/s00018-015-2035-7 PMID: 26350342
42. Neuss S, Schneider RK, Tietze L, Knüchel R, Jahnen-Dechent W. Secretion of fibrinolytic enzymes facilitates human mesenchymal stem cell invasion into fibrin clots. Cells Tissues Organs. 2010; 191(1):36–46. https://doi.org/10.1159/000215579 PMID: 19390164
43. Roy R, Zhang B, Moses MA. Making the cut: protease-mediated regulation of angiogenesis. Exp Cell Res. 2006 Mar; 312(5):608–22. https://doi.org/10.1016/j.yexcr.2005.11.022 PMID: 16442099

44. Pepper MS. Role of the matrix metalloproteinase and plasminogen activator-plasmin systems in angiogenesis. Arterioscler Thromb Vasc Biol. 2001 Jul; 21(7):1104–17. PMID: 11451738

45. Nam HS, Kwon I, Lee BH, Kim H, Kim J, An S, et al. Effects of Mesenchymal Stem Cell Treatment on the Expression of Matrix Metalloproteinases and Angiogenesis during Ischemic Stroke Recovery. PLoS One. 2015; 10(12):e0144218. https://doi.org/10.1371/journal.pone.0144218 PMID: 26637168

46. Park JE, Keller GA, Ferrara N. The vascular endothelial growth factor (VEGF) isoforms: differential deposition into the subepithelial extracellular matrix and bioactivity of extracellular matrix-bound VEGF. Mol Biol Cell. 1993 Dec; 4(12):1317–26. PMID: 8167412

47. Whitelock JM, Murdoch AD, Iozzo RV, Underwood PA. The degradation of human endothelial cell-derived perlecan and release of bound basic fibroblast growth factor by stromelysin, collagenase, plasmin, and heparanases. J Biol Chem. 1996 Apr; 271(17):10079–86. PMID: 8626565

48. Bonnans C, Chou J, Werb Z. Remodelling the extracellular matrix in development and disease. Nat Rev Mol Cell Biol. 2014 Dec; 15(12):786–801. https://doi.org/10.1038/nrm3904 PMID: 25415508

49. Fredriksson L, Li H, Fieber C, Li X, Eriksson U. Tissue plasminogen activator is a potent activator of PDGF-CC. EMBO J. 2004 Oct; 23(19):3793–802. https://doi.org/10.1038/sj.emboj.7600397 PMID: 15372073

50. Kim IS, Song JK, Zhang YL, Lee TH, Cho TH, Song YM, et al. Biphasic electric current stimulates proliferation and induces VEGF production in osteoblasts. Biochim Biophys Acta. 2006 Sep; 1763(9):907–16. https://doi.org/10.1016/j.bbamcr.2006.06.007 PMID: 16930744

51. Bai H, Forrester JV, Zhao M. DC electric stimulation upregulates angiogenic factors in endothelial cells through activation of VEGF receptors. Cytokine. 2011 Jul; 55(1):110–5. https://doi.org/10.1016/j.cyto.2011.03.003 PMID: 21524919

52. Asadi MR, Torkaman G, Hedayati M, Mofid M. Role of sensory and motor intensity of electrical stimulation on fibroblastic growth factor-2 expression, inflammation, vascularization, and mechanical strength of full-thickness wounds. J Rehabil Res Dev. 2013; 50(4):489–98. PMID: 23934870

14

Biophysical effects of high frequency electrical field (4-64 MHz) on muscle fibers in culture

M. Dal Maschio, M. Canato, F. M. Pigozzo, A. Cipullo, G. Pozzato, C. Reggiani

BAM

Basic and Applied Myology

European Journal Of Translational Myology

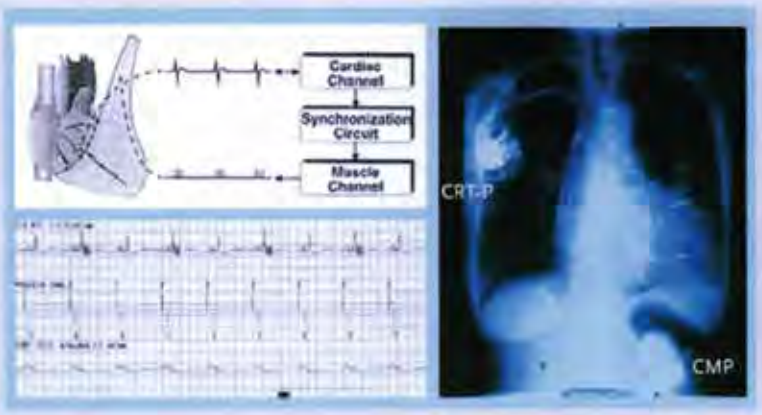

Vol. 19 (1) 2009

UNIPRESS

BAM On-Line

http://www.bio.unipd.it/bam

Biophysical effects of high frequency electrical field (4-64 MHz) on muscle fibers in culture

Marco Dal Maschio (1,2), Marta Canato (1), Filippo M. Pigozzo (3), Alberto Cipullo (4), GianAntonio Pozzato (4), Carlo Reggiani (1)

(1) Department of Anatomy and Physiology, University of Padova; (2) IIT, Italian Institute of Technology, Genova; (3) Department of Information Engineering, University of Padova; (4) Telea srl. Quinto Vicentino, Italy

Abstract

Effects of oscillating electrical fields on living cells depend on the frequency. Electrical field oscillating in the range of MHz can induce cell membrane deformation which may end in cell damage or stimulation. The issue has been studied in red blood cells, but never in excitable cells. In this study we investigated the behaviour of murine muscles and single muscle fibers exposed in vitro to an oscillating electrical field in the MHz range. The commercial set-up Rexonage ™ (Telea srl), providing a particular frequency spectrum in the range 4-64MHz that is patented as "quantum molecular resonance stimulation", was used as a generator of electrical field and a wide range of powers was examined. Muscles or muscle fibers were placed on the bottom of Petri dishes and electrical field was applied between a needle electrode immersed in the medium and movable by means of a micromanipulator and an electrode placed under the bottom of the dish. While high power stimulation produced a fast and well localized cut of the fibers, low power stimulation caused a reversible deformation of the membrane. Such deformation was accompanied by a membrane depolarization and an increase of cytosolic free calcium, which were detected with fluorescent probes. Both the changes of membrane potential and the variations of free calcium concentration strictly followed the time course of electrical field application and removal. In conclusion, the present results demonstrate that excitable cells, such as muscle fibers, respond to the application of high frequency electrical field even when the threshold for action potential is not reached. This might lead to the activation of intracellular signalling pathways even without contraction.

Key Words: High frequency electrical field, membrane potential, cytosolic calcium, muscle fibers

Basic Applied Myology 18 (6): xxx-xxx, 2008

The behaviour of biological materials exposed to electromagnetic fields has become a growing research area in the last years. The interest is stimulated by the variety of frequency-dependent phenomena occurring in the biological tissues that are commonly explained from a theoretical point of view in terms of dielectric dispersion models [7]. The studies are mainly focused on the characterization of the responses of different cell kinds [7, 12] and to possible implications in diagnostic and applications to cell-manipulation [16].

The dispersion phenomena are commonly classified as α-dispersion, β-dispersion and γ-dispersion depending on the corresponding frequency spectrum of the underlying physical processes [1]. The α-dispersion is related to dielectric relaxation of free water and occurs in the range of GHz. The β-dispersion occurs in frequency region between 10 kHz and 100 MHz and is well explained by structural polarization phenomena or the so-called Maxwell-Wagner effect, involving the cytoplasm, the plasma membrane and the surrounding extracellular medium [8]. The γ-dispersion occurs in the range 100 Hz-10 kHz and is related with the variation of the cell membrane capacitance.

Taking advantage from the effects induced by the alternating field stimulation [11], such as the dipole generation leading to cell displacement and to cell deformation, a number of investigations have been carried out on the structural characterization of the cell components [10]. The viscoelastic properties of the cell membrane have been studied in erythrocytes immersed in an oscillating electrical field [5, 6] and applications of these phenomena were developed in order to fabricate devices for cell screening based on dielectrophoretic mechanisms [2, 13]. Some other

studies have considered AC (Alternating Current) stimulation as a mean to break the membrane structure in electrofusion and cell poration experiments not only from the point of view of the dielectrophoretic deformation [15] but also from the point of view of the transmembrane potential variations induced during AC field application [14].

In the present report, we focused mainly onto the effects induced by non uniform low power AC stimulation with high (MHz) frequencies on a specific kind of biological models: muscles and muscle fibers. Taking into account the excitability of these cells, the experiments have examined the physiological effects of the AC stimulation in terms of fluctuations of the trans-membrane potential and alterations of cytoplasmic calcium concentration. The high frequency stimulation was also directly compared on the same preparations with the classical bipolar field stimulation obtained with two platinum electrodes and able to elicit action potentials, calcium transients and contractions.

Materials and Methods

Muscle Tissues and Cells Preparation Protocol

Experiments were carried out on murine adult muscle fibers enzymatically dissociated and kept in culture as described by [4]. Mice were killed by cervical dislocation and Flexor Digitorum Brevis (FDB) muscle was dissected out and placed in Tyrode solution (NaCl 140 mM; KCl 2 mM; CaCl2 0.5 mM; MgCl2 2 mM; HEPES 10 mM; glucose 5 mM) containing 0.2% type I collagenase and 10% fetal bovine serum (FBS) for 1 hour at 4°C and then for 1 hour at 37°C. After several washes in Tyrode solution containing 10% FBS to block the collagenase effect and stabilize the fibers, the muscle was gently dissociated through a Pasteur pipette with a large opening in a glass falcon test tube to obtain single fibers. Isolated fibers were plated on cover slips covered with mouse laminin, which produced fiber attachment within 1 hour. Fibers were maintained in Tyrode solution supplemented with 10% FBS and 1% penicillin-streptomycin in an incubator, with 5% CO2 at 36.5 °C and used for experiments on the second day after dissociation.

Few experiments were carried on whole murine Extensor Digitorum Longus (EDL) muscles freshly dissected from the leg and immediately pinned at both ends on the bottom covered with Silgard of a Petri dish filled with oxygenated Krebs solution.

The use of the animals and the experimental protocol was approved by the Department Ethical Committee. All efforts were made to minimize animal suffering and to use only the number of animals strictly necessary to obtain reliable data.

Experimental Setup

The experimental setup was designed to generate the oscillating electric field around single muscle fibers or EDL muscles placed inside a Petri dish. A commercial stimulator (Rexonage™, Telea), representing the edge technology applied in many surgical and medical tasks, was adopted because of its own peculiar range of stimulation frequency. In fact the stimulator output signal is a periodic sinusoidal signal with a particular harmonic spectrum in the range between 4 and 64 MHz as patented by TELEA s.r.l. as "quantum molecular resonance stimulation". The amplitude ranges from few Volts to about 1 kVolts depending on the power setting. A detailed characterization of the output signal amplitude as function of the power settings was performed in order to evaluate the electric field intensity induced in the extracellular environment. The stimulation protocol envisaged the application of the electric field between a Pt microelectrode of 65 µm diameter, immersed in the perfusing medium very close (<100µm) to the membrane surface, and the bottom side of the culture dish in contact with a ground reference plate in order to close the current pathway. The microelectrode holder was mounted on a 3-axis stepper manipulator stage which allowed the fine control the positioning of the electrode tip in relation to the cell membrane with the help of a stereo-microscope. A simulation of the spatial properties of the stimulation field, generated with the electrode dipped in the perfusion medium (with known dielectric constant and conductivity parameters) at different distances and tilting angles with the muscle fiber surface, was developed. The simulation is shown in Figure 1 and allows the evaluation of the concentration of the electric field and its maximum spatial extension.

Optical Microscopy

A custom upright stereo-microscope from a Mytutoyo stage with very long working distance objectives (10X, 20X and 50X) was used with visible light illumination either for imaging selected regions of isolated muscle or single FDB fibers before, during and after stimulation sessions. By means of a monochromatic camera (SONY-CCD) and video capturing DAQ board installed in a PC, movies of the cell fibers were recorded and digitized. Imaging data analysis was carried out by means of ImageJ software.

Fluorescent Probes and Microscopy

The effects of the stimulation on physiological parameters, cytosolic calcium concentration and membrane potential, were studied by means of fluorescent dyes that change their fluorescence intensity in response to calcium ion binding or to a change in membrane potential. For cytosolic calcium imaging, cell permeant AM ester Fluo4 (F14201, Molecular Probes) was diluted with a concentration of 3µM into the cell loading buffer (125mM NaCl, 5mM KCl, 1mM MgSO4, 1mM KH2PO4, 5,5mM glucose, 1mM CaCl2, 20mM HEPES and 1% BSA). After 30 min loading phase at 37° C, cells were incubated in loading solution

without BSA and Fluo4 for 10 min at 37°C and then the cover-glass was mounted in the imaging chamber. To record transmembrane potential variations, FDB fibers were immersed for 60 min in 4μM Di-8-ANEPPS (D3167, Molecular Probes) dissolved in the loading buffer in order to obtain a homogeneous binding to the cell membrane. The fluorescence imaging setup was composed by a Nikon TE2000 inverted research microscope with a 60X APO TIRF NA1.45 oil immersion objective and a 20X NA 0.8 dry objective. All the imaging data were acquired using a Hamamatsu ImageM back-tinned multiplying camera controlled by the Nikon NIS Advanced Research software and by the Hamamatsu proprietary software Wasabi. The fluorescence filter configuration for Di-8-ANEPPS imaging was based on a 488/30nm excitation filter, a 505nm dicroic mirror and a 590nm long-pass emission filter; for Fluo4 was similar except for the emission filter which was replaced with a 535/50nm. The experimental protocol aimed to compare in the same cell the membrane potential changes/calcium transients obtained with high frequency stimulation electrode with the responses obtained with normal field stimulation with supramaximal 30V square bipolar single stimuli.

Results

Simulation of the High Frequency Electrical Field

The spatial distribution of the high frequency (MHz) electrical field of stimulation in a physical system composed by a Pt electrode, an extracellular medium and a perspex substrate was studied with a computer simulation. Simulation, calculated for stimulation frequency of 4MHz, showed that, because of the particular shape and dimensions of the electrode, the volume interested by the stimulation was very confined (Figure 1).

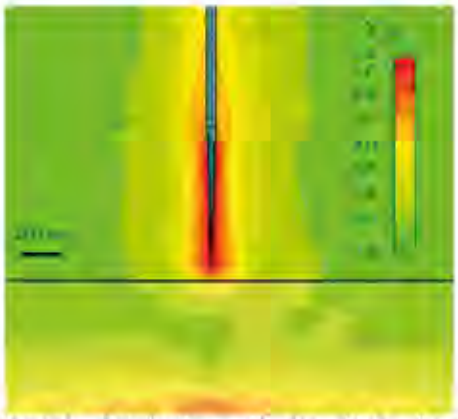

Fig. 1 *Spatial distribution of the high frequency electrical field. The black horizontal line represents the bottom of the petri dish where a second plate electrode is placed. The magnitude of the field is represented by means of a normalized pseudocolor scale.*

At an average distance of 80 μm from the electrode, the absolute value of the induced electric field was about 30% of its maximum value and decrease to 6% at a distance from the tip of 200 μm. Beside the confinement, simulation predicted a very high degree of polarization of the electric field, which is mainly directed along the electrode longitudinal axis (Figure 1). Actually, the transversal components reached at their maximum only the 40% of the longitudinal values, also when the tilting angle was reduced from 90° to lower values.

Effects of MHz Electrical Field on Muscle Fibers in Relation to Power Applied

Taking into account the shape and the polarization of the electrical field predicted by the simulation and exploiting the fine control of the electrode positioning allowed by the micromanipulator, the electrode tip was placed at optimal distance from the cell membrane.

During low power experiments, the tip was located at about 50 μm from the membrane surface, while in higher power experiments, conducted to induce cell permanent morphological changes, the tip was placed even more close to the cell membrane. The power settings corresponded to applied peak-to-peak voltage amplitude in the range of 500V-800V in the high power configuration and in the range 100V-400V in the low power one. The effects on the muscle cells caused by high power and low power application of the electrical field (thereafter indicated as stimulation) were very different and are shown in Figures 2-4.

High power stimulation with the electrode perpendicularly placed 100 μm apart from the membrane caused disorganization in the muscle scaffold with permanent changes in shape and position of the fibers previously aligned along the longitudinal muscle axis. If the tip was more close to the membrane, muscle fibers were transversally cut in a position corresponding to the electrode tip with a background particle chaotic movement (Figure 2).

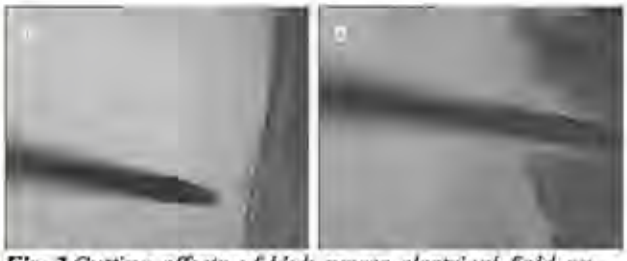

Fig. 2 *Cutting effects of high power electrical field on muscle fibers. Panel A shows the electrode placed perpendicular to the muscle surface before electrical field is applied. Panel B shows the cut produced by high frequency high power electrical field. Note the sharp cut of individual fibers.*

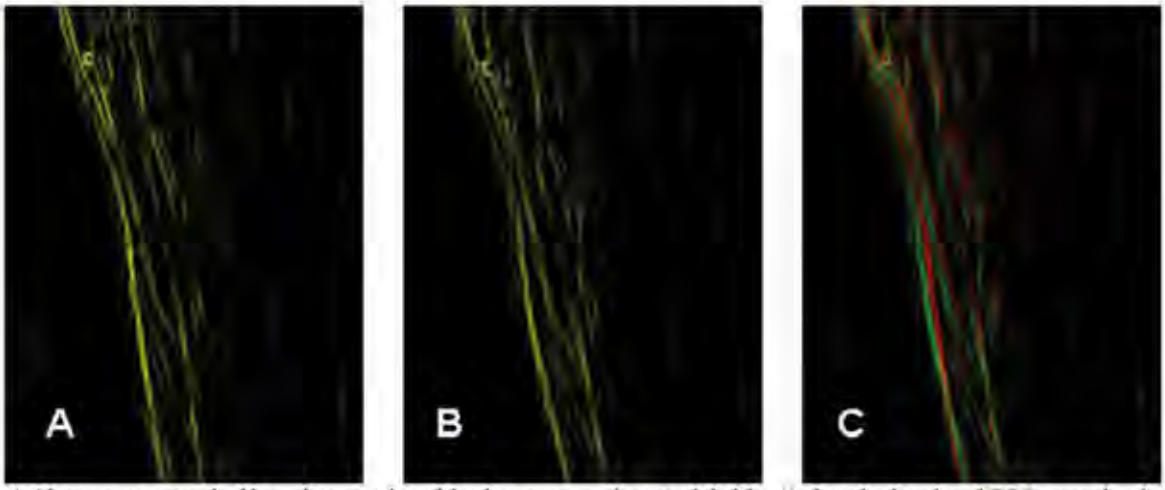

Fig. 3 Changes in muscle fiber shape induced by low power electrical field . A) detail of isolated EDL muscle close to the electrode before stimulation, B) the same region during stimulation, C) merge of the two images : A in red and B in green. Changes in shape of individual fibers are detectable by means after the processing of the images with a "find edge algotithm".

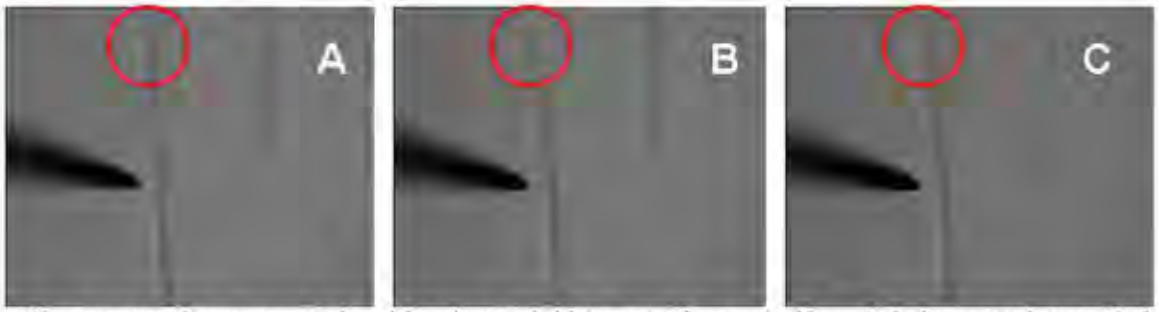

Fig. 4 Slow contractile response induced by electric field in a single muscle fiber. A) before stimulation, B) during stimulation, C) after stimulation. The electrical field was applied for 500 ms (stimulation).

Fig. 5 Migration of particles inside the electrical field during stimulation. A group of three particles are visible close to the tip of the electrode on the left side and a single fiber on the right side. The relative changes in position are detectable by eye comparing the three images taken at subsequent times.

The damage in the fiber membrane morphology was restricted to a small (about 150 µm diameter) region approximately centered around the tip of the electrode, thus corresponding to the predicted size of the electrical field (compare with Figure 1). The surrounding regions appeared almost completely unaffected, thus confirming the extraordinarily confined cut effect.

The low power setting with the tip 50 µm apart the muscle surface induced on the muscles and muscle fibers transient effects that completely disappeared after the end of the stimulation phase. During stimulation, muscle fibers showed a movement reminiscent of a slow contraction (Figure 4). Also in this case, the response was restricted to the limited region of the muscle more close to the electrode tip,

and it was characterized by a contraction phase corresponding to the duration of the stimulation (500ms) followed by a relaxation phase after the end of the stimulation. The same phenomenon with similar temporal features was detectable also in single dissociated muscle fibers where a change in shape, again reminiscent of a slow contraction, occurred in the fiber region nearest to the electrode tip while leaving the rest of the fiber unmodified (Figure 4).

As an additional consequence of the electrical field, non-adherent cells that populate the culture dishes were induced to move and showed a slow continuous movement during stimulation approaching the electrode tip (Figure 5).

Fluorescence Microscopy Reveals Mechanisms Underlying the Cell Change in Shape

The physiological changes induced by the stimulation in muscle fibers were studied by means of fluorescent probes. The parameters analyzed were transmembrane potential monitored by means of Di-8-ANEPPS staining of the fibers, and cytosolic calcium ion concentration monitored with a Fluo4 labeling. For both parameters, a comparison was carried out with the changes induced by classical supra-threshold bipolar stimulation with two electrodes able to induce action potential and trigger contraction.

1. Membrane potential changes during stimulation

Classical single pulse field stimulation induced a change in membrane potential which was very fast, close to the limits of time resolution of the detection system, based on fluorescent light emission of Di-8-ANEPPS and video camera recording. Such fast changes are shown in Figure 6A and likely correspond to action potentials as also confirmed by the accompanying transient change in calcium concentration (see below).

The high frequency and low power stimulation determined slow membrane potential change which lasted for the whole duration of the stimulation phase and was followed by a slow reversal in the interval after the end of the stimulation (Figure 6B). The amplitude of the total change recorded for the membrane potential was about 8% in the membrane region closest to the electrode tip and decreased progressively along the fiber as illustrated in the Figure 7. Thus, with the high frequency stimulation, the cell membrane appeared to go through a charging process toward a steady state level during the stimulation phase, after that the potential slowly returned to its initial level.

2. Cytosolic calcium concentration changes during stimulation

Classical single pulse field stimulation, leading to a fast variation of the membrane potential as described above, triggered the voltage dependent process of calcium release from the sarcoplasmic reticulum and induced a rise in cytosolic calcium concentration. The time course of this process was totally independent of the stimulation timing and lasted about one hundred milliseconds, with a fast rising phase (<20ms) and a slower (<100ms) decay phase as shown in Figure 8A. From a spatial point of view, the process involved the whole muscle fiber, from one end to the other one, so allowing the activation of contraction along the fiber.

High frequency stimulation showed the peculiar property to focus its effects on a limited region of the fiber, inducing increase of calcium concentration mainly in the segments facing the stimulation electrode with a progressively decaying effect along the fiber as shown in Figure 9.

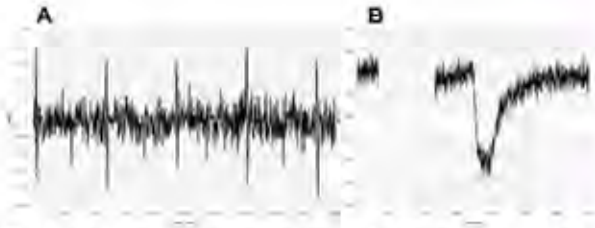

***Fig. 6** Change in membrane potential as monitored by fluorescence of Di-8-ANEPPS. A) Fast changes related to single pulse stimulation, likely corresponding to action potential. B) Long lasting change due to application of high frequency low power electrical field. On the abscissa a small division corresponds to 40 ms in A and 100 ms in B*

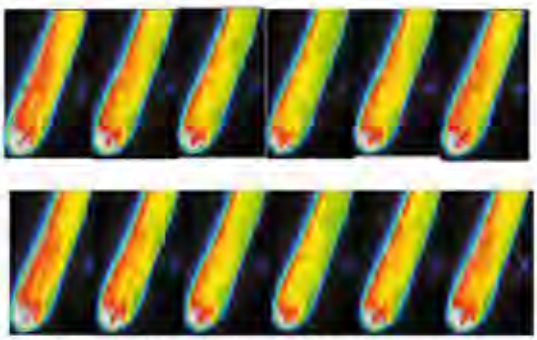

***Fig. 7** Spatial distribution of the changes in fluorescent light emission of a muscle fiber loaded with Di-8-ANEPPS to optically monitor membrane potential before, during and after AC stimulation. The blue spot indicates the position of the electrode. Changes in potential are proportional to emitted green light.*

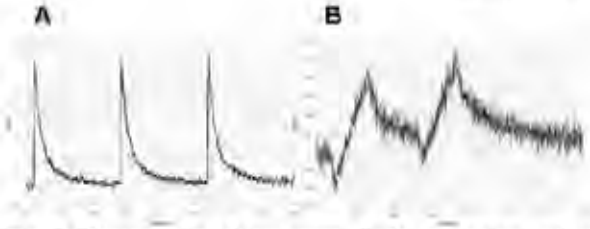

Fig. 8 Changes in fluorescent light emission of a muscle fiber loaded with Fluo4 to optically monitor cytosolic free calcium concentration. A) Changes determined by single pulse bipolar stimulation, likely corresponding to transients following action potentials. B) Slow and low amplitude changes induced by high frequency low power electrical field application. A small division on the abscissa corresponds to 40 ms on A and 100 ms on B

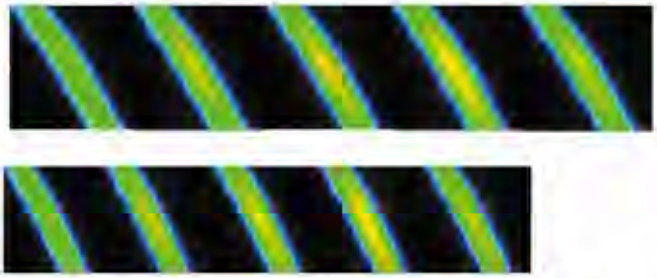

Fig. 9 Spatial distribution of the changes in fluorescent light emission of fibers loaded with Fluo4 to optically monitor cytosolic free calcium concentration. A region of the fiber close to the electrode (not visible) is shown in sequential images. Calcium concentration is proportional to the emitted red light.

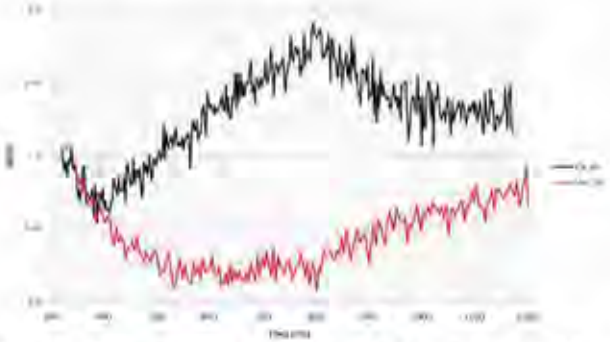

Fig. 10 Time course of the fluorescent signals corresponding to membrane potential (red) and cytosolic calcium concentration (black) during the application of the high frequency low power electrical field for 500 ms, starting at 350 ms. Note that the electrical field induces a slow depolarization which is accompanied by a slow and continuous increase of calcium concentration.

The time course of the increase of calcium concentration was also completely different from that produced by bipolar stimulation as, after the onset of the stimulation, a fast initial deflection in the fluorescence signal was followed by a continuous almost linear rising phase in the fluorescence signal lasting for the duration of the stimulation. A recovery phase with a decrease in the fluorescent signal was detected after the stimulation end, as shown in Figure 8B. The amplitude of the fluorescent signal was also very different as it reached a 50% increase for the bipolar stimulation and only a 10% with the high frequency stimulation. The temporal relation between the changes in membrane voltage gradient and the changes in cytosolic calcium concentration is shown in Figure 10. Importantly, the time course and the amplitude of the cytosolic calcium increase was similar in the presence or in the absence of calcium in extracellular medium, thus indicating that calcium was released from intracellular stores (data not shown).

Discussion

The results obtained in the present study provide the first description of the behavior of muscle fibers exposed to a high frequency (4-64 MHz) oscillating electrical field. The choice of this specific frequency range is related with the recent development of a commercial stimulator (Rexonage™, Telea), which is applied in many surgical and medical tasks and utilizes a well defined and patented frequency range. As outlined in the Introduction many studies have investigated the responses of cells and tissues to oscillating electrical fields. The direct effects of oscillating electrical fields are attributed to dielectric dispersion, i.e. to the variations of the permittivity of a dielectric material in relation to the frequency of the applied electric field.

In this study, an excitable tissue such as skeletal muscle was exposed to an oscillating electrical field and its behavior which depends partly on phenomena of β-dispersion (Maxwell Wagner effect, see [1, 8]) was described in detail. Experiments were carried out using a thin needle electrode to apply the electrical field with high spatial resolution and two distinct ranges of voltage. Whereas at high voltage the main effect of the field application was a fast and sharp cut of the muscle fiber or of the fiber bundle in a position adjacent to electrode tip, at low voltage the field application induced slow changes in muscle fiber shape. Such changes in shape were reminiscent of a contraction, but they developed in a continuous way for the whole period of application of the electrical field, did not involve the whole fiber and remained localized in a region close to the electrode tip. Such changes in shape might be compared to the deformation previously observed in red blood cells exposed to an oscillating electrical field in the MHz range [5, 6].

Muscle fibers, however, are able to modify actively their shape and size, when a contraction is triggered, making important to separate the direct effects of electrical field from active contractile response. Fluorescent probes were employed to follow the changes in membrane potential and in cytoplasmic free calcium concentration and this allowed us to demonstrate that the response to a low voltage electrical field was not a contraction. Actually, the membrane was slowly and progressively depolarized for the whole duration of the field application without reaching a threshold sufficient to trigger an action potential. Apparently, the changes in membrane potential were not sufficient to trigger the opening of the voltage gated sodium channels. Such slow and subliminar depolarization was followed by a small but progressive increase in free calcium concentration.

Experiments carried out in the absence of calcium in the extracellular medium showed that the origin of such calcium increase was likely localized in intracellular calcium stores. We could thus hypothesize that the application of the high frequency electrical field induced a membrane depolarization not sufficient to cause the opening of voltage gated sodium channels, but sufficient to induce the opening of ryanodine receptors calcium channels at the terminal cisternae of the sarcoplasmic reticulum and to cause the release of small amount of calcium. Such increase of intracellular calcium concentration represents a major difference if the effects on muscle fibers are compared to the effects observed in not excitable cells, in particular red blood cells red blood cells [5, 6].

The results obtained are rich of potential applications. At high power oscillating electrical fields are able to cut the membrane and the whole cell in a very fast and effective way. The damage is extremely limited, not only adjacent cells, but even the adjacent region of the same muscle fibers remain not affected. At low power, the oscillating electrical fields are able to cause a prolonged calcium accumulation in the cytosol at a level sufficient to elicit a small contractile response and avoid triggering of a full contraction. A long lasting and low increase of calcium concentration in the cytoplasm is likely an optimal signal to activate calcium-dependent intracellular signaling pathways. For example calmodulin-dependent kinase and phosphatase are known to be activated by low and continuous increase of calcium concentration better than by fast and large transients [3, 9]. In this view, the present study opens the way to further work aimed to assess whether such activation of signaling pathways really occur and to understand completely the possible application of high frequency electrical fields to stimulate muscle fiber plasticity.

Acknowledgements

The study was carried out with the financial support of Biotech II, Regione Veneto.

Address Correspondence to:

Carlo Reggiani, Dept. of Anatomy and Physiology, University of Padua, Via Marzolo 3, I-35131 Padova, Italy. E-mail: carlo.reggiani@unipd.it

References

[1] Adey RD: Tissue interactions with non-ionizing electromagnetic fields. Physiol Rev 1981; 6: 435-514.

[2] Beck JD, Shang L, Marcus MS, Hamers RJ: Manipulation and real-time electrical detection of individual bacterial cells at electrode junctions: A model for assembly of nanoscale biosystems. Nano Letters 2005; 5: 777-781.

[3] Berchtold MW, Brinkmeier H, Müntener M: Calcium ion in skeletal muscle: its crucial role for muscle function, plasticity, and disease. Physiol Rev 2000; 80: 1215-1265.

[4] Defranchi E, Bonaccurso E, Tedesco M, et al: Imaging and elasticity measurements of the sarcolemma of fully differentiated skeletal muscle fibers. Microsc Res Tech 2005; 67: 27-35.

[5] Engelhardt H, Gaub H, Sackmann E: Viscoelastic properties of erythrocyte membranes in high frequency electric fields. Nature 1984; 307: 378-380.

[6] Engelhardt H, Sackmann E: On the measurement of shear elastic moduli and viscosities of erythrocyte plasma membranes by transient deformation in high frequency electric fields. Biophysical J 1988; 54: 495-508,

[7] Foster RK, Schwan HP: Dielectric properties of tissues and biological materials: a critical review. Critical Reviews in Biomedical Engineering, 1989; 17: 25-104.

[8] Gimsa J, Wachner D: A unified resistor-capacitor model for impedance, dielectrophoresis electrorotation, and induced transmembrane potential. Biophysical J 1998; 75: 1107-1111.

[9] Hawley JA, Hargreaves M, Zierath JR: Signalling mechanisms in skeletal muscle: role in substrate selection and muscle adaptation. Essays Biochem 2006; 42: 1-12.

[10] Kurschner M, Nielsen K, Andersen C, et al: interaction of lipophilic ions with the plasma membrane of mammalian cells studied by electrorotation. Biophysical J 1998; 74: 3031-3043.

[11] Mahaworasilpa TH, Coster HGL, George EP: Forces on biological cells due to applied alternating (AC) electric fields. Dielectrophoresis. Biochimica et Biophysica Acta 1994; 1193: 118-126.

[12] Marszalek P, Zielinsky JJ, Fikus M, Tsong Tian Y: Determination of electric parameters of cell membranes by a dielectrophoresis method. Biophysical J 1991; 59: 982-987.

[13] Prasad S, Zhang X, Yang M, et al: Separation of

individual neurons using dielectrophoretic alternative current fields. Journal of Neuroscience Methods 2004; 135: 79-88.

[14] Stenger DA, Kaler VK, Wen Hui S: Dipole interactions in electrofusion. Contributions of membrane potential and effective dipole interaction pressures. Biophysical J 1991; 59: 1074-1084.

[15] Sukhorukov VL, Mussauer H, Zimmermann U: The effect of electrical deformation forces on the electro-permeabilization of erythrocyte membranes in low- and high-conductivity media. J Membrane Biol 1998; 163: 235-245.

[16] Voldman J: Electrical forces for microscale cell manipulation. Annual Review Biomedical Engineering 2006; 8: 425-454.

15

Effects of high frequency and low intensity currents: biostimulation e cell regeneration

Professor C.Reggiani, Scientific Director of Research

UNIVERSITY OF PADUA

Department of Human Anatomy and Physiology
Department of Human Anatomy and Physiology

Effects of high frequency and low intensity currents: biostimulation e cell regeneration

Department of Anatomy and Physiology, University of Padua
Telea Electronic Engineering Srl

Introduction

Electric currents, electric fields and electromagnetic fields are collectively a form of energy that can have important biological effects by acting both on cells and on the extracellular matrix.

The passage of electric currents through tissues, in addition to generating thermal effects, is able to modify the distribution of the charges arranged on the membrane surfaces, inducing modifications of the membrane proteins and among these in particular the opening or closing of ion channels. employees. At suitable intensities, the electric currents are able to cause the appearance of pores (electroporation) in the membranes, allowing the transfer of relatively large molecules across the membrane. These direct effects of the current can subsequently trigger important biological responses: think of the stimulations, with low frequency currents, used to control pain or those used to improve trophism and muscle performance.

The biostimulation equipment developed by Telea Electronic Engineering Srl generates high frequency and low intensity currents which, when applied to the tissues, induce a very modest thermal effect. It is therefore a new approach, different from those generally used and as such of significant interest. The objective of the investigations described in this report is a first characterization of the biological effects of these currents.

Scope

We set out to experimentally investigate the effects on tissues of the high frequency and low intensity currents generated by the above equipment. The effects of the currents were studied at three different levels: in vivo in animals, in vitro in cell culture and in a highly concentrated protein suspension. In particular, it was proposed to verify whether the application of the current could cause 1) cell damage capable of triggering a regeneration process and 2) alterations in the structure of large molecules, such as proteins.

In vivo experimentation

The in vivo experimentation was conducted on mice (subject to the authorization of the departmental ethics committee) by applying a stimulation lasting 1 minute and intensity equal to 2 on an arbitrary scale from 1 to 9, equal to about 6W of power. The animals, after being anesthetized and shaved, were stimulated by applying the electrode on the lower abdomen. Other animals were not stimulated but used as controls. Abdominal wall samples were collected at 1, 3 and 7 days from the date of stimulation. Each sample included the epidermis, dermis and underlying muscle wall of the area that had been stimulated.

From the observation and comparison of images acquired from sections of mouse samples (control and stimulated), there are no significant structural differences attributable to the treatment performed at the level of the skin and the muscle of the abdominal wall. The only significant differences can be identified in the furrier muscle where in animals subjected to stimulation it is possible to identify scattered fibers and modest parvicellular infiltrates. These images are indicative of a regenerative process that represents the probable evolution of minimal current-induced damage.

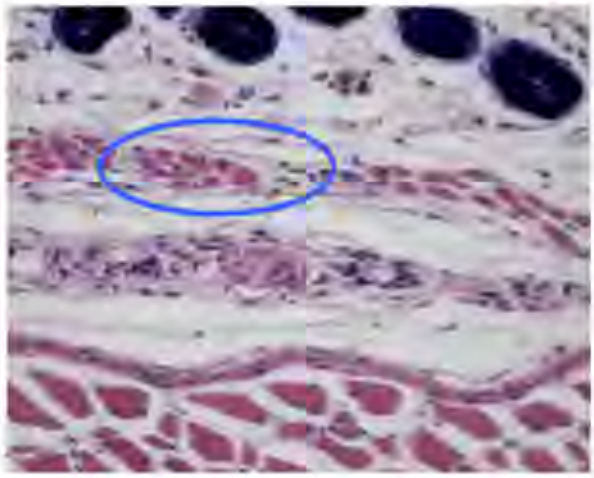

Figure 1: The parvicellular infiltrate in the furrier muscle is visible in the circle. Staining with hematoxylin-eosin.

An alternative approach to the detection of muscle degenerative-regenerative processes triggered by electric currents is represented by the appearance of myosin isoforms typical of immature cells (neonatal and embryonic myosin). These proteins can be considered as molecular markers of regenerative processes and their presence in an adult muscle should be considered as the consequence of cell damage, which occurred a few days earlier.
To visualize the presence of these proteins, the stimulation was performed with intensity 2 (about 6W of power) and for 1 minute at the level of the skin surface overlying the anterior tibialis muscle in the hind limb of the mouse. The muscle of the contralateral, unstimulated limb was used as a control against which to make the comparison. The samples were taken 1, 3 and 7 days after stimulation. The electrophoretic examination of the proteins did not reveal the appearance of bands referable to neonatal and embryonic myosins, nor the presence of a smear attributable to widespread proteolysis.

Via F. Marzolo, 3 - 35131 Padua - Telephone 049 827 5312 - Fax 049 827 5301 - E-Mail: paolina@ux1.unipd.it Via F. Marzolo, 3 - 35131 Padua-Italy-Phone (+39) 049 827 5312- Fax (+39) 049 827 5301- E-Mail: paolina@ux1.unipd.it

Figure 2: Polyacrylamide gel electrophoresis highlighting myosin isoforms (molecular weight 200 kD)

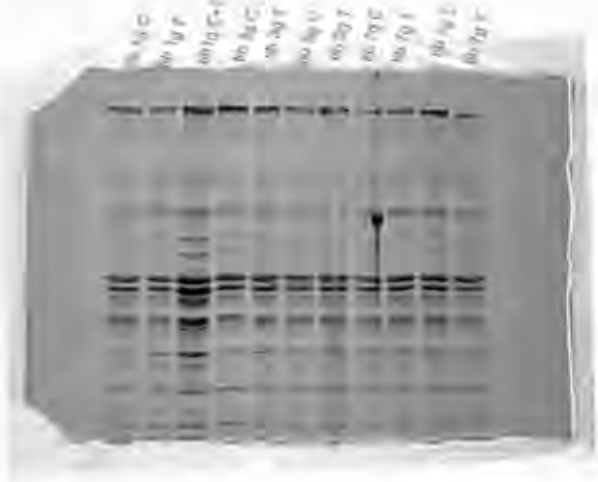

Figure 3 Polyacrylamide gel electrophoresis highlighting all major proteins with molecular weight greater than 10kD

In vitro experimentation on cell cultures:

The possible effect of induction of apoptosis and cell death has been verified on cultures of myoblasts and fibroblasts. Primary cultures were obtained from hind limb muscles of newborn mice. Stimulation with high frequency currents was performed on the cultures approximately 5 days after cell plating, before the culture reached confluence. The stimulation considered different parameters of duration and intensity. Cultures thus stimulated were set at 2 hours, 1 day and 2 days from stimulation. After fixation, the cultures were stained with the Hoechst nuclear dye. The morphology of the cell nuclei was observed using a fluorescence microscope (at wavelength 350 nm).

In no case were there any signs of apoptosis. This suggests that the application of high frequency currents has no harmful effects on the cells (myoblasts and fibroblasts) placed in culture.

Via F. Marzolo, 3 - 35131 Padua - Telephone 049 827 5312 - Fax 049 827 5301- E-Mail: paolina@ux1.unipd.it Via F. Marzolo, 3 - 35131 Padua-Italy-Phone (+39) 049 827 5312- Fax (+39) 049 827 5301- E-Mail: paolina@ux1.unipd.it

Figure 4: Group of nuclei stained with Hoechst. You can see regular appearance.

Experimentation on proteins in solutions

The action of the high frequency currents was studied on an albumin solution at a concentration of 0.5%. The current was applied experimenting varying intensities from 1 to 8 on a conventional 1-9 scale (practically from power 0W up to power of about 15W) and duration varying from 1 to 7 minutes, values higher than those used on tissues and cells in vivo and in vitro. The composition of the protein solution was examined with gel electrophoresis and no signs of protein degradation were observed in any case.

Conclusion

Taken together the experimental investigations conducted:

1) allow to exclude that the application of high frequency currents within the studied intensities and durations can cause direct alterations of the protein structure (see experiments with albumin solutions), can trigger apoptotic phenomena (see experiments on cell cultures) and can cause important degeneration-regeneration phenomena at the tissue level (see experiments on myosin isoforms in the anterior tibialis).
2) show, through histological analysis, the appearance in the abdominal muscle of the stimulated animals of parvicellular infiltrates of modest size and structural disorganization that suggest the possibility of response phenomena to localized degenerative processes. Such phenomena were not observed either in the rectus muscles of the abdominal wall, nor in the anterior tibialis muscle.

Via F. Marzolo, 3 - 35131 Padua - Telephone 049 827 5312 - Fax 049 827 5301- E-Mail: paolina@ux1.unipd.it Via F. Marzolo, 3 - 35131 Padua-Italy-Phone (+39) 049 827 5312- Fax (+39) 049 827 5301- E-Mail: paolina@ux1.unipd.it

The presence of degenerative-regenerative phenomena in the more superficial muscles requires comment. These degenerative-regenerative phenomena that overlap the normal cellular turnover of the muscle and do not upset the structure, due to their modest entity, could represent an important tissue renewal mechanism triggered by stimulation with low intensity and high frequency currents. Further studies should be aimed at clarifying: 1) whether similar phenomena also occur in connective tissues
2) which is the determining mechanism of cellular degeneration-regeneration.

Professor Carlo Reggiani
Scientific Director of Research

Padua 4 April 2005

Via F. Marzolo, 3 - 35131 Padua - Telephone 049 827 5312 - Fax 049 827 5301- E-Mail: paolina@ux1.unipd.it Via F. Marzolo, 3 - 35131 Padua-Italy-Phone (+39) 049 827 5312- Fax (+39) 049 827 5301- E-Mail: paolina@ux1.unipd.it

16

Analysis of quantum molecular resonance effects on human mesenchymal stromal cells

S. Sella, E. Amati, V. Adami, P. Gatto, G. Pozzato, G. Astori

ANALYSIS OF QUANTUM MOLECULAR RESONANCE EFFECTS ON HUMAN MESENCHYMAL STROMAL CELLS

Sabrina Sella[1,2], Eliana Amati[1], Valentina Adami[3], Pamela Gatto[3], Gianantonio Pozzato[4], Giuseppe Astori[1]

1. Hematology and Cellular Therapy, Advanced Cellular Therapy Laboratory, Vicenza Hospital, Italy.
2. Department of Molecular Medicine, University of Padua, Italy.
3. High Throughput Screening Core Facility, Center for Integrative Biology, University of Trento, Trento, Italy.
4. Telea Electronic Engineering srl, Sandrigo, Italy.

Background and aim

Endogenous electric fields play an essential role in cellular functions such as proliferation, migration and gene expression. Quantum Molecular Resonance (QMR) produces waves with a specific form at high frequencies and low intensity through electric fields without increase of temperature. Few is known about QMR mechanism of action on the inter/intracellular processes.

This work aims to evaluate as QMR acts on bone marrow derived mesenchymal stromal cells (BM-MSC).

Materials and Methods

BM-MSC, were treated with QMR (device supplied and patented by Telea, Italy) for 10 minutes for 4 consecutive days a week for 2 weeks (Figure 1). Cell morphology, phenotype, viability, proliferation and migration were investigated.

QMR effects on BM-MSC after the first week of stimulation were further investigated by microarray. For the latter, samples were processed according to the "Agilent Gene Expression Analysis". Data were analyzed by using the Limma package (R language). Differentially expressed genes between conditions were selected based on a p-value cut-off of 0.05. Gene enrichment analysis was performed using ToppGene Suite and Ingenuity Pathway Analysis tools.

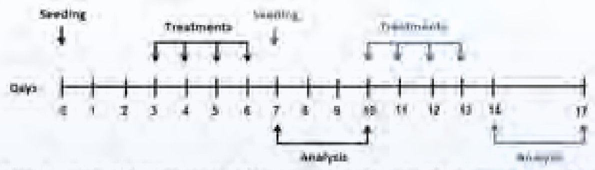

Figure 1. Scheme of QMR treatments. Cells were seeded on day 0, harvested and reseeded on day 7. On day 3 and day 10 the samples were either sham-exposed or treated with 40 or 80 nominal power for 10 minutes a day for 4 days. In black the 1st treatment cycle, in blue the 2nd treatment cycle.

Results

The observations related to morphology and phenotype (Figure 2 and 3, respectively) suggested the maintenance of BM-MSCs identity after 2 weeks of QMR treatment. Furthermore, no alteration of cellular viability, proliferation and migration were observed between samples and controls (Figure 4).

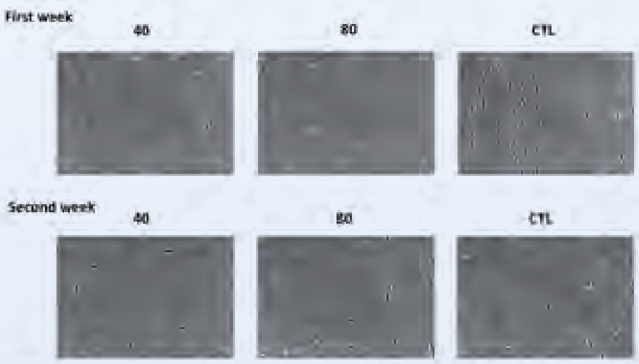

Figure 2. BM-MSCs morphology of a representative sample at Day5 (first week of treatment) and at Day14 (second week of treatment). Scale bar = 100 µm. Total magnification = 100x.

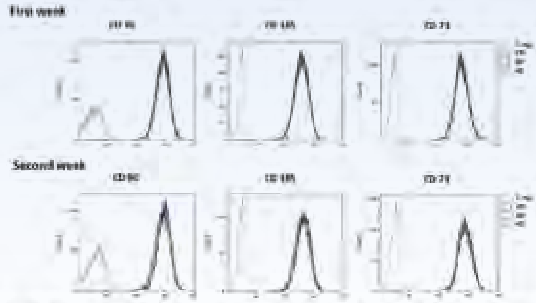

Figure 3. BM-MSCs phenotype of a representative sample after 1 and 2 cycles of QMR stimulation. Grey line=unstained control. Blue line=sham-exposed control. Green line=QMR setting 80. Red line=QMR setting 40.

Figure 4. QMR effects on BM-MSCs viability and proliferation. A) Viability was determined by flow cytometry using LIVE/DEAD Fixable far red stain kit (Invitrogen). B) Cellular proliferation was determined by WST-1 assay (Sigma-Aldrich). Data were expressed as % of proliferation VS control.

At molecular level, the QMR treatment seemed to slightly affect the cell transcriptome: the identified up-regulated genes were mainly involved in cell tissue and vasculature development while the down-regulated genes were involved in cellular growth, phosphorylation, movement and anchoring (Table 2).

[illegible]	[illegible]	[illegible]	[illegible]	[illegible]	[illegible]	[illegible]
40 Treatment vs control	[illegible]	[illegible]	[illegible]	[illegible]	[illegible]	[illegible]
80 Treatment vs control	[illegible]	[illegible]	[illegible]	[illegible]	[illegible]	[illegible]

Table 1. Differentially expressed genes between treated BM-MSC cultures and sham-exposed controls.

Category	[illegible]	Changed genes	Fold-change ≥ 1,3
40 up-regulation	[illegible]	[illegible]	[illegible]
[illegible]	[illegible]	[illegible]	[illegible]
[illegible]	[illegible]	[illegible]	[illegible]
[illegible]	[illegible]	[illegible]	[illegible]
[illegible]	[illegible]	[illegible]	[illegible]
40 down-regulation	[illegible]	[illegible]	[illegible]
[illegible]	[illegible]	[illegible]	[illegible]
[illegible]	[illegible]	[illegible]	[illegible]
[illegible]	[illegible]	[illegible]	[illegible]
[illegible]	[illegible]	[illegible]	[illegible]
80 up-regulation	[illegible]	[illegible]	[illegible]
[illegible]	[illegible]	[illegible]	[illegible]
[illegible]	[illegible]	[illegible]	[illegible]

Table 2. Best enrichment gene lists considering outputs of the software ToppGene Suite and Ingenuity Pathway Analysis (q-value FDR B&H<0.01 and B-H p-value<0.01, respectively). A p-value<0.005 for the changed genes was considered statistically significant. At this level of analysis, the 80 down-regulation condition doesn't show significant genes.

Conclusions

The QMR treatment maintained the BM-MSCs identity and growth and no alteration of the cell phenotype were observed. The microarray analysis evidenced weak transcriptional differences between conditions. Nevertheless, the gene enrichment in tissue and vasculature development processes might suggest that QMR could activate angiogenesis. This hypothesis requires further investigation.

REXONEYE QMR CLINICAL STUDIES | UNIVERSITY RESEARCH | PUBLICATIONS

Rev. 02/2025 - Subject to technical changes as part of product development, as well as errors and omissions

RESONO OPHTHALMIC

Resono Ophthalmic S.r.l.
Via Leonardo da Vinci, 13
36066 Sandrigo (VI) - Italy

+39 044 412 419 47

contact@resono.it

www.resono.it